

# Green Chemistry

Cutting-edge research for a greener sustainable future

[www.rsc.org/greenchem](http://www.rsc.org/greenchem)

Volume 8 | Number 5 | May 2006 | Pages 401–496



Downloaded on 07 November 2010  
Published on 05 May 2006 on <http://pubs.rsc.org> | doi:10.1039/B605747K

ISSN 1463-9262

RSC Publishing

Albrecht *et al.*  
Health implications of  
nanoparticles

Reid *et al.*  
Solventless microwave-assisted  
chlorodehydroxylation

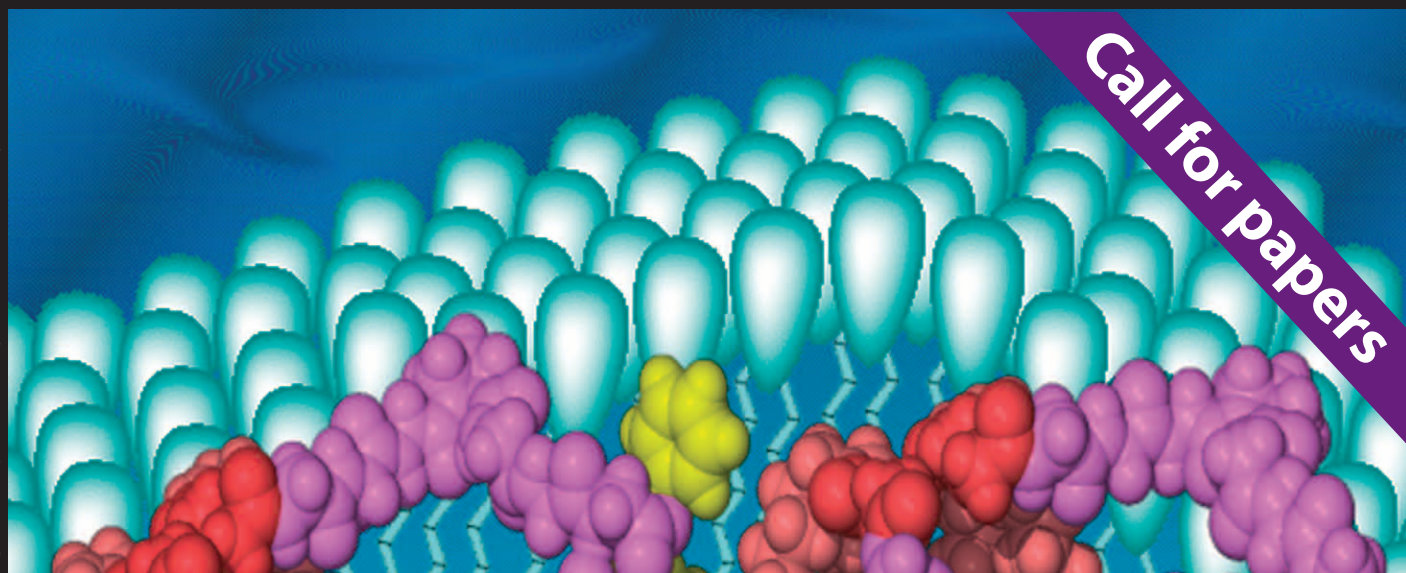
Marci *et al.*  
Cellulose-based superabsorbent  
hydrogels

Li *et al.*  
Preparation of N-sulfonylimines in  
aqueous media



1463-9262(2006)8:5;1-9

Call for papers

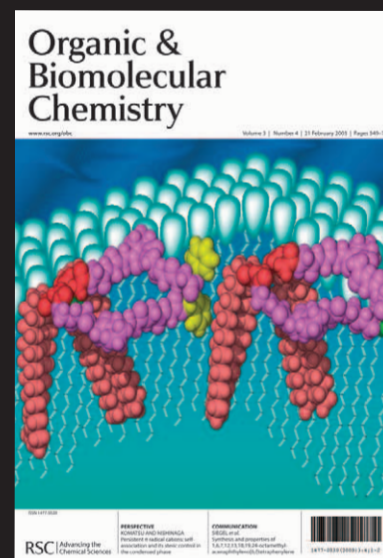


# Organic & Biomolecular Chemistry

A major peer-reviewed international, high quality journal covering the full breadth of synthetic, physical and biomolecular organic chemistry.

Publish your review, article, or communication in OBC and benefit from:

- The fastest times to publication (80 days for full papers, 40 days for communications)
- High visibility (OBC is indexed in MEDLINE)
- Free colour (where scientifically justified)
- Electronic submission and manuscript tracking via ReSource ([www.rsc.org/ReSource](http://www.rsc.org/ReSource))
- A first class professional service
- No page charges



**Submit today!**

RSC Publishing

[www.rsc.org/obc](http://www.rsc.org/obc)

# Green Chemistry

Cutting-edge research for a greener sustainable future

[www.rsc.org/greenchem](http://www.rsc.org/greenchem)

RSC Publishing is a not-for-profit publisher and a division of the Royal Society of Chemistry. Any surplus made is used to support charitable activities aimed at advancing the chemical sciences. Full details are available from [www.rsc.org](http://www.rsc.org)

## IN THIS ISSUE

ISSN 1463-9262 CODEN GRCHFJ 8(5) 401–496 (2006)



### Cover

The cover image depicts a cellulose based superabsorbent hydrogel produced through environmentally sustainable processes. A heterogeneous  $\text{TiO}_2$  photo-catalysed process has been proposed for the detoxification (and a possible re-use) of washing waste waters produced from the hydrogel preparation. Image reproduced by permission of Alessandro Sannino from *Green Chem.*, 2006, 8(5), 439.

## CHEMICAL TECHNOLOGY

T17

Chemical Technology highlights the latest applications and technological aspects of research across the chemical sciences.

## Chemical Technology

May 2006/Volume 3/Issue 5

[www.rsc.org/chemicaltechnology](http://www.rsc.org/chemicaltechnology)

## NEWS

411

### Recalling COIL

John D. Holbrey, Natalia V. Plechkova and Kenneth R. Seddon recall the events of the 1st International Congress on Ionic Liquids (COIL), held in Salzburg, Austria, June 19–22, 2005.



## EDITORIAL STAFF

**Editor**

Sarah Ruthven

**News writer**

Markus Hölscher

**Publishing assistant**

Emma Hacking

**Team leader, serials production**

Stephen Wilkes

**Administration coordinator**

Sonya Spring

**Editorial secretaries**

Lynne Braybrook, Jill Segev, Julie Thompson

**Publisher**

Adrian Kybett

Green Chemistry (print: ISSN 1463-9262; electronic: ISSN 1463-9270) is published 12 times a year by the Royal Society of Chemistry, Thomas Graham House, Science Park, Milton Road, Cambridge, UK CB4 0WF.

All orders, with cheques made payable to the Royal Society of Chemistry, should be sent to RSC Distribution Services, c/o Portland Customer Services, Commerce Way, Colchester, Essex, UK CO2 8HP. Tel +44 (0) 1206 226050; E-mail sales@rscdistribution.org

2006 Annual (print + electronic) subscription price: £859; US\$1571. 2006 Annual (electronic) subscription price: £773; US\$1414. Customers in Canada will be subject to a surcharge to cover GST. Customers in the EU subscribing to the electronic version only will be charged VAT.

If you take an institutional subscription to any RSC journal you are entitled to free, site-wide web access to that journal. You can arrange access via Internet Protocol (IP) address at [www.rsc.org/ip](http://www.rsc.org/ip). Customers should make payments by cheque in sterling payable on a UK clearing bank or in US dollars payable on a US clearing bank. Periodicals postage paid at Rahway, NJ, USA and at additional mailing offices. Airfreight and mailing in the USA by Mercury Airfreight International Ltd., 365 Blair Road, Avenel, NJ 07001, USA.

US Postmaster: send address changes to Green Chemistry, c/o Mercury Airfreight International Ltd., 365 Blair Road, Avenel, NJ 07001. All despatches outside the UK by Consolidated Airfreight.

PRINTED IN THE UK

**Advertisement sales:** Tel +44 (0) 1223 432246; Fax +44 (0) 1223 426017; E-mail [advertising@rsc.org](mailto:advertising@rsc.org)

# Green Chemistry

Cutting-edge research for a greener sustainable future

[www.rsc.org/greenchem](http://www.rsc.org/greenchem)

Green Chemistry focuses on cutting-edge research that attempts to reduce the environmental impact of the chemical enterprise by developing a technology base that is inherently non-toxic to living things and the environment.

## EDITORIAL BOARD

**Chair**

Professor Colin Raston,  
Department of Chemistry  
University of Western Australia  
Perth, Australia  
E-mail [clraston@chem.uwa.edu.au](mailto:clraston@chem.uwa.edu.au)

Dr Janet Scott, Centre for Green  
Chemistry, Monash University,  
Australia

Dr A Michael Warhurst,  
University of Massachusetts,  
USA  
E-mail [michael-warhurst@uml.edu](mailto:michael-warhurst@uml.edu)

Professor Buxing Han, Chinese  
Academy of Sciences  
E-mail [hanbx@iccas.ac.cn](mailto:hanbx@iccas.ac.cn)

**Scientific editor**

Professor Walter Leitner,  
RWTH-Aachen, Germany  
E-mail [leitner@itmc.rwth-aachen.de](mailto:leitner@itmc.rwth-aachen.de)

Professor Tom Welton,  
Imperial College, UK

E-mail [t.welton@ic.ac.uk](mailto:t.welton@ic.ac.uk)  
Professor Roshan Jachuck,  
Clarkson University, USA

**Associate editors**

Professor C. J. Li, McGill  
University, Canada  
E-mail [cj.li@mcgill.ca](mailto:cj.li@mcgill.ca)  
Professor Kyoko Nozaki  
Kyoto University, Japan  
E-mail [nozaki@chembio.tu-tokyo.ac.jp](mailto:nozaki@chembio.tu-tokyo.ac.jp)

**Members**

Professor Joan Brennecke,  
University of Notre Dame, USA  
Professor Steve Howdle, University  
of Nottingham, UK

Dr Paul Anastas, Green Chemistry  
Institute, USA  
E-mail [p\\_anastas@acs.org](mailto:p_anastas@acs.org)

## INTERNATIONAL ADVISORY EDITORIAL BOARD

James Clark, York, UK  
Avelino Corma, Universidad  
Politécnica de Valencia, Spain  
Mark Harmer, DuPont Central  
R&D, USA  
Herbert Hugl, Lanxess Fine  
Chemicals, Germany  
Makato Misono, Kogakuin  
University, Japan  
Robin D. Rogers, Centre for Green  
Manufacturing, USA

Kenneth Seddon, Queen's  
University, Belfast, UK  
Roger Sheldon, Delft University of  
Technology, The Netherlands  
Gary Sheldrake, Queen's  
University, Belfast, UK  
Pietro Tundo, Università ca  
Foscari di Venezia, Italy  
Tracy Williamson, Environmental  
Protection Agency, USA

## INFORMATION FOR AUTHORS

Full details of how to submit material for publication in Green Chemistry are given in the Instructions for Authors (available from <http://www.rsc.org/authors>). Submissions should be sent via ReSource: <http://www.rsc.org/resource>.

Authors may reproduce/republish portions of their published contribution without seeking permission from the RSC, provided that any such republication is accompanied by an acknowledgement in the form: (Original citation) – Reproduced by permission of the Royal Society of Chemistry.

© The Royal Society of Chemistry 2006. Apart from fair dealing for the purposes of research or private study for non-commercial purposes, or criticism or review, as permitted under the Copyright, Designs and Patents Act 1988 and the Copyright and Related Rights Regulations 2003, this publication may only be reproduced, stored or transmitted, in any form or by any means, with the prior permission in writing of the Publishers or in the case of reprographic reproduction in accordance with the terms of

licences issued by the Copyright Licensing Agency in the UK. US copyright law is applicable to users in the USA.

The Royal Society of Chemistry takes reasonable care in the preparation of this publication but does not accept liability for the consequences of any errors or omissions.

Ⓢ The paper used in this publication meets the requirements of ANSI/NISO Z39.48-1992 (Permanence of Paper).

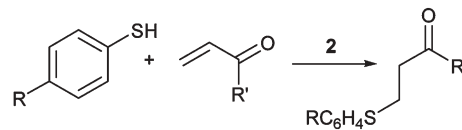
Royal Society of Chemistry: Registered Charity No. 207890

## HIGHLIGHT

415


## Highlights

Markus Hölscher reviews some of the recent literature in green chemistry.



## CRITICAL REVIEW

417


**Green chemistry and the health implications of nanoparticles**

Matthew A. Albrecht, Cameron W. Evans and Colin L. Raston\*

This review scopes the issue of incorporating green chemistry metrics into nanotechnology in the context of potential health effects of nanoparticles, along with medical applications of nanoparticles including imaging, drug delivery, disinfection, and tissue repair.



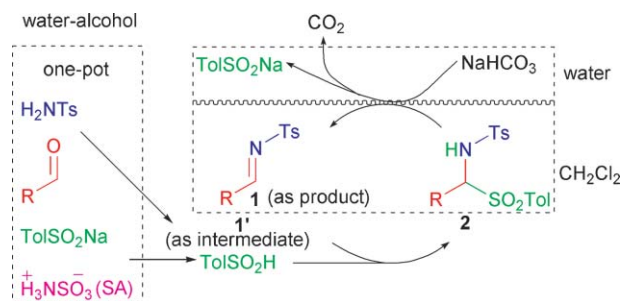
## COMMUNICATIONS

433

**A convenient preparation of aliphatic and aromatic N-sulfonylimines mediated by sulfamic acid in aqueous media**

Zhenjiang Li,\* Xinghua Ren, Ping Wei, Honggui Wan, Yuhu Shi and Pingkai Ouyang

In the presence of sulfamic acid (SA), the intermediate imine **1** was trapped by toluenesulfinic acid in water-alcohol media, the precipitated sulfonamidossulfone **2**, in basic aqueous-biphasic system, was eliminated to afford the imine **1**.

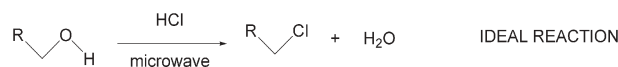


437

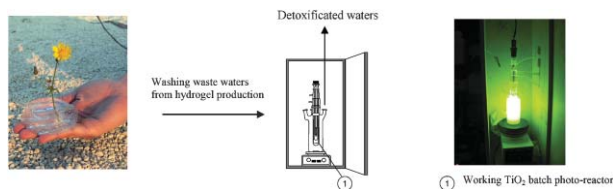
**Solventless microwave-assisted chlorohydroxylation for the conversion of alcohols to alkyl chlorides**

Mark C. Reid, James H. Clark\* and Duncan J. Macquarrie

A genuinely viable auxiliary-free route to the preparation of alkyl chlorides is now available.



439

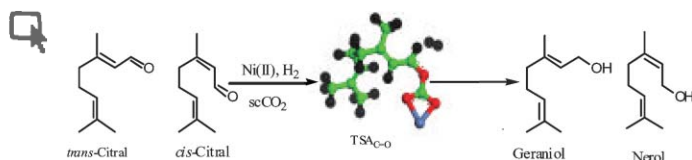


### Environmentally sustainable production of cellulose-based superabsorbent hydrogels

Giuseppe Marci, Giuseppe Mele,\* Leonardo Palmisano, Piero Pulito and Alessandro Sannino

This article deals with the environmentally sustainable synthesis of a novel cellulose based superabsorbent hydrogel for which a heterogeneous  $\text{TiO}_2$  photo-catalysed process has been proposed for the detoxification (and a possible re-use) of washing waste waters.

445

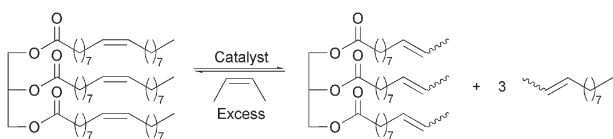


### Hydrogenation of citral in supercritical $\text{CO}_2$ using a heterogeneous $\text{Ni(II)}$ catalyst

Maya Chatterjee, Abhijit Chatterjee, Poovathinthodiyil Raveendran and Yutaka Ikushima\*

$\text{Ni(II)}$ -catalyzed hydrogenation of citral in supercritical carbon dioxide results in the selective hydrogenation of  $\text{C}=\text{O}$  over  $\text{C}=\text{C}$ . With small amounts of  $\text{CO}_2$  in the organic solvent, the catalyst becomes active to the hydrogenation.

450

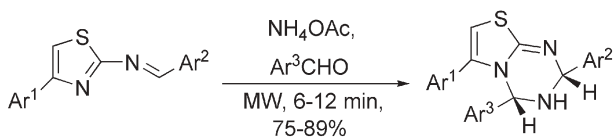


### High conversion and productive catalyst turnovers in cross-metathesis reactions of natural oils with 2-butene

Jim Patel, S. Mujcinovic, W. Roy Jackson,\* Andrea J. Robinson, Algirdas K. Serelis and Chris Such

Ruthenium-alkylidene catalysed butenolysis of triglycerides and unsaturated fatty acid esters gives high yields of products with remarkably high effective TONs of up to 470 000.

455



### Green protocol for annulation of the *s*-triazine ring on thiazoles using a three-component coupling strategy

Lal Dhar S. Yadav,\* Seema Yadav and Vijai K. Rai

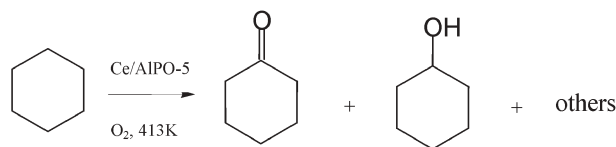
Novel three-component one-pot reactions of thiazole Schiff bases, ammonium acetate and aromatic aldehydes under solvent-free microwave irradiation conditions expeditiously and diastereoselectively annulate the *s*-triazine ring on thiazoles to yield thiazolo-*s*-triazines.

459

### A novel Ce/AlPO-5 catalyst for solvent-free liquid phase oxidation of cyclohexane by oxygen

Rui Zhao, Yanqin Wang, Yanglong Guo, Yun Guo, Xiaohui Liu, Zhigang Zhang, Yunsong Wang, Wangcheng Zhan and Guanzhong Lu\*

A highly efficient oxidation of cyclohexane to cyclohexanol and cyclohexanone is accomplished over a calcined Ce/AlPO-5 molecular sieve catalyst with oxygen as oxidant.

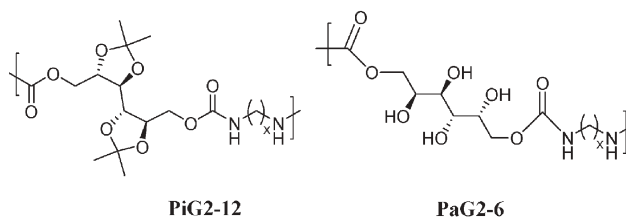


467

### Polyurethanes with pendant hydroxy groups: polycondensation of 1,6-bis-*O*-phenoxy carbonyl-2,3:4,5-di-*O*-isopropylidene galactitol and 1,6-di-*O*-phenoxy carbonyl galactitol with diamines

Günter Prömpers, Helmut Keul\* and Hartwig Höcker

Polyurethanes with four protected hydroxy groups **PiG2-12** and polyurethanes with four free hydroxy groups **PaG2-6** per repeating unit were obtained from renewable sources by an isocyanate-free route.

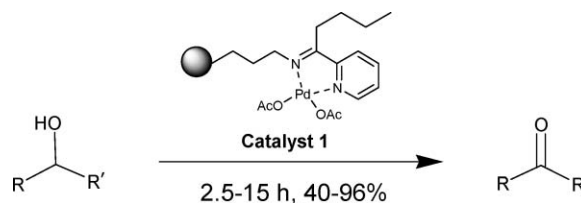


479

### Catalytic properties of several palladium complexes covalently anchored onto silica for the aerobic oxidation of alcohols

Deepak Choudhary, Satya Paul,\* Rajive Gupta and James H. Clark

A series of novel palladium complexes covalently anchored onto silica bearing N–N, N–S and N–O chelating ligands have been prepared and tested for the aerobic oxidation of alcohols to the corresponding carbonyl compounds. The most active catalyst, **1**, was used for the oxidation of a series of alcohols.

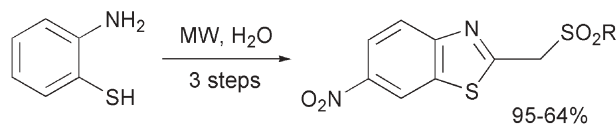


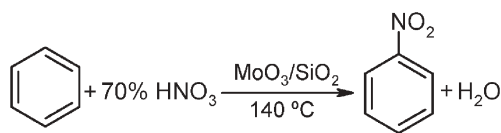
483

### Rapid microwave-promoted synthesis of new sulfonylmethylbenzothiazoles in water

A. Gellis, N. Boufatah and P. Vanelle\*

A simple, fast and inexpensive microwave-irradiated reaction permitting the synthesis of new sulfonylmethylbenzothiazoles in water by *S*-alkylation of 2-chloromethyl-6-nitrobenzothiazole with different benzenesulfinic acid anions is reported.





### Vapor phase nitration of benzene using mesoporous MoO<sub>3</sub>/SiO<sub>2</sub> solid acid catalyst

S. B. Umbarkar, A. V. Biradar, S. M. Mathew, S. B. Shelke, K. M. Malshe, P. T. Patil, S. P. Dagde, S. P. Niphadkar and M. K. Dongare\*

An environmentally benign process for the nitration of benzene has been demonstrated using dilute nitric acid as the nitrating agent, without the use of sulfuric acid, over mesoporous MoO<sub>3</sub>/SiO<sub>2</sub> solid acid catalysts, with high conversion, selectivity and longer catalyst life.

### AUTHOR INDEX

- |                           |                            |                                    |                         |
|---------------------------|----------------------------|------------------------------------|-------------------------|
| Albrecht, Matthew A., 417 | Ikushima, Yutaka, 445      | Patil, P. T., 488                  | Shi, Yuhu, 433          |
| Biradar, A. V., 488       | Jackson, W. Roy, 450       | Paul, Satya, 479                   | Such, Chris, 450        |
| Boufatah, N., 483         | Keul, Helmut, 467          | Plechova, Natalia V., 411          | Umbarkar, S. B., 488    |
| Chatterjee, Abhijit, 445  | Li, Zhenjiang, 433         | Prömpers, Günter, 467              | Vanelle, P., 483        |
| Chatterjee, Maya, 445     | Liu, Xiaohui, 459          | Pulito, Piero, 439                 | Wan, Honggui, 433       |
| Choudhary, Deepak, 479    | Lu, Guanzhong, 459         | Rai, Vijai K., 455                 | Wang, Yanqin, 459       |
| Clark, James H., 437, 479 | Macquarrie, Duncan J., 437 | Raston, Colin L., 417              | Wang, Yunsong, 459      |
| Dagde, S. P., 488         | Malshe, K. M., 488         | Raveendran, Poovathinthodiyil, 445 | Wei, Ping, 433          |
| Dongare, M. K., 488       | Marci, Giuseppe, 439       | Reid, Mark C., 437                 | Yadav, Lal Dhar S., 455 |
| Evans, Cameron W., 417    | Mathew, S. M., 488         | Ren, Xinghua, 433                  | Yadav, Seema, 455       |
| Gellis, A., 483           | Mele, Giuseppe, 439        | Robinson, Andrea J., 450           | Zhan, Wangcheng, 459    |
| Guo, Yanglong, 459        | Mujcinovic, S., 450        | Sannino, Alessandro, 439           | Zhang, Zhigang, 459     |
| Guo, Yun, 459             | Niphadkar, S. P., 488      | Seddon, Kenneth R., 411            | Zhao, Rui, 459          |
| Gupta, Rajive, 479        | Ouyang, Pingkai, 433       | Serelis, Algirdas K., 450          |                         |
| Höcker, Hartwig, 467      | Palmisano, Leonardo, 439   | Shelke, S. B., 488                 |                         |
| Holbrey, John D., 411     | Patel, Jim, 450            |                                    |                         |

### FREE E-MAIL ALERTS AND RSS FEEDS


Contents lists in advance of publication are available on the web *via* [www.rsc.org/greenchem](http://www.rsc.org/greenchem) - or take advantage of our free e-mail alerting service ([www.rsc.org/ej\\_alert](http://www.rsc.org/ej_alert)) to receive notification each time a new list becomes available.

**RSS** Try our RSS feeds for up-to-the-minute news of the latest research. By setting up RSS feeds, preferably using feed reader software, you can be alerted to the latest Advance Articles published on the RSC web site. Visit [www.rsc.org/publishing/technology/rss.asp](http://www.rsc.org/publishing/technology/rss.asp) for details.

### ADVANCE ARTICLES AND ELECTRONIC JOURNAL

Free site-wide access to Advance Articles and the electronic form of this journal is provided with a full-rate institutional subscription. See [www.rsc.org/ejs](http://www.rsc.org/ejs) for more information.

\* Indicates the author for correspondence: see article for details.

 Electronic supplementary information (ESI) is available *via* the online article (see <http://www.rsc.org/esi> for general information about ESI).



'I wish the others were as easy to use.'



'ReSource is the best online submission system of any publisher.'

'It leads the way for online submission and refereeing.'



ReSource



A selection of comments received from just a few of the thousands of satisfied RSC authors and referees who have used ReSource to submit and referee manuscripts. The online portal provides a host of services, to help you through every step of the publication process.

**authors** benefit from a user-friendly electronic submission process, manuscript tracking facilities, online proof collection, free pdf reprints, and can review all aspects of their publishing history

**referees** can download articles, submit reports, monitor the outcome of reviewed manuscripts, and check and update their personal profile

**NEW!!** We have added a number of enhancements to ReSource, to improve your publishing experience even further. New features include:

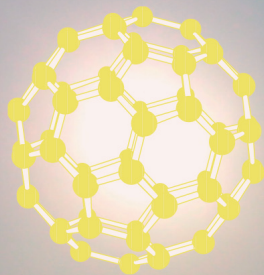
- the facility for authors to save manuscript submissions at key stages in the process (handy for those juggling a hectic research schedule)
- checklists and support notes (with useful hints, tips and reminders)
- and a fresh new look (so that you can more easily see what you have done and need to do next)

A class-leading submission and refereeing service, top quality high impact journals, all from a not-for-profit society publisher ... is it any wonder that more and more researchers are supporting RSC Publishing? Go online today and find out more.

Registered Charity No. 207890

RSC Publishing

[www.rsc.org/resource](http://www.rsc.org/resource)



# NJC

## New Journal of Chemistry

A prime source of international, cutting-edge research,  
encompassing all areas of the chemical sciences

- Impact factor: 2.735
- Fast times to publication
- Multidisciplinary with broad appeal

**Read it today!**

RSC Publishing

[www.rsc.org/njc](http://www.rsc.org/njc)

# Recalling COIL

DOI: 10.1039/b605378p

John D. Holbrey, Natalia V. Plechkova and Kenneth R. Seddon recall the events of the 1st International Congress on Ionic Liquids (COIL), held in Salzburg, Austria, June 19–22, 2005.

The 1st International Congress on Ionic Liquids (COIL; see Fig. 1) was not the first meeting to feature ionic liquids (by a long stretch), but was the first open, truly international, modern meeting to focus entirely on the application and inspiration of ionic liquids, providing a breadth of exciting research and innovation, covering the complete range from fundamental studies to working solutions to 'real-work' industrial problems. It was held in Salzburg (the right venue, as the name suggests), and was attended by over 400 scientists, a healthy mix of industrialists, academics, government scientists and students, travelling from six continents.

Plenary speakers were assembled from both industry and academia, and delivered challenging presentations, describing both the breadth of existing work and exhorting scientists to explore new opportunities that will emerge through the application of ionic liquids. Many interesting talks covered ionic liquid applications and research, from fundamental physico-chemical and computational studies through to existing and current innovations in industrial catalysis, separations, and reactive gas handling. A range of personal opinions and outlooks about the nature of ionic

liquid systems and the future direction of the field were expressed, although the plenary speakers all echoed a common underlying theme, and issued many of the same challenges to the audience, namely that there is a lot more to ionic liquids than just being possible alternative solvent systems for chemical synthesis, and that innovation and future developments emerge when consideration of the characteristics of ionic liquid materials is used as a design criteria for selecting potential solutions to current problems.

*Robin Rogers* (University of Alabama) opened the meeting by setting the scene with a review of some of the progress that had been made in the field (in its modern incarnation) since the pioneering NATO ARW in Crete in 2000, which led to a number of recommendations needed to carry ionic liquid research forwards. What was so exciting was that, throughout this Congress, the products of those recommendations were apparent. Rogers set off persuading the audience that ionic liquids are definitely worthy of study, and exploring how ionic liquids can be designed to behave both like, and unlike, conventional solvents in extraction processes. He exhorted the audience to think beyond our current understanding, and

explore just what the term *ionic liquid* means and how ionic liquid materials can be applied in the context of current chemistry, especially with regards to the fact that no one aspect of ionic liquid properties can be considered as generic—the idea that ionic liquids can be, but are not necessarily, non-volatile, non-flammable, non-toxic solvents was echoed throughout the congress. Safety, health and environment (SHE) issues were discussed, with the observation that while to a first approximation, increased alkyl chain length in the ionic liquid cations increased toxicity, a much more specific study continues to be necessary. Rogers was forced to leave the meeting on the same day in order to attend the EPA's Green Chemistry and Engineering Workshop in Washington DC where he was presented with the (well deserved) 2005 Presidential Award for Green Chemistry and Engineering ([http://www.epa.gov/greenchemistry/past.html#2005\\_award\\_winners](http://www.epa.gov/greenchemistry/past.html#2005_award_winners)) for the work at Alabama on cellulose/ionic liquid systems.

*Joe Magee* (NIST) described the forthcoming NIST ionic liquid database which will go live at the ACS Spring 2006 (Atlanta) meeting, and provide a free, publicly accessible resource of available ionic liquid thermodynamic data. The database has been developed through a IUPAC steering group, and is a direct outcome of the Crete 2000 recommendations, and a highly desirable resource.

Industrial concerns were represented in excellent presentations from Eastman Chemicals, Air Products, BASF, IFP and Degussa, in which materials with ionic liquid characteristics have played significant roles in providing business solutions.

*Daniel Tempel* (Air Products) set the audience buzzing with a talk in which he described a new approach, currently under trial, for storing and delivering reactive gasses (such as  $\text{BF}_3$  and  $\text{PH}_3$ ) at



Fig. 1 COIL.

sub-atmospheric pressures to the electronics industry, by entraining them in ionic liquids. According to Tempel, the new Air Products technology, which is based around the entrainment by chemisorption of the reactive gasses in ionic liquids, has at least twice the performance of the main rival physisorption processes, and provides a method to deliver these reactive gasses in a safe, effective, more easily handled way, reducing both the risks and hazards in the work place—a true green chemistry success.

*Matthias Maase* (BASF) addressed the challenges and successes of current industrial implementation of ionic liquid technologies in a presentation inspired by the famous Mozart opera “Cosi fan tutte” (fitting as Salzburg was Mozart’s birthplace). In addition to highlighting how the recognition that utilising the ionic liquid properties of salts resulted in the drastic process improvements in the BASIL process, the relevance to other chemical processes was described, with the use of ionic liquids entrainers for distillation (again utilising the liquid characteristics of the salts to overcome some difficulties currently faced) highlighted. Maase illustrated the range of existing commercial or piloted industrial processes using ionic liquids, and the diversity of approaches in these systems. Finally, in the spirit of cooperation, BASF/Degussa, and Solvent Innovations jointly announced data from the toxicological screening for registration purposes of two important ionic liquids, 1-ethyl-3-methylimidazolium ethyl sulfate and 1-butyl-3-methylimidazolium chloride, which indicated low toxicities (for [emim][EtSO<sub>4</sub>], LD<sub>50</sub> was > 2000 mg kg<sup>-1</sup>), although these results can’t be used as generic results for all ionic liquids.

*Steve Falling* (Eastman) described the development and details of an ionic liquid catalysed isomerisation process for converting 3,4-epoxybutane to 2,5-dihydrofuran, a useful and versatile chemical intermediate. The process had been run as a commercial success within Eastman from 1996–2004, although Falling noted that currently the plant is non-operational due to a decline in the market for the furan products. Falling clearly covered the development of the catalyst system, highlighting how new

process improvements were made through the introduction and implementation of ionic liquid materials, and how the system was developed with the aid of and cooperation with another company represented at the meeting, Cytec, who are getting known now, not only for their conventional phosphorus-based products, but also as a source of many novel phosphonium ionic liquids.

*Hélène Olivier-Bourbigou* (IFP, France) described examples from the current development of homogeneous and liquid–liquid biphasic catalysis using ionic liquid catalyst phases. The advances and advantages of ionic liquids, compared to heterogeneous catalysis, in terms of increased catalyst life-times and activity, and reductions in reactor volumes for a number of examples, including the olefin dimerisation work pioneered at the IFP was highlighted. It is notable that this IFP Difasol process has been extensively tested under continuous pilot-plant conditions and is a current ‘best technology choice’.

These successful industrial uses of ionic liquids, showing different ways in which ionic liquid systems can be used, reflected many of the other contributing speakers, from whom the use of ionic liquids as solvents for conventional organic synthesis (widely reported in the past few years) took a back seat to recent innovations and developments in materials chemistry, using ionic liquids as rheological fluids, electrochemical enhancers, solvents for polymerisation, enzymatic processes, electrodeposition, and in separations membranes.

*Anna Prodi-Schwab* (Degussa) described a pre-commercial study aimed at integrating ionic liquid electrolytes with other Degussa performance technologies into lithium-ion batteries to deliver future performance demands. While the technology for lithium-ion batteries using ionic liquids does not yet match that of current lithium batteries, there was considerable optimism that both IL–Li<sup>+</sup> ion and IL–polymer systems were rapidly heading in the right direction. This view was supported from the results and talks from *Hiroshi Matsui* (Fujikura, Tokyo) and *Masayoshi Watanabe* (Yokohama National University, Japan), which described the uses of ionic liquids in both battery and solar cell applications.

*Andrew Abbott* (Leicester, UK) highlighted the uses of choline chloride-based ionic liquids in electroplating applications. While the use of reactive, air and moisture-sensitive ionic liquids as solvents for electrochemistry and deposition is well established as one of the fundamental applications of ionic liquids, and still receives active investigation for formation of nanostructured metallic alloys (*Hempelmann*, University of Saarlandes, Germany), Abbott discussed selection of choline chloride as a non-toxic, cheap and readily available component of ionic liquid electrolytes, offering great opportunities as the basis for electroplating baths to compete with current chromic acid systems for industrial chrome plating and polishing. He included pictures of a large portable demonstration tank for chromic acid-free electroplating, which is amenable to deposition of just about all non-reactive metals. Environmental benefits from this technology include reduction in chrome toxicity, emissions, and the energy required to deposit metal, and Abbott claims the process is exceptionally efficient, yielding an enormous energy saving compared to the conventional acid plating technologies.

For utilisation of ionic liquids in scaled-up, industrial applications, knowledge of both the thermodynamics and practical behaviour is needed, and is often neglected by chemists who often forget that there are considerable challenges in scaling from the round-bottomed flask to the full-size reactor. The evaluation of rotating disk columns for separation of aromatic from aliphatic feeds using a counter-current ionic liquid phase was described by *Wytze Meindersma* (Technical University of Twente, Netherlands) while *David Rooney* (QUILL, UK) described studies on the design and kinetics using rotating disk reactors to study gas–ionic liquid–heterogeneous catalyst systems.

Other applications of ionic liquids in synthesis were discussed by *Geldback* (EPFL, Switzerland) and *Kubisa* (Lodz, Poland) who presented approaches to using ionic liquids as solvents for the synthesis of polysiloxanes and radical and ionic polymerisation approaches, respectively. The stability of enzymes in ionic liquids, and their use for biocatalysis, was presented by *Goto*

(Kyushu University) and by *van Rantwijk* (Delft University of Technology). Both talks centred on the need to understand the role of IL–enzyme interactions in controlling reactivity, and made the point that anhydrous ionic liquids are excellent solvents for lipase-catalysed *trans*-esterification reactions.

Different architectures and approaches are sometimes needed to make the greatest use of ionic liquid resources. *Noble* (University of Colorado), *Winterton* (Liverpool University), and *Riisager* (Technical University of Denmark) all reported on aspects of using ionic liquids hosted on polymeric supports either for separations, or as heterogenised catalysts. Moving from solid-supported ionic liquids, the combining of supercritical CO<sub>2</sub>/ionic liquid systems, two neoteric solvents, was first suggested by *Joan Brennecke* (Notre Dame) in 1998 as a means of enabling extractions from non-volatile ionic liquids. Subsequently, the investigation of catalysis and separations from scCO<sub>2</sub>/ionic liquid mixtures has been taken up by a number of groups; *Brennecke*, *Gausepohl* (RWTH Aachen, Germany), and *Peters* (Delft University of Technology) all presented aspects of the development of systems based on scCO<sub>2</sub>/IL.

In a change again to liquid–liquid systems, *Michel Vaultier* (University of Rennes) explained his concepts for ionic liquid-supported chemistry, tethering either reagents or catalysis to ionic liquids and creating, in effect, a liquid analogue to polymer-bead immobilised reaction systems. He showed a demonstration of how free floating ionic liquid-droplets, manipulated and moved in three-dimensional space using electric fields, could be loaded with reagents used as ‘hands-free’ automated microreactors.

Modelling and theory, supported by experimental measurements (*Lopes*, *Rebelo*, *Hardacre*, Padua) help to provide a better picture of ionic liquid structure and fundamental characteristics. There is still a healthy disagreement and debate about procedures, methodologies and analysis of data, and indeed, many approaches to modelling and predicting the behaviour of ionic liquids were presented. As this aspect of the field matures, and methodologies become more robust, their application will

become invaluable to enable ‘*in silico*’ screening and guidance to the design and study of the potential >10<sup>18</sup> IL systems available.

Not that the synthetic chemist should be forgotten: *Jim Davis* (University of South Alabama) again challenged the audience to think about just what an ionic liquid is, and how we might go about exploiting the diversity of chemistry amenable to the formation of new IL materials, particularly addressing the task of preparing new ion families suitable for formulating ionic liquids. The examples included arene sulfonic acid ionic liquids and the use of hydrazine-appended cations to affect reactive separations for solution phase synthesis. The design of new ‘ion core’ compositions and structures as the basis for IL ions was also discussed.

*Doug MacFarlane* (Monash University) first described the uses of ionic liquids containing weakly basic anions, which are capable of interacting with a wide range of chemicals through electron-donor, hydrogen-bond accepting mechanisms, for example, solvating metal cations and carbohydrates. A question arose from this work of how to measure, and indeed what is the meaning of, basicity in non-aqueous systems. *MacFarlane* then proceeded to ask what, fundamentally, ionic liquids are. Is an IL non-volatile, non-flammable, non-toxic and ‘green’, capable of dissolving almost everything (except glass and polythene)? Well both the obvious, and pragmatic answers are, “no!”, at least not in every context, and this was illustrated with examples of definitively volatile ionic liquids based on protic acid + base systems which are important for a number of applications, especially proton transfer systems such as in hydrogen-fuel cells.

*Berndt Jastorff* (University of Bremen) was unable to attend the meeting as scheduled and *J. Brennecke* (Notre Dame, USA) replaced him at very short notice, presenting the results of a diverse range of preliminary toxicological screening studies that have been conducted at Notre Dame. The first results indicate that, in common with all chemicals, the impact of any specific ionic liquid on a diverse eco-system is complex, and in some cases can appear contradictory. Notwithstanding this, it is encouraging

that studies are taking place, both from the industrial perspective aimed at registration (see earlier comments about joint data from BASF, Degussa, and Solvent Innovations) and at the academic level focused on understanding the mechanisms and modes of toxicity in order to understand and assess potential hazards associated with ionic liquids. One question remained however, even after discussions; how would choline-based ionic liquids fair in these tests, considering that this cation is already a required B vitamin and is used as a major food supplement in the poultry industry?

*Hiroyuki Ohno* (Tokyo, Japan) closed the congress in much the same way that *Rogers* opened it, by showing that ionic liquids do not necessarily behave in conventional ways, and highlighted a diverse range of materials under investigation by his group, including polymerisable ionic liquids, zwitterionic systems, acidic ionic liquids for catalysis and hydrogen-transfer, ionic liquids derived from amino acids and self-assembled ionic liquid crystalline salts. He once more issued the challenge for researchers to think beyond the confines of alternative solvents to develop new functional materials utilising the advanced tool-kit presented by ionic liquids. At the end of his talk, the emblem of COIL (see Fig. 2) was passed to him as COIL2 is to be held in Yokohama in 2007 (COIL3 in Australia 2009; COIL4 in Alabama 2011; COIL5 in Portugal 2013). We anticipate an even longer and larger meeting in Japan, but they will be challenged to match the trip



Fig. 2 The emblem of COIL.



**Fig. 3** Congress attendees on a trip to a salt mine.

an underlying theme to much of the meeting, with the recognition that the paradigm of green chemistry is not an inherent feature of any particular system, and in this way ionic liquids are not intrinsically green, but that their use can lead to the design of more efficient, less polluting and greener systems. Synthesis of ionic liquids, end-of-life disposal and toxicity (environmental impact) were strong features of the meeting. Ionic liquids can be designed to possess the properties desired, and tenability results in flexibility rather than compromise. They are what you want them to be!

**John D. Holbrey, Natalia V. Plechkova and Kenneth R. Seddon**

The QUILL Centre, The Queen's University of Belfast, Northern Ireland, UK. E-mail: [quill@qub.ac.uk](mailto:quill@qub.ac.uk)

to a salt mine for all who attended the Congress (see Fig. 3)!!

The marriage of ionic liquids and green chemistry, in its widest sense was

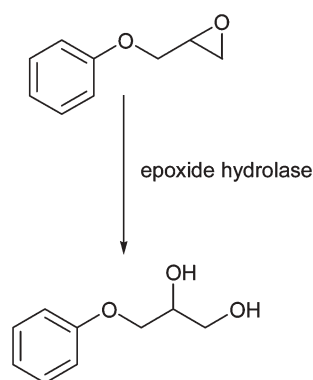
# Highlights

DOI: 10.1039/b605175h

Markus Hölscher reviews some of the recent literature in green chemistry

## Microchip based high speed combined catalysis and analysis

Technologically highly appealing, chemically highly efficient and moreover environmentally very friendly are microchip based synthetic and analytical procedures that are evolving presently from different laboratories. As microfluidic chips for reactions in microchannels and cavities are mainly designed to obtain high reaction and analysis rates their use also reduces the amount of chemical material needed substantially. Progress in recent years has been made both in the analytical and the synthesis sectors, but a combination of both synthesis of chemical compounds and subsequent analysis was not introduced to preparative chemistry. Very recently Belder *et al.* from the Max-Planck-Institut, Mülheim contributed to changing this situation by introducing a microchip based synthesis/analysis protocol.<sup>1</sup> As a model system the authors chose the hydrolytic kinetic separation of glycidyl phenyl ether which is catalyzed by epoxidehydrolase.



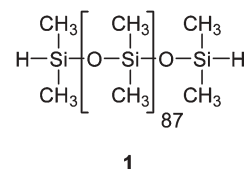
Substrate and catalyst are contained in micro vessels on the chip and are mixed by transferring them into a meander shaped canal allowing the reaction to proceed, the mixture is then transported into a separation channel in which it undergoes an electrophoresis, leading to the separation of the enantiomeric

reaction products from the substrate. Less than 90 s are needed for the whole separation process. Furthermore, it was shown that the microchip could successfully be used for testing the enantioselectivity of novel enzyme mutants from directed evolution. Purified enzymes could be used as efficiently as cell lysates and even complete cells. The data obtained with the microchip system were compared with data obtained with classical reactions on the laboratory scale followed by analysis of the supernatant with HPLC. Both enantioselectivities, *ee*, and selectivity factors, *E*, were shown to agree nicely in all five syntheses investigated. The study demonstrates the usefulness of the integrated synthesis/analysis approach on microchips, and leaves many possibilities for modifications which can increase the speed of the complete process even more.

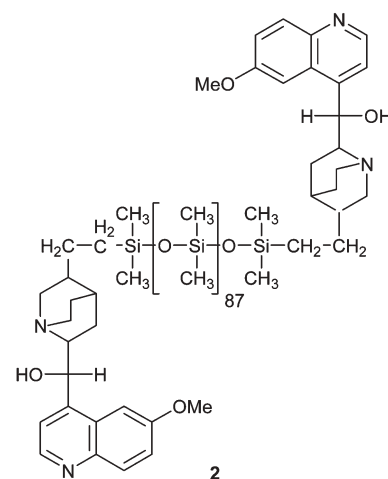
## Novel polysiloxane catalysts in liquid/liquid separable systems

Polymer supported catalysts are usually separated from the reaction mixture during work up by precipitation of the polymer or by membrane separation. As commercially available polysiloxanes can easily be modified due to the presence of silane groups, anchoring of appropriate catalysts to these polymers should generate active catalysts, and the excellent tunable solubility properties of polysiloxanes offer the potential to use them in liquid/liquid separation techniques after a homogeneous reaction. As an underlying principle in this approach thermomorphic solvent mixtures are used, which are biphasic at a certain temperature and monophasic at a different temperature. Bergbreiter *et al.* from Texas A&M University succeeded recently in developing such systems.<sup>2</sup> In a two step study the authors investigated the phase selective solubility of polysiloxanes such as **1**, which were labeled

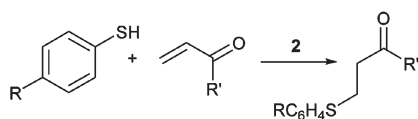
with an azo dye to simulate a catalyst and facilitate analysis.



In this first set of experiments it was shown that four different dye labeled polysiloxanes could be used efficiently in thermomorphic mixtures of heptane/DMF or heptane/EtOH. The heptane/DMF mixture is biphasic at room temperature and monophasic at elevated temperatures. Upon mixing a heptane solution of the polysiloxane with DMF and heating this mixture to 70 °C a monophasic mixture is obtained, which separates forming a biphasic system again upon cooling to 25 °C. High phase selective solubilities were obtained in a number of consecutive runs ranging between 97 and 99% for both solvent systems investigated. In a second set of experiments, the catalytic performance and recovery of a supported quinine catalyst, **2**, was tested.



The vinyl group of quinine was used for immobilisation on the polysiloxane and the resulting catalyst was used in Michael additions of thiols to  $\alpha,\beta$ -unsaturated ketones.



It was shown that in five consecutive cycles for five different reactions tested the product yield remained stable, indicating successful catalyst recovery during the separation process.

## Size and geometry affects catalytic properties of nanoparticles

Increasing attention is focusing on catalytic applications of nanoparticles. Dendrimer-encapsulated nanoparticles (DENs) can be synthesized with a high degree of control over size, composition and structure of the resulting nanoparticles, which makes them very useful for studies related to catalytic properties. Crooks *et al.* from the University of Texas at Austin, very recently reported on the catalytic performance of Pd nanoparticles in the hydrogenation of allylic alcohol.<sup>3</sup> DENs with different sizes ranging from 1.3 to 1.9 nm were synthesized (55 to 250 Pd atoms) and tested for catalytic hydrogenation activity, while care was taken to keep the molar amount of palladium constant for each experiment. As the activity increased with increasing particle size but constant number of Pd atoms present, the activity gain must be related to genuine particle characteristics. When the number of face, surface and defect atoms are compared it becomes clear that only the total number of face atoms increases with increasing particle size. In contrast, the number of surface atoms and defect atoms decreases as the total number of particles decreases. To rule out the potential dependence of the turn over frequency (TOF) on transport phenomena, catalyst solutions of one DEN were prepared with concentrations that span a representative concentration range. The results indicate the TOF to be independent of catalyst concentration, *i.e.* the activity gain with increasing particle size is not transport related

(at very low concentrations  $<0.4 \mu\text{M}$  this is different). As the electronic properties of nanoparticles change from metallic to insulating to molecule-like with decreasing particle size, the authors reasoned that a plot of the TOFs in relation to the number of face, surface and defect atoms together with the number of DENs should help rationalize the size influence. It was shown that the activity of particles with sizes between 1.5 and 1.9 nm mainly arises from the surface atoms. The activity of smaller particles seems to be more dominated by electronic effects than by the amount of surface atoms available. These findings might help in rational design of catalytic properties in the future.

## Design of hyperstable proteins by rationally destabilizing the unfolded state

The performance of protein pharmaceuticals and biocatalysts depends to a large extent on the stability of the protein. Among other factors, heat can lead to fast denaturation of proteins resulting in the loss of activity. Usually rational approaches to improve the stability of proteins focus on the native state. However, the balance between the unfolded and the folded state energetics play an important role for stabilization. Raleigh *et al.* from the State University of New York reasoned that instead of stabilizing the folded state a destabilization of the unfolded state also could lead to improved protein stabilities.<sup>4</sup> As a test case the N-terminal domain of the ribosomal protein L9 (NTL9) was chosen. The protein represents the ABC $\alpha$ D structural motif found in many proteins. Lysine-12 plays a vital role in electrostatic interactions of the unfolded state. Consequently a mutation to methionine should eliminate this interaction, and the mutation had already been shown to stabilize the folded state by  $1.9 \text{ kcal mol}^{-1}$ . As this mutation is specially designed for this protein, a second more generally applicable

mutation was subsequently introduced by changing a glycine to D-alanine and thus decreasing the entropy of the unfolded state, which has already been shown earlier to stabilize NTL-9 by  $1.87 \text{ kcal mol}^{-1}$ . The mutations did not alter the protein's structure significantly according to far-UV CD and 2D-NMR spectra. The stability of K12M-G34D-A-NTL9 was enhanced significantly by these mutations, as no complete melt under native conditions was observed. Furthermore the complete unfolding of the protein took place only upon heating to  $83 \text{ }^\circ\text{C}$  in 6 M urea, while the protein remained completely folded up to  $60 \text{ }^\circ\text{C}$ .

## 2006 Sustainability congress award for Henkel

Awarded for the second time by the Verein zur Förderung des Sustainability Gedankens e.V. (Association for the Support of Sustainability Concepts), Düsseldorf based home care and personal care producer Henkel obtained the award on March 15, 2006 during the second sustainability congress in Bonn. The prize is awarded to companies with a special focus on sustainability. The jury consisting of analysts and fund managers emphasized that Henkel had, for a long time, been following the underlying principle that economy, ecology and social enterprise have equal importance in all activities raised by the company. Henkel chief technology officer Gawrisch was pleased that the companies devotion to sustainability was appreciated by the jury, which puts a central focus on the longterm development of the value of companies.

## References

- 1 D. Belder, M. Ludwig, L.-W. Wang and M. T. Reetz, *Angew. Chem.*, 2006, **118**, 2523–2526.
- 2 M. A. Grunlan, K. R. Regan and D. E. Bergbreiter, *Chem. Commun.*, 2006, DOI: 10.1039/b601120a.
- 3 O. M. Wilson, M. R. Knecht, J. C. Garcia-Martinez and R. M. Crooks, *J. Am. Chem. Soc.*, 2006, DOI: 10.1021/ja058217m.
- 4 B. Anil, R. Craig-Schapiro and D. P. Raleigh, *J. Am. Chem. Soc.*, 2006, **128**, 3144–3145.



# Green chemistry and the health implications of nanoparticles

Matthew A. Albrecht, Cameron W. Evans and Colin L. Raston\*

Received 2nd December 2005, Accepted 3rd March 2006

First published as an Advance Article on the web 23rd March 2006

DOI: 10.1039/b517131h

Until recently the spectacular developments in nanotechnology have been with little regard to their potential effect on human health and the environment. There are no specific regulations on nanoparticles except existing regulations covering the same material in bulk form. Difficulties abound in devising such regulations, beyond self-imposed regulations by responsible companies, because of the likelihood of different properties exhibited by any one type of nanoparticle, which are tuneable by changing their size, shape and surface characteristics. Green chemistry metrics need to be incorporated into nanotechnologies at the source. This review scopes this issue in the context of potential health effects of nanoparticles, along with medical applications of nanoparticles including imaging, drug delivery, disinfection, and tissue repair. Nanoparticles can enter the human body through the lungs, the intestinal tract, and to a lesser extent the skin, and are likely to be a health issue, although the extent of effects on health are inconclusive. Nanoparticles can be modified to cross the brain blood barrier for medical applications, but this suggests other synthetic nanoparticles may unintentionally cross this barrier.

## Introduction

Nanotechnology (and nanoscience, the science leading to nanotechnology) can be defined in a number of ways. In general, however, it is regarded as the ability to manipulate, measure, manufacture and make predictions at the scale of 1–100 nm.<sup>1–3</sup> At the nanometer dimension, materials exhibit novel properties, different to those of both the isolated atom and bulk material, the properties depending largely on the size of the particles from which the material is made. Nanotechnology has not arisen from any one particular scientific discipline. Instead, it is interdisciplinary involving chemistry, physics, biology, and engineering,<sup>2</sup> and in recent times toxicology. Often the plural term, nanotechnologies, is

used because there are many areas and scientific disciplines involved.

Materials at the nanometer dimension are not new. They are common in nature, for example, life depends on many nano-scale objects, including proteins, enzymes and DNA, and nano-sized particles occur naturally in the atmosphere. Silver and gold nanoparticles have been used to colour ceramic glazes and stained glass since the 10th Century AD,<sup>4</sup> and possibly even the 4th Century.<sup>5</sup> Natural sources of nanoparticles include fires and volcanic eruptions. Biological examples include viruses, magnetite (found in cells and animals) and ferritin (a protein which stores excess iron in the body). Nevertheless exposure of humans to nanoparticles has increased dramatically over the last hundred years as a result of nanoparticles produced by simple combustion and other industrialisation processes. Internal combustion engines, power plants and welding fumes, for example, all release nanoparticles into the environment. Even frying or grilling food is a source of nanoparticles.<sup>6</sup>

School of Biomedical, Biomolecular and Chemical Sciences,  
The University of Western Australia, M313, Crawley, Australia 6009.  
E-mail: clraston@chem.uwa.edu.au; Fax: +618 6488 8683;  
Tel: +618 6488 3045



Matthew Albrecht

Matthew Albrecht was born and lives in Perth, Western Australia and has completed a BSc in chemistry and pharmacology at The University of Western Australia (2005). He is currently undertaking an Honours degree in pharmacology at the same institution, researching amphetamine addiction under the supervision of Associate Professor Mathew Martin-Iverson and Dr Kyle Dyer.



Cameron Evans

Cameron Evans was born in Auckland, New Zealand but he has lived in Perth, Western Australia for most of his life. He is a double degree candidate in science and engineering at The University of Western Australia, currently undertaking an Honours degree under the supervision of Professor Colin Raston and Dr Mohamed Makha. Other interests include music, art and computing.

There has been much hype associated with the applications of nanotechnology,<sup>7</sup> and what it can deliver in improving the quality of human life. Short- to medium-term benefits of nanotechnology include environmental pollution cleanup, better drug delivery mechanisms offering fewer side effects (for example more precise anticancer therapies), improvements in information technology, 'smart' fabrics which adjust to suit the temperature, self-cleaning window glass and more efficient chemical processes in industry. Some of these technologies have already been implemented. Longer-term futuristic applications may involve the design of additional 'smart' materials such as food packaging which changes colour when the 'use by' date of its contents expires, or a space-elevator concept being developed by NASA.

Nanotechnology is revolutionary and will impact on economies through new consumer products, and manufacturing methods and materials usage.<sup>2</sup> It will also impact on military technology. Investment in developing new nanotechnologies world-wide is several billion dollars per year, and data suggests that, in 2003, nanotechnology funding was generally equally divided between government and corporations.<sup>8</sup>

Nanotechnology is important in developing sustainable technologies for the future, for humanity and the environment.<sup>6,9</sup> However, care needs to be taken to ensure that nanotechnology is not creating future problems, as has been the case for many technologies of the twentieth century, for example, the dramatic reduction in ozone in the upper atmosphere by chlorofluorocarbons (CFCs). These so-called 'miracle' chemicals were banned from 'nonessential products' in the US in the early 1990s, many years after their detrimental effects were first noted.<sup>10</sup> Similarly, DDT entered widespread commercial use in the US in the late 1940s and was outlawed in 1972.<sup>11</sup> The use of lead in petrol, asbestos as a non-flammable building material, and polychlorinated biphenyls (PCBs) in electronics<sup>12</sup> have also led to environmental disasters. Such examples offer insight into the possible 'double-edged' nature of nanotechnology. Many groups (including the UK Health and Safety Executive) are concerned that possible health effects caused by nanotechnology will be significantly

delayed,<sup>13</sup> and the first detrimental effects, either to human health or the environment, will be noticed long after commercialisation.

It is important to differentiate between 'free' and 'fixed' nanoparticles. The former pose a more direct health threat because they are more difficult to contain, easily become airborne and can be inhaled. Another distinction is the difference between nanoparticles which have been designed intentionally for some purpose (often referred to as 'engineered'), and nanoparticles which are by-products, waste, or naturally-occurring.<sup>14</sup> In general, nanotechnology only deals with engineered particles. This review covers the health implications of both free and fixed nanoparticles, and also engineered, waste and biological nanomaterials.

Another way that nanotechnology can be defined is by differentiating between the production processes of 'top-down' and 'bottom-up'. Top-down refers to the fabrication of nanostructures by miniaturising present methods, such as machining and etching techniques. The other approach is bottom-up, sometimes labelled as molecular nanotechnology, whereby nano-sized objects are constructed from smaller units, even down to the manipulation of individual atoms.<sup>3</sup>

For the purpose of this review, nanotechnology is defined as nano-scale materials, structures and devices covering the transport of substances such as biological materials on nanoparticulate surfaces, the interactions of biological materials with nanotubes, and the direct effect of nano-sized materials on human health. Minimising the impact of nanoparticles on human health and the environment requires the implementation of green chemistry principles at the source. This includes minimising both waste and the use and generation of toxic materials. Issues relating to minimising the impact of nanotechnology on human health and the environment are summarised in Fig. 1, and are elaborated upon below.

## Types of nanomaterials

Nanostructures can be classified according to the number of dimensions at the nanometer level. Features at the nanometer level on a surface are one-dimensional, nanotubes have two nano-sized dimensions, and nanoparticles are nano-sized in all three dimensions. Nanoparticles can be engineered (intentional) or incidental/waste nanoparticles (unintentional), and are the most basic structure that can feature in nanotechnology. They can also be referred to as nanocrystals if they have



Colin Raston

*Professor Colin Raston is an Australian Research Council Professorial Fellow at The University of Western Australia, being appointed to the University in 2003. He completed a PhD under the guidance of Professor Allan White, and after postdoctoral studies with Professor Michael Lappert at the University of Sussex, he was appointed a Lecturer at The University of Western Australia (1981) then to the Chair of Chemistry at Griffith University (1988),*

*being awarded a DSc there in 1993, Monash University (1995) and Leeds (2001). His research interests cover aspects of nanochemistry and green chemistry.*

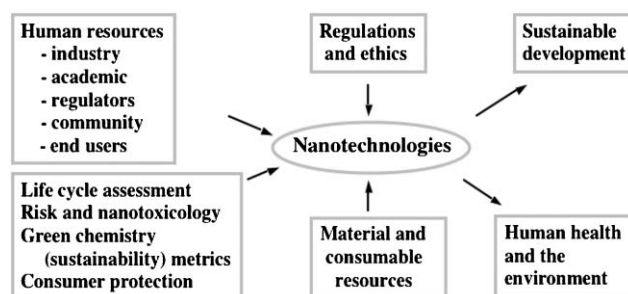


**Fig. 1** Key issues in dealing with the potential impact of nanotechnology on human health.

highly ordered crystalline structures, and as quantum dots (QDs) when such structures are semiconducting.<sup>2</sup>

Nanoparticles can be fixed in a matrix or free. This distinction is important because it directly affects human exposure. Free nanoparticles can enter and move within the human body, depending on the biological compatibility of the surface, whereas fixed nanoparticles are immobilised and thus cannot be inhaled.<sup>14</sup> Free nanoparticles can also be named as ultrafine particles which is principally a term used in toxicology.<sup>6</sup>

Engineered nanoparticulates cover a broad range of substances, including elemental metals, inorganic substances like titanium dioxide (TiO<sub>2</sub>), zinc sulfide (ZnS) and oxide (ZnO), and carbon-based fullerenes and their derivatives and composites. Metallic nanoparticles have been formed from a variety of elements including iron, nickel, zinc, titanium, gold, silver, palladium, iridium and platinum.<sup>15–18</sup> Such materials are sometimes used as catalysts, and the more inert metals are being studied for their use in medicine, for example in the thermal treatment therapy of tumours.<sup>19</sup>

Inorganic nanoparticles of TiO<sub>2</sub>, ZnS and ZnO have already entered the consumer market as sunscreens and cosmetic products. Nanocrystals of TiO<sub>2</sub>, an inorganic solid obtained from natural ores, have been found in the lungs of a 5300-year-old iceman, suggesting that such nanoparticles exist naturally in the atmosphere.<sup>20</sup> Examples of the material used in quantum dots include inorganic cadmium selenide and related materials.<sup>21–24</sup>

Fullerenes can be both engineered and unintentional nanoparticles. They are generated in combustion and cooking, and are the subject of intense research. Mitsubishi recently commissioned a plant to produce a few hundred tonnes of C<sub>60</sub> per year.<sup>25</sup> Incidental nanoparticles are formed as a result of combustion processes, including soot from diesel exhaust<sup>26</sup> and power generation, and the natural weathering of silicates and iron oxides.<sup>2</sup> Anthropogenic sources of nanoparticles have increased considerably over the last century with industrialisation.<sup>6</sup> Algae and plants are also capable of producing colloids of nanoparticles.<sup>27</sup> Nanoparticles also encompass nanorobots which are synthetic machines designed for a specific function.

Initially nanotubes were constructed only from carbon atoms, arranged in rolled-up, graphite-like sheets. They can be made from other light elements including boron and nitrogen,<sup>28,29</sup> and metal complexes. Carbon nanotubes (CNTs) are the most common type of nanotubes under current investigation, and come in two principal types, single-walled (SW) and multi-walled (MW). The latter can consist of up to thirty concentric tubes, and have diameters of up to 50 nm. SWCNTs generally have a diameter close to 1.4 nm.<sup>2</sup>

The length of nanotubes can be up to one thousand times their diameter, and they can form fibrous crystalline materials. For the purpose of toxicology, an analogy can be made to other fibres such as asbestos, which are sufficiently small to make their way deep into the lungs, where they can enter lung tissue cells. The long, thin geometry and insolubility of nanotubes may have the potential to cause effects similar to those arising from inhalation of asbestos fibres.<sup>30</sup> Such bio-persistent substances can remain in the lungs for decades, and can result in fibrosis (scarring of the lung tissue) and increase the risk of cancer.

Materials with engineered surfaces at the nanometer dimensions feature in many nanotechnologies. Such surfaces are used to prevent coagulation of 'naked' material, especially nanoparticles, and can alter the hydrophilic/hydrophobic balance of the underlying material for biological applications, for example, in preparing water repelling surfaces and delivery of material across the blood brain barrier (BBB).<sup>31,32</sup> The latter raises concerns about the entry of unintentional nanoparticles into the human body, and any associated toxicological effects.

## Applications of nanotechnology impacting on human health

The examples of nanotechnology discussed below are representative of current, developing and futuristic applications which relate to human health. For many applications the toxicology of the nanomaterial has not been addressed, although its importance is now being realised. The quantities of nanomaterials being generated range from multi-tonne carbon black production and fuming silica through to microgram quantities for speciality applications in biological imaging.<sup>33</sup>

### Device technology

(i) Programmed DNA that can hold molecule-size electronic devices, which may lead to devices that can replicate, and DNA machines with moving parts have potential as nanosensors, switches and tweezers.<sup>34,35</sup> (ii) Soft lithography techniques for moulding or printing nanopatterns on curved as well as flat surfaces.<sup>36</sup> (iii) CNT or other nano-scaled bars for mechanical quantum computers,<sup>37</sup> and nanocrystalline cylinders surrounded by silica as capacitors for storing data.<sup>38</sup> (iv) Less toxic batteries with rapid recharge capabilities.<sup>39</sup> (v) Photovoltaic cells for capturing infrared.<sup>40</sup> (vi) Optical/holographic tweezers for assembling nanocomputers from nanotubes, purifying drugs, performing non-invasive surgery, and creating spinning liquid vortices that can act as microscopic pumps.<sup>41</sup> (vii) Solar cell technology using less material with lower processing costs.<sup>42</sup>

### Medical

This comes under the realms of nanomedicine, as the application of nanotechnology for the treatment, diagnosis, monitoring, and control of biological systems.<sup>34</sup> Synthetic nanostructured biomaterials can be designed to self-assemble and create structures for tissue engineering, effectively mimicking biomineralization processes.<sup>43</sup> Self-assembled peptides can direct mineralisation of hydroxyapatite including formation of collagen fibrils which is of interest in mineralised tissue repair.<sup>44</sup> Light irradiation of gold-coated silica spheres trigger the release of heat that can destroy cancer cells.<sup>19,45–47</sup> Gold nanoparticles themselves inhibit the growth of blood vessels. Such growth is an important process in the growth of tumours.<sup>48</sup> Disinfection of surfaces is possible using UV photocatalytic oxidation with nanocrystalline TiO<sub>2</sub>.<sup>49,50</sup> Artificial mechanical red blood cells (respirocytes) are mimics for the oxygen and carbon dioxide transport function of red

blood cells. They can deliver 236 times more oxygen per unit volume than a natural red blood cell.<sup>51</sup> Adsorption of antibodies on assemblies of single wall carbon nanotubes (SWCNT) forms the basis of an amperometric immunosensor.<sup>52</sup> Functionalised CNTs are strong candidates for the delivery of drugs, antigens and genes, having been used as new platforms to detect antibodies associated with human autoimmune diseases with high specificity.<sup>53</sup> Modified carboxy-fullerene C<sub>60</sub> acts as a free radical scavenger, and can be used as a drug for a target activity on human cells of the immune system and their mitochondria, specifically for protection against apoptosis.<sup>54</sup> The parent fullerene C<sub>60</sub> and other derivatives have application as antioxidants against radical-induced biological processes.<sup>55</sup>

### Medical imaging

Superparamagnetic iron oxide nanoparticles feature in *in vivo* applications including magnetic resonance, tissue repair, detoxification of biological fluids, drug delivery, imaging contrast enhancement (see below), and the treatment of hypothermia.<sup>56,57</sup> Semiconducting QDs have a number of advantages over organic fluorophores for following cells *in vivo* at high resolutions.<sup>58,59</sup>

### Drug delivery

Drugs (or contrasting agents) can be trapped physically within the hydrophobic cores of micelles, or similarly trapped in the aqueous space or be intercalated into the lipid bilayer of liposomes, depending on the physicochemical characteristics of the drug. There are also nanospheres where the drug of interest is dissolved, entrapped, attached or encapsulated throughout or within a polymeric matrix.<sup>34</sup> Nanospheres loaded with antigen have possible applications in vaccine delivery.<sup>60</sup> Drug delivery across the BBB is possible using nanoparticles.<sup>31,32</sup> Natural polymers such as chitosan can be used for the delivery of anti-cancer drugs, genes and vaccines.<sup>61–64</sup> Chitosan-DNA nanoparticles can be used as gene carriers.<sup>62</sup> Nanoparticle aerosols are attractive for drug delivery because of their bioavailability in deep lung tissue and ease of delivery.<sup>57</sup> SWCNTs have potential in drug, antigen and gene delivery,<sup>53</sup> and functionalised SWCNTs with DNA attached can increase DNA uptake and gene expression more so than free DNA.<sup>53,65</sup>

### Food additives

There appears to be resistance to applications of nanotechnology in food, in contrast to applications in medicine. Antioxidant catalytic devices keep deep-frying oil fresh significantly longer, resulting in better taste, crispier fried foods, better consistency of product, lower costs and greater profits, with substantial benefits to health and the environment. There is a US patent and FDA approval.<sup>66</sup> Nano-based product packaging and nanodevices feature in tracking food origins and its freshness.<sup>67</sup> Novel carriers including nanomolecular capsules have been developed for nutraceuticals to be incorporated in food systems and cosmetics formulations, increasing the bioavailability of the product.<sup>68</sup>

### Molecular machines

A large research effort involves developing molecular machines based on molecules and macromolecules including DNA. They feature in the bottom up approach to nanotechnology, and incorporate molecular switches, logic gates, memory devices, photonic devices, non-linear optics, conducting wires, molecular magnets, and more.<sup>69</sup>

### Military

CNTs have high electrical conductivity, and plastic composites based on them could provide lightweight shielding material for electromagnetic radiation. Computers and electronic devices for battlefield command, control and communication need to be protected from weapons that emit electromagnetic pulses.<sup>5</sup> Smart materials may be able to change in response to their surroundings. Tiny computers embedded in materials could send signals to notify their status with the material changing colour on command, or generate electricity during the day and store it for later use. There is the prospect for coatings that stay clean and possibly the ability to heal themselves when damaged.<sup>70</sup> CNTs spun into fibres are undergoing rapid development, along with composite fibres containing the same material, having potential in body and vehicle armour through to transmission line cables to woven fabrics and textiles.<sup>71</sup>

### Chemical decomposition

Combustion-synthesized nanoparticles of TiO<sub>2</sub> are more effective than bulk commercial material for the catalytic photodecomposition of various organic compounds. The high catalytic activity of the nanoparticles is attributed to their high surface area and the density of the surface hydroxyl groups.<sup>72</sup> MgO nanoparticles adsorb and destroy various organophosphorus mimics of 'warfare agents' and can destroy fluorocarbons.<sup>73</sup> Exxon Mobil use mesoporous material with pores less than one nanometer to improve breakdown of large hydrocarbon molecules to form gasoline.<sup>74</sup> Conversion of polychlorobiphenyls (PCBs), organochlorine pesticides, and halogenated solvents to benign hydrocarbons (environmental decontamination) is possible using catalytic nanoparticles.<sup>75</sup>

### Metal decontamination

Recombinant DNA techniques are being used to protein engineer biopolymers with novel molecular arrangements and tuneable properties, with high affinity for the selective removal of toxic heavy metals such as cadmium, mercury and arsenic.<sup>76</sup> Poly(amidoamine) dendrimers have functional nitrogen groups which can act as chelating agents for binding toxic metal ions, electron transfer mediators, redox active metal clusters and metal clusters with catalytic properties.<sup>77</sup> Brushes have been developed for sweeping up nano-dust, painting microstructures, and cleaning up pollutants in water, for example, the soaking up of silver ions from contaminated water.<sup>78</sup>

### Regulatory bodies and legislation

There are new directives of the European Parliament restricting the use of certain hazardous substances in electrical and

electronic equipment,<sup>79</sup> including heavy metals such as mercury and cadmium. Chronic overexposure to cadmium may result in lung, liver and kidney damage, and cadmium and its compounds are carcinogenic to humans. Mercury is a bioaccumulative poison and targets the kidneys and brain. Chronic poisoning (mercurialism) causes depression of the central nervous system. A recent study revealed that cadmium selenide QDs release toxic cadmium ions and as such cannot be considered biocompatible.<sup>80</sup>

Food Standards Australia New Zealand (FSANZ) is the regulatory body responsible for protecting public health in Australia by maintaining a safe food supply. Procedures set in place require that 'all foods that have not traditionally been part of our diet' pass a pre-market safety assessment. FSANZ claims that improved knowledge pertaining to safety and nutrition is being applied to the latest and emerging developments, which in the future may include the use of nanoparticles in food products.<sup>81</sup> The US Food and Drug Administration (FDA) adopts a similar approach in the assessment of food safety in that pre-market assessments are required. It is dismissive of any risks posed by nanotechnology entering the food market and states that 'the existing battery of pharmacological tests is probably adequate' for the majority of products requiring regulation and that 'If the manufacturer makes no nanotechnology claims... FDA may be unaware at the time that the product is in the review and approval process that nanotechnology is being employed'. Furthermore, they make the claim that in the use of nanotechnology in food, 'size is not the issue'.<sup>82</sup> An independent study in the UK suggests that substances in nanoparticulate form should be considered independent of their bulk counterparts. Current UK regulation does not require any additional testing of a substance produced in nanoparticulate form. The report recommends that the 'regulatory gap' be addressed.<sup>27</sup>

Advances in nanotechnology are keeping ahead of regulatory bodies, with most legislation as of late 2004 making no differentiation between bulk materials and their nano-counterparts. This is a problem because separate tests for nanomaterials are not required if the bulk material is certified as safe. However, it is well documented that benign bulk substances can show significant toxicity at the nanometer level. The EC and EPA are now addressing this deficiency. The first International Symposium on Nanotechnology and Occupational Health, co-sponsored by the British Health and Safety Executive (HSE) and the US National Institute for Occupational Health, was held in October 2004.<sup>83</sup>

Current recommendations<sup>27,84</sup> call for: (i) Treating nanoparticles and nanotubes as hazardous substances. (ii) Assessing the risks posed by the release of nanoparticles during the product lifecycle. (iii) Studying the toxicity, bioaccumulation and epidemiology of the products of nanotechnology as a preventative measure.

In the UK the Control of Substances to Health Regulations (2002) require assessment of risk and suitable controls to be put in place for any substance. However, nano-featured materials do not qualify as new materials. There are clearly significant gaps in nanotechnology—nomenclature, measurement of exposure, when a nanomaterial is considered new, the difference in the effect of a nanoparticle of one size relative to

another, test data that is required, whether new toxicology models are needed, and the level of exposure that will cause harm.<sup>83</sup> Other issues on the agenda include:<sup>83</sup> (i) The toxicological epidemiological hazards posed by nanoparticles reflecting exposure levels likely to be encountered in industry. (ii) Hazard testing is likely to take several years to complete and a cautionary approach needs to be adopted in handling nanoparticles. (iii) It is unclear how exposure limits will be established for nanoparticles, and how this can be achieved. (iv) New standards for testing and guaranteeing suitable filtration of nanoparticles may be required.

If regulators, industry and the public get it right there is a bright future.<sup>83</sup> There are many potential benefits to society (medical, devices, *etc.*), potential for growth in public confidence in science and industry, and it could lead to intrinsically safer products at the design stage, and sustainable growth. Moreover, the availability of data on environmental effects of nanotechnology could go a long way towards building community trust.<sup>3</sup>

The National Science Foundation (NSF) has identified 'Nanoscale Processes in the Environment' and 'Societal and Educational Implications of Nanotechnology' as two of the main research and education themes in 2000. The EPA has had an annual program on nanotechnology and the environment since 2002, focusing on manufactured nanoparticles including QDs, CNTs, and TiO<sub>2</sub>.

The US EPA has identified a number of critical risk assessment issues regarding the manufacture of nanoparticles including: (i) Exposure assessment. (ii) Toxicology of the nanoparticles. (iii) Extrapolating the nanoparticle toxicity from existing particle and fibre toxicological databases. (iv) Environmental and biological fate, transport, persistence, and transformation of nanoparticles. (v) Recyclability and overall sustainability of the nanoparticles.<sup>85</sup>

The EU has dedicated projects on risk assessment dealing with nanosafe risk assessment, nanopathologies (nanoparticles in biomaterial-induced pathologies), and nanoderm (skin as the barrier to ultra fine particles).

Several organisations are calling for moratoriums or total bans on the development of nanotechnology. Notably, since mid-2002 the Action Group on Erosion, Technology and Concentration (ETC) has called for a moratorium on the use of synthetic nanoparticles in the laboratory and in any new commercial products until governments adopt 'best practices' for research.<sup>86</sup>

Since it is the novel properties that are being exploited, nanomaterials need to be treated as 'new' compounds and this should be reflected in the legislation. In the last five years nanotoxicology has come to the fore, but there are no specific regulations covering the manufacture, transport and use of nanomaterials, despite the well known change in properties of materials at the nanometer level, and variable properties, depending on the actual size of the nanostructures.

## Sustainability and nanotechnology

Nanotechnology is an integral part of getting the planet onto a sustainable trajectory with all the benefits of current technology, based on smaller products which use less energy to run,

less energy and materials to build, and incorporate the potential for recycling. Nanotechnology also includes the development of renewable energy sources such as solar energy and fuel cells. The implementation of science and technology in general is necessary to make the shift towards sustainability and a zero waste society.<sup>9</sup>

Sustainable development can be defined as ‘the ability to meet the needs of the current generation while preserving the ability of future generations to meet their needs’.<sup>87</sup> Sustainability is an ethical issue (see below) since it relates to the needs of the present and future generations.<sup>88</sup> The UN Commission on Environment and Development reported that sustainable development requires the provision of basic needs, and the opportunity to improve quality of life. This definition encompasses all of the global population.<sup>87</sup> Therefore, sustainable development can be interpreted as an ethical responsibility—in particular, to those who currently enjoy high standards of living. An evaluation of the sustainability of nanotechnology in this global sense is necessary, since there is the possibility of downstream health implications. In the *Western Australian State Sustainability Strategy*, sustainability has been described as the ability to meet these needs through environmental protection, social advancement and economic prosperity.<sup>88</sup>

## Ethical issues

In all risk analyses carried out in nanotechnology, social, ethical and cultural issues need to be considered. This is especially true in medical applications, where the ethics of any new drug or procedure must be investigated. However, it is difficult to define what is acceptable in any new technology.

In relation to human health, industry has the most impact. It is important that in developing new nanotechnology, corporations act in the best public interest, ideally being self-regulating. Ignorance of important ethical considerations is still an issue in society. For example, asbestos is still used with global producers of the material continuing aggressive marketing operations to export their product to developing countries.<sup>89</sup>

Nanotechnology could be used to enhance sections of the community creating an ‘elite’ class division. This ‘performance enhancement’, which might include the use of artificial red blood cells, in medical applications, or extend to the improvement of physical or mental capacity, and could eventually lead to a situation where the elite are chosen for employment which challenges individual choice.

The ‘digital divide’ has already been established—the gap that exists between those who have technology, and those who do not. For example, the users of the internet account for 6% of the world population, with 85% of these users living in developed countries.<sup>90</sup> The development of a similar ‘nano divide’ is anticipated. The risk is that resources and expertise will all be applied to developed-world ‘market opportunities’ and not towards critical applications such as the purification of drinking water, renewable energy and gels preventing the spread of HIV/AIDS in developing countries, and more.<sup>91</sup>

The development of nanosensors could result in a decrease in privacy. For example, as new tests are developed, there is

the possibility that genetic disposition to a particular condition could be measured. Health insurance companies might then require that such vulnerabilities be tested—and thus the individual in question may learn that they will develop a life-compromising condition in the future. This raises issues pertaining to the individual’s right to confidentiality and quality of life.

Negative coverage of nanotechnology in the media includes the so called ‘grey goo’, whereby nano-sized robots replicate out of control, ultimately resulting in the formation of untreatable waste and hence destruction of the planet. The concept of ‘grey goo’ was conceived by Eric Drexler in 1986<sup>92</sup> and was endorsed in 2000 in an article by Bill Joy,<sup>93</sup> revisited in science fiction literature,<sup>94</sup> and again brought to light in 2003 when Prince Charles expressed concern over nanotechnology and requested that a study into nanotechnology health effects be undertaken.<sup>95</sup> The ensuing study, by the Royal Society and the Royal Academy of Engineering, reported that the ‘grey goo’ concept is unrealistic and that ‘the complete details of operation of even a simple cell are far beyond our understanding’. The general consensus among the scientific community is that the concept of ‘grey goo’ belongs in the realms of science fiction.<sup>1,95–98</sup> Indeed, in 2004, Drexler published a paper acknowledging that self-replication was not necessary for nanomanufacture.<sup>98</sup> He is quoted as saying, ‘I wish I had never used the term ‘grey goo... Researchers resent it and I want to clean up the mess’.<sup>99</sup> Nevertheless, the scepticism of authors about nanotechnology abound which is highlighted by a publication in 2002 by Crichton, ‘Prey’, which describes an experiment that went wrong with a cloud of nanorobots escaping and becoming self sustaining and self replicating.<sup>94</sup>

## Green chemistry metrics

Nanotechnology needs to address the principle of green chemistry and associated metrics.<sup>100</sup> These are summarised in Fig. 2. Examples of nanotechnology considerations in the context of green chemistry are developed below.

### 1. Preventing the generation of waste

Advances in drug delivery include overcoming insolubility issues, uneven distribution throughout the body and poor selectivity, healthy tissue damage and drug toxicity,<sup>58,101</sup> thereby reducing the amount of drug to be administered with less going to waste in the body. There is also the need for minimising the generation of waste during the production of nanomaterials.

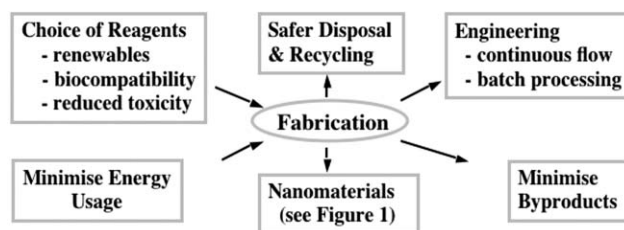


Fig. 2 Green chemistry considerations in preparing nanomaterials.

## 2. Atom economy

Bottom-up nanotechnology can be intrinsically more atom efficient since products can be built atom-by-atom, or molecule-by-molecule, in self-repairing assembly processes, and without generating waste.

## 3. Less hazardous chemical syntheses

The release of fine dust including nanoparticles into the air should be avoided through appropriate preventative measures including the packaging and transport of the nanoparticles under a liquid.

## 4. Designing safer materials

Often the novel properties of nanomaterials are employed to replace a less efficient mechanism which may induce adverse effects. Drug delivery is one example where safety is improved by nanotechnology, helping to reduce side effects.<sup>102</sup>

## 5. Safer solvents and auxiliaries

There are already emerging examples of green syntheses of nanoparticles.<sup>93</sup>

## 6. Design for energy efficiency

The manufacture of nano-sized systems can require less energy than is used in traditional systems, for example in the fabrication of nanoparticles by self-assembly involving inherently weak interactions.

## 7. Use of renewable feedstocks

Carbon forms the basis of many nanoparticulates (including carbon black, fullerenes and nanotubes) and can be obtained from renewable biomass, an important issue at least for large volume nanomaterials such as composite fibres.

## 8. Reduce the use of derivatives

Bottom-up self assembly processes do not require the use of protection/deprotection and associated techniques used in traditional organic chemistry.

## 9. Catalysis

Nanoparticles of catalysts can enhance the selectivity of reactions,<sup>15,103</sup> which reduces the amount of energy required to initiate a reaction, and the reaction can be effected at lower temperature. This is important because energy considerations are often the most important issue in environmental and economic analysis.<sup>100</sup>

## 10. Design for degradation

Nanoparticles can be designed to degrade to innocuous products. Drug delivery applications, for example, require that the nanoparticles are broken down within the body. Nanoparticles released into the environment for decontamination must decompose to benign products. Iron nanoparticles have been shown to be useful in treating the estimated 15 000–25 000 US sites contaminated by halogenated organic

compounds. Here, the iron particles form rust, which is almost impossible to differentiate from that naturally found in the environment.<sup>18,104</sup>

## 11. Real-time analysis for pollution prevention

This involves the use of chemical processes using nanoparticles as catalysts for example, to monitor chemical reactors, to ensure excess energy is not used and that by-products are not formed.

## 12. Inherently safer chemistry

This relates to the manufacture of nanomaterials and their applications.

A full life-cycle assessment (LCA) is needed before nanotechnology is integrated into society. LCA is defined as: 'An objective process to evaluate the environmental burdens associated with a product, process, or activity by identifying energy and materials used and wastes released to the environment, being used to evaluate and implement opportunities for environmental improvements.'<sup>105</sup> Particularly, wastes released into the environment are of concern, since the size of airborne particulates released from the handling of nanoparticles affects their toxicity.<sup>20</sup> Issues relating to toxicity of nanoparticles are summarised in Fig. 3.

Clearly ethical issues are important in nanotechnology. There are serious implications in advantaging/disadvantaging sectors of the community in consumer products, IT, and privacy. There is also a duty of care at the manufacturing stage, to incorporate sustainability metrics into the nanotechnology, with a full LCA before the technology is incorporated into consumer products.

## Nanoparticles and human health

Nanoparticles can enter the human body in several ways; (i) *via* the lungs where a rapid translocation through the blood stream to vital organs is possible, including crossing the BBB, and absorption by (ii) the intestinal tract, or (iii) the skin.<sup>33</sup> Biocompatibility of the material is important. Noble metals such as gold, platinum and palladium are very biocompatible, silver is moderately biocompatible, and titanium is biocompatible being widely used in implants.<sup>106</sup> Single crystal silicon is not biocompatible. Luminescent semiconducting QDs are biocompatible but they often contain toxic arsenic or cadmium.<sup>106</sup> Exceptions are the indium gallium phosphide (InGaP) QDs produced by Evident Technologies.<sup>107</sup>

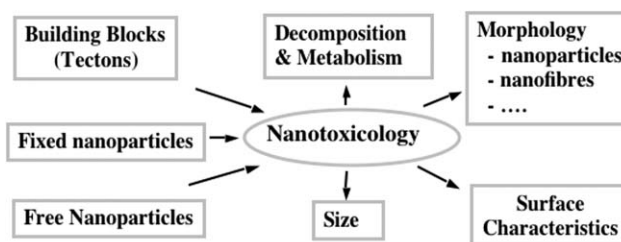


Fig. 3 Key nanotoxicology issues relating to the nature of the particles.

Spheroidal like nanoparticles <100 nm deposit in the alveolar area of the lungs. The same is true of small diameter nano-fibres. The lungs can clear spheroidal nanoparticles, the retention half life being  $\sim 70$  days as long as the clearance mechanism is not affected by the particles themselves. Fibres, on the other hand, can stay in the lungs for years with the increased risk of developing lung cancer. Intestinal uptake of nanoparticles is better understood than uptake in the lungs and skin uptake, and is of importance in designing nanoparticles for drug delivery and stabilising food. There appears to be no information on the damage or irritation to the skin caused by fibres <100 nm.<sup>31</sup>

Key issues on whether nanoparticles can enter the human body, beyond the lungs for airborne nanoparticles, are the nature of the surface and size of the nanomaterial, and the point of entry. After entry the nature of the surface becomes dominant in whether the nanoparticles are toxic. Radicals formed on the surface of nanoparticles have toxicological consequences, for example, the cytotoxicity of silica correlates with the appearance of surface radicals and reactive oxygen species, and these are thought to play a key role in the development of fibrosis and lung cancer by this material.<sup>31</sup> Other compounds including ZnO and TiO<sub>2</sub> nanoparticles in sunscreen may behave similarly, and may have an adverse effect on the underlying skin.

TiO<sub>2</sub> nanoparticles catalyse DNA damage.<sup>106</sup> Fullerene C<sub>60</sub> is a singlet oxygen generating agent, and this also presents potential health risks.<sup>106</sup> Molecular components of nanoparticles are likely to have aromatic ring systems which have the size and shape to interact with DNA, and thus have the potential to promote cancer.<sup>106</sup> Toxicity of nanomaterials relates directly to the nature of the surfaces—functionality and charge, including induced charge. All this is an integral part of nanotoxicology, the safety evaluation of engineered nanostructures and devices.<sup>6</sup> For nanotoxicology to arrive at an appropriate risk assessment an interdisciplinary approach is required, also covering research in materials science, medicine, molecular biology, bioinformatics, and more.<sup>6</sup> This comes at a time when occupational and public exposure to engineered nanoparticles is dramatically increasing.<sup>85</sup>

### Transport of substances on nanoparticulate surfaces

Very little is known about the transport of substances on nanoparticulate surfaces but it will clearly depend on the nature of the surfaces. Airborne nanoparticles with surface bound substances can enter the body, and nanoparticles that contain mutagenic substances, which remain in the lungs for years, increase the risk of developing cancer.<sup>33</sup>

For cells to be able to react to any topography they must be able to sense shape. Strong responses from cells to nanotopography have been seen even though the dimensions of these shapes are much smaller than the dimensions of the cells.<sup>108</sup>

CNTs can easily enter into cells which is the basis for some concern,<sup>53</sup> and this relates to the way DNA can wrap around the nanotubes. The cellular response of murine fibroblasts to nano-scale silica topography has been investigated. The cells become rounded and do not replicate. When they are placed back onto a regular surface, their activity returns to normal,

spreading out and proliferating.<sup>109</sup> This result nicely demonstrates surface effects on living cells.

How small a feature can a cell sense? The interplay of cells with material at the nanometer level has been demonstrated by looking at different pit sizes on silicon substrates (35, 75 and 120 nm). Human fibroblasts placed on these surfaces interact with pits of all sizes although the response for 35 nm pits is weak. Thus cells are sensitive to surface features at the nanometer scale, and designing materials with nanoscale features need to take this into account.<sup>108</sup>

In developing sensors that use biological detecting components, care must be taken in immobilization of the detector molecules so that they preserve their shape and function and hence original recognition specificity. To do this the surface needs to be pre-coated to allow sufficiently strong binding of detector molecules and sufficiently weak and gentle perturbations so that the molecules retain their shape and functionality.<sup>110</sup>

Surfaces of nanoparticles of zirconia can undergo reversible adsorption–desorption of DNA depending on the pH of the solutions, with basic solutions resulting in desorption.<sup>111</sup> This relates to a change in charge on the surface of the zirconia particles.

Surface topography at the nano- and micrometer range of titanium devices critically determines cellular attachment and subsequent biological function. There is an increase of cell attachment to micron and sub-micron patterned surfaces in comparison to smooth surfaces which is attributed to pores acting as positive attachment sites.<sup>112</sup>

Cell migration, proliferation and differentiated function are dependent on adhesion, and cell adhesion is enhanced by a high surface to volume ratio in nano-fibrous scaffolds. Synthetic nano-fibrous scaffolds which can mimic collagen feature in tissue engineering and have the benefit of overcoming possible immunogenicity and disease transmission problems.<sup>113</sup>

Creating nano-featured surfaces is important in the biocompatibility of artificial material. Silicon-based surfaces are prone to fouling in the presence of biological fluids, but this can be overcome by grafting PEG (polyethylene glycol) of various densities on silicon. The decrease in protein adsorption on PEG surfaces is due to its hydrophilicity and ability to shield the surface from direct contact from proteins and charged particles.<sup>114</sup>

Chitosan is a polysaccharide which is biocompatible and does not cause allergic reactions, breaking down to harmless products which are easily removed. Chitosan-based nanoparticulate drug delivery systems have the advantages of improved efficacy, reduced toxicity and improved patient compliance over standard preparations. This is a form of green chemistry in nanotechnology—utilising a renewable resource which is non-toxic.

### Interactions of biological materials with nanotubes

This covers carbon based nanotubes and those of other elements, binary systems and more complex systems. Little is known on the effects of exposure of nanotubes to biological environments and the release of the entrapped particles, and



how this will affect the body, and the general principles of fibre toxicology as applied to nanofibres need to be determined.<sup>6</sup>

The health hazard of nanotubes depends on the nature of the material, how easily they can become airborne, the size of the clumps or aggregates of the material, and the ability to deaggregate to form smaller particles following entry to the lungs. A further hazard is created by the presence of other small particles or metal catalysts embedded in the tubes (which may be a consequence of the method of fabrication of the tubes as in the synthesis of CNTs).<sup>115</sup>

Entry into biological systems by means other than respiration can occur *via* (i) supramolecular complexation where the nanotubes are wrapped up by material involving non-covalent interactions, or (ii) by covalent functionalisation where polar groups are attached to the surface of the material. In this way CNTs bearing water solubilising peptide groups have been shown to cross the cell membrane and to accumulate in the cytoplasm or reach the nucleus without being toxic to the cell.<sup>116</sup>

As a comparison, graphite is biocompatible with cells, and graphite-coated plastic valves *in vivo* show little or no blood clotting. This has led to the development of artificial heart valves and dental implants comprised of carbon fibre reinforced carbon composites.<sup>117</sup>

CNTs have been reported to be harmful to living organisms.<sup>118–120</sup> They come in varying lengths and a study of 220 nm and 825 nm long CNTs showed no severe inflammatory response, although the degree of inflammation was larger for the longer nanotubes. This suggests that macrophages can envelop the shorter nanotubes more readily. Thus longer nanotubes may pose more of a health issue than shorter ones.

Single walled carbon nanotubes (SWCNT) can inhibit the proliferation of cells. They induce a signal inside a cell and the nucleus, resulting in decrease of cell adhesion, causing the cell to detach, float and shrink in size. Cells have a self protection response, secreting proteins to wrap the nanotubes into nodular structures, which isolate the cells attached to the CNTs from other cells.<sup>121</sup>

Unfunctionalised multiwalled carbon nanotubes (MWCNTs) are capable for both localising within and initiating an irritation response in human cells, but there is no information as to whether MWCNTs structures are an occupational risk.<sup>122</sup>

A study involving mice showed that, for equal masses in the lungs, CNTs can be more toxic than quartz (a form of silica), which is known to cause silicosis following chronic exposure.<sup>123</sup> However, a study by the National Institute for Occupational Safety and Health (NIOSH) revealed that with normal handling, the amount of fine particulate matter released into the air is minimal.<sup>115</sup> Hence, although nanotubes are expected to show considerable pulmonary toxicity, fine material which can be inhaled is unlikely to be generated through normal handling.

The hierarchy of *in vitro* cytotoxicity of carbon nanomaterials (and quartz) follow a sequence of order based on mass: SWCNT > MWCNT (10–20 nm diameter) > quartz > C<sub>60</sub>. Profound toxicity of SWCNT is observed after a six hour exposure with a 35% increase in cytotoxicity when the dosage of SWCNT is 11.3  $\mu\text{g cm}^{-2}$ . In comparison there is no

significant toxicity for spheroidal C<sub>60</sub>, up to a dose of 226.0  $\mu\text{g cm}^{-2}$ .<sup>124</sup> Thus cytotoxicity depends on the different geometric shapes of carbon nanomaterials.<sup>124</sup>

SWCNTs induce dose dependent epithelioid granulomas and interstitial inflammation in mice. Carbon black treated mice are normal and quartz treated mice have mild to moderate inflammation.<sup>123</sup> On an equal weight basis, if SWCNTs reach the lungs, they are much more toxic than carbon black, and can be more toxic than quartz, which is a serious health hazard in chronic inhalation exposures.

Functionalised CNTs by themselves are not toxic, but they can help transport other molecules that are cytotoxic into cells.<sup>125</sup> A SWCNT-biotin conjugate causes extensive cell death. Nanotubes non-specifically associate with hydrophobic regions of the cell surface and internalize by endocytosis, and accumulate in the cytoplasm in the cells. DNA can wrap around CNTs and this is the basis of a method for separating different size CNTs. At the same time it raises concerns over the entry of CNTs into the human body.<sup>33</sup>

Studies in animal models revealed that mesothelioma could be induced by asbestos and other related fibres < ~0.25–1.5 microns in diameter and > ~4–8 microns in length, regardless of composition.<sup>106</sup>

### Effect of nano-sized systems on human health

Nanoparticles have high surface area per unit mass and can have different effects on human health relative to bulk material from which they are made. Increased biological activity can be beneficial (*e.g.* antioxidant activity, carrier capacity for therapeutics, penetration of cellular barrier for drug delivery), detrimental (toxic, induction of oxidative stress or of cellular dysfunction) or a mix of both.<sup>6</sup> There is inadequate information available as to the possible adverse effects of nanoparticles through either intentional or unintentional exposure. Nevertheless, the safety analysis of nanotechnology, especially nanoparticles, is of utmost priority given the expected worldwide use and the probability of exposure. There are currently no standards on the toxicology of nanoparticles.

Several sources of environmental contamination with nanoparticles have been identified: in mass production, spillage during handling and transport, and from the washing off of consumer products like sunscreens and cosmetics. Furthermore, the use of nanoparticles in filters and other disposable materials may be a source of environmental contamination through landfill.<sup>6</sup>

### Detrimental aspects of nanotechnology

Inadvertent contact with nanoparticles can occur *via* the skin, lungs or intestinal tract. Nanoparticles may induce undesirable genetic changes as a side effect of their presence in the human body—mutagenicity. Carcinogenicity associated with nanorobots will depend on the nature of the surface, and the limited results thus far are guardedly optimistic.<sup>106</sup>

Nanoparticles are a constituent of air pollution and result from combustion. When made from insoluble, non-toxic materials, they induce a greater inflammatory response than (larger) fine particles composed of the same material. A possible explanation for this observation is that ultrafine

particles can hinder the body's cell-level defences against inhaled particles in the lungs.<sup>126</sup> Epidemiological studies have shown that an increase in airborne particulates in urban areas result in adverse health effects in the population, especially in susceptible groups.<sup>127</sup> As a specific example, ultra-fine (20 nm) nickel has a much more toxic effect on the lungs than fine (5  $\mu\text{m}$ ) particles.<sup>16</sup>

Although it has been shown that nanoparticles can penetrate the skin, this method of entry is of less significance than through the lungs or intestinal tract, since the skin acts predominantly as a barrier and does not allow material exchange. Particles 500–1000 nm in size, theoretically beyond the realms of nanotechnology, can penetrate and reach the lower levels of human skin,<sup>128</sup> and smaller particles are likely to move deeper into the skin. Despite this penetration there is no direct evidence of particles entering the circulation through the skin.<sup>33</sup> Thus, adverse effects resulting from skin contact seem to be of less importance. However, some small fibres (like fibreglass) have the potential to cause mechanical skin irritation, although this is not an allergic or chemical response.

The lungs constitute the most likely entry route for nanoparticles, and can facilitate the spread of nanoparticles to other organs. The distribution of nanoparticles in the body is essentially dependent on size and other physical and chemical properties. Very small biopersistent particles, including silica dust, asbestos fibres and also diesel exhaust (non-engineered nanoparticles) in the lungs can result in significant physiological damage.<sup>33</sup> Inhaled nanoparticles have the potential to aggravate existing airway conditions, like asthma or bronchitis,<sup>127</sup> and there is a close association between particulate air pollution and cardiovascular adverse effects such as myocardial infarction.<sup>129</sup>

Studies in rats show that it is possible for nanoparticles to cross the BBB *via* the olfactory nerve.<sup>120</sup> This mechanism shows promise in drug delivery but unintentional exposure to nanoparticles with this capability could pose a health risk.

Spheroidal nano-sized particles entering the lungs can be cleared as long as the clearance mechanism is not affected by the nanoparticles or any other cause.<sup>130</sup> Nanoparticles are likely to hamper such clearance. In the case of nano-fibres their clearance will depend on the length of the fibres. Bio-persistent types of asbestos, where breakage occurs longitudinally, result in more fibres of the same length but smaller diameter. Amorphous fibres break perpendicular to their long axis, resulting in fibres that can be engulfed by the macrophages in the lungs and are therefore less persistent and less toxic.

In addition to size of nanoparticles, their charge and surface chemistry is important for the material entering the lungs. Not only is the charge density important, but so is the distribution of charge over the particles. However, more studies are required.<sup>33</sup> Regardless of the surface chemistry, particles entering the lungs will be submersed into the lining layer, and any reactive groups will modify the biological effects. Surface modification of silica results in a great decrease in toxicity, with the appearance of surface radicals for 'naked' silica particles considered the key event in the development of fibrosis and lung cancer by this material. Thus it appears that reactive groups on nanoparticles influence their interaction

with the lungs, and ultimately it may be possible to predict the reactivity of nano-surfaces in the lungs,<sup>32</sup> and elsewhere.

The first toxicological studies on CNTs indicate that they can be a risk for human health, while exposure assessment indicates that these materials are probably not inhaled.<sup>131</sup>

Translocation of nanoparticles from the lungs towards other organs can occur. For example, inhalation experiments with rats, using <sup>13</sup>C labelled particles, showed that nano-sized particles (25 nm) are present in several organs 24 h after exposure.<sup>33</sup> Studies on the role of factors governing translocation of nanoparticles, including exposure, dose, size and surface chemistry and time course, is limited.<sup>33</sup>

Engineered nanoparticles can be taken up *via* the intestinal tract, and this is better understood and studied in more detail than pulmonary (lung) and skin uptake.

Nanoparticles designed to stabilise food or to deliver drugs *via* intestinal uptake need to satisfy more demanding rules before the products can be marketed. QDs and other 'throw away' nanodevices may become a class of nano-biodegradable pollutants for which there is little understanding of their effect on human health and the environment.<sup>3</sup>

### Beneficial aspects of nanotechnology

This is essentially covered above with an additional aspect of drug delivery being the ability of nanoparticles to cross the BBB *via* the olfactory nerve, and this has clear benefits, but it implies that unintended passage of nanoparticles across the BBB is possible which is a concern. Toxicity evaluation of nanoparticles is critical for all materials entering the human body, including nanoparticles in food technology.

Biodegradable polymers have been used in cardiac tissue engineering, the function of which can be modulated by the nature of the nano- and micro-textured surfaces.<sup>132</sup>

QD's in biological systems are not completely innocuous, but a safe concentration range likely exists in which they can complete their task without major interference.<sup>133</sup>

Overall, entry of nanoparticles into the human body depends on the nature of the surface (functionality and charge), size of the nanoparticles, and point of entry—lungs, intestinal or skin. The lungs can clear spheroidal nanoparticles but fibres can stay in the lungs for years with the risk of developing lung cancer. Once inside the body the nature of the surface determines whether the particles have beneficial or detrimental effects, and nanoparticles can be engineered to move across the BBB. Nanoparticles may induce undesirable genetic changes and the onset of cancers. Others may be benign, with application in drug delivery and imaging, and tissue engineering.

### Status of nanotechnology relating to human health

#### Toxicity

Research into the toxicity of nanoparticles has, in the past, been largely uncoordinated. Recent articles highlight the need for a systematic approach to studying this important aspect of nanotechnology<sup>1,6,27</sup> and additionally, the need for a regulatory framework for the protection of workers exposed to nanoparticles during their production.<sup>30</sup>

Nanotoxicology is now an established discipline having evolved from studies on nanoparticles, where it is well known that such particles cause morbidity and mortality in susceptible populations.<sup>6</sup> In comparison, there is a paucity of data for human or environmental exposure levels of nanoparticles.<sup>6</sup> There are significant differences between nanoparticles and larger particles in terms of their deposition and clearance from the respiratory system. Nanoparticles, in contrast to larger particles, move throughout the body and can reach other organs.<sup>6</sup>

In a study on the effect of nanotubes on rats, aggregation of the nanotubes results in blockage of the airway and suffocation, rather than effects of the nanoparticles themselves entering the lungs.<sup>6</sup> While the most prevalent mechanism for solid particle clearance is by macrophages in the alveoli of the lungs,<sup>6</sup> it cannot be assumed that all nanoparticles will follow expected clearance mechanisms due to their small size.<sup>6</sup> During the life-cycle of a product it is likely that nanomaterials will enter the environment. The stability of coatings on nanoparticles therefore need to be investigated both *in vivo* and in the environment.<sup>6</sup> A significant factor in risk assessment is the likelihood of exposure—which has been shown to be negligible with due care in handling procedures.<sup>6,115</sup>

The National Institute for Occupational Health and Safety (NIOSH) is conducting a five-year study into the toxicity and health risks associated with occupational exposure to nanoparticles addressing the following health issues:<sup>19</sup>

- (i) The ability of unrefined carbon nanotubes to release airborne particulates during handling.
- (ii) Pulmonary toxicity of carbon nanotube particles.
- (iii) Surface activity of inhaled particles.
- (iv) Nanoparticle exposure in the workplace and an evaluation of the risks involved.

Carcinogenicity of nanorobot building materials has barely begun. This includes looking at non-leaching surfaces.<sup>106</sup>

The so-called 'Nanoderm' project funded by the European Commission is based on the understanding that there is a lot of exposure in the population to nanoparticles (<20 nm). Outcomes of the project include quantitative information on the penetration of nanoparticles, health implications of such, assessment of the risk for such particles, and strategies pertaining to their risk and better information reaching the consumer.<sup>134</sup>

Many polluted sites have been injected with nanoparticles as part of environmental remediation programs, however, the safety of this practice has not yet been evaluated.<sup>6</sup>

### Benign nanotechnology

The US Environmental Protection Agency (EPA) is interested primarily in the environmental aspects of the health implications of nanotechnology. It has a program to develop 'green' nanotechnology.<sup>135</sup> Examples of the applications of the research being undertaken include the synthesis of nanoparticles for the treatment of groundwater, nanosensors used to detect the presence of heavy metals, and the treatment of exhaust from vehicles.

Silver nanoparticles have been synthesised using a totally green method. The use of water as an 'environmentally benign

solvent' and sugars ( $\beta$ -D-glucose as a non-toxic reducing agent, and starch as a stabilising agent) illustrate the opportunity for the possible implementation of benign solvents and reagents in the synthesis of nanoparticles.<sup>92</sup>

Little development in the field is being specifically targeted towards sustainability. This is a problem because the opportunity to develop green processes from the beginning is not being taken. The transformation to sustainable development is an enormous economic opportunity.<sup>136</sup> Moreover, past achievement aimed at being able to watch the next generation prosper has come *via* terribly destructive methods. What is needed now is redevelopment—a paradigm shift in the approaches in providing energy, technology and agriculture. Clearly if nanotechnology is to be the key to the future, it should be developed with sustainability in mind from the outset, Fig. 1.

Benign nanoparticles are in cosmetic products including TiO<sub>2</sub>. Anatase TiO<sub>2</sub> (10 and 20 nm) particles induce oxidative stress in human bronchial epithelial cells without photoactivation, noting that oxidative stress is implicated in aging, atherosclerosis, carcinogenesis and inflammatory disorders. The larger particles (>200 nm) do not have the same effect, and it therefore seems that the smaller the particle the easier it is to induce oxidative damage. This suggests that ultrafine anatase TiO<sub>2</sub> particles, intratracheally, could cause an inflammatory response, whereas TiO<sub>2</sub> particles larger than 100 nm are classified as benign in humans and animals.<sup>138</sup> Rutile TiO<sub>2</sub> (200 nm) particles induce hydrogen peroxide and oxidative damage in the absence of light.

Kertész *et al.* observed nanoparticles penetrating into the corneocyte layers of stratum corneum with no particles in the cytoplasm of the granular cells.<sup>138</sup>

Schulz *et al.* found that surface characteristics, particle size or shape of micronised pigments result in the dermal absorption of the substance. TiO<sub>2</sub> is only observed in the outer surface of the stratum corneum and has not been detected in deeper layers, the epidermis and dermis. The results highlight the safe use of micro-fine TiO<sub>2</sub> for topical application to humans.<sup>139</sup>

Nanoscale particles of PVC, TiO<sub>2</sub>, SiO<sub>2</sub> and cobalt metal (Co) are taken up into human endothelial cells. Only exposure of HDMECs (human dermal microvascular endothelial cells) to Co particles leads to enlargement of vacuoles, and HDMECs exposed to Co, SiO<sub>2</sub> and TiO<sub>2</sub> nanoparticles induce pro-inflammatory effects. Co and SiO<sub>2</sub> particles produce a larger effect than TiO<sub>2</sub> particles. The inflammatory lung disease caused by SiO<sub>2</sub> particles might share a common mechanism with that shown by the endothelial cells.<sup>149</sup>

### Toxicological analysis

Most nano-products can be designed in such a way as to either increase or decrease toxicity depending on the desired outcome. For treatment in drug delivery, minimising toxicity of the carrier is necessary and in most cases this can be done. On the other hand for chemotherapeutic agents, toxicity is designed to be magnified and targeted to specific tissues or areas. Altering the coating of many of these therapeutic agents can increase selectivity and toxicity.

Care must also be taken in the profiling of the pharmacokinetics and release of the products. The nanoparticle may be designed for human consumption knowing that it will stay intact in the body. If afterwards, the coating designed to alleviate toxicity is broken down, what are the ensuing products once released from the body and exposed to a different environment?

Increasing concentrations of mercapto-undecanoic acid (MUA) QDs show a decrease in cell viability in Vero cells (African green monkey's kidney cell), HeLa cells and human primary hepatocyte cells. The Vero cells are affected less than the others. Four to six hours incubation in the presence of the QDs resulted in cell death. There is a range of concentrations for QDs where cell viability can decrease without cell death.<sup>140</sup>

When QDs remain intact, toxicity is dependent on the surface presented to the cell rather than what is in the core. A MUA coated QD is toxic when treated for twelve hours at 100  $\mu\text{g mL}^{-1}$  and above, with DNA damage observed after two hours treatment at a dose of 50  $\mu\text{g mL}^{-1}$  and above. Cysteamine coated QDs induce some DNA damage when treated for twelve hours, the other coatings showing little to no signs of toxicity.<sup>141</sup>

Toxicity of QDs is also associated with oxidation of the surface of the nanoparticles. This leads to reduced cadmium on the surface deteriorating the CdSe lattice, releasing free  $\text{Cd}^{2+}$  which then results in cell death. The toxicity can be modified by altering the QD coating; mercaptoacetic acid (MAA) renders CdSe QDs non-toxic and coating with ZnS and bovine serum albumin molecules reduce toxicity.<sup>21</sup>

Water soluble CdSe/ZnS QDs induce DNA damage in the presence of UV light and to a lesser extent DNA damage in the absence of UV. This nicking of DNA is attributed to free radicals that are both photo-generated and surface oxide generated. Formation of radicals can be avoided by doping the lattice with  $\text{Mn}^{2+}$  ions to hold charge carriers in the internal structure.<sup>22</sup>

Michalet *et al.* found that most of the papers on QDs used *in vivo* and *in vitro* did not find any notable adverse effects arising from QDs at labelling concentrations, while the  $\text{Se}^{2-}$  and  $\text{Cd}^{2+}$  ions are released from the QDs and so they are not completely without risk but can be used effectively within a safe range.<sup>133</sup>

In another study, pathogenic bacteria *S. aureus* were found to extract  $\text{Se}^{2-}$  and  $\text{Cd}^{2+}$  ions from CdSe QDs. The extraction is dependent on the surface conjugation; holotransferrin conjugates show a significant increase in the amount of  $\text{Se}^{2-}$  ions inside the cytoplasm compared to the original QDs and mercaptoacetic acid coated QDs.<sup>23</sup>

Studies on the injection of QDs into the blood stream of pigs and mice show no toxicity. Even for QDs loaded in cells growing *in vitro*, there is no toxicity evident after two weeks.<sup>24</sup> Nano-sized selenium is less toxic than selenite and high selenium protein that is administered to rats.<sup>142</sup>

Inhaled nanoparticles are of great concern, since the most likely accidental contact with nanoparticles occurs through the lungs.<sup>33</sup> The effect of environmental factors in the development of Parkinson's disease has become increasingly apparent, and the high exposure to airborne particulates in urban areas is a cause for concern.<sup>26</sup> Suitable industrial hygiene should be

maintained to minimise exposure during the manufacture of carbon nanotubes.<sup>143</sup>

The onset of pathogenic effects generally requires the achievement of a sufficient lung burden.<sup>33</sup> When inhaled, nanoparticles are deposited in all regions of the respiratory tract.<sup>6</sup> Numerous studies have found that for equal masses, nanoparticles exert a more marked effect in the detriment to respiratory function, compared with 'normal' sized particles.<sup>4,20</sup> There are significant differences between nanoparticles and larger entities during deposition and clearance in the respiratory tract.<sup>6</sup> In the case of nanoparticles, the most prevalent mechanism for clearance is phagocytosis by macrophages.<sup>6</sup>

A study of the pulmonary toxicity of carbon nanotubes in mice showed they could be more toxic than quartz which is known to cause significant health problems after chronic exposure.<sup>123</sup>

Although nanoparticles often form larger clusters, such airborne aggregates can disintegrate in the lungs and this might result in increased toxicity.<sup>20</sup> With normal handling of carbon nanotube material, the concentration of splinters in the air is minimal.<sup>115</sup>

The majority of *in vivo* studies into the pulmonary toxicity of nanoparticles has been conducted in rodents, but it is known that rats are especially sensitive when it comes to adverse lung responses.<sup>144</sup> In addition, all *in vivo* studies use instillation into the trachea (as a mass of particles) out of necessity.<sup>27</sup> Intratracheal instillation of nanoparticles may cause oxidative stress which can lead to atherosclerosis, carcinogenesis or acute or chronic inflammatory disorders.<sup>137</sup> A thorough inhalation study still remains to be undertaken to investigate the respirability of nanoparticles,<sup>143</sup> that is, their ability to pass beyond the airways and move to the low-level structures of the lungs.<sup>144</sup>

Normal-sized  $\text{TiO}_2$  is classified as biologically inert although more research is warranted.<sup>137</sup> The 'precautionary principle' should be applied to nanoparticle toxicity.<sup>143</sup> Conclusions about the toxicity of nanoparticles cannot be made until the reaction of lung tissue to these particles is established.<sup>145</sup> Such a response may take many years to develop.<sup>13</sup>

Diesel exhaust contains nanoparticles which have been linked to inflammation and oxidative stress in the lungs and cardiovascular system.<sup>26</sup> Inhalation of diesel particles may result in the formation of reactive oxygen species.<sup>26</sup> Another substance with this ability is  $\text{TiO}_2$ , which can absorb UV light and produce various oxygen-containing, reactive species in solution.<sup>137</sup> Reactive oxygen species are known to attack lipids and proteins and have been implicated in carcinogenesis.<sup>137</sup> A hypothesis has been suggested that smaller particles have a higher potency in inducing oxidative stress in the absence of photoactivation.<sup>137</sup>

Long fibres (greater than 20 microns—easily achieved by carbon nanotubes) in lungs are not cleared effectively.<sup>33</sup> At the alveolar level, these long fibres result in 'frustrated' phagocytosis or the attempt by multiple macrophages to ingest the particle. This results in an inflammatory response and leads to scarring of lung tissue (fibrosis).<sup>144</sup> At this stage, it remains unknown whether the asbestos mechanism of toxicity is relevant to carbon nanotubes.<sup>144</sup>

If MWCNTs reach the lungs, they are biopersistent, and induce lung inflammation and fibrosis.<sup>143</sup> However, short term tests *in vitro* fail to accurately model the breakdown of nanomaterials in the lungs.<sup>144</sup> Thus, a false positive result may be obtained when a substance is, in fact, non-persistent in the lungs.

Rat tracheal explants have been used to examine how nanoparticles interact with cells in the lungs.<sup>146</sup> Nanoparticulates persist as aggregates but larger particle aggregates get smaller over time. It is hard to tell if the inflammatory response is caused by the smaller-sized nanoparticles, or just the large number of particles administered.

Donaldson *et al.* have shown a very clear distinction between normal and nano-sized particles. Ultrafine TiO<sub>2</sub> (20 nm) and 500 nm particles induce free radical activity and break the strands of super-coiled plasmid DNA, but the ultrafine TiO<sub>2</sub> results in complete destruction of DNA. Some of the damage caused by TiO<sub>2</sub> particles can be alleviated in the presence of mannitol, which shows that hydroxyl free radicals are involved. Free radical activity is also detected on the surface of asbestos fibres, environmental particles, ceramic fibres and glass fibres.<sup>147</sup>

Ingested nanoparticles: Gold nanoparticles are being studied for use as transfection vectors, DNA-binding agents, protein inhibitors and spectroscopic markers. Cationic gold nanoparticles (quaternary ammonium terminal groups) increase vesicle lysis while anionic (carboxyl terminal groups) are relatively harmless. The cationic particles presumably have a strong electrostatic interaction with the negatively charged cell membrane.<sup>148</sup>

Two fullerene C<sub>60</sub> derivatives, a dendritic C<sub>60</sub> mono-adduct and a malonic acid C<sub>60</sub> tris-adduct, have been tested for cell growth and viability on Jurkat cells (human T-lymphocytes). The dendritic mono-adduct inhibits cell growth (over two weeks it decreased to 19%) but has no effect on cell vitality, while the tris-malonic acid adduct has little effect on either. Growth inhibition arising from the dendritic C<sub>60</sub> is reversible; the same cells grown without the fullerene resume normal growth. The tris-malonic (TMA) acid fullerene is more phototoxic than the dendritic derivative. The two different fullerenes possibly interact with the cell membrane in different ways. The dendritic adduct has very large branches, while the tris-malonic adduct is more compact, the branches keeping the C<sub>60</sub> away from the cell. Also the dendrofullerene molecules aggregate lowering the interaction with cell membranes.<sup>149</sup>

Foley *et al.* have demonstrated that a fullerene derivative (C<sub>60</sub>(CO<sub>2</sub>H)<sub>2</sub>) could cross the cell membrane and be localized preferentially in compartments within the cell. This is thought to strengthen the case for using fullerenes for drug delivery.<sup>150</sup>

Three C<sub>60</sub> fullerene derivatives, namely (i) di-malonic acid, DMA, (ii) TMA, and (iii) tetra-malonic acid (QMA) C<sub>60</sub>, have been tested on HeLa cells to determine growth inhibition. The cytotoxicity of these fullerenes is dose and irradiation dependent with the hierarchy of toxicity DMA > TMA > QMA. Mannitol, which is able to prevent hydroxyl radical damage, does not prevent the damage induced by the C<sub>60</sub> compounds.<sup>151</sup>

Fullerene C<sub>60</sub> forms stable nano-aggregates 25–500 nm, which are also stable in ionic solutions for months. There is a

need, therefore, to study the properties of such nanoparticles – which are likely to be different from bulk C<sub>60</sub>.<sup>152</sup>

Less-derivatised, less-soluble forms of C<sub>60</sub> are the most toxic to HDF (human dermal fibroblasts) and HepG2 (human liver carcinoma) cells. They cause oxidative damage to cell membranes which can lead to cell death, yet with a notable lack of damage to DNA, proteins and mitochondria. In water C<sub>60</sub> aggregates and can form superoxide anions that seem to be the most likely cause of membrane damage. More soluble derivatives of C<sub>60</sub> like C<sub>60</sub>(OH)<sub>24</sub> and Na<sup>+</sup><sub>2-3</sub>[C<sub>60</sub>O<sub>7-9</sub>(OH)<sub>12-15</sub>]<sup>(2-3)-</sup> are much less toxic (C<sub>60</sub> is toxic at 0.020 ppm compared to C<sub>60</sub>(OH)<sub>24</sub> at >5000 ppm which is limited by its solubility). Given the differential cytotoxicity, strategies can be developed for increasing toxicity to target bacteria or cancer and minimised for safety in other applications.<sup>153</sup>

Exposure of juvenile largemouth bass fish to C<sub>60</sub> resulted in lipid peroxidation in their brains after 48 h of exposure to 0.5 ppm of uncoated C<sub>60</sub>. This is the first study to show the oxidative effects of fullerenes *in vivo*. The fullerenes also keep the water clearer, possibly owing to its anti-bacterial effects.<sup>154</sup>

Huang *et al.* found that chitosan toxicity depends chiefly on the degree of deacetylation. Decreasing the degree of deacetylation increases cell viability. Turning chitosan into nanoparticles does not influence the toxicity but it increases its endocytosis, and molecular weight has little effect on the toxicity.<sup>62</sup>

Super paramagnetic iron oxide nanoparticles (SPIONs) have been modified with a pullulan coating. This has the desired result of reducing toxicity and increasing cellular uptake compared with uncoated SPIONs. Uncoated SPIONs are toxic (determined by cytotoxicity and adhesion studies) and their internalisation results in disruption of the cytoskeletal organisation in human dermal fibroblasts. The difference in toxicity may be due to the pullulan coating being hydrophilic which protects the surfaces from interacting with biological materials. These coatings may add additional specificity for magnetic nanoparticles in drug delivery.<sup>155</sup>

## Conclusions

A study commissioned by the Royal Society and the Royal Academy of Engineering in the UK in 2003 found that most nanotechnology poses no new health or safety risks.<sup>7</sup> However, it highlighted uncertainties on the potential effects on human health and the environment of manufactured nanoparticles and nanotubes if they are free and not incorporated into a material. It is impossible to assess the toxicity of nanoparticles by testing the material in bulk form.

The concern over nanotechnology being the ‘the next GMT’ appears to be ill founded,<sup>7</sup> but there needs to be care in bringing any nanotechnology to the marketplace. Much needs to be done in establishing toxicity thresholds and measuring exposures in the work place and the environment. Finally it would be prudent to examine and address environmental and human health concerns before the widespread adoption of specific nanotechnologies,<sup>6</sup> and to incorporate green chemistry metrics into the production and distribution of nanoparticles.

## Acknowledgements

Support of this by DSTO Australia is graciously acknowledged.

## References

- 1 K. Donaldson and V. Stone, *Commun. ACM*, 2004, **47**, 113–115.
- 2 T. Masciangioli and W. Zhang, *Environ. Sci. Technol.*, 2003, **37**, 102A–108A.
- 3 *Future Technologies, Today's Choices*, Greenpeace UK, 2003, <http://www.greenpeace.ork.uk/contentlookup.cfm?ucidparam=2003072113521&menupoint=\A-L>.
- 4 A. P. Dowling, *Mater. Today*, 2004, **7**, 30–35.
- 5 *Introduction to Nanotechnology*, ed. C. P. Poole and F. J. Owens, Wiley, Hoboken, New Jersey, 2003.
- 6 G. Oberdörster, E. Oberdörster and J. Oberdörster, *Environ. Health Perspect.*, 2005, **113**, 823–839.
- 7 A. Dowling, *New Sci.*, 2005, 19.
- 8 Nano Investment, *Technol. Rev.*, 2005, **108**, 20.
- 9 P. T. Anastas, *Green Chem.*, 2003, **5**, G29–G34.
- 10 Regulatory History of CFCs and Other Stratospheric Ozone Depleting Chemicals (to 1993)—Press Release 1993, Environmental Protection Agency (EPA), Washington DC, 2005, <http://www.epa.gov/history/topics/ozone/03.htm>.
- 11 DDT Ban Takes Effect—Press Release 1972, Environmental Protection Agency (EPA), Washington DC, 2005, <http://www.epa.gov/history/topics/ddt/01.htm>.
- 12 EPA Bans PCB Manufacture; Phases Out Uses—Press Release 1979, Environmental Protection Agency (EPA), Washington DC, 2005, <http://www.epa.gov/history/topics/pcbs/01.htm>.
- 13 P. Davies, Managing the Risks from Nanotechnology, Health and Safety Executive, UK, 2004, <http://www.hse.gov.uk/aboutus/hsc/meetings/2004/060404/c42.pdf>.
- 14 Nanotechnologies: A Preliminary Risk Analysis on the Basis of a Workshop Organized in Brussels on 1–2 March 2004 by the Health and Consumer Protection Directorate General of the European Commission, European Community, 2004, [http://europa.eu.int/comm/health/ph\\_risk/events\\_risk\\_en.htm](http://europa.eu.int/comm/health/ph_risk/events_risk_en.htm).
- 15 S. Özkar and R. G. Finke, *J. Am. Chem. Soc.*, 2005, **127**, 4800–4808.
- 16 Q. Zhang, Y. Kusaka, X. Zhu, K. Sato, Y. Mo, T. Kluz and K. Donaldson, *J. Occup. Health*, 2003, **45**, 23–30.
- 17 E. E. Connor, J. Mwamuka, A. Gole, C. J. Murphy and M. D. Wyatt, *Small*, 2005, **1**, 325–327.
- 18 C.-B. Wang and W.-X. Zhang, *Environ. Sci. Technol.*, 1997, **31**, 2145–2156.
- 19 L. R. Hirsch, R. J. Stafford, J. A. Bankson, S. R. Sershen, B. Rivera, R. E. Price, J. D. Hazle, N. J. Halas and J. L. West, *Proc. Natl. Acad. Sci. U. S. A.*, 2003, **100**, 13549–13554.
- 20 L. E. Murr, E. V. Esquivel and J. J. Bang, *J. Mater. Sci.: Mater. Med.*, 2004, **15**, 237–247.
- 21 A. M. Derfus, W. C. W. Chan and S. N. Bhatia, *Nano Lett.*, 2004, **4**, 11–18.
- 22 M. Green and E. Howman, *Chem. Commun.*, 2005, 121–123.
- 23 J. A. Kloepfer, R. E. Mielke, M. S. Wong, K. H. Nealson, G. Stucky and J. L. Nadeau, *Appl. Environ. Microbiol.*, 2003, **69**, 4205–4213.
- 24 J. K. Jaiswal and S. M. Simon, *Trends Cell Biol.*, 2004, **14**, 497–504.
- 25 Fullerenes by the Ton: Mitsubishi's Frontier Carbon Opens 40 metric ton/year fullerene plant using TDA reactors and technology, *Chem. Eng. News*, August 11, 2003.
- 26 M. L. Block, X. Wu, Z. Pei, G. Li, T. Wang, L. Qin, B. Wilson, J. Yang, J. S. Hong and B. Veronesi, *Fed. Am. Soc. Exp. Biol. J.*, 2004, **18**, 1618–1620.
- 27 Nanoscience and nanotechnologies: Opportunities and uncertainties, The Royal Society & The Royal Academy of Engineering, 2004, <http://www.nanotec.org.uk/finalreport.htm>.
- 28 N. G. Chopra, R. J. Luyken, K. Cherrey, V. H. Crespi, M. L. Cohen, S. G. Louie and A. Zettl, *Science*, 1995, **269**, 966–967.
- 29 Y. Zhang, K. Suenaga, C. Colliex and S. Iijima, *Science*, 1998, **281**, 973–975.
- 30 A. Seaton and K. Donaldson, *Lancet*, 2005, **365**, 923–924.
- 31 J. Kreuter, P. Ränge, V. Petrov, S. Hamm, S. E. Gelperina, B. Engelhardt, R. Alyautdin, H. Briesen and D. J. Begley, *Pharm. Res.*, 2003, **20**, 409–416.
- 32 R. N. Alyautdin, V. E. Petrov, K. Langer, A. Berthold, D. A. Kharkevich and J. Kreuter, *Pharm. Res.*, 1997, **14**, 325–328.
- 33 P. H. M. Hoet, I. Brüske-Hohlfeld and O. V. Salata, *J. Nanobiotechnol.*, 2004, **2**.
- 34 S. M. Moghimi, A. C. Hunter and J. C. Murray, *Fed. Am. Soc. Exp. Biol. J.*, 2005, **19**, 311–327.
- 35 Y. Liu, C. Lin, H. Li and H. Yan, *Angew. Chem., Int. Ed.*, 2005, **44**, 4333–4338.
- 36 W. W. Wayt, *Sci. Am.*, 1999, 281/1.
- 37 C. Q. Choi, *Sci. Am.*, 2005, 292/2.
- 38 G. Stix, *Sci. Am.*, 2004, 290/3.
- 39 D. Graham-Rowe, *New Sci.*, 2005, 7 March.
- 40 S. A. McDonald, G. Konstantatos, S. Zhang, P. W. Cyr, E. J. D. Klem, L. Levina and E. H. Sargent, *Nat. Mater.*, 2005, **4**, 138–142.
- 41 G. Stix, *Sci. Am.*, 2003, 289/2.
- 42 P. J. Sebastian and S. A. Gamboa, *Sol. Energy Mater. Sol. Cells*, 2005, **88**, 129–130.
- 43 W. L. Murphy and D. J. Mooney, *Nat. Biotechnol.*, 2002, **20**, 30–31.
- 44 J. D. Hartgerink, E. Beniash and S. I. Stupp, *Science*, 2001, **294**, 1684–1688.
- 45 C. Lok, *Technol. Rev.*, 2004, **107**, 81.
- 46 A. Goho, *Sci. News*, 2003, **164**, 381–382.
- 47 Nanoshells for cancer therapy, *Mater. Today*, 2003, **6**, 6.
- 48 Nano-drug may starve tumours, *New Sci.*, 2004, **184**, 17.
- 49 K. P. Kühn, I. F. Chaberny, K. Massholder, M. Stickler, V. W. Benz, H. Sonntag and L. Erdinger, *Chemosphere*, 2003, **53**, 71–77.
- 50 J. C. Yu, W. Ho, J. Yu, H. Yip, P. K. Wong and J. Zhao, *Environ. Sci. Technol.*, 2005, **39**, 1175–1179.
- 51 K. Bogunia-Kubik and M. Sugisaka, *BioSystems*, 2002, **65**, 123–138.
- 52 M. O'Connor, S. N. Kim, A. J. Killard, R. J. Dorster, M. R. Smyth, F. Papadimitrakopoulos and J. D. Rusling, *Analyst*, 2004, **129**, 1176–1180.
- 53 A. Bianco, K. Kostarelos, C. D. Partidos and M. Prato, *Chem. Commun.*, 2005, 571–577.
- 54 D. Monti, L. Moretti, S. Salvioli, E. Straface, W. Malorni, R. Pellicciari, G. Schettini, M. Bisaglia, C. Pincelli, C. Fumelli, M. Bonafè and C. Franceschi, *Biochem. Biophys. Res. Commun.*, 2000, **277**, 711–717.
- 55 C. Wang, L. A. Tai, D. D. Lee, P. P. Kanakamma, C. K. F. Shen, T. Luh, C. H. Cheng and K. C. Hwang, *J. Med. Chem.*, 1999, **42**, 4616–4620.
- 56 A. J. Gupta and M. Gupta, *Biomaterials*, 2005, **26**, 3995–4021.
- 57 D. A. LaVan, T. McGuire and R. Langer, *Nat. Biotechnol.*, 2003, **10**, 1184–1191.
- 58 E. B. Voura, J. K. Jaiswal, H. Mattoussi and S. M. Simon, *Nature Med.*, 2004, **10**, 993–998.
- 59 B. Ballou, B. C. Lagergölm, L. A. Ernst, M. P. Bruchez and A. S. Waggoner, *Bioconjugate Chem.*, 2004, **15**, 79–86.
- 60 J. E. Eyles, V. W. Bramwell, J. Singh, E. D. Williamson and H. O. Alpar, *J. Controlled Release*, 2003, **86**, 25–32.
- 61 M. Huang, E. Khor and L. Lim, *Pharm. Res.*, 2004, **21**, 344–353.
- 62 H.-Q. Mao, K. Roy, V. L. Troung-Le, K. A. Janes, K. Y. Lin, Y. Wang, J. T. August and K. W. Leong, *J. Controlled Release*, 2001, **70**, 399–421.
- 63 K. A. Janes, M. P. Fresneau, A. Marazuela, A. Fabra and M. L. Alonso, *J. Controlled Release*, 2001, **73**, 255–267.
- 64 S. A. Agnihotri, N. N. Mallikarjuna and T. M. Aminabhavi, *J. Controlled Release*, 2004, **100**, 5–28.
- 65 D. Pantarotto, R. Singh, D. McCarthy, M. Erhardt, J.-P. Briand, M. Prato, K. Kostarelos and A. Bianco, *Angew. Chem., Int. Ed.*, 2004, **43**, 5242–5246.
- 66 OilFresh®1000, antioxidant catalytic device, OilFresh Corporation, 2005, <http://www.oilfresh.com/of1000.html>.
- 67 Kraft, AtomWorks, 2005, <http://atomworks.org/Companies/kraft/kraft>.
- 68 Nutralease Ltd., Israeli Life Science Industry, 2005, [http://www.ilsi.org/il/companies\\_life\\_science\\_company.asp?ID=545](http://www.ilsi.org/il/companies_life_science_company.asp?ID=545).

- 69 J. D. Badji, V. Balzani, A. Credi, S. Silvi and J. F. Stoddart, *Science*, 2004, **303**, 1845–1849.
- 70 The nanotechnology page, University of Technology, Sydney: Institute for nanoscale research <http://www.nano.uts.edu.au/nano.html>.
- 71 Buckytube properties and uses, Carbon Nanotechnologies Incorporated, Houston Texas, [http://www.cnanotech.com/pages/buckytube\\_properties\\_uses/buckytube\\_uses/5-2-8\\_fibers\\_fabrics.html](http://www.cnanotech.com/pages/buckytube_properties_uses/buckytube_uses/5-2-8_fibers_fabrics.html).
- 72 K. Nagaveni, G. Sivalingam, M. S. Hegde and G. Madras, *Environ. Sci. Technol.*, 2004, **38**, 1600–1604.
- 73 E. M. Lucasa and K. J. Klabunde, *Nanostruct. Mater.*, 1999, **12**, 179–182.
- 74 J. Zink, University of South Florida Magazine, 2002, [http://www.usf.edu/hpic\\_entry.html](http://www.usf.edu/hpic_entry.html).
- 75 W.-X. Zhang, C.-B. Wang and H.-L. Lien, *Catal. Today*, 1998, **40**, 387–395.
- 76 W. Chen, M. Matsumoto and A. Mulchandani, *EPA grant number-R829606*, 2002–2005.
- 77 M. S. Diallo, L. Balogh and W. A. Goddard, *EPA grant number-R829626*, 2002–2005.
- 78 R. Pease, *BBC News*, 2005, 22 June.
- 79 Directive 2002/95/EC of the European Parliament and of the Council, *Official Journal of the European Union*, 2003, **37**, 19–23.
- 80 C. Kirchner, T. Liedl, S. Kudera, T. Pellegrino, A. M. Javier, H. E. Gaub, S. Stözl, N. Fertig and W. J. Parak, *Nano Lett.*, 2005, **5**, 331–338.
- 81 Food Standards Australia New Zealand, 2000, <http://www.foodstandards.gov.au>.
- 82 FDA Regulation of Nanotechnology Products, <http://www.fda.gov/nanotechnology/regulation.html>.
- 83 D. Mark, Nanomaterials. A risk to health at work? Proceedings of the 1st International Symposium on Occupational Health Implications of Nanomaterials, 2004.
- 84 P. H. M. Hoet, A. Nemmar and B. Nemery, *Nat. Biotechnol.*, 2004, **22**, 19.
- 85 K. L. Dreher, *Toxicol. Sci.*, 2004, **11**, 3–5.
- 86 Nanotech: Unpredictable and Un-Regulated, ETC Group, 2004, <http://etcgroup.org/article.asp?newsid=469>.
- 87 Our Common Future: Report of the World Commission on Environment and Development (“The Brundtland Report”), United Nations, 1987.
- 88 Hope for the future: The Western Australian State Sustainability Strategy, Department of the Premier and Cabinet, Perth, 2003, <http://www.sustainability.dpc.wa.gov.au/>.
- 89 L. Kazan-Allen, *Lung Cancer*, 2005, **49**, S3–S9.
- 90 S. S. Rao, *Telemat. Inform.*, 2005, **22**, 361–375.
- 91 M. H. A. Hassan, *Science*, 2005, **309**, 65–66.
- 92 K. E. Drexler, Engines of creation: The coming era of nanotechnology, Anchor-Doubleday, New York, 1986.
- 93 B. Joy, Why the future doesn’t need us, 2000, [http://www.wired.com/wired/archive/8.04/joy\\_pr.html](http://www.wired.com/wired/archive/8.04/joy_pr.html).
- 94 M. Crichton, Prey, HarperCollins, New York, 2002.
- 95 Beware the grey goo; Nanotech scare stories are blinding us to more pressing perils, *New Sci.*, 2003, **178**, 3.
- 96 K. Kleiner and J. Hogan, *New Sci.*, 2003, **177**, 14.
- 97 R. F. Service, *Science*, 2000, **290**, 1526–1527.
- 98 C. Phoenix and E. Drexler, *Nanotechnology*, 2004, **15**, 869–872.
- 99 J. Giles, *Nature*, 2004, **429**, 591.
- 100 P. T. Anastas and J. C. Warner, *Green Chemistry: Theory and Practice*, Oxford University Press, New York, 1998.
- 101 G. A. Hughes, *Nanomedicine: Nanotech. Biol. Med.*, 2005, **1**, 22–30.
- 102 P. Raveendran, J. Fu and S. L. Wallen, *J. Am. Chem. Soc.*, 2003, **125**, 13940–13941.
- 103 G. A. Somorjai and K. McCrea, *Appl. Catal., A*, 2001, **222**, 3–18.
- 104 A. Goho, *Sci. News*, 2005, **167**, 266–268.
- 105 Glossary of Green Chemistry Terms, Green Chemistry Institute, ACS, 2005, [http://www.chemistry.org/portal/a/c/s/1/acdisplay.html?DOC=greenchemistryinstitute%5Cglossary\\_al.html](http://www.chemistry.org/portal/a/c/s/1/acdisplay.html?DOC=greenchemistryinstitute%5Cglossary_al.html).
- 106 R. A. Freitas, *Nanomedicine*, vol. IIA: Biocompatibility, Landes Bioscience, 2003.
- 107 S. Talbot, *Evident Technologies*, 2005, 1–2, <http://www/evident-tech.com>.
- 108 M. J. Dalby, N. Gadegaard, M. O. Riehle, C. D. W. Wilkinson and A. S. G. Curtis, *Int. J. Biochem. Cell Biol.*, 2004, **36**, 2005–2015.
- 109 B. G. Cousins, P. J. Doherty, R. L. Williams, J. Fink and M. J. Garvey, *J. Mater. Sci.: Mater. Med.*, 2004, **15**, 355–359.
- 110 B. Kasemo, *Surf. Sci.*, 2002, **500**, 656–677.
- 111 S.-Q. Liu, J.-J. Xu and H.-Y. Chen, *Colloids Surf., B*, 2004, **36**, 155–159.
- 112 X. Zhu, J. Chen, L. Scheideler, T. Altebaeumer, J. Geisgerstorfer and D. Kern, *Cells Tissues Organs*, 2004, **178**, 13–22.
- 113 L. A. Smith and P. X. Ma, *Colloids Surf., B*, 2004, **39**, 125–131.
- 114 S. Sharma, R. W. Johnson and T. A. Desai, *Biosens. Bioelectron.*, 2004, **20**, 227–239.
- 115 A. D. Maynard, P. A. Baron, M. Foley, A. A. Shvedova, E. R. Kisin and V. Castranova, *J. Toxicol. Environ. Health A*, 2004, **67**, 87–107.
- 116 D. Panterotto, J.-P. Briand, M. Prato and A. Bianco, *Chem. Commun.*, 2004, 16–17.
- 117 Y. Sato, A. Yokoama, K. Shibata, Y. Akimoto, S. Ogino, Y. Nodasaka, T. Kohgo, K. Tamura, T. Akasaka, M. Uo, K. Motomiya, B. Jeyadvan, M. Ishiguro, R. Hatakeyama, F. Watari and K. Tohji, *Mol. Biosyst.*, 2005, **1**, 176–182.
- 118 P. H. M. Hoet, A. Nemmar and B. Nemery, *Nat. Biotechnol.*, 2004, **22**, 19.
- 119 D. B. Warheit, B. R. Laurence, K. L. Reed, D. H. Roach, G. A. M. Reynolds and T. R. Webb, *Toxicol. Sci.*, 2004, **77**, 117–125.
- 120 C. W. Lam, J. T. James, R. McCluckey and R. L. Hunter, *Toxicol. Sci.*, 2004, **77**, 1126–1230.
- 121 D. Cui, F. Tian, C. S. Ozkan, M. Wang and H. Gao, *Toxicol. Lett.*, 2005, **155**, 73–85.
- 122 N. A. Monteiro-Riviere, R. J. Nemanich, A. O. Inman, Y. Y. Wang and J. E. Riviere, *Toxicol. Lett.*, 2005, **155**, 377–384.
- 123 C.-W. Lam, J. T. James, R. McCluskey and R. L. Hunter, *Toxicol. Sci.*, 2004, **77**, 126–134.
- 124 G. Jia, H. Wang, L. Yan, X. Wang, R. Pei, T. Yan, Y. Zhao and X. Guo, *Environ. Sci. Technol.*, 2005, **39**, 1378–1383.
- 125 N. W. S. Kam, T. C. Jessop, P. A. Wender and H. Dai, *J. Am. Chem. Soc.*, 2004, **126**, 6850–6851.
- 126 K. Donaldson, D. Brown, A. Clouter, R. Duffin, W. MacNee, L. Renwick, L. Tran and V. Stone, *J. Aerosol Med.*, 2002, **15**, 213–220.
- 127 G. Oberdörster, *Int. Arch. Occup. Environ. Health*, 2001, **74**, 1–8.
- 128 S. S. Tinkle, J. M. Antonini, B. A. Rich, J. R. Roberts, R. Salmen, K. DePree and E. J. Adkins, *Environ. Health Perspect.*, 2003, **111**, 1202–1208.
- 129 A. Peters, D. W. Dockery, J. E. Mullere and M. A. Mittleman, *Circulation*, 2001, **103**, 2810–2815.
- 130 D. B. Warheit, B. R. Laurence, K. L. Reed, D. H. Roach, G. A. M. Reynolds and T. R. Webb, *Toxicol. Sci.*, 2004, **77**, 117–125.
- 131 A. D. Maynard, P. A. Baron, M. Foley, A. A. Shvedova and E. R. Kistin, *J. Toxicol. Environ. Health*, 2004, **67**, 87–107.
- 132 X. Zong, H. Bien, C.-Y. Chung, L. Yin, D. Fang, B. S. Hsiao, B. Chu and E. Entcheva, *Biomaterials*, 2005, **26**, 5330–5338.
- 133 X. Michalet, F. F. Pinaud, L. A. Bentolila, J. M. Tsay, S. Doose, J. J. Li, G. Sundaresan, A. M. Wu, S. S. Gambhir and S. Weiss, *Science*, 2005, **307**, 538–544.
- 134 Nanoderm quality of skin as a barrier to ultra-fine particles, European Commission, 2003, <http://www.uni-leipzig.de/~nanoderm>.
- 135 Environmental Tools of the Future, Today: Nanotechnology, National Center for Environmental Research, within the Environmental Protection Agency, 2003, [http://es.epa.gov/ncer/events/news/2003/01\\_15\\_03a.html](http://es.epa.gov/ncer/events/news/2003/01_15_03a.html).
- 136 The natural advantage of nations: Business opportunities, innovation and governance in the 21st century, ed. K. C. Hargroves and M. H. Smith, Earthscan, London, 2005.
- 137 J.-R. Gurr, A. S. S. Wang, C.-H. Chen and K.-Y. Jan, *Toxicology*, 2005, **213**, 66–73.
- 138 Zs. Kertész, Z. Szikszai, E. Gontier, P. Moretto, J.-E. Surlève-Bazeille, B. Kiss, I. Juhász, J. Hunyadi and Á. Z. Kiss, *Nucl. Instrum. Methods Phys. Res., Sect. B*, 2005, **231**, 280–285.

- 139 J. Schulz, H. Hohenerg, F. Pflücker, E. Gärtner, T. Will, S. Pfeiffer, R. Wepf, V. Wendel, H. Gers-Barlag and K.-P. Wittern, *Adv. Drug Delivery Rev.*, 2002, **54**, S157–S163.
- 140 A. Shiohara, A. Hoshino, K. Hanaki, K. Suzuki and K. Yamamoto, *Microbiol. Immunol.*, 2004, **48**, 669–675.
- 141 A. Hoshino, K. Fujioka, T. Oku, M. Suga, Y. F. Sasaki, T. Ohta, M. Yasuhara, K. Suzuki and K. Yamamoto, *Nano Lett.*, 2004, **4**, 2163–2169.
- 142 X. Jia, N. Li and J. Chen, *Life Sci.*, 2005, **76**, 1989–2003.
- 143 J. Muller, F. Huaux, N. Moreau, P. Misson, J.-F. Heilier, M. Delos, M. Arras, A. Fonseca, J. B. Nagy and D. Lison, *Toxicol. Appl. Pharmacol.*, 2005, **207**, 221–231.
- 144 K. Donaldson and C. Lang Tran, *Mutat. Res.*, 2004, **553**, 5–9.
- 145 R. F. Service, *Science*, 2003, **300**, 243.
- 146 A. Churg, B. Stevens and J. L. Wright, *Am. J. Physiol.: Lung Cell. Mol. Physiol.*, 1998, **274**, L81–L86.
- 147 K. Donaldson, P. H. Beswick and P. S. Gilmour, *Toxicol. Lett.*, 1996, **88**, 293–298.
- 148 C. M. Goodman, C. D. McCusker, T. Yilmaz and V. M. Rotello, *Bioconjugate Chem.*, 2004, **15**, 897–900.
- 149 F. Rancan, S. Rosan, F. Boehm, A. Cantrell, M. Brellreich, H. Schoenberger, A. Hirsch and F. Moussa, *J. Photochem. Photobiol., B*, 2002, **67**, 157–162.
- 150 S. Foley, C. Crowley, M. Smaih, C. Bonfils, B. F. Erlanger, P. Seta and C. Larroque, *Biochem. Biophys. Res. Commun.*, 2002, **294**, 116–119.
- 151 X. L. Yang, C. H. Fan and H. S. Zhu, *Toxicol. in Vitro*, 2002, **16**, 41–46.
- 152 J. D. Fortner, D. Y. Lyon, C. M. Sayes, A. M. Boyd, J. C. Falkner, E. M. Hotze, L. B. Alemany, Y. J. Tao, W. Guo, K. D. Ausman, V. L. Colvin and J. B. Hughes, *Environ. Sci. Technol.*, 2005, **39**, 4307–4316.
- 153 C. M. Sayes, J. D. Fortner, W. Guo, D. Lyon, A. M. Boyd, K. D. Ausman, Y. J. Tao, B. Sitharaman, L. J. Wilson, J. B. Hughes, J. L. West and V. L. Colvin, *Nano Lett.*, 2004, **4**, 1881–1887.
- 154 E. Oberdörster, *Environ. Health Perspect.*, 2004, **112**, 1058–1062.
- 155 A. K. Gupta and M. Gupta, *Biomaterials*, 2005, **26**, 1565–1573.

# Chemical Science

An exciting news supplement providing a snapshot of the latest developments across the chemical sciences



Free online and in print issues of selected RSC journals!\*

**Research Highlights** – newsworthy articles and significant scientific advances

**Essential Elements** – latest developments from RSC publications

**Free access** to the original research paper from every online article

\*A separately issued print subscription is also available

RSC Publishing

[www.rsc.org/chemicalscience](http://www.rsc.org/chemicalscience)



# A convenient preparation of aliphatic and aromatic *N*-sulfonylimines mediated by sulfamic acid in aqueous media

Zhenjiang Li,\* Xinghua Ren, Ping Wei, Honggui Wan, Yuhu Shi and Pingkai Ouyang

Received 16th December 2005, Accepted 27th March 2006

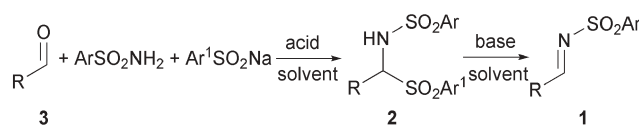
First published as an Advance Article on the web 3rd April 2006

DOI: 10.1039/b517864a

A facile synthesis of *N*-sulfonylimines by the condensation of aldehydes, sulfonylamide, and sodium arenesulfinate in the presence of sulfamic acid (NH<sub>2</sub>SO<sub>3</sub>H) in water–alcohol solvent and subsequent aqueous–biphasic basic elimination is reported.

## Introduction

Imines bearing electron-withdrawing *N*-substitutions are useful intermediates in organic synthesis.<sup>1</sup> Sulfonyl imines have been increasing in importance in the last decade<sup>2</sup> as they are one of the few types of electron-deficient imines<sup>3</sup> that are stable enough to be isolated but reactive enough to undergo addition reactions.<sup>4</sup> Several kinds of synthetic routes toward *N*-sulfonylimines (SI) have been developed.<sup>2a</sup> Generally speaking, direct condensation<sup>5</sup> of carbonyl compounds with sulfonamides was the straightforward route, but it was always forced by dehydrating agents or apparatus. Due to the weak nucleophilicity of sulfonamide, activation of the carbonyl by Lewis acids<sup>6</sup> or employment of acetals in place of the carbonyl<sup>7</sup> under harsh conditions was unavoidable. Mild and more efficient indirect methods were developed for enolizable or heat sensitive aldehydes/ketones. Among these preparation procedures, the Kresze reaction<sup>8</sup> and Hudson reaction<sup>9</sup> were widely investigated. In Kresze's method, *N*-sulfonyl sulfonamides were used instead of sulfonamides to generate SI *in situ* via a [2 + 2] cycloaddition and extrusion of sulfur dioxide. SI was prepared by treatment of oxime with sulfonyl chloride or sulfonyl cyanide<sup>9e</sup> in the Hudson reaction. Indirect preparation of SI by methods such as oxidation of *N*-sulfenimines or *N*-sulfinimines,<sup>10</sup> catalyzed isomerization or rearrangement of *N*-sulfonyl aziridines,<sup>11</sup> and imido-transfer of aldehydes<sup>12</sup> were reported recently. Other methods<sup>13</sup> through  $\alpha$ -substitution of SI,<sup>13a</sup> tellurium mediated reaction of aldehydes with chloramine T,<sup>13b</sup> photo-imino group migration,<sup>13c</sup> reaction of *N*-TMS imines with sulfonyl chloride,<sup>13d</sup> microwave facilitated acid catalyzed direct condensations,<sup>13e,13g</sup> and utilization of acetic anhydride as dehydrating and acylation reagent<sup>13f</sup> were used in some cases. An important two-step route (Scheme 1) to *N*-arenesulfonyl imines **1**, which is based on the fundamental works of Strating's group<sup>14</sup> for the preparation of sulfonamidossulfones **2**, was developed as a general strategy. By analogy to the preparation of *N*-acyl imines,<sup>15</sup> **2** was subject to basic elimination, from condensation of aldehydes **3**, arenesulfonylamide, and sodium arenesulfinate in the presence



Scheme 1 Two-step route by acidic 3-component condensation and subsequent basic elimination to *N*-arenesulfonylimines.

of acid, to afford **1**.<sup>16</sup> Chemla's group<sup>16c</sup> reported a similar elegant procedure for the preparation of SI with mild reaction conditions and easy work-up.

By careful comparison of the works of Chemla *et al.*<sup>16c</sup> and others<sup>15,16a</sup> with the earlier studies,<sup>14</sup> it showed that formic acid was employed as acid and co-solvent in most cases and a large excess of formic acid, ordinarily more than 30 equivalents, was used. Because formic acid ( $pK_a$  3.77) is much weaker than sulfinic acid ( $pK_a$  2.1), the proportion of sulfinic acid formed *in situ* from sodium sulfinate would be scarce. The formic acid–water solvent also restricted the adjustability of solvent and was not ideal for more efficient reactions. For large scale preparations, the treatment of the excess formic acid would be problematic. The choice of formic acid might be more a habit than a necessary. An acid of moderate strength would facilitate the formation of sufficient amount of sulfinic acid, push the addition to proceed effectively, and avoid enolization of aldehydes/ketones.

In searching for a candidate acid, sulfamic acid (SA) caught our attention due to its appropriate acidity ( $pK_a$  1.0) and unique structure.<sup>17</sup> SA has emerged as a powerful solid acid catalyst in many organic reactions.<sup>18</sup> It has many prominent properties,<sup>19</sup> such as, it is moderately acidic, non-volatile, non-corrosive, insoluble in common organic solvent, has outstanding physical stability, is inexpensive, and readily available. To our surprise, this potential solid acid has not been employed as a Brønsted acid in current organic preparations.

Use of aqueous media for green, sustainable organic synthesis is of significant interest.<sup>20</sup> The development of non-hazardous alternatives to conventional organic solvents is a challenge for academia, industrial, and regulatory bodies.<sup>21</sup> However, performing organic reactions in pure water is not always feasible. As aqueous media is highly recommended in green chemical processes, water–lower alcohols and aqueous–biphasic systems are highly preferred when considering the solubility and compatibility of organic compounds in aqueous media.<sup>22</sup> Herein we report a green two-step synthetic route through a 3-component condensation mediated by SA in water–alcohol solvent and subsequent aqueous–biphasic basic elimination to afford *N*-sulfonyl imines at ambient temperature in open vessels.

College of Life Science and Pharmaceutical Engineering, Nanjing University of Technology, Nanjing, 210009, China.  
E-mail: zjli@njut.edu.cn; Fax: +86 25 8347 9464

## Results and discussion

In continuing our work on asymmetric synthesis of special amino acids,<sup>23</sup> we needed to prepare SI on the liter scale. At the beginning, SI was produced as described in the literature.<sup>16c</sup> Most preparations proceeded smoothly in the first condensation step. After filtering off the solid products, the acidic water proved troublesome when handled. In light of the plethora of uses of SA in organic synthesis, we envisioned SA would perform better for this preparation. The use of free sulfinic acid in Strating's method already had precedents.<sup>15b,16b</sup> A catalytic amount of camphor-sulfonic acid (CSA) was used in the latter case, but the CSA was too strong and the imine was protonated to form an iminium ion, which was added by an amide to afford *bis*-amide. Although free arenesulfinic acid made the condensation faster, the acid decomposed readily on storage and had to be prepared carefully on the spot. SA as a moderate acid can produce sulfinic acid *in situ*, keeping its concentration at a reasonable level, and avoiding the possible iminium ion and *bis*-amide formation.

Initially, one equivalent of SA was added to the formic acid–water system. The condensation proceeded faster as expected. Then we realized that the formic acid was not necessary if solvent(s) of similar strength and polarity could be found. Furthermore, multiple combinations of different solvents may offer comparable apparent polarity but disparity solvent effects on reactions. One of the merits of the Strating condensation was that in polar solvent the reactants can be dissolved but the product **2** was insoluble. On the other hand, SA is very soluble in water, slightly soluble in alcohols, but insoluble in common organic solvents. Thus, combinations of acetonitrile–water, DMF–water, DMSO–water, dioxane–water, ethanol–water, methanol–water, and *i*-propanol–water as solvents were trialled and showed promising effects on the condensations. Aqueous–biphasic systems composed of water/CH<sub>2</sub>Cl<sub>2</sub> or water/dichloroethane were tested without success. Pure water as solvent was denied because most aldehydes used in the preparation were not soluble in it. Finally, water–methanol and water–ethanol were chosen for their good performance, benign environmental influence,<sup>22</sup>

**Table 1** Three-component condensations mediated by sulfamic acid in water–alcohol solvents and aqueous–biphasic basic elimination to *N*-tosylimines

Entry	<b>3</b>	R	<b>1</b>	Method <sup>a</sup>	Yield <sup>b</sup> /%	Mp/ <sup>c</sup> °C	$\delta_{\text{H}}$ (500 MHz; CDCl <sub>3</sub> ; Me <sub>4</sub> Si)/10 <sup>-6</sup> ; J/Hz	$\nu_{\text{max}}$ (KBr)/cm <sup>-1</sup>
1 <sup>c</sup>	<b>3a</b>	Phenyl	<b>1a</b>	A	66	113–114	2.45 (s, 3H), 7.36 (d, 2H, <i>J</i> 8.0), 7.50 (t, 2H, <i>J</i> 7.5), 7.64 (t, 1H, <i>J</i> 7.5), 7.90–7.95 (q, 4H), 9.05 (s, 1H)	1652 (C=N) 1326 (S=O)
2	<b>3b</b>	4-Methoxyphenyl	<b>1b</b>	A	68	121–122	2.45 (s, 3H), 3.90 (s, 3H), 6.98 (d, 2H, <i>J</i> 9.0), 7.35 (d, 2H, <i>J</i> 8.0), 7.88–7.91 (m, 4H), 8.96 (s, 1H)	1668 (C=N) 1320 (S=O)
3	<b>3c</b>	2,4-Dichlorophenyl	<b>1c</b>	C	47	106–107	2.47 (s, 3H), 7.35 (d, 1H, <i>J</i> 8.0), 7.38 (d, 2H, <i>J</i> 8.5), 7.51 (s, 1H), 7.91 (d, 2H, <i>J</i> 8.0), 8.11 (d, 1H, <i>J</i> 8.5), 9.44 (s, 1H)	1694 (C=N) 1306 (S=O)
4	<b>3d</b>	2-Chlorophenyl	<b>1d</b>	B	64	133–134	2.47 (s, 3H), 7.27–7.38 (m, 4H), 7.48 (d, 1H, <i>J</i> 8.0), 7.53 (d, 1H, <i>J</i> 8.5), 7.92 (d, 2H, <i>J</i> 8.5), 8.17 (d, 1H, <i>J</i> 8.0), 9.52 (s, 1H)	1690 (C=N) 1325 (S=O)
5	<b>3e</b>	3-Nitrophenyl	<b>1e</b>	A	67	141–142	2.48 (s, 3H), 7.41 (d, 2H, <i>J</i> 8.0), 7.74 (t, 1H, <i>J</i> 8.0), 7.93 (d, 2H, <i>J</i> 8.0), 8.27 (d, 2H, <i>J</i> 7.5), 8.47 (d, 1H, <i>J</i> 7.5), 8.79 (s, 1H), 9.13 (s, 1H)	1675 (C=N) 1317 (S=O)
6	<b>3f</b>	4-Methylphenyl	<b>1f</b>	A	68	114–115	2.45 (s, 6H), 7.30 (d, 2H, <i>J</i> 8.0), 7.36 (d, 2H, <i>J</i> 8.0), 7.83 (d, 2H, <i>J</i> 8.0), 7.90 (d, 2H, <i>J</i> 8.0), 9.00 (s, 1H)	1660 (C=N) 1324 (S=O)
7	<b>3g</b>	2-Furyl	<b>1g</b>	A	61	99–100	2.45 (s, 3H), 6.67 (q, 1H), 7.28 (d, 2H), 7.35 (d, 2H, <i>J</i> 8.0), 7.76 (d, 1H), 7.89 (d, 2H, <i>J</i> 8.0), 8.83 (s, 1H)	1638 (C=N) 1341 (S=O)
8	<b>3h</b>	<i>n</i> -Propyl	<b>1h</b>	A	81	Oil	0.97 (m, 3H), 1.67 (m, 2H), 2.45 (s, 3H), 2.51 (m, 2H), 7.34 (d, 2H, <i>J</i> 7.5), 7.83 (d, 2H, <i>J</i> 8.0), 8.61 (t, 1H, <i>J</i> 4.5)	1649 (C=N) 1336 (S=O)
9	<b>3i</b>	Isobutyl	<b>1i</b>	A	75	Oil	0.97 (d, 6H, <i>J</i> 6.5), 2.08 (m, 1H), 2.39 (m, 2H), 2.44 (s, 3H), 7.32 (m, 2H), 7.82 (d, 2H), 8.60 (t, 1H, <i>J</i> 5.0)	1630 (C=N) 1335 (S=O)
10	<b>3j</b>	2-Propyl	<b>1j</b>	A	59	Oil	0.96 (d, 6H, <i>J</i> 7.0), 2.10 (m, 1H), 2.44 (s, 3H), 7.33 (m, 2H), 7.83 (d, 2H), 8.62 (d, 1H, <i>J</i> 5.5)	1647 (C=N) 1329 (S=O)

<sup>a</sup> Solvent compositions by volume: **A** (water–methanol 1 : 1), **B** (water–methanol 3 : 4), **C** (water–ethanol 3 : 4). <sup>b</sup> Overall, separated yields.

<sup>c</sup> The preparation of **1a** was scaled-up to 3 l (1 mole of **3a**), the separated yield was 71%.

economy, and adjustability of solvent strength tunable for different aldehydes.

Investigations on the ratio of SA to sodium sulfinate showed that 1.5–3 equivalents of SA were effective to furnish the condensation. Although 1.2 equivalents of SA were enough for the first-step reaction, 2 equivalents were chosen for faster reactions without further optimization. As we have focused on the influence of acid and solvents on the condensation reactions, the molar ratio of the three reactants was fixed as 1 : 1 : 1. The elimination step was carried out in the presence of sodium hydrogencarbonate<sup>6a,15a,16</sup> quantitatively.

As summarized in Table 1, we have established preparation procedures using SA (2 equiv.) as acid in water–alcohol solvents of adjustable compositions to furnish the condensations and subsequent aqueous–biphasic basic elimination in open vessels at ambient temperature to afford both aromatic and aliphatic *N*-tosyl imines **1** in good yields.

## Conclusions

In conclusion, we have developed a new procedure for the synthesis of *N*-tosylimines of aromatic and aliphatic aldehydes with less environmental impact and easier preparations. Sulfamic acid was an ideal acid to facilitate the condensation and to avoid the possible enolization of aldehydes. Water–alcohol solvents improved the reactions and resulted in simple work-up. The process was appropriate for synthesis of SI by diversity of aldehydes and amenable to larger quantity preparations.

## Experimental

A typical experimental procedure is as follows: a mixture of TsNH<sub>2</sub> (1.71 g, 10.0 mmol), TolSO<sub>2</sub>Na (1.78 g, 10.0 mmol), and sulfamic acid (1.94 g, 20.0 mmol) was dissolved in water–methanol (1 : 1, v/v, 30 cm<sup>3</sup>) by stirring. Benzaldehyde **3a** (1.06 g, 1.00 cm<sup>3</sup>, 10.0 mmol) was added in one portion. The reaction mixture was stirred for 12 h at rt. The white solid product **2a** was collected by filtration, washed with water (2 × 10 cm<sup>3</sup>) and hexane (10 cm<sup>3</sup>), and then dissolved in CH<sub>2</sub>Cl<sub>2</sub> (50 cm<sup>3</sup>). Saturated aqueous NaHCO<sub>3</sub> solution (50 cm<sup>3</sup>) was added and the biphasic liquid was stirred for 2 h at rt. The organic phase was separated and the aqueous phase was extracted with CH<sub>2</sub>Cl<sub>2</sub> (30 cm<sup>3</sup>). The combined organic phase was dried (MgSO<sub>4</sub>) and solvent was vacuum evaporated. The residue obtained was pure **1a** as shown by <sup>1</sup>H NMR and HPLC.

## Acknowledgements

We thank the Major Basic R & D Program of China (Grant No. 2003CB716004) and the Hi-tech R & D Program of China (Grant No. 2003AA235051) for financial support.

## References

- (a) R. Bloch, *Chem. Rev.*, 1998, **98**, 1407–1438; (b) S. Kobayashi and H. Ishitani, *Chem. Rev.*, 1999, **99**, 1069–1094; (c) H. Miyabe, M. Ueda and T. Naito, *Synlett*, 2004, 1140–1157.
- (a) S. M. Weinreb, *Top. Curr. Chem.*, 1997, **190**, 131–184; (b) D. Enders and U. Reinhold, *Tetrahedron: Asymmetry*, 1997, **8**, 1895–1946.
- (a) F. A. Davis, P. Zhou and B. C. Chen, *Chem. Soc. Rev.*, 1998, **27**, 13–18; (b) J. A. Ellman, T. D. Owens and T. P. Tang, *Acc. Chem. Res.*, 2002, **35**, 984–995; (c) J. A. Ellman, *Pure Appl. Chem.*, 2003, **75**, 39–46; (d) P. Zhou, B.-C. Chen and F. A. Davis, *Tetrahedron*, 2004, **60**, 8003–8030.
- (a) C. H. Senananake, D. Krishnamurthy, Z.-H. Lu, Z. Han and I. Gallou, *Aldrichimica Acta*, 2005, **38**, 3, 93–104; (b) J.-P. Begue, D. Bonnet-Delpon, B. Crousse and J. Legros, *Chem. Soc. Rev.*, 2005, **34**, 562–572; (c) S. M. Weinreb and R. K. Orr, *Synthesis*, 2005, 1205–1227.
- (a) L. C. Vishwakarma, O. D. Stringer and F. A. Davis, *Org. Synth.*, 1987, **66**, 203–208; (b) D. L. Boger, W. L. Corbett, T. T. Curran and A. M. Kasper, *J. Am. Chem. Soc.*, 1991, **113**, 1713–1729; (c) B. E. Love and J. Ren, *J. Org. Chem.*, 1993, **58**, 5556–5557; (d) B. E. Love, P. S. Raju and T. C. Williams, II., *Synlett*, 1994, 493–494; (e) J. H. Wynne, S. E. Price, J. R. Rorer and W. M. Stalick, *Synth. Commun.*, 2003, **33**, 341–352.
- (a) W. R. McKay and G. R. Proctor, *J. Chem. Soc., Perkin Trans. 1*, 1981, 2435–2442; (b) W. B. Jennings and C. J. Lovely, *Tetrahedron Lett.*, 1988, **29**, 3725–3728; (c) F. A. Davis, R. ThimmaReddy and M. C. Weismiller, *J. Am. Chem. Soc.*, 1989, **111**, 5964–5965; (d) 5 b; (e) W. B. Jennings and C. J. Lovely, *Tetrahedron*, 1991, **47**, 5561–5568; (f) R. N. Ram and A. A. Khan, *Synth. Commun.*, 2001, **31**, 841–846; (g) 5 e.
- (a) R. Albrecht and G. Kresze, *Chem. Ber.*, 1964, **97**, 490–493; (b) F. A. Davis, J. M. Kaminski, E. W. Kluger and H. S. Freilich, *J. Am. Chem. Soc.*, 1975, **97**, 7085–7091; (c) F. A. Davis, J. Lamendola, Jr., U. Nadir, E. W. Kluger, T. C. Sedergran, T. W. Panunto, R. Billmers, R. Jenkins, Jr., I. J. Turchi, W. H. Watson, J. S. Chen and M. Kimura, *J. Am. Chem. Soc.*, 1980, **102**, 2000–2005.
- (a) R. Albrecht, G. Kresze and B. Mlakar, *Chem. Ber.*, 1964, **97**, 483–489; (b) R. Albrecht and G. Kresze, *Chem. Ber.*, 1965, **98**, 1431–1434; (c) G. Kresze and W. Wucherpfennig, *Angew. Chem., Int. Ed.*, 1967, **6**, 149–167; (d) M. J. Melnick, A. J. Freyer and S. M. Weinreb, *Tetrahedron Lett.*, 1988, **29**, 3891–3894; (e) J. Sisko and S. M. Weinreb, *Tetrahedron Lett.*, 1989, **30**, 3037–3040; (f) J. Sisko and S. M. Weinreb, *J. Org. Chem.*, 1990, **55**, 393–395; (g) P. Hamley, A. B. Holmes, A. Kee, T. Ladduwahetty and D. F. Smith, *Synlett*, 1991, 29–30.
- (a) B. F. Hudson and F. A. F. Record, *J. Chem. Soc., Chem. Commun.*, 1976, 831–832; (b) C. Brown, R. F. Hudson and K. A. F. Record, *J. Chem. Soc., Chem. Commun.*, 1977, 540–542; (c) C. Brown, R. F. Hudson and K. A. F. Record, *J. Chem. Soc., Perkin Trans. 1*, 1978, 822–828; (d) 5 b; (e) D. L. Boger and W. L. Corbett, *J. Org. Chem.*, 1992, **57**, 4777–4780; (f) M. C. McIntosh and S. M. Weinreb, *J. Org. Chem.*, 1993, **58**, 4823–4832; (g) G. D. Artman, III., A. Bartolozzi, R. W. Franck and S. M. Weinreb, *Synlett*, 2001, 232–233.
- (a) 7 b; (b) 7 c; (c) J. L. G. Ruano, J. Aleman, M. B. Cid and A. Parra, *Org. Lett.*, 2005, **7**, 179–182.
- (a) Y. Sugihara, S. Iimura and J. Nakayama, *Chem. Commun.*, 2002, 134–135; (b) J. P. Wolfe and J. E. Ney, *Org. Lett.*, 2003, **5**, 4607–4610.
- (a) S. L. Jian, V. B. Sharma and B. Sain, *J. Mol. Catal. A: Chem.*, 2005, **239**, 92–95; (b) V. B. Sharma, S. L. Jain and B. Sain, *J. Chem. Res. (S)*, 2005, 182–183.
- (a) F. A. Davis, P. Zhou and G. S. Lal, *Tetrahedron Lett.*, 1990, **31**, 1653–1656; (b) B. M. Trost and C. Marrs, *J. Org. Chem.*, 1991, **56**, 6468–6470; (c) T. Fujii, T. Kimura and N. Furukawa, *Tetrahedron Lett.*, 1995, **36**, 1075–1078; (d) G. I. Georg, G. C. B. Harriman and S. A. Peterson, *J. Org. Chem.*, 1995, **60**, 7366–7268; (e) A. Vass, J. Dudas and R. S. Varma, *Tetrahedron Lett.*, 1999, **40**, 4951–4954; (f) K. Y. Lee, C. G. Lee and J. N. Kim, *Tetrahedron Lett.*, 2003, **44**, 1231–1234; (g) T. Jin, G. Feng, M. Yang and T. Li, *Synth. Commun.*, 2004, **34**, 1277–1283.
- (a) J. B. Engberts and J. Strating, *Recl. Trav. Chim. Pays-Bas*, 1964, **83**, 733–736; (b) J. B. Engberts and J. Strating, *Recl. Trav. Chim. Pays-Bas*, 1965, **84**, 942–950; (c) J. B. Engberts, T. Olijnsma and J. Strating, *Recl. Trav. Chim. Pays-Bas*, 1966, **85**, 1211–1222; (d) T. Olijnsma, J. B. Engberts and J. Strating, *Recl. Trav. Chim. Pays-Bas*, 1967, **86**, 463–473; (e) T. Olijnsma, J. Strating and J. B. Engberts, *Recl. Trav. Chim. Pays-Bas*, 1972, **91**, 209–212; (f) H. Meijer, R. M. Tel, J. Strating and J. B. Engberts, *Recl. Trav. Chim. Pays-Bas*, 1973, **92**, 72–82.
- (a) A. M. van Leusen, J. Wildeman and O. H. Oldenziel, *J. Org. Chem.*, 1977, **42**, 1153; (b) 6 a; (c) J. Morton, A. Rahim and E. R. H. Walker, *Tetrahedron Lett.*, 1982, **23**, 4123–4126.

- 16 (a) A. M. Kanazawa, J.-N. Denis and A. E. Greene, *J. Org. Chem.*, 1994, **59**, 1238–1240; (b) J. Sisko, M. Mellinger, P. W. Sheldrake and N. H. Baine, *Tetrahedron Lett.*, 1996, **37**, 8113–8116; (c) F. Chemla, V. Hebbe and J.-F. Normant, *Synthesis*, 2000, 75–77.
- 17 (a) D. Philip, A. Eapen and G. Aruldas, *J. Solid State Chem.*, 1995, **116**, 217–223; (b) M. Canageratna, M. E. Ott and K. R. Leopold, *Chem. Phys. Lett.*, 1997, **281**, 63–68.
- 18 (a) T.-S. Jin, G. Sun, Y.-W. Li and T.-S. Li, *Green Chem.*, 2002, **4**, 255–256; (b) P. R. Singh, D. U. Singh and S. D. Samant, *Synlett*, 2004, 1909–1912; (c) R. Nagarajan, C. J. Magesh and P. T. Perumal, *Synthesis*, 2004, 69–74; (d) B. Wang, Y. Gu, C. Luo, T. Yang, L. Yang and J. Suo, *Tetrahedron Lett.*, 2004, **45**, 3369–3372; (e) J. S. Yadav, P. P. Rao, D. Sreenu, R. S. Rao, V. N. Kumar, K. Nagaiah and A. R. Prasad, *Tetrahedron Lett.*, 2005, **46**, 7249–7253; (f) B. Rajitha, B. S. Kumar, Y. T. Geddy, P. N. Reddy and N. Sreenivasulu, *Tetrahedron Lett.*, 2005, **46**, 8691–8693.
- 19 B. Wang, *Synlett*, 2005, 1342–1343.
- 20 (a) C.-J. Li, *Chem. Rev.*, 2005, **105**, 3095–3165; (b) U. M. Lindström, *Chem. Rev.*, 2002, **102**, 2751–2772.
- 21 (a) R. A. Sheldon, *Green Chem.*, 2005, **7**, 267–278; (b) H.-U. Blaser and M. Studer, *Green Chem.*, 2003, **5**, 112–117; (c) J. M. DeSimone, *Science*, 2002, **297**, 799–803.
- 22 S. Hellweg, U. Fischer, M. Scheringer and K. Hungerbühler, *Green Chem.*, 2004, **6**, 418–427.
- 23 (a) Z. Li, H. Wan, P. Wei, Y. Shi and P. Ouyang, *Chin. J. Org. Chem.*, 2005, **25**, 881–892; (b) W. Qin, F. Cao, Z. Li, H. Zhou, H. Wan, P. Wei, Y. Shi and P. Ouyang, *J. Chem. Crystallogr.*, 2006, **36**, DOI: 10.1007/s10870-005-9025-9.

# ReSource

## Lighting your way through the publication process

A website designed to provide user-friendly, rapid access to an extensive range of online services for authors and referees.

### ReSource enables authors to:

- Submit manuscripts electronically
- Track their manuscript through the peer review and publication process
- Collect their free PDF reprints
- View the history of articles previously submitted

### ReSource enables referees to:

- Download and report on articles
- Monitor outcome of articles previously reviewed
- Check and update their research profile

**Register today!**

RSCPublishing

[www.rsc.org/resource](http://www.rsc.org/resource)

02030508

# Solventless microwave-assisted chlorodehydroxylation for the conversion of alcohols to alkyl chlorides

Mark C. Reid, James H. Clark\* and Duncan J. Macquarrie

Received 26th October 2005, Accepted 8th March 2006

First published as an Advance Article on the web 21st March 2006

DOI: 10.1039/b515223b

The atom and energy-efficient and low hazardous direct chlorodehydroxylation of alcohols can be achieved in very short times using aqueous HCl under microwave activation. Traditional catalysts generally inhibit the reaction except for some phosphonium phase transfer catalysts. The results can be explained by the transfer of HCl to the non-aqueous reaction phase being rate-limiting.

## Introduction

The conversion of primary alcohols to their corresponding chlorides has previously been reported utilizing various regimes almost entirely relying on stoichiometric conversion technologies. One traditional method of choice involves the use of thionyl chloride (Scheme 1 i) giving yields in the region of 60% (1-chlorohexane) over 5 h.<sup>1–3</sup> Numerous literature citations exist relating to various attempts to improve these reactions using alternative reagents and greener methodologies. The reaction of hydrogen chloride with the primary alcohol is most desirable due to the inherently high atom economy, and avoidance of hazardous stoichiometric co-products (Scheme 1 ii).

Early attempts using a (1 mol%) zinc (II) chloride catalyst (160 °C) gave yields in excess of 95% (cetyl-1-chloride, C<sub>16</sub>H<sub>33</sub>Cl) over 20 h with similar yields observed using anhydrous HCl.<sup>4,5</sup> Use of quaternary phosphonium salts as phase-transfer catalysts (PTCs) in solventless aqueous systems gave yields of the order of 90% (1-chlorooctane) over 30 h (105 °C).<sup>6</sup> Tundo and co-workers attempted to continue this work in generating continuous flow methods based on these catalysts in gas-liquid PTC systems with some success.<sup>7–9</sup>

Recently, much interest has been shown in microwave-assisted chemistry to facilitate reactions and efforts are now being made to scale up reactions using this technology.<sup>10,11</sup> Microwave-assisted alcohol halodehydroxylation using halide-based ionic liquids have

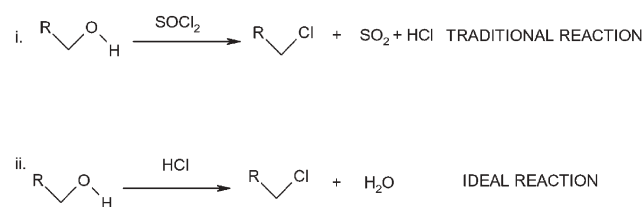
been reported with fast reaction rates<sup>12–14</sup> (compared to the non-assisted reaction) and giving reasonable product yields. This has encouraged us to explore the use of simple aqueous HCl for a range of commercially important chlorodehydroxylation under microwave conditions with and without added catalysts (Table 1). We have been able to achieve extremely rapid reactions, enabling quantitative conversions with often excellent selectivities in minutes rather than hours. We have also observed unexpected and quite complex effects in the presence of different types of catalysts.

## Experimental

Reactions were carried out in a microwave reactor using 1 cm<sup>3</sup> alcohol mixed with 3 cm<sup>3</sup> 37% aqueous HCl and (where appropriate) 0.1 or 0.2 g of catalyst. The reaction time was 10 min with 90 W microwave power and a threshold temperature of 130 °C or 170 °C using a computer controlled CEM-Discover focussed microwave synthesis system. After organic layer separation, quenching and drying, the product yield and conversion of substrate was determined by <sup>1</sup>H NMR spectroscopy and confirmed by GC.

## Results and discussion

The results show that in the absence of any catalyst, the smaller alcohols studied are converted to the corresponding alkyl chlorides in high yields and selectivity with microwave assistance. These represent excellent examples of green chemistry in that they are quick and efficient with high atom efficiency and involve no auxiliaries. The remarkable accelerating effect of the microwaves is unlikely to be due to rapid heating alone since non-microwave chlorodehydroxylation carried out at high temperature are of the order of 100 times slower.<sup>4–6</sup> It is likely that the known ability of microwaves to excite OH groups especially in such a highly polar environment contributes to the rapid reactions through activation of the alcohol substrates. Larger chain alcohols are less reactive presumably due to the lower solubility of HCl as the alcohols become more hydrophobic. In these cases at least, the transfer of HCl to the alcohol phase can be considered as rate limiting. This effect is confirmed by the somewhat unexpected detrimental effect of ZnCl<sub>2</sub> on the reaction rate. ZnCl<sub>2</sub> is a Lewis acid and might be expected to catalyse these reactions. However, any positive catalytic effect is overwhelmed by the negative effect of the salt increasing the difference in polarities of the aqueous and non-aqueous layers and thus further inhibiting the transfer of HCl to the latter. Iron (III) chloride has a different effect, giving low yields and selectivities (Table 1) which may be due to the FeCl<sub>3</sub> activating



Scheme 1 Chlorodehydroxylation.

Clean Technology Centre, Department of Chemistry, The University of York, York, UK YO10 5DD. E-mail: jhc1@york.ac.uk

**Table 1** Chlorodehydroxylation of primary alcohols using microwave irradiation

Substrate	Catalyst sample	Yield (%) (130 °C)	Selectivity (%) (130 °C)	Yield (%) (170 °C)	Selectivity (%) (170 °C)
1-Hexanol	No catalyst	85	97	88	98
1-Hexanol	ZnCl <sub>2</sub>	78	93	70	93
1-Hexanol	FeCl <sub>3</sub>	48	57	41	58
1-Hexanol	n-BuPPh <sub>3</sub> Br	82	98	92	98
1-Hexanol	PhCH <sub>2</sub> PPh <sub>3</sub> Br	82	96	93	99
1-Hexanol	C <sub>16</sub> H <sub>33</sub> PBu <sub>3</sub> Br <sup>b</sup>	90	95	94	98
1-Hexanol	C <sub>16</sub> H <sub>33</sub> NMe <sub>3</sub> Cl <sup>b</sup>	53	96	64	97
1-Octanol	No catalyst	78	99	77	96
1-Octanol	ZnCl <sub>2</sub>	68	94	73	94
1-Octanol	FeCl <sub>3</sub>	44 <sup>a</sup>	59	35	51
1-Octanol	n-BuPPh <sub>3</sub> Br	73	97	76	96
1-Octanol	PhCH <sub>2</sub> PPh <sub>3</sub> Br	72	96	81	98
1-Octanol	C <sub>16</sub> H <sub>33</sub> PBu <sub>3</sub> Br <sup>b</sup>	72	97	91	98
1-Octanol	C <sub>16</sub> H <sub>33</sub> NMe <sub>3</sub> Cl <sup>b</sup>	52	96	66	99
1-Decanol	ZnCl <sub>2</sub>	69	94	—	—
1-Decanol	FeCl <sub>3</sub>	30	40	—	—
1-Decanol	n-BuPPh <sub>3</sub> Br	70	99	—	—
1-Decanol	PhCH <sub>2</sub> PPh <sub>3</sub> Br	69	96	—	—
1-Decanol	C <sub>16</sub> H <sub>33</sub> PBu <sub>3</sub> Br <sup>b</sup>	86	99	—	—
1-Decanol	C <sub>16</sub> H <sub>33</sub> NMe <sub>3</sub> Cl <sup>b</sup>	53	98	—	—
1-Dodecanol	No catalyst	53	94	57	93
1-Dodecanol	ZnCl <sub>2</sub>	56	96	44	98
1-Dodecanol	FeCl <sub>3</sub>	33	47	30	45
1-Dodecanol	n-BuPPh <sub>3</sub> Br	61	96	63	95
1-Dodecanol	PhCH <sub>2</sub> PPh <sub>3</sub> Br	65	96	68	99
1-Dodecanol	C <sub>16</sub> H <sub>33</sub> PBu <sub>3</sub> Br <sup>b</sup>	86	98	89	99
1-Dodecanol	C <sub>16</sub> H <sub>33</sub> NMe <sub>3</sub> Cl <sup>b</sup>	48	96	54	98

<sup>a</sup> Plus 17% dialkylether. <sup>b</sup> 0.1 g catalyst.

the RCl product to further attack by unreacted alcohol giving ether as a significant by-product. Evidence for this comes from experimentation using analogous microwave conditions (90 W, 130 °C, 10 min) with no HCl. Alcohol and FeCl<sub>3</sub> alone did not react but when alkyl chloride was introduced (10 alcohol : 1 chloride by volume) ether formation occurred (monitored by GC) with almost no change in the alkyl chloride levels in the reaction (indicating that it was being regenerated during the reaction). Zinc chloride had a similar though smaller effect in that system. Addition of quaternary phosphonium and ammonium salts as PTCs had negligible or detrimental results in most cases except hexadecyltributylphosphonium bromide which led to elevated product yields with almost no change in the selectivity of the reaction. This effect was seen with all the alcohols screened and can be attributed to a phase-transfer effect of HCl to the organic layer (presumably due to the formation of HCl<sub>2</sub><sup>-</sup> ions) thereby increasing the reaction rate of HCl with the alcohol. This is again consistent with HCl phase transfer being rate-limiting.

## Conclusions

In conclusion, it has been shown that a solventless microwave-assisted chlorodehydroxylation of alcohols to alkyl chlorides using aqueous HCl can be carried out with dramatically short reaction times (10 min) with very high yields and selectivities (90%+). The reactions do not use hazardous S or P halogenating reagents, are very atom- and energy-efficient and generate no hazardous co-products. Thus, for the first time, a genuinely viable auxiliary-free route to the preparation of these important products is available.

The effects of added 'catalysts' are often unexpected but they can all be explained on the basis of a rate-limiting transfer of HCl to the non-aqueous reaction phase.

## Acknowledgements

We thank EPSRC and C6 Solutions Ltd for financial support and Mr T Lowden for his helpful advice and discussions.

## References

- 1 A. I. Vogel, *Textbook of Practical Organic Chemistry*, Longman, London, 5th edn, 1989, pp. 555–559.
- 2 J. March, *Advanced Organic Chemistry*, Wiley, New York, 4th edn, 1992, pp. 431–433.
- 3 R. C. Larock, *Comprehensive Organic Transformations*, VCH, New York, 1989, pp. 353–360.
- 4 A. Guyer, A. Bieler and E. Hardmeyer, *Helv. Chim. Acta*, 1937, **20**, 1462–1467.
- 5 M. T. Atwood, *J. Am. Oil Chem. Soc.*, 1963, **40**, 64–66.
- 6 D. Landini, F. Montanari and F. Rolla, *Synthesis*, 1974, 37–38.
- 7 P. Tundo, P. Venturello and E. Angeletti, *J. Chem. Soc., Perkin Trans. I*, 1987, 2157–2158.
- 8 P. Tundo, G. Moraglio and F. Trotta, *Ind. Eng. Chem. Res.*, 1989, **28**, 881–890.
- 9 P. Tundo and M. Selva, *Green Chem.*, 2005, **7**, 6, 464–467.
- 10 Evaluserve, *Developments in Microwave Chemistry, CW Special Reports, Chemistry World*, RSC, 2005.
- 11 CEM Corp., Matthews, NC-USA, www.cemsynthesis.com.
- 12 R. X. Ren and J. X. Wu, *Org. Lett.*, 2001, **3**, 3727–3728.
- 13 N. E. Leadbeater, H. M. Torenius and Heather Tye, *Tetrahedron*, 2003, **59**, 2253–2258.
- 14 H. P. Nguyen, H. Matondo and M. Baboulene, *Green Chem.*, 2003, **5**, 303–305.

# Environmentally sustainable production of cellulose-based superabsorbent hydrogels

Giuseppe Marci,<sup>a</sup> Giuseppe Mele,<sup>\*b</sup> Leonardo Palmisano,<sup>a</sup> Piero Pulito<sup>b</sup> and Alessandro Sannino<sup>b</sup>

Received 26th October 2005, Accepted 28th February 2006

First published as an Advance Article on the web 16th March 2006

DOI: 10.1039/b515247j

The development of new products and materials, especially those which are non-petrolchemical reserves and based on renewable organic resources, using innovative sustainable processes is nowadays of increasing interest and deserves the attention of both academic and industrial research. Cellulose and its derivatives, as renewable organic resources, have been used to synthesize novel superabsorbent hydrogels. Although the production of cellulose is one of the causes connected to deforestation, the production of suitably engineered cellulose superabsorbent hydrogel materials has been proposed to preserve water in typically arid areas in the world. Paradoxically, divinylsulfone (DVS), a small di-functional highly toxic molecule, was used as a crosslinker for the preparation of the hydrogel. An environmentally sustainable heterogeneous TiO<sub>2</sub> photo-catalysed process has been performed in order to achieve the detoxification (and a possible re-use) of washing waters deriving from the purification process carried out after the synthesis of a bio-degradable cellulose based superabsorbent hydrogel. The main species present in the washing water was DVS. DVS is a well known toxic agent and it was efficiently removed along with the unreacted polymers and oligomers by irradiating the washing waters in the presence of suspended polycrystalline TiO<sub>2</sub>. The photoprocess was studied not only by monitoring the total organic carbon (TOC) present in the solution but also by following the evolution of sulfate anions.

## Introduction

Hydrogels are 3D polymeric networks whose main feature is the ability to absorb large amounts of water, up to 5 L per g of dry product.<sup>1</sup> Chemical hydrogels are a particular class of macromolecular gels, obtained by chemical stabilization of hydrophilic polymers in a tridimensional network, in which the dispersed phase is water, present in substantial quantities.

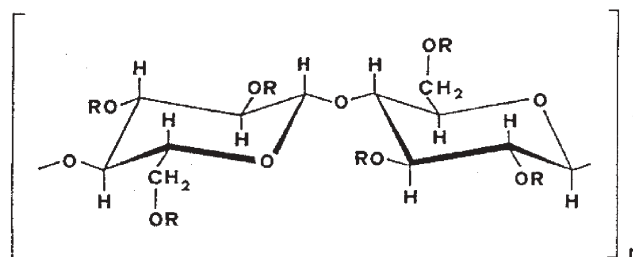
In the last fifty years, research in the field of superabsorbent products has come from the rapidly increasing demand for their application in the market of personal care absorbent products.<sup>2</sup>

The production of superabsorbents for personal care products covers almost 80% of the overall hydrogel production nowadays, and this attractive business has pushed multinational groups toward the development of new technologies both in the chemistry definition<sup>3,4</sup> and the production processes<sup>5,6</sup> of these materials. However, they are widely used also in other fields such as drug delivery,<sup>7-9</sup> biosensing,<sup>10</sup> soft actuators/valves,<sup>11</sup> and catalysis.<sup>12</sup>

An important focus of the research in this field is the material's biodegradability. Modern superabsorbents are non-biodegradable acrylamide-based products. The renewed attention of institutions and public opinion toward environmental-protection issues has awoken some producers to the

development of biodegradable superabsorbents.<sup>13</sup> A potential biodegradable cellulose-based superabsorbent, with sorption properties similar to those displayed for acrylate-based products<sup>14</sup> was recently patented.<sup>15</sup> This material was obtained by chemical crosslinking of cellulose polyelectrolyte derivatives, carboxymethylcellulose (CMC) and hydroxyethylcellulose (HEC) using small di-functional molecules as crosslinkers (divinylsulfone, DVS) which covalently bound different polymer molecules in a 3D hydrophilic network as shown in Fig. 1 and Fig. 2.

However, biodegradable superabsorbents synthesis scale up, necessary for the large scale production of these materials,



CMCNa	R= -H, -CH <sub>2</sub> COONa
HEC	R= -H, -CH <sub>2</sub> CH <sub>2</sub> OH, -CH <sub>2</sub> CH <sub>2</sub> O CH <sub>2</sub> CH <sub>2</sub> OH, -CH <sub>2</sub> CH <sub>2</sub> O CH <sub>2</sub> CH <sub>2</sub> O CH <sub>2</sub> CH <sub>2</sub> O CH <sub>2</sub> CH <sub>2</sub> OH

Fig. 1 The cellulose derivative's repeating units.

<sup>a</sup>Dipartimento di Ingegneria Chimica dei Processi e dei Materiali, Università di Palermo, Viale delle Scienze, 90128, Palermo, Italy

<sup>b</sup>Dipartimento di Ingegneria dell'Innovazione, Università di Lecce, Via Arnesano, 73100, Lecce, Italy. E-mail: giuseppe.mele@unile.it; Fax: +39 0832 297279; Tel: +39 0832 297281

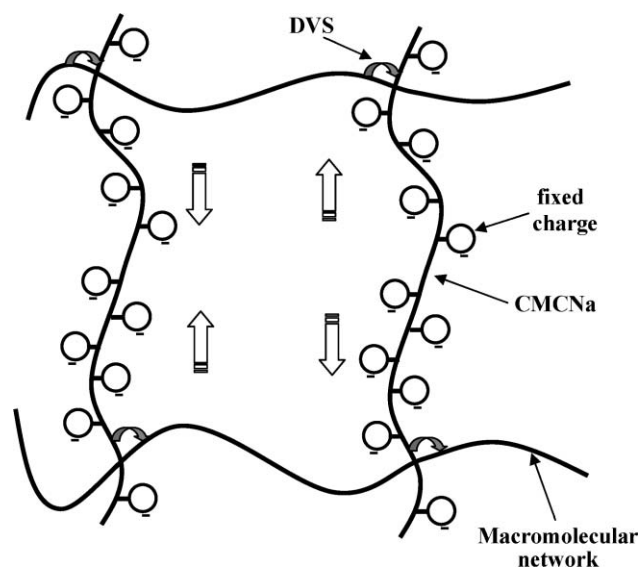


**Fig. 2** CMCNa/HEC macromolecular network, with the charged chains acting as contraction or expansion devices. Large arrows indicate the contraction or expansion of the polyelectrolyte chains.

requires large amounts of pure water. In fact, during the washing stage, the hydrogel absorbs large amounts of water, which are then expelled during the following desiccation stage.<sup>14</sup> Moreover, in order to design a connected microporosity inside the material, it has to be synthesized in a partially swollen state, and thus dried by phase inversion in a non-solvent for the polymer. Waste water contains unreacted crosslinker (DVS), unreacted polymers (cellulose derivatives) and potassium hydroxide (KOH), used as a catalyst in the crosslinking reaction, which significantly affect waste water toxicity.

In fact, over the past several years, the mutagenicity and clastogenicity of compounds capable of Michael-type reactions have been studied. These compounds, including acrylamide, several acrylate and methacrylate esters, vinyl sulfones, and phorone, have been evaluated using  $TK \pm -3.7.2$  C mouse lymphoma cells. Mutagenic chemicals induced increases in the number of small colony TK-deficient mutants. This suggested a clastogenic mechanism which was confirmed by demonstrating increases in aberrations and micronucleus frequencies in cultured cells. Vinyl sulfone was found to be the most effective chemical mutagen with induction of genotoxic effects at concentrations as low as  $0.25 \mu\text{g mL}^{-1}$ .<sup>16</sup>

Thus, a system of water purification after the synthesis-washing stage would reduce significantly the amount of waste water, allowing its re-utilization and improving the whole process environmental impact and production costs.

The oxidative purification process would be a good route for the treatment of water coming from the synthesis-washing stage. However, the complete mineralisation of organic compounds (largely beneficial in many cases) is not always achieved by means of the usual homogeneous oxidizing treatments.

Among the advanced oxidation processes aiming for environment remediation, in this case heterogeneous photocatalysis has been applied, which showed successful results in the abatement of organic and inorganic pollutants both in basic and applied research. This technique works in the presence

of irradiated polycrystalline semiconductors and  $\text{TiO}_2$  is the most popular photocatalyst due to its optical and electronic properties, low cost, chemical stability and non-toxicity.<sup>17-21</sup> Heterogeneous photocatalysis is becoming a commercial technology<sup>22,23</sup> and it is receiving increasing interest by industry. The main advantage with respect to the chemical methods is the possibility to obtain a complete mineralisation of toxic substrates even in the absence of added reagents. Additional advantages are: (i) its non-specificity; (ii) the possibility of treating effluents with very low concentrations of contaminants without lowering the reaction rate to negligible values; (iii) the possibility of operation at ambient temperature and pressure; (iv) the use of a cheap oxidant as molecular oxygen; (v) the possibility to use sunlight instead of artificial light.

## Experimental

### Materials and methods

**Hydrogel synthesis.** The hydrogel synthesis procedure is reported in this section, with the aim of highlighting all the steps of the process in which a significant amount of water and a procedure for its recovery are required.

The reaction is performed in an aqueous solution at 2% in polymer concentration by weight; DVS is added to the solution as a crosslinking agent, at a concentration which can be modulated as a function of the degree of crosslinking to be induced in the network. After complete mixing, KOH is added to the solution as a catalyst, up to a 0.02 M concentration. At this stage, the crosslinking reaction takes place and the solution viscosity rapidly increases. Reaction products are partially swollen gels. In consideration of the low concentration of polymer in the reactive mixture required to get the final product with high sorption properties, a significant amount of water is required in this step.

At this stage, a purification and desiccation procedure are required to remove the KOH, the unreacted DVS, and all the other organic impurities from the hydrogel.

The purification is carried out by swelling the material several times in distilled water, until the equilibrium sorption capacity is reached (*i.e.* the sample weight remains constant). This is, actually, the limiting stage in terms of water waste. In fact, here the hydrogel swells up to 800 times its initial weight in water, and thus large amounts of water are required to properly soak the material. As the washing stage has to be repeated several times (from 3 to 7), water coming from each washing step can be purified and reintroduced in the process with a small refill.

An environmentally friendly process of water detoxification focused on the elimination of DVS (free, partially bonded to small pieces of suspended hydrogel or bonded to small amounts of soluble oligomers) deriving from the synthesis-washing stage as well as the monitoring of the amount of harmless  $\text{SO}_4^{2-}$  anion produced by its oxidation (see Results and discussion section) allowed us to perform the safe re-utilisation of water improving the whole process environmental impact.

Two desiccation techniques can be adopted: the first of which is a phase inversion in a non-solvent for the polymer,



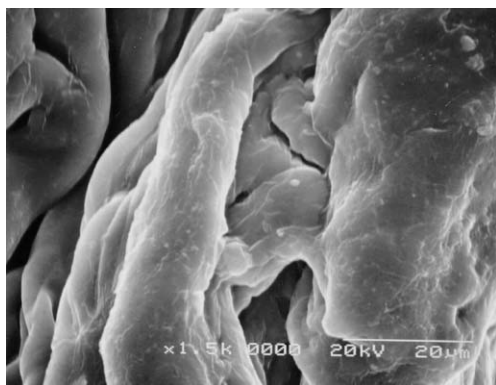


**Fig. 3** SEM picture of the CMCNa/HEC-based hydrogel desiccated by extraction in acetone. An interconnected microporosity seems to be present after the desiccation procedure.

such as acetone and the second is a simple water elimination by air atmosphere evaporation at ambient conditions. Both techniques can be applied in sequence. Although it has been demonstrated that the desiccation by phase inversion in acetone induces a connected microporosity in the dry hydrogel, which increases its sorption capacity for capillary retention effects, they scarcely influence the consumption and possibility of toxic contamination of the water in the whole process.

### Morphological analysis

The morphology of acetone dehydrated samples was examined by means of scanning electron microscopy (SEM), with the aim of detecting qualitatively the presence of a connected microporosity. Micrographs of gel surfaces were obtained using a JEOL JSM-6500 F scanning electron microscope (see Fig. 3).

### Photocatalytic experiments

A Pyrex batch photoreactor of cylindrical shape of *ca.* 0.5 L was used for the photodegradation experiments of the organics contained in the water coming from the synthesis-washing stage; three ports in its upper section allowed the inlet and outlet of air, the sampling and the temperature measurements. A 125 W medium pressure Hg lamp (Helios Italquartz) was placed in the cylinder axial position, in the middle of the photoreactor. The lamp was cooled by water circulating through a surrounding Pyrex jacket in order to avoid overheating and to cut off radiations with wavelength below 300 nm (see Fig. 4). The catalyst used for all of the experiments was commercial TiO<sub>2</sub> Degussa P25 (*ca.* 80% anatase and 20% rutile, BET surface area *ca.* 50 m<sup>2</sup> g<sup>-1</sup>) and a magnetic stirrer guaranteed a satisfactory mixing of the suspension and the uniformity of the reacting mixture. For all of the experiments the amount of catalyst was 0.8 g L<sup>-1</sup>. In this condition the photon flow transmitted by the suspension was negligible. The radiant power incident on the suspension was determined by using an UV radiometer (Digital, UVX) able to measure radiation with wavelength in the 300–400 nm range. The mean value of the radiation power impinging on the reacting suspension was equal to 13.5 mW cm<sup>-2</sup>.

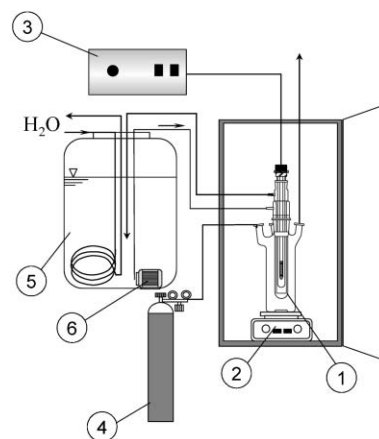


**Fig. 4** Setup of the apparatus: (1) photoreactor, (2) magnetic stirrer, (3) power supply, (4) oxygen cylinder, (5) cooling apparatus, (6) pump.

The temperature inside the reactor during the runs was  $300 \pm 2$  K. The photoreactivity runs lasted 6–7 h; before switching on the lamp the aqueous suspension was stirred and saturated by bubbling oxygen at atmospheric pressure. After 0.5 h a sample of suspension was withdrawn from the reactor, the lamp was switched on and the reactivity run started. During the runs the gas was continuously bubbled so that the steady state concentration of dissolved oxygen did not change.

Samples of 5 ml volume were withdrawn at fixed time intervals for analyses. The catalyst was immediately separated from the solution by filtration through 0.45 µm cellulose acetate filter (HA, Millipore).

The quantitative determination of total organic carbon (TOC) dissolved in the starting solution and present in the samples withdrawn from the reactor during the photocatalytic tests was performed using a 5000A Shimadzu total organic carbon (TOC) analyser.

The initial TOC concentration was *ca.* 125 mg L<sup>-1</sup> when the water coming from the synthesis-washing stage was directly treated, and *ca.* 31 mg L<sup>-1</sup> when it was diluted with distilled water.

The evolution of sulfate anion deriving from the degradation of DVS, by far the largest amount of compound present in the washing water, was followed by using an ionic chromatography system (Dionex DX 120) equipped with an Ion Pac AS14 4 mm column (250 mm long, Dionex). An aqueous solution of NaHCO<sub>3</sub> (8 mM) and Na<sub>2</sub>CO<sub>3</sub> (1 mM) was used as eluant at a flow rate of  $1.67 \times 10^{-2}$  cm<sup>3</sup> s<sup>-1</sup>.

A photoreactivity run was carried out after sonication for 0.5 h of the solution coming from the synthesis-washing stage in order to break hydrogel micro-pieces with  $\phi > 0.45$  µm (that could be retained by the filter) and to perform the TOC measurements on all the organic species present in the system.

## Results and discussion

### Hydrogel synthesis and morphological analysis

Details on the hydrogel synthesis have been extensively reported in the Experimental section. The polyelectrolyte nature of the CMC makes the development of a Donnan

equilibrium between the hydrogel and the external solution possible, strongly increasing the polymer swelling capacity.<sup>24,25</sup> High field NMR techniques<sup>26</sup> revealed a  $0.66 \pm 0.03$  degree of substitution for the carboxylic group on the CMC backbone.<sup>27</sup> The degree of substitution and the relative distribution of substituents in the C-2, C-3 and C-6 position in cellulose ethers may strongly affect the properties and the behavior of these polymers.<sup>28</sup> The distribution of substituents at the C-2, C-3 and C-6 positions of the anhydro D-glucose moiety has been determined by <sup>1</sup>H and <sup>13</sup>C NMR in solution;<sup>26</sup> the substituent groups ( $\text{CH}_2\text{COO}^- \text{Na}^+$ ) turn out to be  $\approx 40\%$  in position 3,  $\approx 40\%$  in position 6 and  $\approx 20\%$  in position 2. <sup>1</sup>H NMR studies also gave information on the network stability of the cellulose based hydrogels cross-linked through DVS.<sup>29</sup>

On the other hand, HEC is a highly hydrophilic cellulose derivative, but it is not a polyelectrolyte. The presence of HEC is necessary to promote quantitatively intermolecular rather than intramolecular crosslinking. In fact poor crosslinking efficiency is reported<sup>13</sup> if only CMCNa is used, seemingly due to the electrostatic repulsion between charged macromolecules and to the fact that few hydroxyl groups remain available for reaction at C6, the most reactive position.

Intrinsic viscosities of polymers in water have also been determined using an Ubbelohde capillary viscometer at 25 °C. Tests have been performed on a filtered solution of polysaccharides and distilled water. The values obtained were 4.5 and 3.37 dL g<sup>-1</sup> respectively for CMCNa and HEC.

Both CMCNa/HEC weight ratio and the degree of crosslinking significantly affect hydrogel equilibrium swelling properties. In fact, it has been demonstrated<sup>14,30,31</sup> that increasing the CMCNa concentration in the reactive mix increases the hydrogel swelling capacity. This is related to an osmotic pressure between the internal of the gel and the external solution, which favours the water to enter into the hydrogel, due to a Donnan effect associated to the presence of fixed charges on the polymer backbone. Moreover, increasing the DVS concentration in the reactive mixture (*i.e.* the degree of crosslinking of the network), decreases the material's equilibrium swelling capacity, and this was related to an increase of the elastic (entropic in nature) response to network expansion.

The desiccation procedure also affects dry hydrogel swelling properties. In fact, hydrogels desiccated by phase inversion with acetone show a higher degree of microporosity when compared to those desiccated in air atmosphere at ambient conditions<sup>14,30</sup> and thus a higher capillary retention capacity which increases the overall material equilibrium swelling properties.

Thus, acting both on chemical network parameters (*i.e.* CMCNa/HEC weight ratio and degree of crosslinking) and physical properties (*i.e.* dry hydrogel microporosity), it is possible to modulate the hydrogel swelling properties, designing the appropriate characteristics for each specific application.

### Photocatalytic experiments

A preliminary run was carried out in the absence of TiO<sub>2</sub>, under the same experimental conditions used for the heterogeneous systems, at the initial TOC concentration of 31.3 mg L<sup>-1</sup>. The experimental result, not reported for the sake of brevity, showed a continuous increasing of the TOC up

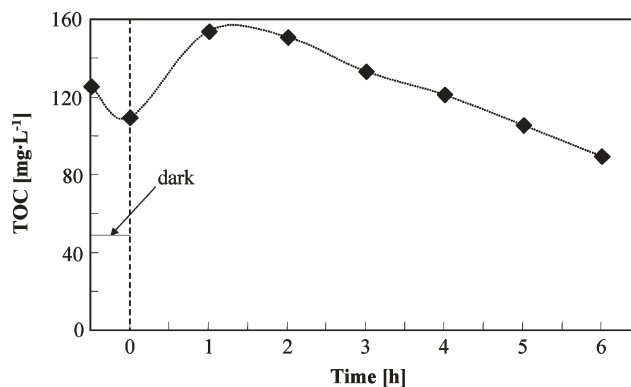


Fig. 5 Total organic carbon concentration (TOC) versus time for a representative run. TOC initial concentration: 125.7 mg L<sup>-1</sup>.

to a plateau. This finding indicates that the incident radiation is able only to break the small pieces of hydrogel present in the solution that in such a way are not retained by the 0.45 μm filter and give rise to the increase of the TOC.

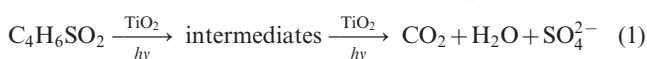
Fig. 5 reports the experimental results obtained for a representative run carried out in the presence of TiO<sub>2</sub> with an initial dissolved TOC concentration of 125.7 mg L<sup>-1</sup>. From the figure a significant decrease of the dissolved TOC during the first 0.5 h in the dark can be seen.

This finding can be attributed to the adsorption of organic molecules onto the catalyst surface. On the contrary, an initial increase of TOC was observed during the first hour when the lamp was switched on. This increase was due both to a photodesorption of organic species and also to the break of the small pieces of hydrogel present in the solution. Subsequently the dissolved TOC content continuously decreased although, due to the high initial concentration, the duration of the run (6 h) was not sufficient to obtain the total mineralization of the organic molecules present in the solution.

Some runs were carried out diluting the washing-water to study the feasibility of the process by reducing the mineralization times. In Fig. 6 results from a representative run are reported: a behavior similar to that observed for runs performed in the presence of larger amounts of initial dissolved TOC can be seen and an almost complete mineralization was achieved after *ca.* 6 h.

Although the dilution process implies the use of additional volumes of water, it is worth noticing that the treated effluents can be reutilized in the preparation and washing processes. On the other hand, the initial concentration of DVS could be modulated not only as a function of the degree of crosslinking to be induced in the network, but also in order to obtain more diluted solutions to be treated more efficiently by heterogeneous photocatalysis.

As mentioned in the Experimental section, sulfate anions were produced during the oxidative degradation of soluble DVS and its derivatives obtained from the synthetic and washing processes. The evolution of sulfate anions indicated that all the sulfur deriving from DVS and dissolved in the washing water was transformed in SO<sub>4</sub><sup>2-</sup> (eqn (1)).



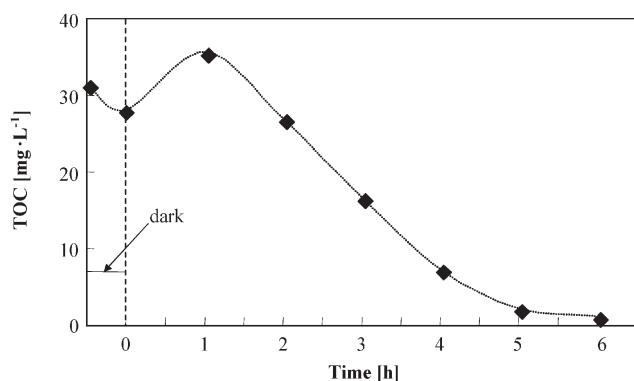
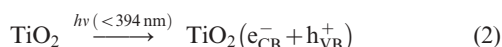
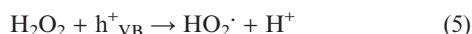
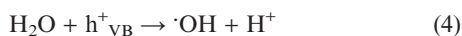


**Fig. 6** Total organic carbon concentration (TOC) versus time carried out by using a diluted solution. TOC initial concentration: 31.3 mg L<sup>-1</sup>.

As it is well known, the photoinduced process of charge separation promoted by UV radiation, reported in eqn (2), represents the key step to produce  $\cdot\text{OH}$ ,  $\cdot\text{O}_2\text{H}$ ,  $\cdot\text{O}_2^-$  radical species responsible for the effective oxidative degradation processes.<sup>19–21,32</sup>



In eqns (3)–(5) the role of holes to induce the formation of oxidant radical species is reported:



As far as the electrons are concerned, eqns (6) and (7) show some possible reactions producing reactive intermediates.

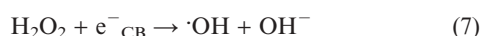
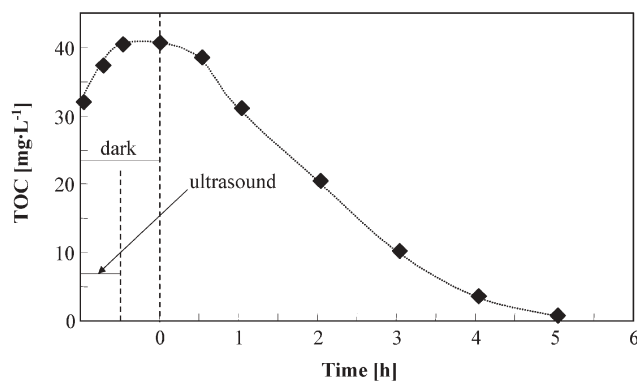
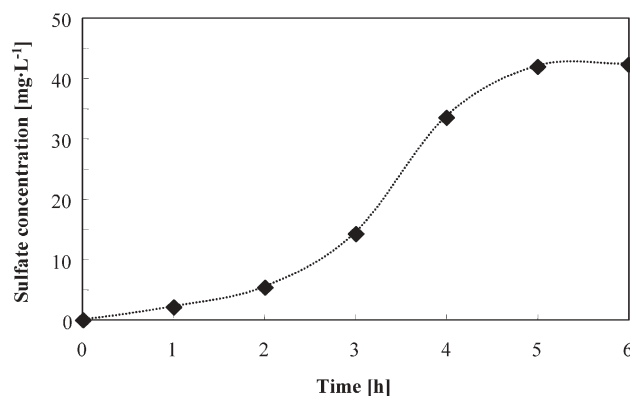


Fig. 7 reports TOC results for a run carried out by using the diluted solution after an ultrasound treatment that lasted 0.5 h. It can be observed that TOC concentration increased during the ultrasound treatment from 31.3 mg L<sup>-1</sup> to 40.5 mg L<sup>-1</sup>, due to breaking of the small pieces of hydrogel present in the solution, it remained almost constant for the further 0.5 h in the dark and then decreased when the lamp was switched on. It is worth noticing that for this run carried out after an ultrasound treatment, an almost complete mineralization was reached after *ca.* 5 h instead of 6 h of irradiation needed for the corresponding run performed without any preliminary ultrasound treatment.

In Fig. 8 the formation of sulfate ions during a representative photodegradation run carried out by using a diluted solution after its sonication is reported. It can be observed the achievement of a plateau after 5 h irradiation time corresponding to the complete disappearance of TOC (see Fig. 7). The plateau corresponds to an initial TOC concentration, due to



**Fig. 7** Organic carbon concentration (TOC) versus time carried out by using a diluted solution and a 0.5 h ultrasound pre-treatment. TOC initial concentration: 31.3 mg L<sup>-1</sup> (40.5 mg L<sup>-1</sup> after sonication).



**Fig. 8** Sulfate concentration versus irradiation time for a run carried out by starting from an initial TOC concentration of 31.3 mg L<sup>-1</sup> (40.5 mg L<sup>-1</sup> after sonication).

the presence of DVS, equal to *ca.* 21 mg L<sup>-1</sup>. Consequently *ca.* 19 mg L<sup>-1</sup> of TOC can be attributed to the other organic species present in the aqueous effluent.

## Conclusions

A preparation procedure has been set up for a novel class of superabsorbents, which consists of cellulose-based crosslinked hydrogels, able to absorb large amounts of water and is totally biodegradable.

Since hydrogels are prepared in their swollen state, and they need to be abundantly washed before the desiccation—most applications are needed in the dry state—significant amounts of waste water are produced during synthesis, which would make the process environmentally harvesting and not economically interesting. Here, a photocatalytic process has been set up in order to largely reduce the amounts of waste water, allowing its re-utilization with a low environmental impact procedure.

The results indicate that complete photodegradation of the organics present in the washing water can be achieved after *ca.* 5 h of irradiation and a previous ultrasound treatment.

## Acknowledgements

The authors wish to thank the “Ministero dell’Istruzione, Università e Ricerca” (MIUR) for financial support.

## References

- 1 J. R. Gross, *The Evolution of Absorbent Materials in Absorbent Polymer Technology*, ed. L. Brannon-Peppas and R. S. Harland, Elsevier, Amsterdam, 1990.
- 2 F. Masuda, *Superabsorbent Polymers*, Japan Polymer Society, Kyoritsu Shuppan, 1987.
- 3 J. P. Baker, D. R. Stephens, H. W. Blanch and J. M. Prausnitz, *Macromolecules*, 1992, **25**, 1955–1958.
- 4 H. H. Hooper, D. R. Baker, H. W. Blanch and J. M. Prausnitz, *Macromolecules*, 1990, **23**, 1096–1104.
- 5 H. Takeda and Y. Taniguchi, *US Pat.*, 4 525 527, 1985.
- 6 Y. Irie, K. Iwasaki, T. Hatsuda, K. Kimura, N. Harada, K. Ishizaki, T. Shimomura and T. Fujiwara, *US Pat.*, 4 920 202, 1990.
- 7 T. G. Park, *Biomaterials*, 1999, **20**, 517–521.
- 8 K. Makino, J. Hiyoshi and H. Ohshima, *Colloids Surf., B*, 2001, **20**, 341–346.
- 9 H. Ichikawa and Y. Fukumori, *J. Controlled Release*, 2000, **63**, 107–119.
- 10 J. H. Holtz and S. A. Asher, *Nature*, 1997, **389**, 829–832.
- 11 D. J. Beebe, J. S. Moore, J. M. Bauer, Q. Yu, R. H. Liu, C. Devadoss and B. H. Jo, *Nature*, 2000, **404**, 588–590.
- 12 D. E. Bergbreiter, B. L. Case, Y. S. Liu and J. W. Caraway, *Macromolecules*, 1998, **31**, 6053–6062.
- 13 U. Anbergen and W. Opperman, *Polymer*, 1990, **31**, 1854.
- 14 F. Esposito, M. A. Del Nobile, G. Mensitieri and L. Nicolais, *J. Appl. Polym. Sci.*, 1996, **60**, 2403–2407.
- 15 M. A. Del Nobile, F. Esposito, G. Mensitieri and A. Sannino, *WO Pat.* 98/58686, 1998.
- 16 K. L. Dearfield, K. Harrington-Brock, C. L. Doerr, J. R. Rabinowitz and M. M. Moore, *Mutagenesis*, 1991, **6**, 519–525.
- 17 V. Augugliaro, L. Palmisano, A. Sclafani, C. Minero and E. Pelizzetti, *Toxicol. Environ. Chem.*, 1988, **16**, 89–109.
- 18 V. Augugliaro, V. Loddo, G. Marci, L. Palmisano and M. J. López-Muñoz, *J. Catal.*, 1997, **166**, 272–283.
- 19 E. Pelizzetti and N. Serpone, *Photocatalysis. Fundamental and Applications*, Wiley, New York, 1989.
- 20 *Heterogeneous Photocatalysis*, ed. M. Schiavello, *Wiley Series in Photoscience and Photoengineering*, John Wiley and Sons, Chichester, 1997, vol. 3.
- 21 L. Palmisano, *Processi e Metodologie per il Trattamento delle Acque*, Edizioni Spiegel, Milano, Italy, 2000.
- 22 *Photocatalytic Purification and Treatment of Water and Air*, ed. D. F. Ollis and H. Al-Ekabi, Elsevier, Amsterdam, 1993.
- 23 *TiO<sub>2</sub> Photocatalysis. Fundamentals and Applications*, ed. A. Fujishima, K. Hashimoto and T. Watanabe, BKC Inc., Tokyo, 1999.
- 24 I. Kagawa and K. Katsura, *J. Polym. Sci.*, 1951, **7**, 89.
- 25 F. H. Chowdhury and S. M. Neale, *J. Polym. Sci.*, 1963, **1**, 2881.
- 26 D. Capitani, F. Porro and A. L. Segre, *Carbohydr. Polym.*, 2000, **42**, 3, 283–286.
- 27 D. Capitani, M. A. Del Nobile, G. Mensitieri, A. Sannino and A. L. Segre, *Macromolecules*, 2000, **33**, 430–437.
- 28 S. P. Rowland, in *Encyclopedia of Polymer Science*, ed. F. Mark and W. M. Bikales, Wiley, New York, 1976, pp. 146–175.
- 29 A. Sannino, M. Madaghiele, F. Conversano, G. Mele, A. Maffezzoli, P. A. Netti, L. Ambrosio and L. Nicolais, *Biomacromolecules*, 2004, **5**, 92–96.
- 30 A. Sannino, G. Mensitieri and L. Nicolais, *J. Appl. Polym. Sci.*, 2004, **91**, 3791–3796.
- 31 A. Sannino and L. Nicolais, *Polymer*, 2005, **46**, 4676–4685.
- 32 G. Mele, R. Del Sole, G. Vasapollo, G. Marci, E. García-López, L. Palmisano, J. M. Coronado, M. D. Hernández-Alonso, C. Malitesta and R. Guascito, *J. Phys. Chem. B*, 2005, **109**, 12347–12352.

# Hydrogenation of citral in supercritical CO<sub>2</sub> using a heterogeneous Ni(II) catalyst†

Maya Chatterjee,<sup>a</sup> Abhijit Chatterjee,<sup>b</sup> Poovathinthodiyil Raveendran<sup>a</sup> and Yutaka Ikushima<sup>\*ac</sup>

Received 8th December 2005, Accepted 22nd February 2006

First published as an Advance Article on the web 20th March 2006

DOI: 10.1039/b517440f

Ni(II)-catalyzed hydrogenation of citral in supercritical carbon dioxide (scCO<sub>2</sub>) results in the selective hydrogenation of C=O over C=C. The catalyst is completely inactive in conventional organic solvents. However, in presence of small amounts of CO<sub>2</sub> in the organic solvent, the catalyst become active to the citral hydrogenation. Theoretical calculations and spectroscopic studies suggest the probability of the formation of a complex between CO<sub>2</sub> and Ni(II) during the reaction. This, along with unique physical properties of scCO<sub>2</sub>, may be an important factor in directing the activity and selectivity of the reaction.

## Introduction

Supercritical carbon dioxide (scCO<sub>2</sub>) is currently considered as a promising “green” reaction medium for rapid and selective organic synthesis, and several other industrial processes.<sup>1–5</sup> Over the past few years, a number of heterogeneously catalyzed reactions have been successfully carried out in scCO<sub>2</sub>, often with higher reaction rates and different product distributions, as well as high selectivity, in comparison with those in conventional organic solvents.<sup>6–8</sup> The origin of the observed selectivity is of importance in view of the current developments in the understanding of the solvent attributes of supercritical CO<sub>2</sub><sup>9–12</sup> and the interesting supramolecular interactions<sup>13</sup> reported for CO<sub>2</sub>.

Most often, scCO<sub>2</sub> is described as a non-polar solvent with a low dielectric constant (and zero dipole moment), comparable to that for hydrocarbons. However, recent papers<sup>9–13</sup> have indicated that the charge polarized CO<sub>2</sub> molecule can act as a Lewis acid or a Lewis base. In fact, it has been reported that the oxygen atoms of CO<sub>2</sub> can participate in conventional<sup>14</sup> and unconventional<sup>15</sup> hydrogen bonds with various proton donor systems. The supramolecular interactions of CO<sub>2</sub> give rise to interesting electronic and optical properties in various systems<sup>13</sup> and govern the solvation of several molecular systems carrying relatively polar functional groups, such as acetates.<sup>15</sup> In addition, some previous reports show that CO<sub>2</sub> also plays the role of a protecting group in chemical reactions.<sup>6–8</sup> Thus, it is pertinent to explore whether CO<sub>2</sub> is capable of mediating any selectivity in homogeneously or heterogeneously catalyzed organic reactions, as opposed to its conventional description as an inert reaction medium. The unique physical properties of scCO<sub>2</sub> is also relevant in this context.

In the present study, we report the highly selective Ni(II)-catalyzed hydrogenation of an  $\alpha,\beta$ -unsaturated aldehyde (citral) into the corresponding unsaturated alcohol in scCO<sub>2</sub>. We also explore the plausible reaction paths using density functional (DFT) calculations, since such studies often provide excellent insights to understand the reaction mechanisms.

Selective hydrogenation of  $\alpha,\beta$ -unsaturated aldehydes to form unsaturated alcohols is an important issue in the manufacturing of fine chemicals and pharmaceutically important molecular systems. For example, unsaturated alcohols such as geraniol have been widely used for flavor and fragrance, as well as in the production of biologically active systems such as phomactin (a platelet activating factor antagonist).<sup>16</sup> Although, there are several homogeneous and heterogeneous catalytic approaches reported for this transformation, in most cases selective hydrogenation of the C=O bond in preference to the C=C bond is still a challenge. In search of suitable catalysts, extensive studies have been carried out in conventional organic solvents.<sup>17</sup> However, those methods require extreme conditions like high temperature and raise environmental concerns. In order to follow the ‘green’ footsteps,<sup>18</sup> scCO<sub>2</sub>, ionic liquid and a combination of these were used for the selective hydrogenation of  $\alpha,\beta$ -unsaturated aldehyde using noble metal catalyst on various supports. Nickel catalysed selective hydrogenation in scCO<sub>2</sub> is not so well documented. Here, we used Ni(II) and Ni(0) supported on mesoporous silica (MCM-41) as catalysts for the selective hydrogenation of citral and extended the method to other  $\alpha,\beta$ -unsaturated aldehydes in scCO<sub>2</sub>.

## Results and discussions

Citral hydrogenation presents a complex reaction network. Scheme 1 displays a sufficiently descriptive reaction network under the present reaction conditions. Table 1 summarises the conversion and selectivities obtained at various CO<sub>2</sub> pressures using Ni(II) and Ni(0) catalysts. The effect due the change in phase behavior is important and can give rise to significant changes in conversion and selectivity. From the phase behavior studies it is observed that, the solubility of citral increases with

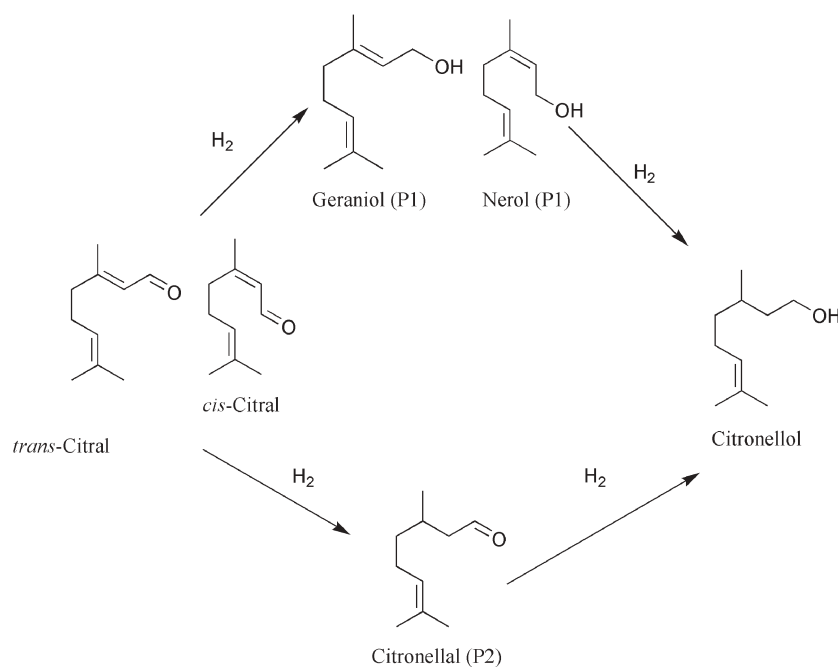
<sup>a</sup>Research Center for Compact Chemical Process, AIST, Tohoku, 4-2-1 Nigatake, Miyagino-ku, Sendai-983-8551, Japan.

E-mail: y-ikushima@aist.go.jp; Fax: 81 22 237 5214; Tel: 81 22 237 5211

<sup>b</sup>Accelrys K K, Nishi-shimbashi, Minato-ku, Tokyo 105-0003, Japan

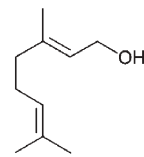
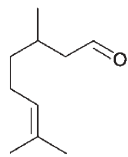
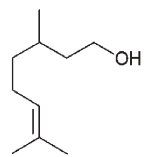
<sup>c</sup>CREST, Japan Science and Technology, Kawaguchi, Japan

† Electronic supplementary information (ESI) available: hydrogenation of citral in supercritical carbon dioxide using a Ni(II) catalyst. See DOI: 10.1039/b517440f



**Scheme 1** Reaction network of citral hydrogenation under the reaction conditions studied.

**Table 1** Conversion and product selectivity for Ni(II) and Ni(0) catalyzed citral hydrogenation. Data in parenthesis are for Ni(0)<sup>a</sup>

Run	Total pressure/MPa	Conversion (%)	Selectivity (%)		
					
1	11	50.5 (37.2)	10.6 (0.0)	50.1 (55.1)	39.3 (44.9)
2	12	52.1 (40.1)	18.2 (0.0)	48.9 (67.5)	32.8 (42.8)
3	13	53.5 (51.5)	40.2 (0.0)	41.0 (68.3)	18.8 (31.7)
4	14	60.9 (56.5)	75.0 (0.0)	25.0 (77.8)	0.0 (22.2)
5	16	76.5 (62.5)	87.8 (0.0)	12.2 (88.2)	0.0 (11.8)
6	17	80.5 (70.2)	97.3 (0.0)	2.8 (95.3)	0.0 (4.7)
7	20	81.2 (72.5)	96.0 (0.0)	4.0 (96.8)	0.0 (3.2)

<sup>a</sup> Reaction conditions: temperature = 70 °C; time = 2 h; total pressure =  $P_{H_2}$  (4 MPa) +  $P_{CO_2}$ .

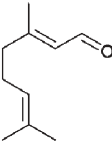
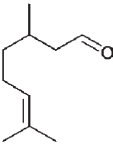
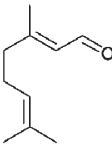
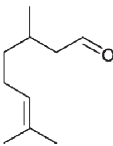
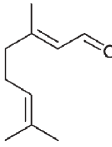
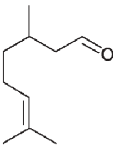
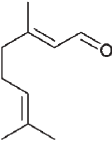
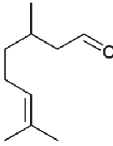
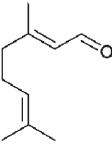
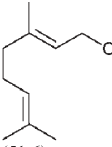
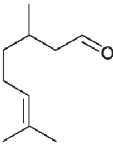
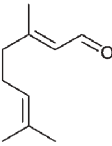
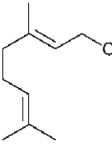
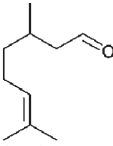
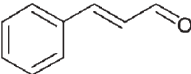
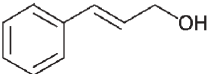
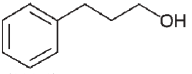
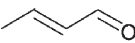


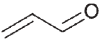


increasing CO<sub>2</sub> pressure/density and a single phase appears at a total pressure of ~16 MPa ( $P_{H_2}$  = 4 MPa and the rest is CO<sub>2</sub>; temperature = 70 °C; amount of citral = 1.5 mmol; size of the view cell = 10 ml). Typically, in the biphasic region, the conversion is low, but it increases from ~50% to ~80% with the transformation of the system from biphasic to single phase because of the absence of mass transfer limitation caused by phase borders. At a constant temperature of 70 °C, CO<sub>2</sub> pressure dependant selectivity of geraniol/nerol shows a maximum selectivity of 97% (Table 1; run 6) as the system reaches single phase. For supercritical fluid the variation of density causes a change in the physical or chemical equilibrium and can affect the catalytic activity of the reaction.

On the contrary, over the entire pressure range studied, the Ni(0)-catalyzed reaction does not hydrogenate the C=O of citral. The maximum selectivity observed of citronellal (hydrogenated product of C=C) is 96.8% (Table 1; run 7; data in the parentheses).

In order to compare the conversion and selectivity in scCO<sub>2</sub> with those in conventional solvents, we have carried out systematic investigations in several organic solvents and the results are given in Table 2. Surprisingly, the Ni(II) catalyzed reaction did not take place at all in conventional organic solvents (Table 2; runs 1–4), whereas Ni(0) hydrogenates C=C selectively. Furthermore, other  $\alpha,\beta$ -unsaturated aldehydes also undergo similar selective hydrogenation of C=O in scCO<sub>2</sub> in the presence of Ni(II) catalyst (Table 2; run 7–9). For example, cinnamaldehyde produces cinnamyl alcohol (~78%), crotyl alcohol was obtained from crotonaldehyde and allyl alcohol from acrolein with ~83% and ~70% selectivity, respectively.

For Ni(II) the trend in catalytic activity differs widely depending on the reaction medium. In scCO<sub>2</sub>, Ni(II) is active and selective to the hydrogenation of C=O; however, it remains inactive in the conventional organic solvents used. This drastic change in the behaviour of Ni(II) in organic solvents in comparison with that in scCO<sub>2</sub> suggests an

**Table 2** Product selectivity for Ni(II) and Ni(0) catalyzed hydrogenation of various substrates in scCO<sub>2</sub> and in different organic solvents<sup>c</sup>

Run	Substrate	Solvent	Product selectivity (%)	
			Ni(II)	Ni(0)
1		Hexane	No reaction	 (50.1)
2		Propanol	No reaction	 (77.4)
3		Ethanol	No reaction	 (80.6)
4		Toluene	No reaction	 (100.0)
5 <sup>a</sup>		Toluene + CO <sub>2</sub> (0.2 MPa)	 (51.6)	 (99.5)
6		scCO <sub>2</sub>	 (97.9)	 (95.3)
7		scCO <sub>2</sub>	 (77.8)	 (100.0)
8 <sup>b</sup>		scCO <sub>2</sub>	 (83.0)	 (71.4)
9 <sup>b</sup>		scCO <sub>2</sub>	 (72.5)	 (86.5)

<sup>a</sup> For toluene experiments in the presence of CO<sub>2</sub>: toluene (5 ml),  $P_{H_2} = 4$  MPa. <sup>b</sup> Time = 4 h. <sup>c</sup> Reaction conditions: temperature = 70 °C; time = 2 h; total pressure =  $P_{H_2}$  (4 MPa) +  $P_{CO_2} = 20$  MPa; volume of the organic solvent = 5 ml.

important role for the medium. The role of solvents in catalytic processes is complicated, especially for scCO<sub>2</sub>. In some cases it is inert: however in other cases CO<sub>2</sub> interacts with some functional groups and can thus impact on the chemical

transformation.<sup>19</sup> In order to probe whether the surprising selectivity can be attributed to the specific nature of CO<sub>2</sub> (since the supercritical phase itself can give rise to differences in chemical reactivity because of its physical differences from the

conventional media), citral hydrogenation was carried out in a mixture of toluene and a very small amount of CO<sub>2</sub> (0.2 MPa; Table 2; run 5). Interestingly, in the presence of CO<sub>2</sub>, Ni(II) shows catalytic activity in toluene medium although the conversion (10.9%) is low. The activity of the Ni(II) catalyst in the CO<sub>2</sub>-toluene phase might also result from the CO<sub>2</sub>-expanded properties of solvent. However, in the present case, such a contribution is insignificant, in view of the low concentration of CO<sub>2</sub> in the medium.

Considering the entire scenario, it might be possible to hypothesize that the chemical and physical attributes of scCO<sub>2</sub> play significant roles in the observed conversion and selectivity of the Ni(II) catalyzed reaction. The chemical participation of the medium might also result from the direct interaction between the substrate and CO<sub>2</sub>, which is particularly important in view of the Lewis acid-Lewis base interactions and hydrogen bonding reported<sup>6</sup> in acetaldehyde-CO<sub>2</sub> complexes. But, we observed that the reaction does not take place in the absence of the Ni(II) catalyst as well as without scCO<sub>2</sub>. This suggests that the observed selectivity is either due to a direct interaction between Ni(II) and the substrate or a coupled three-body interaction operating among the catalyst, solvent, and the substrate. The possibility of Ni(II)-substrate interaction is expectedly similar in scCO<sub>2</sub> and conventional organic solvents. Since the reaction does not take place in the conventional organic solvents studied, the possibility of a coupled substrate-catalyst-solvent interaction guiding the observed reaction and the selectivity becomes important. In other words, scCO<sub>2</sub> not only acts as a medium, but also takes part in the transition of the reactant to the product, by participating in an energetically favorable mechanism involving the substrate, catalyst and CO<sub>2</sub>. It is plausible that the electron deficient Ni(II) can attack CO<sub>2</sub> easily, forming a complex. As we have mentioned earlier, CO<sub>2</sub> is not a non-polar solvent but a quadrupolar solvent. There is a clear charge separation in the CO<sub>2</sub> molecule leaving a partial positive and negative charge towards the carbon and oxygen, respectively. The complex formation of Ni(II) with CO<sub>2</sub> makes the carbon more positive, which then probably dictates the preferential hydrogenation of C=O over C=C. It is difficult to probe such a complex solvent participation, although there is experimental evidence reported for the formation of complexes between CO<sub>2</sub> and transition metal ions.<sup>20</sup> *In-situ* FTIR studies on the catalyst surface during the reaction furnish an asymmetric stretching band at 2360 cm<sup>-1</sup> (see Electronic Supplementary Information (ESI)†). This band is shifted by 11 cm<sup>-1</sup> from that for free CO<sub>2</sub> (2349 cm<sup>-1</sup>),<sup>21</sup> which may be due to a weak attachment of Ni(II) to CO<sub>2</sub>.<sup>22</sup>

Although experimental evidence can be correlated to intuitive models to some extent, it is important to identify the transition states, which could have a decisive influence on the selectivity of a particular reaction. In this context, we carried out calculations using density functional theory (see ESI for details†) to give an accurate description of transition states and the reaction mechanism. In view of the reported geometries for the transition metal complexes of CO<sub>2</sub>, we have considered two different types of geometries in the present case: (A) coordination *via* O only<sup>23</sup> and (B) C=O coordination.<sup>24</sup> However, based on energy considerations, the B-type

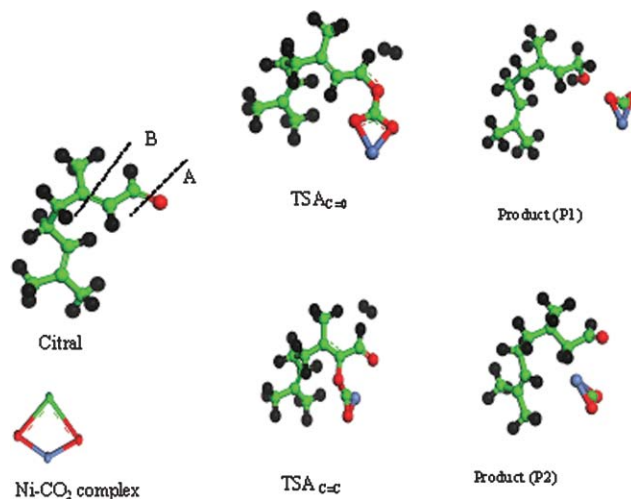


**Fig. 1** Interaction of citral with Ni-CO<sub>2</sub> complex: (A) through C=O, proposed reaction intermediates TSA<sub>C=O</sub> and the corresponding product (P1); (B) through C=C, proposed reaction intermediates TSA<sub>C=C</sub> and the corresponding product (P2) in scCO<sub>2</sub>. The colour schemes for various atoms are: red (O); black (H); blue (Ni) and green (C).

geometries were excluded. Fig. 1 presents the probable transition states obtained from the calculations, for the interaction of the Ni(II)-CO<sub>2</sub> complexes of type A with the C=O (TSA<sub>C=O</sub>) and C=C (TSA<sub>C=C</sub>) bonds of citral, respectively. The calculations showed that the interactions involving the C=O bond are more favorable than those with the C=C bond. A comparison between the two transition state energies (TSA<sub>C=O</sub> and TSA<sub>C=C</sub>) indicates that the TSA<sub>C=O</sub> state is energetically favored by ~25.63 kcal mol<sup>-1</sup> over the TSA<sub>C=C</sub> state, suggesting a preferential hydrogenation of the carbonyl group. This makes the C=O of citral more susceptible to Ni(II)-catalyzed hydrogenation. The energy differences for the TSA<sub>C=O</sub> and TSA<sub>C=C</sub> with the corresponding products are 61.175 kcal mol<sup>-1</sup> and 99.150 kcal mol<sup>-1</sup>, respectively. This suggests that the low barrier height of TSA<sub>C=O</sub> dictates the preferential C=O hydrogenation of citral. Thus, in the Ni(II) catalyzed reaction there could be a possibility of the chemical participation of the medium.

In organic solvent, Ni(0) selectively hydrogenates the C=C bond of citral, producing citronellal (Table 2; column 5, run 1-6). It also catalyzed reduction of cinnamaldehyde produced hydrocinnamyl alcohol (100%: Table 2, run 7, column 5), in which both the C=C and C=O bonds underwent reduction. On the other hand, crotonaldehyde (71.4%: Table 2, run 8) and acrolein (86.5% run 9, column 5) were converted to the corresponding saturated aldehydes (reduction of C=C) selectively in scCO<sub>2</sub>. For Ni(0) it is tempting to assume that, it favors C=C (146.3 kcal/mol) compared to C=O (177.6 kcal mol<sup>-1</sup>) to hydrogenate as supported by previous *ab-initio* MO studies.<sup>25</sup>

## Experimental

Citral (Aldrich, 95%, 4:3 isomers *trans:cis*), *trans*-cinnamaldehyde (Wako Pure Chemicals 98%), crotonaldehyde (Aldrich,



99%) and acrolein (Tokyo Kasei 90%) were used as received. Carbon dioxide (>99.99%) was supplied by Nippon Sanso Co. Ltd.

### Catalyst synthesis and characterization

Ni-MCM-41 was prepared by hydrothermal reaction (140 °C for 96 h) of Ni(II) sulfate (Aldrich), cetyl trimethylammonium bromide (CTAB; Merck) and tetraethyl orthosilicate (TEOS; Wako) in the presence of NaOH. The chemical composition of the starting gel was as follows: TEOS: 0.48 CTAB: 0.43 Na<sub>2</sub>O: (0.0–0.04) Ni: 62.5 H<sub>2</sub>O. The resultant gel was treated hydrothermally at 100 °C for 3 d. After that, solid product was recovered by filtration, dried, followed by calcination at 550 °C in air. To determine the oxidation state of the metal ion, XPS studies were carried out (see ESI†). Calcined catalyst indicates the presence of Ni(II) as Ni 2p<sub>3/2</sub> signal is centered at 853.5 eV as the main peak, along with a satellite peak at 561.0 eV, which can be assigned to the octahedral Ni(II) by taking into account that the same peak appears at 854.2 eV for unsupported NiO.<sup>26</sup> After the *ex-situ* reduction, at 350 °C for 2 h, the Ni 2p<sub>3/2</sub> signal obtained at 852.0 (SI-1) reveals the formation of Ni(II). Remarkably, changes in the main peak position and satellite peak were noticed between the calcined sample (SI-2) and during the reaction of Ni(II) in scCO<sub>2</sub> (SI-3). These changes are possibly consistent with the formation of different Ni species.

### Catalytic activity

All the reactions were carried out in a 50 ml stainless steel batch reactor placed in hot air circulating oven and the details are given elsewhere.<sup>18</sup> Briefly, 0.1 g of catalyst and 7.5 mmol of the reactant were introduced in the reactor 70 °C. After the required temperature was attained, H<sub>2</sub>, followed by CO<sub>2</sub>, was charged into the reactor using a high-pressure liquid pump and then compressed to the desired pressure. The product liquid was separated from the catalyst simply by filtration and identified by GC-MS, followed by quantitative analysis using a GC (HP 6890) equipped with capillary column and flame ionization detector. For all results reported, the selectivity is defined as follows:

% selectivity = concentration of the product/total concentration of product × 100.

For Ni(0), before the catalytic test, the catalyst was *ex-situ* reduced under hydrogen flow at 350 °C for 2 h and then performed the same reaction process. For organic solvent in place of CO<sub>2</sub>, 5 ml of organic solvent was used.

### Conclusions

In this work, we present the data on the selective hydrogenation of Ni(II) catalyst in scCO<sub>2</sub> and also in conventional organic solvents. The results suggested that the solvent attributes of scCO<sub>2</sub> are an important factor in dictating the activity and the selectivity of the the hydrogenation of some  $\alpha$ - $\beta$  unsaturated aldehydes. An analysis of the catalytic

activity data of Ni(II) under various solvents and reaction environments indicates that both the unique physical and chemical characteristics of scCO<sub>2</sub> play significant roles in the observed conversion and selectivity. At this stage it is difficult to differentiate the individual contribution of the physical and chemical behavior of the solvent medium and it remains an open question. Increasing research efforts are needed to elucidate the role of scCO<sub>2</sub> in different catalytic systems, which is of potential importance for this “green” alternative medium.

### References

- 1 J. M. De Simone, Z. Guan and C. S. Elsbernd, *Science*, 1992, **267**, 945.
- 2 P. G. Jessop, T. Ikariya and R. Noyori, *Science*, 1995, **269**, 1065.
- 3 J. M. Xi, X. Chen, C. M. Wai and J. L. Fulton, *J. Am. Chem. Soc.*, 1999, **121**, 2631.
- 4 K. P. Johnston, K. L. Harrison, M. J. Clarke, S. M. Howdle, M. P. Heitz, F. V. Bright, C. Carlier and T. W. Randolph, *Science*, 1996, **271**, 624.
- 5 J. Ke, B. X. Han, M. W. George, Y. K. Yan and M. Poliakoff, *J. Am. Chem. Soc.*, 2001, **123**, 3661.
- 6 A. Baiker, *Chem. Rev.*, 1999, **99**, 453.
- 7 A. Fürstner, L. Ackermann, K. Beck, H. Hori, D. Koch, K. Langeman, M. Liebl, C. Six and W. Leitner, *J. Am. Chem. Soc.*, 2001, **123**, 9000.
- 8 K. Wittmann, W. Wisniewski, R. Mynott, W. Leitner, C. L. Kranemann, T. Rische, P. Eilbracht, S. Kluwer, J. M. Ernsting and C. J. Elsevier, *Chem.–Eur. J.*, 2001, **7**, 4584.
- 9 S. G. Kazarian, M. F. Vincent, F. V. Bright, C. L. Liotta and C. A. Eckert, *J. Am. Chem. Soc.*, 1996, **118**, 1729.
- 10 P. Raveendran and S. L. Wallen, *J. Am. Chem. Soc.*, 2002, **124**, 12590; P. Raveendran, Y. Ikushima and S. L. Wallen, *Acc. Chem. Res.*, 2005, **38**, 478.
- 11 L. Reynolds, J. A. Gardecki, S. J. V. Frankland, M. L. Horng and M. Maroncelli, *J. Phys. Chem.*, 1996, **100**, 10337.
- 12 S. Saharay and S. Balasubramanian, *ChemPhysChem*, 2004, **5**, 1442.
- 13 D. M. Rudkevitch, *Angew. Chem., Int. Ed. Engl.*, 2004, **43**, 558.
- 14 A. Fuji, T. Ebata and N. Mikami, *J. Phys. Chem. A*, 2002, **106**, 10124.
- 15 P. Raveendran and S. L. Wallen, *J. Am. Chem. Soc.*, 2002, **124**, 7274; M. A. Blatchford, P. Raveendran and S. L. Wallen, *J. Am. Chem. Soc.*, 2002, **124**, 14818.
- 16 P. J. Mohr and R. L. Halcomb, *J. Am. Chem. Soc.*, 2003, **125**, 1712.
- 17 U. K. Singh and M. A. Vanice, *J. Catal.*, 2001, **199**, 73; C. Milone, M. L. Tropeano, G. Gulino, G. Neri, R. Ingoglia and S. Galvagno, *Chem. Commun.*, 2002, 868.
- 18 M. Chatterjee, F. Y. Zhao and Y. Ikushima, *Adv. Synth. Catal.*, 2004, **346**, 459; M. Chatterjee, A. Chatterjee and Y. Ikushima, *Green Chem.*, 2004, **6**, 114; M. Chatterjee, F. Zhao and Y. Ikushima, *Appl. Catal. A*, 2004, **262**, 93.
- 19 W. Leitner, *Acc. Chem. Res.*, 2002, **35**, 746.
- 20 J. Mascetti, F. Galan and I. Papai, *Coord. Chem. Rev.*, 1999, **190**, 557.
- 21 T. Shimanouchi, ‘Molecular Vibrational Frequencies’ in *NIST Chemistry Web Book. NIST standard reference database no. 69*, ed. P. J. Linstorm and W. G. Mallard, NIST, Gaithersburg, MD, 2001.
- 22 N. R. Walker, G. A. Grieves, R. S. Walters and M. A. Duncan, *Chem. Phys. Lett.*, 2003, **380**, 230.
- 23 A. M. Mebel and D.-Y. Hwang, *J. Phys. Chem. A*, 2000, **104**, 11622.
- 24 W. Leitner, *Coord. Chem. Rev.*, 1996, **153**, 257.
- 25 S. Sasaki, K. Mine, D. Taguchi and T. Arai, *Bull. Chem. Soc. Jpn.*, 1993, **66**, 3289.
- 26 J. C. Klein and D. M. Hercules, *J. Catal.*, 1983, **82**, 424.

# High conversion and productive catalyst turnovers in cross-metathesis reactions of natural oils with 2-butene†

Jim Patel,<sup>a</sup> S. Mujcinovic,<sup>a</sup> W. Roy Jackson,\*<sup>a</sup> Andrea J. Robinson,<sup>a</sup> Algirdas K. Serelis<sup>b</sup> and Chris Such<sup>b</sup>

Received 20th January 2006, Accepted 3rd March 2006

First published as an Advance Article on the web 22nd March 2006

DOI: 10.1039/b600956e

High conversion and selectivity can be obtained for the cross-metathesis of 2-butene with triglycerides and unsaturated fatty acid esters derived from natural oils. This can be achieved with remarkably high productive catalyst turnovers using second-generation ruthenium-based olefin metathesis catalysts.

## Introduction

Vegetable oils have long been established as useful raw materials for the chemical industry, and the current focus on the preference for renewable materials has stimulated a heightened interest in their application.<sup>2</sup> Recent years have seen a large amount of work based on olefin metathesis chemistry<sup>3</sup> of natural oils containing unsaturated fatty acids for the production of oleochemicals. The first report described the self-metathesis of methyl oleate and also its cross-metathesis with 3-hexene using a multi-component tungsten-based catalyst system.<sup>4</sup> Other examples of cross-metathesis of oil-derived fatty acid esters with a range of simple alkenes have since been reported using a number of catalyst systems based on W, Re and Mo.<sup>5</sup> More recent work has focused on cross-metathesis of oil-derived unsaturated esters with ethylene.<sup>6</sup>

Significant improvements in effective TONs for both self-metathesis and cross-metathesis reactions have been achieved by the use of homogeneous ruthenium-based catalysts.<sup>7–10</sup> A detailed study by workers at the Dow Chemical Company reported the most successful conditions for the cross-metathesis of methyl oleate with ethylene.<sup>11</sup> They pointed out however, that high conversions could only be achieved in a reasonable amount of time by the use of high catalyst loadings,

and that this problem needed to be overcome in order to achieve an economically viable process.

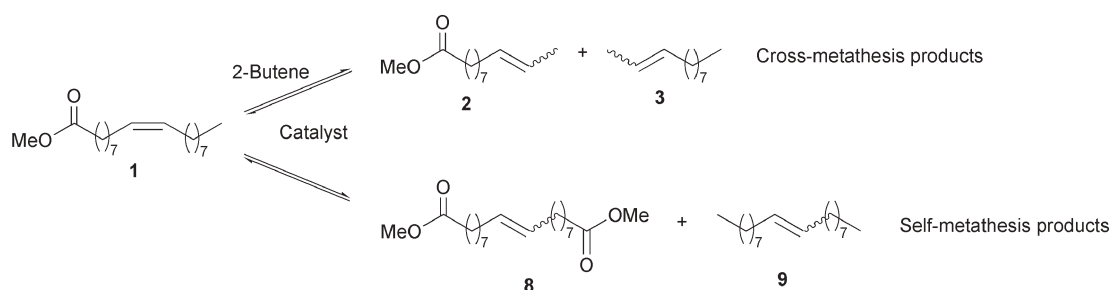
In this paper we report on experiments that extend our initial observations on cross-metathesis of 2-butene with both natural and synthetic triglycerides, showing that they can be conducted on a significant scale (300 g of triglyceride). We also describe cross-metathesis reactions of 2-butene with methyl oleate where effective TONs of up to 470 000 can be achieved if the methyl oleate is of sufficient quality.

## Results and discussion

### Cross-metathesis of 2-butene with methyl oleate

2-Butene was chosen for cross-metathesis in place of ethylene as no terminal alkenes should be present in the equilibrium system (see Scheme 1). Terminal olefins form methylidene–ruthenium intermediates and successfully compete with internal alkenes in binding to the catalyst with adverse effects on reaction time, conversion and effective TONs.<sup>11</sup> 2-Butene overcomes these problems by avoiding terminal alkenes and involving ethylidene–ruthenium intermediates, which have been shown to be more efficient initiators of metathesis reactions than methylidene intermediates and to have significantly longer half-lives.<sup>12,13</sup> Thus the reaction of 2-butene with methyl oleate (**1**) to give methyl 9-undecenoate (**2**) and 2-undecene (**3**) was attempted using homogeneous Ru-based catalysts under a variety of conditions (Scheme 1).

All metathesis reactions were conducted at atmospheric pressure and low temperature using a 10 : 1 molar ratio of 2-butene to methyl oleate. Methyl oleate was found to be soluble in liquid 2-butene at  $-5\text{ }^{\circ}\text{C}$ , and reactions were



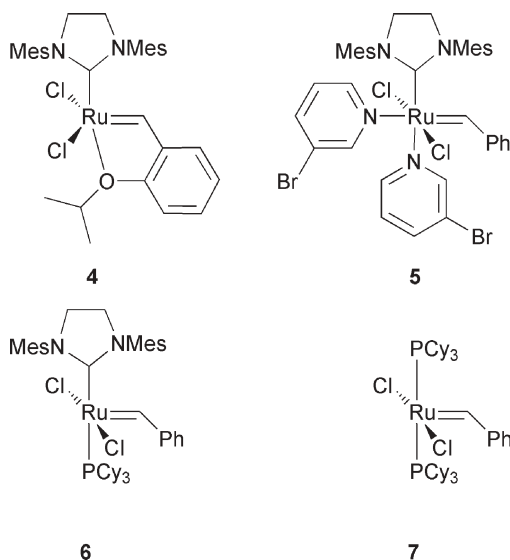
Scheme 1 Butenolysis of methyl oleate.

<sup>a</sup>Centre for Green Chemistry, School of Chemistry, P.O. Box 23, Monash University, Victoria 3800, Australia.  
E-mail: william.roy.jackson@sci.monash.edu.au; Fax: +61 399054597; Tel: +61 399054552

<sup>b</sup>Dulux Australia Technology, 1970 Princes Highway, Clayton, Victoria 3168, Australia

† For the preceding communication, see ref. 1.

conducted without additional solvent. Aliquots were removed using a pre-cooled syringe and reactions quenched by adding the samples to a solution of an excess of ethyl vinyl ether in dichloromethane prior to GC analysis.



A series of ruthenium–benzylidene olefin metathesis catalysts (**4–7**)<sup>14–17</sup> was trialled under these conditions. The best results, corresponding to effective TONs >9500, were obtained with catalysts **4** and **5** using a catalyst to methyl oleate ratio of 1 : 10 000. GC analysis of the reaction mixture after two hours showed near quantitative conversion of the methyl oleate (95%) and excellent selectivity (95%) for butenolysis products. The formation of self-metathesis products of methyl oleate (**8** and **9**) was suppressed by the use of an excess of 2-butene (Scheme 1). On the other hand, first- and second-generation Grubbs catalysts, **7** and **6** respectively, each gave very low conversion (<1%) under the same reaction conditions. The low conversion obtained with catalyst **7** was not unexpected, as 1,2-disubstituted olefins are known to display poor reactivity with this catalyst. Catalyst **6**, however, which generally gives excellent reactivity with internal olefins, probably failed to initiate under the low reaction temperature used in this study.<sup>18</sup>

Pure *cis*-2-butene was used in each of these reactions. Attempts to use a less expensive and unpurified commercially available mixture of *cis*- and *trans*-2-butene with catalysts **4** and **5** produced poor results, and only traces of butenolysis products were observed. In contrast, a laboratory-generated mixture of *cis*- and *trans*-2-butene (70 : 30), produced by isomerisation of *cis*-2-butene with catalyst **4**, gave almost identical results to those observed when pure *cis*-2-butene was employed. GC analysis of each of the 2-butene sources revealed that the commercial *cis*- and *trans*-2-butene mixture contained 2.6% of 1,3-butadiene. This diene was not observed in the commercial *cis*-2-butene source nor the laboratory-generated *cis*- and *trans*-2-butene. These results suggested that 1,3-butadiene was acting as a poison. This was supported by the observation that the addition of 1,3-butadiene (1%) to pure *cis*-2-butene produced a mixture that no longer displayed metathesis activity for the butenolysis of methyl oleate. These results are consistent with a report that the vinyl

alkylidene–ruthenium complex produced by addition of 1,3-butadiene to **7** is inactive for the metathesis of acyclic olefins.<sup>17</sup>

The influence of methyl oleate on the cross-metathesis reaction was also investigated by reacting and comparing three samples of varying purity: an as-received commercial sample, a carefully fractionated sample (single distillation) and a rigorously purified sample (triple distillation). A detailed examination of the reaction involving singly distilled methyl oleate at the 1 : 200 000 catalyst to methyl oleate ratio was shown to have maximum conversion after 60 minutes. To ensure complete conversion of all reactions a longer reaction time (4 hours) was chosen. Results are summarised in Table 1.

It can be seen that the purity of the methyl oleate has a significant impact on the effectiveness of the reaction, with high catalyst loadings necessary to obtain good conversions for reactions using the unmodified commercial sample. Dramatic improvements were observed when the commercial sample was carefully fractionated with effective TONs of up to  $470 \times 10^3$  for the triply distilled sample.

<sup>1</sup>H NMR, GC and GC–MS analysis of the three methyl oleate samples of varying purity and reactivity showed no discernible differences. The quality of the methyl oleate samples could be readily evaluated by studying their reactivity in self-metathesis reactions using catalyst **4**. Appropriate catalyst loadings for the butenolysis reactions were found to be closely related to those required to achieve equilibrium for the self-metathesis reaction.

In addition, it was found that the initially formed 2-undecene contained approximately equal amounts of the *cis* and *trans* isomers, but this mixture equilibrated over time to give an *ca.* 80 : 20 *trans* : *cis* ratio. The cross-metathesis and alkene isomerization appeared to have comparable rates and thus achievement of an 80 : 20 *trans* : *cis* ratio could be used to indicate when the cross-metathesis reaction had reached equilibrium.

A preparative scale reaction (79 g of methyl oleate) was carried out using the singly distilled sample with a catalyst : methyl oleate ratio of 1 : 100 000. A conversion of 97% (by GC) was achieved after 1 hour, and the reaction was terminated by addition of an excess of tricyclohexylphosphine relative to the catalyst. The butene was removed by distillation at temperatures below 10 °C and ethyl vinyl ether was added to the product to ensure that all traces of the very active catalyst had been quenched. A simple ambient temperature distillation at *ca.* 0.13 Pa gave a sample of 2-undecene containing 7% of

**Table 1** The effects of methyl oleate purity on reaction efficiency.

Sample of methyl oleate	Ratio of <b>4</b> to methyl oleate	Conversion (%)	Effective TON <sup>a</sup>
Commercial	1 : $5 \times 10^3$	36	$1.8 \times 10^3$
	1 : $1 \times 10^5$	<1	<1 × 10 <sup>3</sup>
Single distillation	1 : $1 \times 10^5$	95	$95 \times 10^3$
	1 : $2 \times 10^5$	80	$160 \times 10^3$
	1 : $3 \times 10^5$	58	$174 \times 10^3$
	1 : $4 \times 10^5$	21	$84 \times 10^3$
Triple distillation	1 : $5 \times 10^5$	94	$470 \times 10^3$

<sup>a</sup> Reactions were carried out with a methyl oleate : 2-butene ratio of 1 : 10 using the second-generation Hoveyda–Grubbs catalyst (**4**) at –5 °C. Analysis was performed after 4 hours.

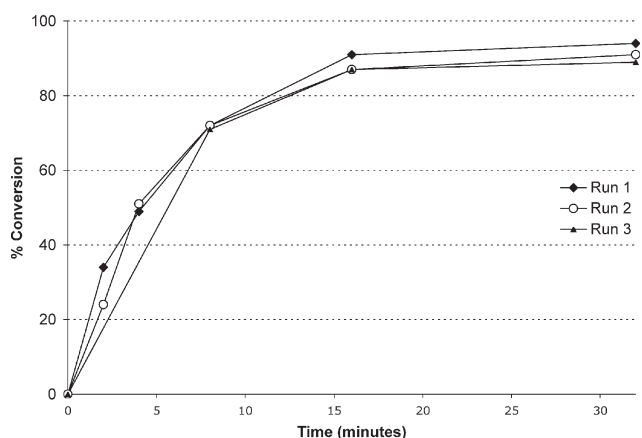


**Fig. 1** % Conversions vs. time for reactions using recovered 2-butene. Run 1, *cis*-2-butene; Run 2, recycled 2-butene (76 : 24 *trans* : *cis* mixture); Run 3, 2-butene recycled a second time (76 : 24 *trans* : *cis* mixture).

methyl 9-undecenoate and a sample of methyl 9-undecenoate containing 6% of 2-undecene. The total yield of the two products was 96%, and no other products were detected other than traces of unreacted methyl oleate and self-metathesis products.

The recovery and re-use of excess 2-butene was investigated in a series of reactions with *cis*-2-butene, singly distilled methyl oleate and **4** (**4** : methyl oleate = 1 : 200 000). Reactions were sampled periodically and quenched after 1 hour by addition of tricyclohexylphosphine. The unconsumed 2-butene was recovered by distillation below 10 °C and re-used as a 76 : 24 *trans* : *cis* mixture in further reactions, as summarised in Fig. 1. No significant loss of catalytic activity was observed after two recycles. Butene recoveries of *ca.* 75% of theoretical were achieved in these reactions, but a recovery of greater than 90% was achieved in the large-scale reaction described above.

### Cross-metathesis of 2-butene with triolein

Cross-metathesis reactions of 2-butene with a commercial sample of triolein (**10**), a model triglyceride, were carried out under identical conditions to those described for the methyl oleate reactions. Aliquots were removed using a cooled

syringe, quenched with ethyl vinyl ether and the products were transesterified by reaction with methanol and *p*-toluenesulfonic acid prior to GC analysis (Scheme 2).

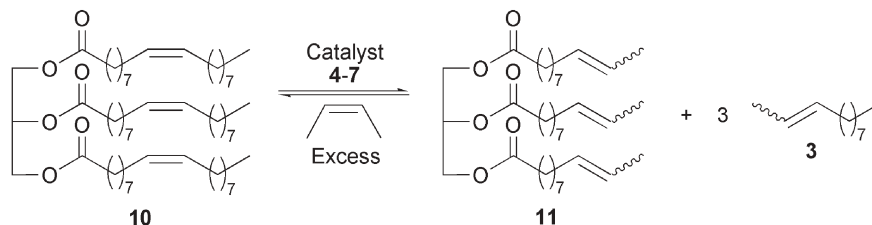
Again only traces of butenolysis products were obtained with the first- and second-generation Grubbs catalysts. A reaction using second-generation Hoveyda–Grubbs catalyst (**4**), with a catalyst to triglyceride C=C bond ratio of 1 : 100 000, gave a conversion of 92% to **11** in *ca.* 4 hours, representing an effective TON of  $92 \times 10^3$ . Reactions using a higher loading of catalyst **4** (**4** : triglyceride C=C bond = 1 : 10 000) led to 95% conversion in less than 4 minutes. The use of catalyst **5** at a similar concentration, however, resulted in a much slower reaction rate, and greater than 200 minutes was required to achieve a similar conversion.

### Cross-metathesis of 2-butene with vegetable oils

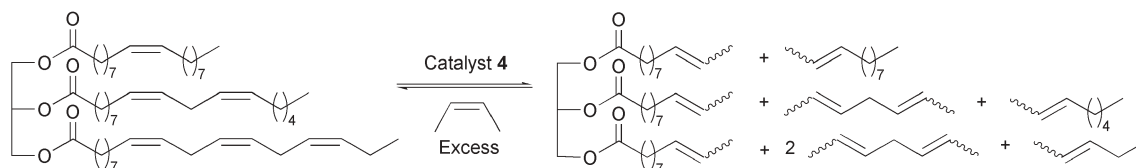
Four vegetable oils were reacted with 2-butene in the presence of catalyst **4** under conditions as close as possible to those used for the reactions with methyl oleate and triolein (**10**). Scheme 3 shows the range of alkenes which can be obtained from a model triglyceride.

The ratio of the triglyceride to 2-butene for the different vegetable oils was adjusted so that the ratio of triglyceride C=C bonds to 2-butene was maintained at 1 : 10. The type and proportion of fatty acids, and thus alkenes, in each of the oils was determined using the NMR method described by Knothe and Kenar, and the fatty acid compositions are summarised in Table 2.<sup>19</sup> Conversions were determined by quenching the reactions and converting the triglycerides to methyl esters, which were then analysed by GC. An unreactive saturated ester, methyl palmitate, was used as an internal standard.

The results in Table 2 show that effective TONs were influenced by the degree of unsaturation of the vegetable oil, with values of *ca.*  $93 \times 10^3$  for triolein,  $37\text{--}38 \times 10^3$  for canola and sunflower oils and  $23\text{--}24 \times 10^3$  for linseed and soyabean oils. The non-ester-containing alkenes shown in Scheme 3 were characterised by GC–MS. The alkenes were obtained in approximately the proportions expected for each of the vegetable oils. Each monoalkene was present as a mixture of *cis* and *trans* isomers with the *trans* isomer predominating



**Scheme 2** Cross-metathesis of 2-butene with triolein (**10**).



**Scheme 3** Products from the cross-metathesis of 2-butene with a model unsaturated natural oil containing oleic, linoleic and linolenic acids.

**Table 2** Butenolysis of natural oils with catalyst **4**

Oil	Fatty acid composition in the oil (%)				Relative number of C=C bonds	Effective TON <sup>a</sup>
	C18:1	C18:2	C18:3	Saturated		
Triolein <sup>c</sup>	100	0	0	0	1	93 × 10 <sup>3</sup>
Sunflower <sup>b,d</sup>	81	10	0	9	1	38 × 10 <sup>3</sup>
Canola <sup>d</sup>	63	18	11	8	1.3	37 × 10 <sup>3</sup>
Soya <sup>e</sup>	22	54	7	17	1.5	24 × 10 <sup>3</sup>
Linseed <sup>e</sup>	22	13	53	12	2	23 × 10 <sup>3</sup>

<sup>a</sup> Reaction time = 18 h. <sup>b</sup> High oleic. <sup>c</sup> Catalyst (**4**) : C=C = 1 : 100 × 10<sup>3</sup>. <sup>d</sup> Catalyst (**4**) : C=C = 1 : 40 × 10<sup>3</sup>. <sup>e</sup> Catalyst (**4**) : C=C = 1 : 25 × 10<sup>3</sup>.

in each case. The 2,5-heptadiene was obtained as the three possible isomers with the *trans,trans* isomer predominating.

Several large-scale reactions (300–400 g of oil) were carried out using sunflower oil (high oleic). After quenching, the non-ester alkenes were distilled off under a high vacuum and the triglycerides were subjected to methanolysis to liberate the fatty acids as their methyl esters. After separation from glycerol a single distillation gave methyl 9-undecenoate (>95% purity by GC) in high yield (*ca.* 92% based on the proportion of unsaturated fatty acids in the oil). The yield of non-ester alkenes was estimated as 83% based on the composition of the fatty acids in the oil. The major alkene product, 2-undecene, could be purified by straightforward fractional distillation.

## Conclusion

The butenolysis technology described above offers a potentially commercially applicable method for the conversion of vegetable oils into useful fine chemicals. The conversion of sunflower oil (high oleic) into methyl 9-undecenoate, and hence its commercially desirable derivative acid, and useful alkenes such as 2-undecene, has been demonstrated on a several hundred gram scale. Reaction times to achieve high conversions and effective TONs are dramatically superior to those obtained for reactions using ethylene.

## Experimental

### General

All reactions and manipulations of organometallic compounds were carried out under an argon atmosphere using glovebox and Schlenk techniques. Solvents were purified and dried according to standard procedures, stored under a nitrogen atmosphere, and freshly distilled prior to use. The catalysts **4–7** were prepared according to literature procedures.<sup>14–17</sup> Methyl oleate (99%+) was purchased from Sigma and 2-butene (*cis*-butene and a mixture of *cis* and *trans* isomers, both certified as 99%+) was sourced from Aldrich. Methyl oleate and methyl palmitate were purified by vacuum distillation through a 25 cm Vigreux column and stored under argon. Commercial samples of triolein and vegetable oils were degassed and passed through a short plug of activated alumina under argon immediately prior to use. Similarly, liquid 2-butene was passed through a short alumina plug at –5 °C under argon. All other reagents were purchased and used without further purification. GC analyses were performed on a Varian Model 3700 gas

chromatograph equipped with a 30 m × 0.53 mm 30QC51-BPX5 column (1 μm film thickness, He at 4 × 10<sup>2</sup> kPa). GC–MS analyses were performed using a Hewlett Packard gas chromatograph equipped with an Agilent MSD and a 30 m × 0.25 mm HP5S column (0.25 mm film thickness) using He as a carrier gas. NMR spectra were recorded with a Bruker 400 MHz spectrometer (<sup>1</sup>H NMR, 400.130 MHz).

### Standard procedure for butenolysis reactions

A Schlenk flask under an argon atmosphere was equipped with a magnetic stirrer bar and placed in a cold-bath set at –5 °C. The flask was charged with a fatty acid ester and *cis*-2-butene (*ca.* 4g). The reaction was initiated by the addition of a freshly prepared solution of the appropriate amount of catalyst in dichloromethane (~20 μL). The reaction mixture was monitored by removal of 50 μL samples using a pre-cooled gas-tight syringe. Each sample was quenched by addition to a solution of ethyl vinyl ether (100 μL) in dichloromethane (1 mL). Products from methyl oleate reactions were analysed directly by GC, while the products from reactions of triglycerides were transesterified with methanol by conventional means prior to analysis by GC. A known amount of methyl palmitate (as an internal standard) was added to reactions involving methyl oleate and triolein. The palmitate esters naturally present in various samples were used as the standard for the vegetable oils.

### Preparative scale butenolysis of methyl oleate

Methyl oleate (79.0 g, 0.27 mol), 2-butene (153 g, 2.73 mol) and Second-Generation Hoveyda–Grubbs catalyst (**4**) (1.70 mg, 2.66 × 10<sup>–6</sup> mol) were reacted as above for 2 h, by which time GC analysis of an aliquot showed conversion of >97%. The reaction was quenched by addition of PCy<sub>3</sub> (0.1 g) and the excess 2-butene (125 g, 91% of the theoretical recovery) was recovered by distillation under a slight vacuum at 10 °C. Ethyl vinyl ether (1 mL) was added to the residue which was distilled under vacuum (<0.13 Pa, short path) at ambient temperature to give 2-undecene (39.6 g, containing 7% methyl 9-undecenoate). The residue from the distillation was shown to be methyl 9-undecenoate (51.8 g, containing 6% 2-undecene). Pure samples of each of the products (>99% by GC) were obtained by redistillation through a 25 cm Vigreux column. 2-Undecene: <sup>1</sup>H NMR: 5.42 (m, 2H), 1.97 (m, 2H), 1.64 (m, 3H), 1.27 (m, 12H), 0.88 (t, *J* = 7.2 Hz, 3H); 18% *cis*, 82% *trans*, determined by GC and <sup>13</sup>C NMR. Methyl 9-undecenoate: <sup>1</sup>H NMR: 5.41 (m, 2H), 3.67 (s, 3H), 2.30 (t, *J* = 7.4 Hz,

2H), 1.96 (m, 2H), 1.63 (m, 5H), 1.29 (m, 8H); 18% *cis*, 82% *trans* determined by GC and  $^{13}\text{C}$  NMR.

#### Preparative scale butenolysis of sunflower seed oil (high oleic)

Sunflower seed oil (high oleic) (301 g, 0.34 mol), 2-butene (620 g, 11.1 mol) and Second-Generation Hoveyda–Grubbs catalyst (**4**) (1.60 mg,  $2.55 \times 10^{-5}$  mol) were reacted as above for 90 minutes by which time a GC analysis of an aliquot showed a high proportion of the *trans* isomer of 2-undecene (*trans* : *cis* = 4.56 : 1). The reaction was quenched by addition of  $\text{PCy}_3$  (0.15 g) and the excess 2-butene (413 g, 74% of theoretical recovery) was recovered by distillation under a slight vacuum at 10 °C. Ethyl vinyl ether (1 mL) was added to the residue, which was distilled under vacuum (<0.13 Pa, short path) at ambient temperature to give a mixture of 2,5-heptadiene, 2-octene, and 2-undecene in a *ca.* 1 : 1.4 : 43.6 ratio (determined by GC). The residue was stirred vigorously at 60 °C with anhydrous MeOH (80 mL) in the presence of NaOMe (0.23 g) for 1 h. The glycerol formed a separate layer and was removed. Additional anhydrous MeOH (40 mL) and NaOMe (0.23 g) were added and vigorous stirring was continued for 1 h at 60 °C. A second crop of glycerol was then removed, the methanol was distilled off using a rotary evaporator, and the residue was flash-distilled under vacuum (13 Pa) to give methyl 9-undecenoate (170 g, 95% pure by GC, 93% yield).

#### Acknowledgements

We thank Orica Pty Ltd for provision of funds through their Strategic Research Initiative.

#### References

- 1 J. Patel, J. Elaridi, W. R. Jackson, A. J. Robinson, A. K. Serelis and C. Such, *Chem. Commun.*, 2005, **44**, 5546.
- 2 U. Biermann, W. Friedt, S. Lang, W. Lühs, G. Machmüller, J. O. Metzger, M. Rüschen, Klaas, H. J. Schäfer and M. Schneider, *Angew. Chem., Int. Ed.*, 2000, **39**, 2206.
- 3 *Handbook of Metathesis*, ed. R. H. Grubbs, Wiley-VCH, Weinheim, 2003.
- 4 P. B. van Dam, M. C. Mittelmeijer and C. J. Boelhouwer, *J. Chem. Soc., Chem. Commun.*, 1972, **22**, 1221.
- 5 J. C. Mol, *Green Chem.*, 2002, **4**, 5.
- 6 R. H. A. Bosma, F. Van Den Aardweg and J. C. Mol, *J. Chem. Soc., Chem. Commun.*, 1981, 1132.
- 7 R. H. Grubbs, S. T. Nguyen, L. K. Johnson, M. S. Hillmyer and G. C. Fu, *World Pat.* WO 9604289, 1996.
- 8 S. Warwel, F. Bruse, C. Demes, M. Kunz and M. R. Klaas, *Chemosphere*, 2001, **43**, 39.
- 9 M. B. Dinger and J. C. Mol, *Adv. Synth. Catal.*, 2002, **344**, 671.
- 10 S. H. Hong, D. P. Sanders, C. W. Lee and R. H. Grubbs, *J. Am. Chem. Soc.*, 2005, **127**, 17160.
- 11 K. A. Burdett, L. D. Harris, P. Margl, B. R. Maughon, T. Mokhtar-Zadeh, P. C. Saucier and E. P. Wasserman, *Organometallics*, 2004, **23**, 2027.
- 12 S. E. Lehman and K. B. Wagener, *Organometallics*, 2005, **24**, 1477.
- 13 M. S. Sanford, J. A. Love and R. H. Grubbs, *J. Am. Chem. Soc.*, 2001, **123**, 6543.
- 14 S. B. Garber, J. S. Kingsbury, B. L. Gray and A. H. Hoveyda, *J. Am. Chem. Soc.*, 2000, **122**, 8168.
- 15 J. A. Love, J. P. Morgan, T. M. Trnka and R. H. Grubbs, *Angew. Chem., Int. Ed.*, 2002, **41**, 4035.
- 16 M. Scholl, S. Ding, C. W. Lee and R. H. Grubbs, *Org. Lett.*, 1999, **1**, 953.
- 17 P. Schwab, R. H. Grubbs and J. W. Ziller, *J. Am. Chem. Soc.*, 1996, **118**, 100.
- 18 S. E. Lehman and K. B. Wagener, *Macromolecules*, 2002, **35**, 48.
- 19 G. Knothe and J. A. Kenar, *Eur. J. Lipid Sci. Technol.*, 2004, **106**, 88.

# Green protocol for annulation of the *s*-triazine ring on thiazoles using a three-component coupling strategy

Lal Dhar S. Yadav,\* Seema Yadav and Vijai K. Rai

Received 13th February 2006, Accepted 3rd March 2006

First published as an Advance Article on the web 17th March 2006

DOI: 10.1039/b602123a

Novel three-component one-pot reactions of thiazole Schiff bases, ammonium acetate, and aromatic aldehydes under solvent-free microwave irradiation conditions expeditiously and diastereoselectively annulate the *s*-triazine ring on thiazoles to yield thiazolo-*s*-triazines.

## Introduction

In the context of green chemistry, the development of eco-friendly synthetic methods would be most welcome. In this respect, organic synthesis involving multi-component reactions (MCRs) under solvent-free conditions is a basic protocol because multi-step synthesis produces considerable amounts of environmentally unfavorable waste, mainly due to a series of complex isolation procedures often involving expensive, toxic and hazardous solvents after each step. Thus, MCRs are perfectly suited for combinatorial library syntheses, and are finding increasing use in discovery processes for new drugs and agrochemicals.<sup>1–7</sup>

The application of microwave (MW) irradiation as a non-conventional energy source for activation of reactions, in general and under solvent-free conditions in particular, has now gained popularity over the usual homogeneous and heterogeneous reactions, as it provides chemical processes with special attributes, such as enhanced reaction rates, higher yields of pure products, better selectivity, improved ease of manipulation, rapid optimization of reactions in parallel, and several eco-friendly advantages.<sup>8–15</sup> The application of MW irradiation to provide enhanced reaction rates and improved product yields in chemical synthesis has been extended to modern drug discovery processes,<sup>16,17</sup> and it is proving quite successful in the formation of carbon–heteroatom and carbon–carbon bonds.<sup>18,19</sup> Thus, the present synthetic protocol should be welcome in these environmentally conscious days.

Thiazole and *s*-triazine ring systems have a long history of applications in pharmaceutical and agrochemical industries. Thus, *s*-triazine annulated thiazoles appear to be attractive scaffolds to be utilized for exploiting chemical diversity.

Considering the above reports and the recently reported results of the MW-accelerated version of the Ugi three-component coupling (3cc) reactions<sup>20–22</sup> as well as our interest in devising new solvent-free cyclization methods,<sup>23–26</sup> we decided to investigate the potential of microwaves to accelerate the 3cc reaction between thiazole Schiff bases, ammonium acetate and aromatic aldehydes yielding new thiazolo-*s*-triazines, **6** (Scheme 1).

In view of achieving our goal expeditiously, we relied upon significant advantages of multi-component reactions (MCRs)

under solvent-free MW irradiation. Interestingly, the MCRs reported herein, yielding thiazolo-*s*-triazines, are among the few examples showing increased stereoselectivity under MW irradiation compared to conventional heating.<sup>12,27</sup>

## Results and discussion

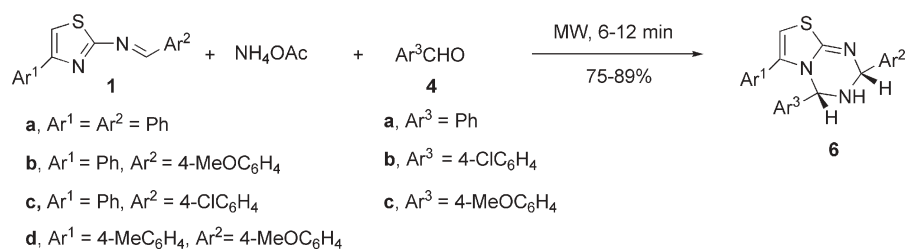
After some preliminary experimentation, it was found that the envisaged three-component synthesis (Scheme 1) was successful with an intimate mixture of the thiazole Schiff base **1**, ammonium acetate and an aromatic aldehyde **4** under intermittent MW irradiation at 100 W in a CEM Discover microwave system for the time specified in Table 1. Isolation and purification by recrystallization from ethanol afforded the thiazolo-*s*-triazines **6** in excellent yields (75–89%) with >95% diastereoselectivity (Table 1).

For comparison purposes, the final temperature was recorded immediately after the MW irradiation for 2 min and was found to reach about 90 °C from 30 °C (room temperature). The reactions were also carried out using a thermostatted oil-bath at the same temperature (90 °C) as for the MW-activated method but for a longer (optimized) period of time (Table 1) to ascertain whether the MW method improves the yield or simply increases conversion rates. It was found that significantly lower yields (21–35%) were obtained using oil-bath heating rather than the MW-activated method (Table 1). This observation may be rationalized on the basis of the formation of a dipolar activated complex from an uncharged educt in these reactions (as an example, Scheme 2 shows an activated complex **2**), and the greater stabilization of the more dipolar activated complex by dipole–dipole interactions with the electric field of microwaves, as compared to the less dipolar educt, which may reduce the activation energy ( $G^\ddagger$ ), resulting in the rate enhancement.<sup>12</sup>

The formation of **6** may be tentatively rationalized by the conjugate addition of ammonia to the Schiff base **1**, followed by condensation of the adducts **3** with aromatic aldehydes **4** to yield the final products **6** (Scheme 2). However, the possibility of *in situ* generation of aldimines **5** followed by a [4 + 2] cycloaddition to the Schiff base **1** leading to the formation of **6** (Scheme 2) could not be ruled out. The isolation of intermediates **3** and **5** was unsuccessful in the present reaction conditions.

The formation of **6** was highly diastereoselective in favor of the *cis* isomers. The diastereomeric ratios of the crude products

Department of Chemistry, University of Allahabad, Allahabad, 211 002, India. E-mail: ldsyadav@hotmail.com



6	Ar <sup>1</sup>	Ar <sup>2</sup>	Ar <sup>3</sup>	6	Ar <sup>1</sup>	Ar <sup>2</sup>	Ar <sup>3</sup>
<b>a</b>	Ph	Ph	Ph	<b>f</b>	Ph	4-ClC <sub>6</sub> H <sub>4</sub>	4-ClC <sub>6</sub> H <sub>4</sub>
<b>b</b>	Ph	Ph	4-ClC <sub>6</sub> H <sub>4</sub>	<b>g</b>	4-MeC <sub>6</sub> H <sub>4</sub>	4-ClC <sub>6</sub> H <sub>4</sub>	Ph
<b>c</b>	Ph	4-MeOC <sub>6</sub> H <sub>4</sub>	Ph	<b>h</b>	4-MeC <sub>6</sub> H <sub>4</sub>	4-ClC <sub>6</sub> H <sub>4</sub>	4-ClC <sub>6</sub> H <sub>4</sub>
<b>d</b>	Ph	4-MeOC <sub>6</sub> H <sub>4</sub>	4-ClC <sub>6</sub> H <sub>4</sub>	<b>i</b>	4-MeC <sub>6</sub> H <sub>4</sub>	4-ClC <sub>6</sub> H <sub>4</sub>	4-MeOC <sub>6</sub> H <sub>4</sub>
<b>e</b>	Ph	4-ClC <sub>6</sub> H <sub>4</sub>	Ph				

Scheme 1

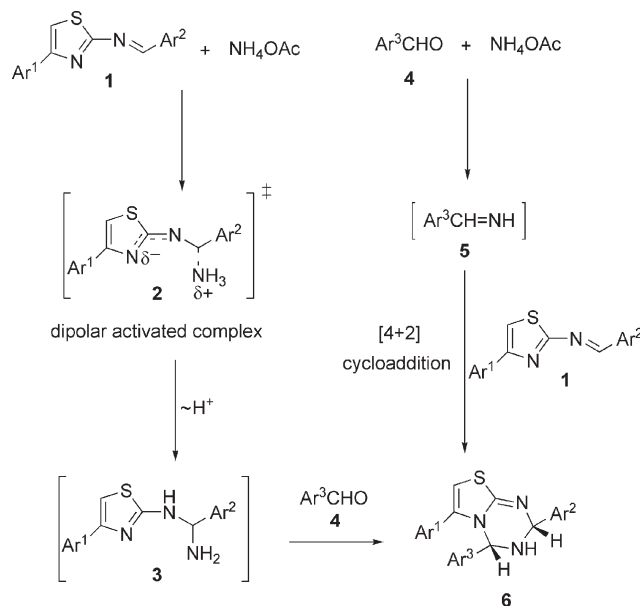
**Table 1** Solvent-free three-component synthesis of thiazolo-*s*-triazines **6**

Product	Time		Yield (%) <sup>c,d</sup>		<i>cis</i> : <i>trans</i> ratio <sup>e</sup>		Mp/ <sup>o</sup> C
	MW <sup>a</sup> /min	Thermal <sup>b</sup> /h	MW	Thermal	MW	Thermal	
<b>6a</b>	10	5	78	23	93 : 7	51 : 49	77–78
<b>6b</b>	8	4	84	31	94 : 6	53 : 47	73–74
<b>6c</b>	12	5	75	21	93 : 7	52 : 48	70–71
<b>6d</b>	10	5	81	28	94 : 6	54 : 46	75–76
<b>6e</b>	8	4	83	30	93 : 7	53 : 47	84–85
<b>6f</b>	6	3	89	35	95 : 5	57 : 43	95–96
<b>6g</b>	10	5	82	29	94 : 6	55 : 45	116–118
<b>6h</b>	8	3	86	33	96 : 4	58 : 42	82–83
<b>6i</b>	12	4	80	27	95 : 5	56 : 44	80–81

<sup>a</sup> Microwave irradiation time (power = 100 W). <sup>b</sup> Time for oil-bath heating at 90 °C. <sup>c</sup> Yield of isolated and purified product. <sup>d</sup> All compounds gave C, H and N analyses within ±0.35%, and satisfactory spectral (IR, <sup>1</sup>H NMR, <sup>13</sup>C NMR and EIMS) data. <sup>e</sup> As determined by <sup>1</sup>H NMR spectroscopy.

were checked by <sup>1</sup>H NMR prior to purification, to ensure that accurate and true diastereomeric ratios are reported. The diastereomeric ratios in the cases of MW activation were found to be >95 : <5 and those from oil-bath heating were >53 : <47 as determined by <sup>1</sup>H NMR spectroscopy. The high diastereoselectivity (>95%) in favor of the *cis* isomers under MW irradiation may be explained if the activated complex leading to the formation of the *cis* isomers is more polar than that leading to the *trans* isomers because MW irradiation favors reactions occurring *via* more polar activated complexes.<sup>12</sup> It was found that there was no evolution of any *trans* form under prolonged MW-induced and oil-bath heating of compounds **6** at 90 °C. This indicates that there is no equilibrium between the *cis* and *trans* forms.

In summary, we have developed a general, straightforward and highly diastereoselective three-component green synthetic protocol for thiazolo-*s*-triazines from readily and widely available substrates (thiazole Schiff bases and aromatic aldehydes) employing solvent-free microwave irradiation conditions.



Scheme 2

## Experimental

### General

Melting points were determined by the open glass capillary method and are uncorrected. IR spectra in KBr were recorded on a Perkin–Elmer 993 IR spectrophotometer. <sup>1</sup>H (400 MHz) and <sup>13</sup>C (100 MHz) NMR spectra were recorded on a Bruker WM-40C FT spectrometer in DMSO-*d*<sub>6</sub> using TMS as internal reference. *J* values are given in Hz. Mass spectra (EI, 70 eV) were recorded on a JEOL D-300 mass spectrometer. Elemental analyses were carried out in a Coleman automatic carbon, hydrogen, and nitrogen analyzer. A CEM Discover Focused Microwave Synthesis System operating at 2450 MHz was used at an output of 100 W for all the experiments. All



commercially available chemicals were used without further purification. Silica gel-G was used for TLC.

**Thiazolo[3,2-*a*]-*s*-triazines (6 a–i).** An intimate mixture of thiazole Schiff base **1** (2.0 mmol), ammonium acetate (3.0 mmol) and an aromatic aldehyde **4** (2.0 mmol) was placed in a 10 mL vial and subjected to MW irradiation at 100 W in a CEM Discover microwave system for 2 min. The reaction mixture was then thoroughly mixed outside the MW oven for 2 min and again irradiated for another 2 min. This intermittent irradiation–mixing cycle was repeated for the total irradiation time (Table 1). After completion of the reaction as indicated by TLC (hexane–AcOEt, 8 : 2, v/v), water (5 mL) was added, and the reaction mixture stirred well. The yellow precipitate obtained was washed with water to give the crude product, which was recrystallized from ethanol to afford a diastereomeric mixture (>95 : <5; in the crude products the ratio was >94 : <6 as determined by <sup>1</sup>H NMR spectroscopy). The product on second recrystallization from ethanol furnished analytically pure pale yellow needles of a single diastereomer **6** (Table 1), which was assigned the *cis* stereochemistry on the basis of <sup>1</sup>H NMR spectra.

**6a:** Yellowish needles (Found: C, 74.46; H, 5.39; N, 11.21). C<sub>23</sub>H<sub>19</sub>N<sub>3</sub>S requires C, 74.77; H, 5.18; N, 11.37%; mp 77–78 °C (from EtOH);  $\nu_{\max}(\text{KBr})/\text{cm}^{-1}$  3342, 3050, 1604, 1574, 1460, and 1310;  $\delta_{\text{H}}(400 \text{ MHz; DMSO-}d_6/\text{TMS})$  3.13 (1 H, br s, NH exchanges with D<sub>2</sub>O), 6.69 (1 H, d, *J* 8, 4-H), 6.79 (1 H, d, *J* 8, 2-H), and 7.61–7.88 (16 H<sub>arom</sub>, m);  $\delta_{\text{C}}(100 \text{ MHz; DMSO-}d_6/\text{TMS})$  75.2 (4-C), 76.3 (2-C), 118.1 (7-C), 127.0, 127.7, 128.3, 129.0, 129.6, 130.5, 131.1, 131.8, 132.6, 133.5, 134.1, 134.8 (3 × Ph), 150.1 (6-C), and 159.5 (SC=N); *m/z* 369 (M<sup>+</sup>).

**6b:** Yellowish needles (Found: C, 68.09; H, 4.61; N, 10.58). C<sub>23</sub>H<sub>18</sub>ClN<sub>3</sub>S requires C, 68.39; H, 4.49; N, 10.40%; mp 73–74 °C (from EtOH);  $\nu_{\max}(\text{KBr})/\text{cm}^{-1}$  3346, 3059, 1605, 1586, 1442, and 1315;  $\delta_{\text{H}}(400 \text{ MHz; DMSO-}d_6/\text{TMS})$  3.16 (1 H, br s, NH exchanges with D<sub>2</sub>O), 6.71 (1 H, d, *J* 8, 4-H), 6.83 (1 H, d, *J* 8, 2-H), and 7.18–7.92 (15 H<sub>arom</sub>, m);  $\delta_{\text{C}}(100 \text{ MHz; DMSO-}d_6/\text{TMS})$  75.4 (4-C), 76.5 (2-C), 118.4 (7-C), 127.2, 127.8, 128.5, 129.1, 129.7, 130.4, 131.1, 131.7, 132.3, 133.0, 133.8, 134.6 (2 × Ph, 4-ClC<sub>6</sub>H<sub>4</sub>), 150.3 (6-C), and 159.8 (SC=N); *m/z* 403 (M<sup>+</sup>).

**6c:** Yellowish needles (Found: C, 72.42; H, 5.11; N, 10.41). C<sub>24</sub>H<sub>21</sub>N<sub>3</sub>OS requires C, 72.15; H, 5.30; N, 10.52%; mp 70–71 °C (from EtOH);  $\nu_{\max}(\text{KBr})/\text{cm}^{-1}$  3344, 3058, 1603, 1585, 1440, and 1313;  $\delta_{\text{H}}(400 \text{ MHz; DMSO-}d_6/\text{TMS})$  3.15 (1 H, br s, NH exchanges with D<sub>2</sub>O), 3.73 (3 H, s, OMe), 6.70 (1 H, d, *J* 8, 4-H), 6.81 (1 H, d, *J* 8, 2-H), and 7.15–7.91 (15 H<sub>arom</sub>, m);  $\delta_{\text{C}}(100 \text{ MHz; DMSO-}d_6/\text{TMS})$  51.5 (OMe), 75.3 (4-C), 76.4 (2-C), 118.3 (7-C), 127.1, 127.7, 128.4, 129.0, 129.7, 130.8, 131.5, 132.2, 132.9, 133.5, 134.1, 134.8 (2 × Ph, 4-MeOC<sub>6</sub>H<sub>4</sub>), 150.4 (6-C), and 159.6 (SC=N); *m/z* 399 (M<sup>+</sup>).

**6d:** Yellowish needles (Found: C, 66.09; H, 4.83; N, 9.73). C<sub>24</sub>H<sub>20</sub>ClN<sub>3</sub>OS requires C, 66.43; H, 4.65; N, 9.68%; mp 70–71 °C (from EtOH);  $\nu_{\max}(\text{KBr})/\text{cm}^{-1}$  3347, 3059, 1605, 1587, 1446, and 1315;  $\delta_{\text{H}}(400 \text{ MHz; DMSO-}d_6/\text{TMS})$  3.17 (1 H, br s, NH exchanges with D<sub>2</sub>O), 3.75 (3 H, s, OMe), 6.72 (1 H, d, *J* 8, 4-H), 6.83 (1 H, d, *J* 8, 2-H), and 7.60–7.91 (14 H<sub>arom</sub>, m);  $\delta_{\text{C}}(100 \text{ MHz; DMSO-}d_6/\text{TMS})$  51.7 (OMe), 75.5 (4-C), 76.3

(2-C), 118.3 (7-C), 127.0, 127.7, 128.5, 129.2, 129.9, 130.7, 131.4, 132.1, 132.9, 133.6, 134.3, 134.9 (Ph, 4-ClC<sub>6</sub>H<sub>4</sub>, 4-MeOC<sub>6</sub>H<sub>4</sub>), 150.5 (6-C), and 159.8 (SC=N); *m/z* 433 (M<sup>+</sup>).

**6e:** Yellowish needles (Found: C, 68.04; H, 4.68; N, 10.53). C<sub>23</sub>H<sub>18</sub>ClN<sub>3</sub>S requires C, 68.39; H, 4.49; N, 10.40%; mp 84–85 °C (from EtOH);  $\nu_{\max}(\text{KBr})/\text{cm}^{-1}$  3345, 3060, 1604, 1584, 1441, and 1314;  $\delta_{\text{H}}(400 \text{ MHz; DMSO-}d_6/\text{TMS})$  3.16 (1 H, br s, NH exchanges with D<sub>2</sub>O), 6.70 (1 H, d, *J* 8, 4-H), 6.82 (1 H, d, *J* 8, 2-H), and 7.18–7.90 (15 H<sub>arom</sub>, m);  $\delta_{\text{C}}(100 \text{ MHz; DMSO-}d_6/\text{TMS})$  75.5 (4-C), 76.5 (2-C), 118.2 (7-C), 127.3, 127.9, 128.6, 129.3, 130.0, 130.6, 131.4, 132.0, 132.7, 133.4, 134.5 (2 × Ph, 4-ClC<sub>6</sub>H<sub>4</sub>), 150.4 (6-C), and 159.5 (SC=N); *m/z* 403 (M<sup>+</sup>).

**6f:** Yellowish needles (Found: C, 63.32; H, 3.72; N, 9.41). C<sub>23</sub>H<sub>17</sub>Cl<sub>2</sub>N<sub>3</sub>S requires C, 63.02; H, 3.91; N, 9.59%; mp 95–96 °C (from EtOH);  $\nu_{\max}(\text{KBr})/\text{cm}^{-1}$  3348, 3068, 1595, 1583, 1456, and 1317;  $\delta_{\text{H}}(400 \text{ MHz; DMSO-}d_6/\text{TMS})$  3.16 (1 H, br s, NH exchanges with D<sub>2</sub>O), 6.74 (1 H, d, *J* 8, 4-H), 6.85 (1 H, d, *J* 8, 2-H), and 7.15–7.94 (14 H<sub>arom</sub>, m);  $\delta_{\text{C}}(100 \text{ MHz; DMSO-}d_6/\text{TMS})$  75.6 (4-C), 76.7 (2-C), 118.5 (7-C), 127.1, 127.7, 128.3, 129.0, 129.7, 130.3, 131.0, 131.6, 132.3, 133.0, 133.8, 134.5 (Ph, 2 × 4-ClC<sub>6</sub>H<sub>4</sub>), 150.6 (6-C), and 159.8 (SC=N); *m/z* 439 (M<sup>+</sup>).

**6g:** Yellowish needles (Found: C, 68.68; H, 4.61; N, 10.29). C<sub>24</sub>H<sub>20</sub>ClN<sub>3</sub>S requires C, 68.97; H, 4.82; N, 10.05%; mp 116–118 °C (from EtOH);  $\nu_{\max}(\text{KBr})/\text{cm}^{-1}$  3343, 3052, 1596, 1579, 1465, and 1311;  $\delta_{\text{H}}(400 \text{ MHz; DMSO-}d_6/\text{TMS})$  2.27 (3 H, s, Me), 3.14 (1 H, br s, NH exchanges with D<sub>2</sub>O), 6.69 (1 H, d, *J* 8, 4-H), 6.80 (1 H, d, *J* 8, 2-H), and 7.14–7.89 (14 H<sub>arom</sub>, m);  $\delta_{\text{C}}(100 \text{ MHz; DMSO-}d_6/\text{TMS})$  20.2 (Me), 75.3 (4-C), 76.5 (2-C), 118.4 (7-C), 127.0, 127.8, 128.4, 129.1, 129.7, 130.4, 131.1, 131.8, 132.4, 133.1, 133.7, 134.6 (Ph, 4-ClC<sub>6</sub>H<sub>4</sub>, 4-MeC<sub>6</sub>H<sub>4</sub>), 150.2 (6-C), and 159.3 (SC=N); *m/z* 417 (M<sup>+</sup>).

**6h:** Yellowish needles (Found: C, 63.99; H, 4.48; N, 9.15). C<sub>24</sub>H<sub>19</sub>Cl<sub>2</sub>N<sub>3</sub>S requires C, 63.72; H, 4.23; N, 9.29%; mp 82–83 °C (from EtOH);  $\nu_{\max}(\text{KBr})/\text{cm}^{-1}$  3347, 3063, 1601, 1585, 1443, and 1315;  $\delta_{\text{H}}(400 \text{ MHz; DMSO-}d_6/\text{TMS})$  2.29 (3 H, s, Me), 3.17 (1 H, br s, NH exchanges with D<sub>2</sub>O), 6.73 (1 H, d, *J* 8, 4-H), 6.81 (1 H, d, *J* 8, 2-H), and 7.16–7.90 (13 H<sub>arom</sub>, m);  $\delta_{\text{C}}(100 \text{ MHz; DMSO-}d_6/\text{TMS})$  20.5 (Me), 75.6 (4-C), 76.5 (2-C), 118.6 (7-C), 127.2, 127.8, 128.5, 129.2, 129.8, 130.5, 131.2, 131.8, 132.5, 133.2, 133.9, 134.7 (2 × 4-ClC<sub>6</sub>H<sub>4</sub>, 4-MeC<sub>6</sub>H<sub>4</sub>), 150.5 (6-C), and 159.7 (SC=N); *m/z* 453 (M<sup>+</sup>).

**6i:** Yellowish needles (Found: C, 67.37; H, 4.71; N, 9.53). C<sub>24</sub>H<sub>20</sub>ClN<sub>3</sub>OS requires C, 67.03; H, 4.95; N, 9.38%; mp 80–81 °C (from EtOH);  $\nu_{\max}(\text{KBr})/\text{cm}^{-1}$  3345, 3061, 1602, 1578, 1449, and 1313;  $\delta_{\text{H}}(400 \text{ MHz; DMSO-}d_6/\text{TMS})$  2.28 (3 H, s, Me), 3.16 (1 H, br s, NH exchanges with D<sub>2</sub>O), 3.74 (3 H, s, OMe), 6.70 (1 H, d, *J* 8, 4-H), 6.82 (1 H, d, *J* 8, 2-H), and 7.13–7.93 (13 H<sub>arom</sub>, m);  $\delta_{\text{C}}(100 \text{ MHz; DMSO-}d_6/\text{TMS})$  20.3 (Me), 51.7 (OMe), 75.5 (4-C), 76.3 (2-C), 118.5 (7-C), 127.3, 128.0, 128.6, 129.2, 129.9, 130.5, 131.3, 132.9, 132.5, 133.4, 134.0, 134.8 (4-ClC<sub>6</sub>H<sub>4</sub>, 4-MeOC<sub>6</sub>H<sub>4</sub>, 4-MeC<sub>6</sub>H<sub>4</sub>), 150.4 (6-C), and 159.5 (SC=N); *m/z* 447 (M<sup>+</sup>).

## Acknowledgements

We sincerely thank RSIC, Lucknow, India, for providing microanalyses and spectra.

## References

- 1 I. Ugi and A. Domling, *Endeavour*, 1994, **18**, 115.
- 2 S. Heck and A. Domling, *Synlett*, 2000, 424.
- 3 G. A. Kraus and J. O. Nagy, *Tetrahedron*, 1985, **41**, 3537.
- 4 G. H. Posner, *Chem. Rev.*, 1986, **86**, 831.
- 5 I. Ugi, *J. Prakt. Chem.*, 1997, **339**, 499.
- 6 H. Bienayme and K. Bouzid, *Tetrahedron Lett.*, 1988, **39**, 2735.
- 7 T. Ziegler, H. J. Kaiser, R. Schlomer and C. Koch, *Tetrahedron*, 1999, **55**, 8397.
- 8 S. Caddick, *Tetrahedron*, 1995, **51**, 10403.
- 9 A. Loupy, A. Petit, J. Hamelin, F. Texier-Bouller, P. Jacquault and D. Mathe, *Synthesis*, 1998, 1213.
- 10 R. S. Varma, *Green Chem.*, 1999, **1**, 43.
- 11 P. Lidstrom, J. Tierney, B. Wathey and J. Westman, *Tetrahedron*, 2001, **57**, 9225.
- 12 L. Perreux and A. Loupy, *Tetrahedron*, 2001, **57**, 9199.
- 13 M. Balogh and P. Laszlo, *Organic chemistry using clays*, Springer, Berlin, 1993.
- 14 J. Chisem, I. C. Chisem, J. S. Rafelt, D. J. Macquarrie and J. H. Clark, *Chem. Commun.*, 1997, 2203.
- 15 H. M. Meshram, K. C. Shekhar, Y. S. S. Ganesh and J. S. Yadav, *Synlett*, 2000, 1273.
- 16 G. A. Strohmeier and C. O. Kappe, *J. Comb. Chem.*, 2002, **4**, 154.
- 17 F. R. Alexandre, L. Domon, S. Frere, A. Testard, V. Thiery and T. Besson, *Mol. Diversity*, 2003, **7**, 273.
- 18 R. S. Varma, *J. Heterocycl. Chem.*, 1999, **36**, 1565.
- 19 M. Larhed, C. Moberg and A. Hallberg, *Acc. Chem. Res.*, 2002, **35**, 717.
- 20 R. S. Varma and D. Kumar, *Tetrahedron Lett.*, 1999, **40**, 7665.
- 21 P. Lidstrom, J. Westman and A. Lewis, *Comb. Chem. High-throughput Screening*, 2002, **5**, 441.
- 22 S. M. Ireland, H. Tye and M. Whittakar, *Tetrahedron Lett.*, 2003, **44**, 4369.
- 23 L. D. S. Yadav and A. Singh, *Synthesis*, 2003, 2395.
- 24 L. D. S. Yadav, B. S. Yadav and V. K. Rai, *Tetrahedron Lett.*, 2004, **45**, 5351.
- 25 L. D. S. Yadav and R. Kapoor, *J. Org. Chem.*, 2004, **69**, 8118.
- 26 L. D. S. Yadav, S. Yadav and V. K. Rai, *Tetrahedron*, 2005, **61**, 10013.
- 27 Q. Cheng, W. Zhang, Y. Tagami and T. Oritani, *J. Chem. Soc., Perkin Trans. 1*, 2001, 452.

# Chemical Biology

An exciting news supplement providing a snapshot of the latest developments in chemical biology



Free online and in print issues of selected RSC journals!\*

**Research Highlights** – newsworthy articles and significant scientific advances

**Essential Elements** – latest developments from RSC publications

**Free links** to the full research paper from every online article during month of publication

\*A separately issued print subscription is also available

RSC Publishing

[www.rsc.org/chemicalbiology](http://www.rsc.org/chemicalbiology)

# A novel Ce/AlPO-5 catalyst for solvent-free liquid phase oxidation of cyclohexane by oxygen

Rui Zhao, Yanqin Wang, Yanglong Guo, Yun Guo, Xiaohui Liu, Zhigang Zhang, Yunsong Wang, Wangcheng Zhan and Guanzhong Lu\*

Received 16th December 2005, Accepted 27th February 2006

First published as an Advance Article on the web 15th March 2006

DOI: 10.1039/b517656e

Cerium-containing AlPO-5 with an AFI structure has been prepared by hydrothermal synthesis in the presence of HF, and characterized by XRD, XPS, SEM, N<sub>2</sub> adsorption/desorption, solid state <sup>27</sup>Al, <sup>31</sup>P MAS NMR and TG-DTA techniques. The results show that all the samples have good crystallinity, high dispersity of Ce and high surface area, and Ce(III) replaces the position of Al(III) and enters the framework of AlPO-5. Ce/AlPO-5 is a very efficient catalyst for the oxidation of cyclohexane in a solvent-free system with oxygen as an oxidant. In the condition of 0.5 MPa O<sub>2</sub> and 413 K for 4 h, the conversion of cyclohexane is 13%, the total selectivity of cyclohexanol and cyclohexanone is above 92%. In addition, the Ce/AlPO-5 catalyst is very stable in the cyclohexane oxidation system.

## 1. Introduction

Selective oxidations using heterogeneous catalysts are of growing importance for the modern chemical industry. The oxidation products of cyclohexane, *viz.*, cyclohexanol and cyclohexanone, are important intermediates in the production of adipic acid and caprolactam, which is used to manufacture nylon-6 and nylon-66 polymers.<sup>1–4</sup> In addition, they are also used as solvents for lacquers, shellacs, and varnishes as well as stabilizers and homogenizers for soaps and synthetic detergent emulsions. Furthermore, cyclohexanol ester, *viz.*, cyclohexyl phthalate, is widely used as a plasticizer as well as in the surface-coating industry. Other uses of cyclohexanone are as starting material in the synthesis of insecticides, herbicides, and pharmaceuticals. However, in most cases, extreme reaction conditions such as high pressure (2 MPa) and high temperature (450 K) in conjunction with low activity make this process less attractive. In addition, leaching of active metal ions has often been observed under the reaction conditions. Thus, the oxidation of cyclohexane over environmentally friendly heterogeneous catalysts under mild/moderate reaction conditions is a topic of great interest. Molecular oxygen is the cheapest and cleanest oxidant. However, the technology for the oxidation of cyclohexane to cyclohexanol and cyclohexanone by oxygen has not been improved very well up to now.

Recently, some new catalytic systems have been developed for cyclohexane oxidation with O<sub>2</sub> as an oxidant. Using a nanosized iron oxide supported in the pores of mesoporous material (titania) as a catalyst, cyclohexane could be oxidized under mild conditions to gain mainly cyclohexanol and cyclohexanone.<sup>5</sup> However, this process produced a large amount of isobutyraldehyde and used acetic acid as a

co-catalyst. Good results were obtained using *N*-hydroxyphthalimide (NHPI) derivatives as catalysts and air as an oxidant,<sup>6</sup> but the preparation of catalysts was complex, and some co-catalysts were also used. Selvam *et al.* used (Cr) MCM-41<sup>7</sup> and (Fe) MCM-41<sup>8</sup> as catalysts for the selective oxidation of cyclohexane, and obtained excellent results. Unfortunately, acetic acid was used as a solvent, and initiator (methyl ethyl ketone) must be used. Guo *et al.*<sup>9</sup> reported the oxidation of cyclohexane with cobalt porphyrins as catalysts and air as oxidant in solvent-free systems. The results indicated that the catalyst is very efficient, but the cobalt porphyrin catalyst is too expensive.

In most processes of catalytic cyclohexane oxidation, the solvent plays an important role. However, the use of solvent leads to many environmental problems. Up to now, the development of a solvent-free system is still a challenge, and only a few systems have been reported.<sup>6,9–11</sup> More recently, we reported that the oxidation of cyclohexane over Au/ZSM-5,<sup>12</sup> Au/MCM-41<sup>13</sup> and Bi/MCM-41<sup>14,15</sup> is very efficient. However, the leaching of gold nanoparticles from ZSM-5 is quite serious. As for the Bi/MCM-41 catalyst, although it solved the leaching problem of active metals, the very high price of the bismuth metal would prevent its application as a catalyst on an industrial scale. So in further work, we tried to find more stable and cheaper catalysts for the oxidation of cyclohexane.

CeO<sub>2</sub> and CeO<sub>2</sub>-based materials have attracted much attention in catalysis because of their unique catalytic activities associated with environmental concerns.<sup>16–18</sup> The facile redox cycle of Ce<sup>4+</sup>/Ce<sup>3+</sup> often leads to higher oxygen storage capacity (OSC) with reversible addition and removal of oxygen in the fluorite structure of ceria. For further improvement of the redox cycle between Ce<sup>4+</sup> and Ce<sup>3+</sup>, various CeO<sub>2</sub>-based binary oxides, such as CeO<sub>2</sub>-SiO<sub>2</sub>,<sup>19</sup> CeO<sub>2</sub>-TiO<sub>2</sub>,<sup>20</sup> and CeO<sub>2</sub>-ZrO<sub>2</sub>,<sup>20</sup> V<sub>2</sub>O<sub>3</sub>-CeO<sub>2</sub>,<sup>21</sup> CuO-CeO<sub>2</sub>,<sup>22</sup> SrCeO<sub>3</sub>,<sup>23</sup> Co<sub>x</sub>-CeO<sub>2</sub><sup>24</sup> have been widely investigated. A general conclusion is that an incorporation of MO<sub>x</sub> into the CeO<sub>2</sub> lattice

Lab for Advanced Materials, Research Institute of Industrial Catalysis, East China University of Science and Technology, Shanghai 200237, P. R. China. E-mail: gzhluc@ecust.edu.cn; Fax: +86 21 64253703

forms  $Ce_{1-x}M_xO_y$  solid solutions with higher OSC and better redox properties than those of  $CeO_2$  alone.

In 1982, Wilson and co-workers<sup>25</sup> developed a new class of zeolite-like molecular sieve AIPO-*n* (*n* denotes a structure type). Their structures are typically built up from strict alternation of  $AlO_4$  and  $PO_4$  tetrahedral through corner sharing to form a neutral open-framework. Part of the Al sites can be replaced by catalytically active transition metal ions. One of the important promising applications of AIPO-*n* is the aerial oxidations of linear and cyclic hydrocarbons.<sup>26</sup> They are also available in the growing field of solvent-free industrial reactions in the important area of clean technology.<sup>27,28</sup>

In this paper, we report the first example of a cerium doped AIPO-5 microporous molecular sieve synthesized in the presence of HF acid. The Ce/AIPO-5 samples were characterized by numerous physical-chemical methods, including power X-ray diffraction (PXRD), nitrogen adsorption/desorption, scanning electron microscopy (SEM), solid state  $^{27}Al$ ,  $^{31}P$  MAS NMR spectra, Raman spectroscopy, and X-ray photoelectron spectroscopy (XPS). The catalytic performance of Ce/AIPO-5 was also investigated by the oxidation of cyclohexane in a solvent-free system, with  $O_2$  as an oxidant.

## 2. Experiment

### 2.1 Catalyst preparation

All chemical reagents used were of AR grade. The Ce/AIPO-5 samples were synthesized according to ref. 29 with minor modifications, in which HF acid was used. A calculated amount of phosphoric acid (85 wt%), triethylamine (TEA), cerous nitrate and deionized water were mixed together at 303 K and stirred for 2 h, then aluminium isopropylate was added to this mixture under stirring. After the slurry was stirred for 2 h at 303 K, HF (40% in water) diluted with water was added under stirring, and this mixture was stirred continually for another 2 h. Finally, the matrix gel was transferred into a Teflon-lined stainless steel autoclave, and crystallized at 453 K for 6 h under static conditions. After the autoclave was quenched in cold water, the product was separated by centrifugation, washed with de-ionized water repeatedly, dried at 373 K for one day and calcined in air at 823 K for 5 h. Pure ceria was also synthesized with the same procedure as Ce/AIPO-5, except that no aluminium isopropylate and phosphoric acid were added. The molar composition of the matrix gel is:  $xCe(NO_3)_3 \cdot 6H_2O : Al_2O_3 : 1.3P_2O_5 : 1.6TEA : 1.3HF : 425H_2O$ , and the molar ratio of Al/Ce is 100, 50 and 25. The corresponding samples are named Ce(A)/AIPO-5, Ce(B)/AIPO-5, and Ce(C)/AIPO-5, their Ce content in the solid samples are 0.88, 1.62, 3.20 wt%, respectively (Table 1), which was analyzed by ICP-AES.

### 2.2 Catalyst characterization

The chemico-physical properties of Ce/AIPO-5 microporous materials were analyzed by Powder XRD (RigakuD/MAX 2550 PC),  $N_2$  adsorption/desorption (Micromeritics ASAP 2010), scanning electron microscopy (SEM) (JSM-6360LV/JEOL), solid state  $^{27}Al$ ,  $^{31}P$  CP-MAS NMR (AVANCE 500 NMR), Raman spectroscopy (Nicolet Raman 910), XPS

**Table 1** Ce content and BET surface area of Ce/AIPO-5 samples

Sample	Al/Ce (mol) in matrix gel	Ce content in solid (wt%) <sup>a</sup>	BET surface area/m <sup>2</sup> g <sup>-1</sup>	Pore volume/cm <sup>3</sup> g <sup>-1</sup>
AIPO-5	∞	0	120.5	2.3
Ce(A)/AIPO-5	100	0.88	102.2	2.5
Ce(B)/AIPO-5	50	1.62	112.3	2.6
Ce(C)/AIPO-5	25	3.20	122.4	2.7

<sup>a</sup> Analyzed by ICP-AES.

(Vgescalab 210), and TG/DTA (PerKinElmer Diamond TG/DTA).

XRD patterns were recorded with a RigakuD/MAX 2550 PC diffractometer equipped with Ni-filtered  $Cu K\alpha$  radiation (scanning step 0.15°/s). BET surface areas were measured by  $N_2$  adsorption at 77 K in a Micromeritics ASAP 2010. The samples were pre-degassed at 383 K overnight before measuring. TG/DTA analysis was carried out on a PerkinElmer Diamond TG/DTA at a heating rate of 5 K min<sup>-1</sup>. XPS spectra were recorded on a Vgescalab 210 spectrometer using Al  $K\alpha$  radiation (1486.6 eV), operated at 13 kV and 23 mA. All binding energies were determined with respect to the C1s line (284.6 eV) originating from adventitious carbon, and the standard deviation of the peak areas (in counts eV s<sup>-1</sup>) with integral subtraction of the background. Solid state  $^{27}Al$ ,  $^{31}P$  CP-MAS NMR spectra were recorded with an AVANCE 500 NMR spectrometer at 130.3 and 202.4 MHz, respectively. Solid state  $^{27}Al$  and  $^{31}P$  chemical shifts were externally referenced to  $[Al(H_2O)_6]^{3+}$  in aqueous  $Al(NO_3)_3$  and  $H_3PO_4$  (85 wt% in water), respectively.

### 2.3 Catalytic oxidation of cyclohexane

The catalytic oxidations were carried out in a 25 ml stainless steel reactor equipped with a magnetic stirrer. In a typical reaction, cyclohexane (2 ml) was mixed with Ce/AIPO-5 catalysts (10 mg) and heated to 413 K under a 0.5 MPa  $O_2$  atmosphere. After reaction, the reactants and products were directly analyzed by GC or GC-MS.

### 2.4 Leaching and recycling tests

The leaching tests were carried out in a 25 ml stainless steel reactor equipped with a magnetic stirrer and two test methods were used. Method I was that the catalyst was separated from the reaction solution by filtration after stirring for 12 h at room temperature under 0.5 MPa  $O_2$ , and then the matrix solution was immediately allowed to react further in 413 K. After reaction, the reaction solution was analyzed by GC immediately. Furthermore, the Ce content in the reaction solution was also determined by ICP-AES. Method II was similar to method I, but the catalyst was separated by filtration from the reaction solution after 12 h under 0.5 MPa  $N_2$  at 413 K.

Recycling tests were carried out by repeatedly using Ce/AIPO-5 in four consecutive reactions. After the reaction was finished, the catalyst was separated by filtration from the reaction solution, washed with acetone, dried at 393 K for 6 h, and reused in the next catalytic run under the same reaction conditions.

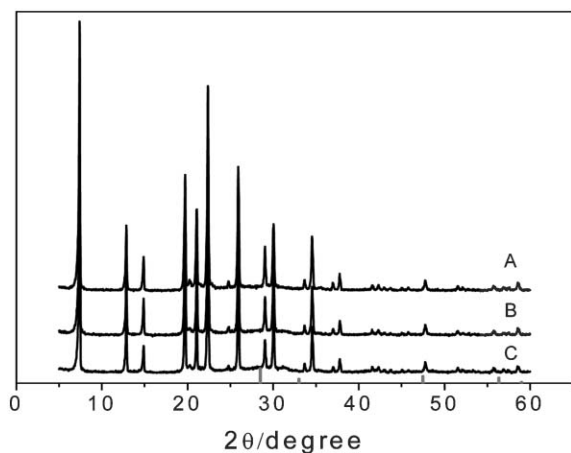


**Fig. 1** XRD patterns of Ce/AIPO-5 as-synthesized with different Ce content ((A) 0.88 wt%; (B) 1.60 wt%; (C) 3.20 wt%).

### 3. Results and discussion

#### 3.1 Catalyst characterization

**3.1.1 Powder X-ray diffraction.** The XRD patterns in Fig. 1 and 2 show that three samples synthesized have the typical AFI type structures<sup>30</sup> and the intense (211) or (210) peaks are located at  $2\theta = 22.4^\circ$  or  $19.7^\circ$ , respectively. The patterns of the calcined samples remained unchanged (Fig. 2), indicating a good thermal stability of the materials.

Compared with the XRD of pure  $\text{CeO}_2$ , the four strongest diffraction peaks at  $2\theta$  ( $3.116$ ,  $2.699$ ,  $1.909$ ,  $1.629$   $\text{A}^\circ$ ), corresponding to the (111), (200), (220), (311) crystal faces of cubic ceria, are not observed in the XRD patterns, which indicates that ceria may be highly dispersed<sup>31</sup> or cerium atoms partially substituted aluminium atoms in the framework by forming a new CeAIPO structure.<sup>32–34</sup>

**3.1.2 Raman spectroscopy.** Raman spectroscopy (RS) is a good technique to elucidate the structures of transition metal oxides present either as bulk phases or as two-dimensional supported phases, because RS can directly probe the surface structures and bonds of solid compounds by their vibration spectra. Therefore, this technique has been successfully used to discriminate the different structures of oxide surfaces.<sup>35</sup> Fig. 3

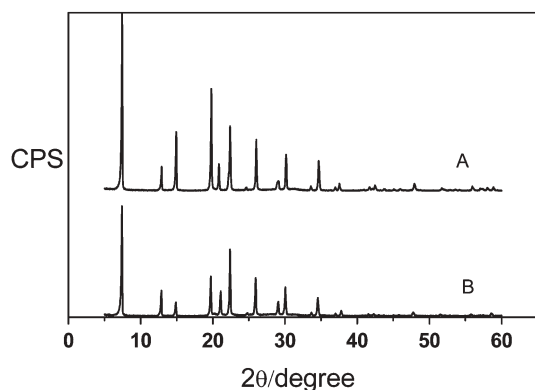


**Fig. 2** XRD patterns of Ce(A)/AIPO-5 as-synthesized (A) and calcined (B).

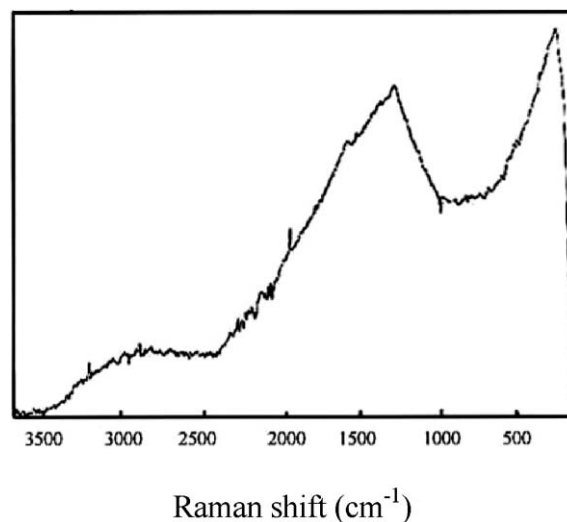


**Fig. 3** Raman spectrum of Ce(A)/AIPO-5 sample.

shows the Raman spectrum of Ce(A)/AIPO-5 (0.88 wt%Ce) and no classical band at  $460\text{--}465\text{ cm}^{-1}$  can be observed. This band corresponds to the triply degenerate  $\text{F}_{2g}$  mode and can be viewed as a symmetric breathing mode of the oxygen atoms around cerium ions.<sup>36</sup> This result indicates that Ce is highly dispersed or enters the framework of AIPO-5.

**3.1.3 X-ray photoelectron spectroscopy.** X-ray photoelectron spectroscopy was used to analyze the surface chemical composition of the samples. The photoelectron peaks of O1s, Ce3d, P2p, and Al2p are depicted in Fig. 4–6, respectively. The corresponding binding energy and the full width at half-maximum (fwhm) values are shown in Table 2. It is well known that the binding energy of  $\text{Ce}^{4+}$  in the XPS spectrum of Ce3d is different to that of  $\text{Ce}^{3+}$ . In  $\text{CeO}_2$  ( $\text{Ce}^{4+}$ ) the strong hybridization of the oxygen 2p valence band with Ce 4f orbital gives rise to the presence of the three peaks, due to final state effects caused by the creation of a core hole. By contrast,  $\text{Ce}_2\text{O}_3$  ( $\text{Ce}^{3+}$ ) is an almost pure  $4f^1$  state, showing only two photoemission peaks. According to the thoroughly accepted

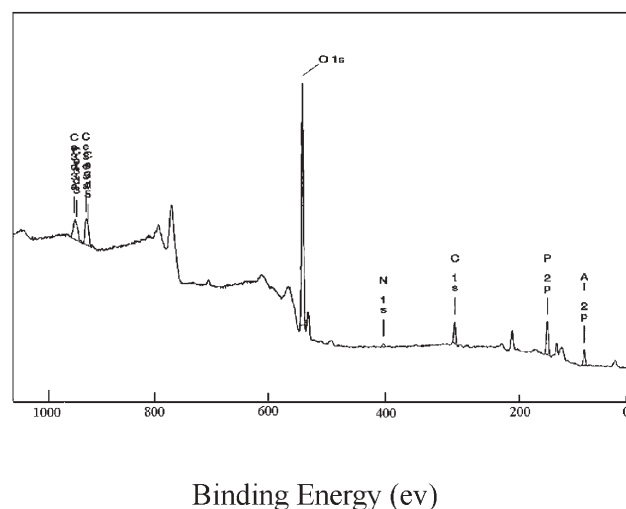


**Fig. 4** XPS spectrum of Ce(A)/AIPO-5 sample.

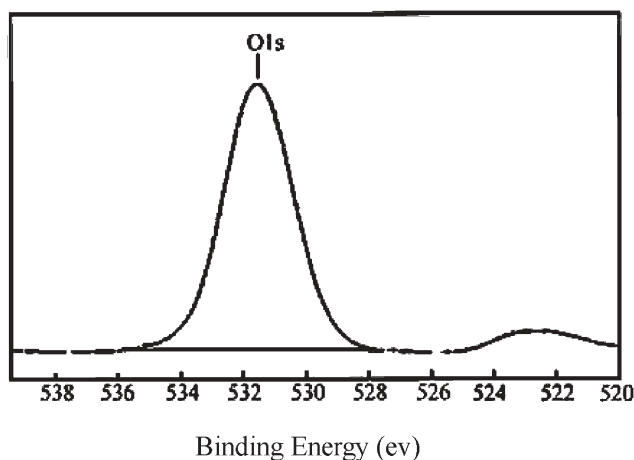


Fig. 5 XPS spectrum of O1s of Ce(A)/AlPO-5 sample.

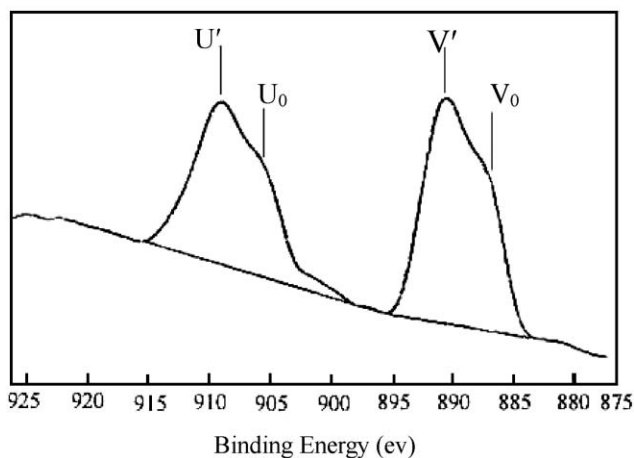


Fig. 6 XPS spectrum of Ce3d core levels of Ce(A)/AlPO-5 sample.

convention as suggested by Burroughs *et al.*,<sup>37</sup> Ce 3d<sub>3/2</sub> multiplets are labeled U, whereas those of 3d<sub>5/2</sub> are labeled V. In the case of pure Ce(IV) oxide, V, V' and V'' peaks for the Ce 3d<sub>5/2</sub> core level and U, U' and U'' peaks for the Ce 3d<sub>3/2</sub> level can be identified in its XPS spectrum (from low to high binding energy). For pure Ce(III) oxide, V<sub>0</sub> and V' features for the Ce 3d<sub>5/2</sub> core level and U<sub>0</sub> and U' features for the Ce 3d<sub>3/2</sub> core level can be seen. When Ce(IV) and Ce(III) oxidation states coexist in a cerium oxide, up to 10 features can be recognized,<sup>38</sup> taking also into account the spin-orbit coupling.

The XPS spectrum of the Ce 3d level of the Ce/AlPO-5 sample (Fig. 6) exhibits a typical spectrum of Ce(III). There are not any signals of Ce(IV) ions. So we can propose that Ce(III) partially occupied the position of Al(III) and entered the framework of AlPO-5. The binding energies of O1s, Al2p and

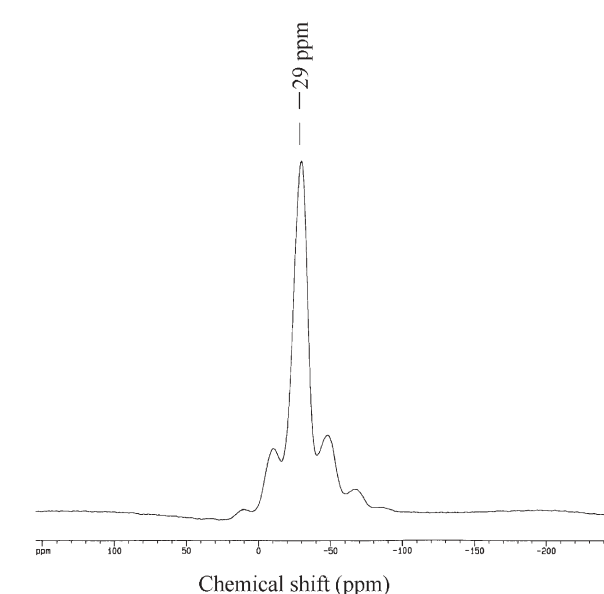
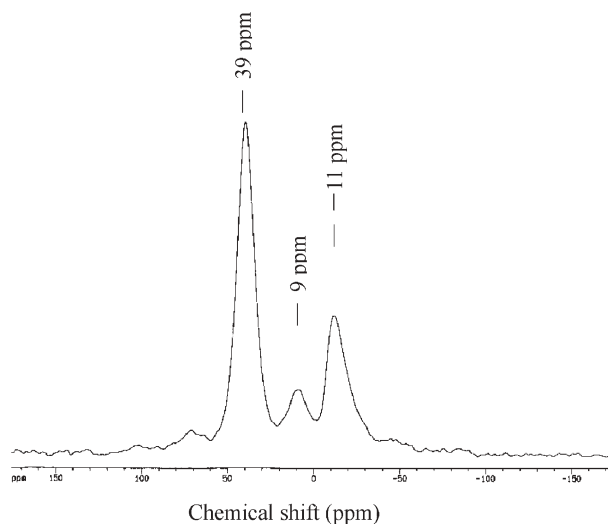


Fig. 7 Solid state <sup>27</sup>Al (top) and <sup>31</sup>P (bottom) MAS NMR spectra of Ce(A)/AlPO-5.

P2p on the Ce/AlPO-5 sample are quite similar to those reported for AlPO-5.<sup>39</sup> Detailed XPS core level electron binding energies are also presented in Table 2.

**3.1.4 Solid state <sup>27</sup>Al and <sup>31</sup>P MAS NMR measurements.** Fig. 7 presents the solid state <sup>27</sup>Al and <sup>31</sup>P MAS NMR spectra of calcined Ce(A)/AlPO-5 sample. The solid state <sup>27</sup>Al NMR spectrum of Ce/AlPO-5 is composed of three peaks at 39, 9 and -11 ppm. The main line at 39 ppm is ascribed to the tetrahedral aluminium in the aluminophosphate framework.

Table 2 XPS core level electron binding energies (BE in eV) and surface atom concentration (AT in %) of Ce/AlPO-5 samples

Al/Ce (mol)	O1s		Al2p		P2p		Ce3d3a BE	Ce3d3 BE	Ce3d5a		Ce3d5	
	BE	AT	BE	AT	BE	AT			BE	AT	BE	AT
100	531.68	57.8	74.48	9.9	133.90	10.5	903.96	900.53	885.56	5.3	881.99	3.5
50	531.60	57.0	74.40	9.8	133.70	10.4	904.21	900.78	886.48	6.3	883.12	4.1
25	531.50	57.4	74.36	8.9	133.60	9.9	904.45	900.80	885.62	7.5	882.14	5.3

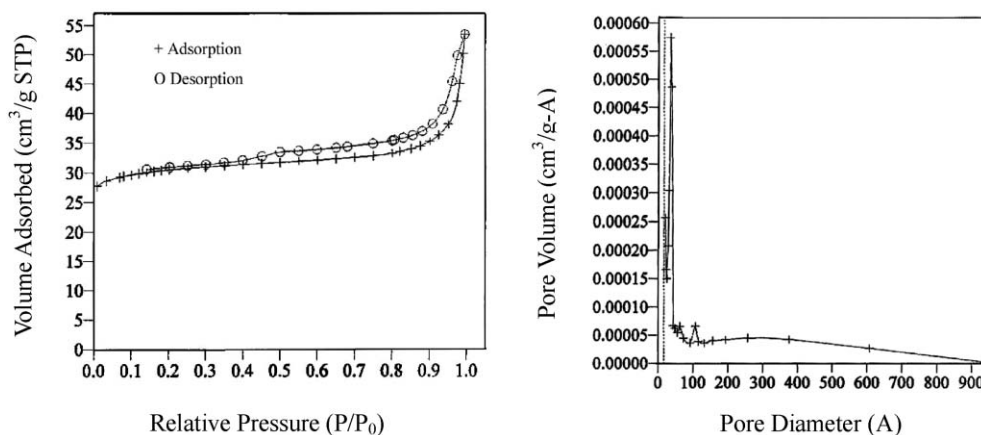


Fig. 8  $N_2$  adsorption/desorption isotherm of Ce(A)/AIPO-5.

The peak at 9 ppm is assigned to the remaining pseudo-boehmite. The resonance peak at  $-11$  ppm is attributed to hexacoordinated Al. This kind of hexacoordinated aluminium is possibly formed by water adsorption. It was reported that in aluminophosphate molecular sieves the adsorption of water caused the appearance of resonance peaks in the pentacoordinated and octahedral regions in the solid state  $^{27}\text{Al}$  MAS NMR spectrum.<sup>40</sup>

Solid state  $^{31}\text{P}$  MAS NMR spectrum of calcined Ce(A)/AIPO-5 shows a central band at around  $-29$  ppm, with asymmetry at low field. The broad resonance at *ca.*  $-29$  ppm can be readily attributed to the tetrahedral phosphorus in a  $\text{P}(\text{O}-\text{Al})_4$  environment.<sup>41</sup> It is known that the solid state  $^{31}\text{P}$  resonance is considerably shifted because of the contact interaction of paramagnetic species. However, this NMR spectrum of Ce(A)/AIPO-5 is much more similar to that of AIPO-5. Neither the shifts of the central peaks nor new resonance peaks are observed with the introduction of cerium atoms, which suggests that only one kind of coordination mode of phosphorus exists in Ce/AIPO-5. It also means that the coordination environment of P atoms may not be influenced by the addition of cerium.

**3.1.5  $N_2$  adsorption/desorption isotherm.** Fig. 8 shows  $N_2$  adsorption/desorption isotherms of the Ce(A)/AIPO-5 sample, by which the BET surface area and pore volume of samples are calculated as shown in Table 1. For all three samples, the BET surface area is more than  $100 \text{ m}^2 \text{ g}^{-1}$ . With an increase of Ce amount, the pore size increases from 2.3 nm to 2.6 nm, although the specific surface area changes less. These results above clearly demonstrate that incorporation of Ce in the AIPO-5 sample results in a modification of its surface texture.

**3.1.6 Thermal analysis.** The TG and DTA curves of Ce(A)/AIPO-5 as-prepared are shown in Fig. 9. As can be noted from this figure, this sample exhibits one major and one minor weight loss peak. The major peak at 323–373 K is primarily due to the loss of adsorbed water. The minor weight loss peak at 473–873 K may be the loss of water held in the micropores of the sample. The loss of weight from ambient to 373 K is about 14% and from 473 to 873 K is 2%. This result indicates that synthesized Ce/AIPO-5 has a high thermal stability.

**3.1.7 Surface microstructure.** Scanning electron microscopy (SEM) is used to determine the particle size and particle morphology of the synthesized sample. The SEM picture of the Ce(A)/AIPO-5 in Fig. 10 shows the morphology of hexangular rhombic-like rods. It is clear that most of the particles are rod-like, although some agglomerates are detected.

### 3.2 Catalytic performance

The catalytic performances for the cyclohexane oxidation in 0.5 MPa  $\text{O}_2$  at 413 K are given in Table 3. Good conversion and selectivity are obtained over the Ce/AIPO-5 catalysts with different cerium content. GS-MS analysis indicates that the main by-products are acid and hexane. In the blank reaction over pure AIPO-5 as a catalyst, trace amount of oxidative products were detected by GC analysis. Thus, it is clear that the presence of cerium in AIPO-5 plays a role in the catalytic reaction, that is to say, the Ce ions in Ce/AIPO-5 are the active sites. Among three Ce/AIPO-5 catalysts, Ce(A)/AIPO-5 shows the best activity for the oxidation of cyclohexane. With an increase of Ce content, the conversion of cyclohexane decreases somewhat, and the selectivity to cyclohexanol decreases and the selectivity to cyclohexanone increases. For a comparison, the data for the cyclohexane oxidation over Mn/AIPO-5<sup>42</sup> are also listed in Table 3. It can be seen that

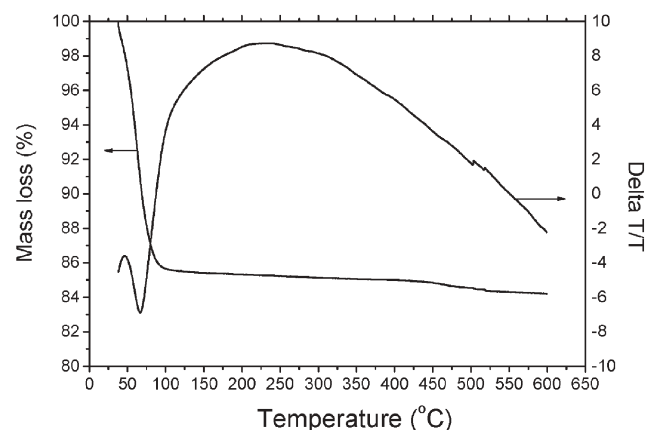


Fig. 9 TG and DTA curves of Ce(A)/AIPO-5 as-synthesized.

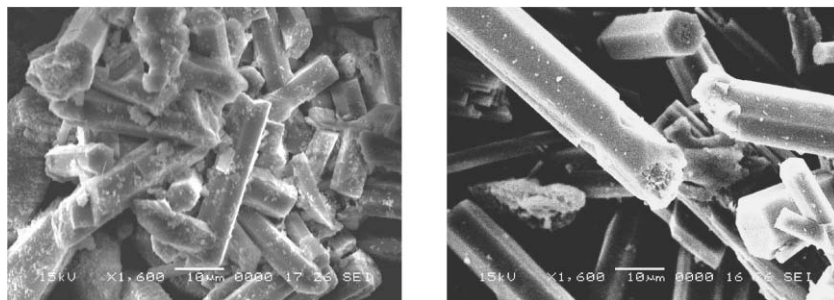


Fig. 10 SEM micrographs of Ce(A)/AlPO-5

Table 3 Performance of Ce/AlPO-5 for the cyclohexane oxidation<sup>a</sup>

Catalyst	Time/h	Atmosphere/MPa	Conversion (%)	Selectivity (%)	
				Cyclohexanol	Cyclohexanone
AlPO-5	4	N <sub>2</sub> /0.5	—	—	—
Ce(A)/AlPO-5	4	N <sub>2</sub> /0.5	—	—	—
Ce(A)/AlPO-5	4	O <sub>2</sub> /0.5	13.5	42	50
Ce(A)/AlPO-5 <sup>b</sup>	4	O <sub>2</sub> /0.5	13.0	40	51
Ce(B)/AlPO-5	4	O <sub>2</sub> /0.5	12.0	35	58
Ce(C)/AlPO-5	4	O <sub>2</sub> /0.5	11.5	30	60
Mn/AlPO-5 <sup>42</sup>	24	Air/1.0	6.0	19	43
Mn/AlPO-5 <sup>42c</sup>	24	Air/1.0	16.5	20	43
CeO <sub>2</sub>	4	O <sub>2</sub> /0.5	7.0	30	52

<sup>a</sup> Reaction conditions: 18.5 mmol cyclohexane, 10 mg catalyst, at 413 K. <sup>b</sup> After using repeatedly 4 times. <sup>c</sup> Small amounts (3 wt% cyclohexane) of hydroquinone (free-radical scavenger) added.

Mn/AlPO-5 is a very efficient catalysts for the cyclohexane oxidation with air as oxidant. However, it should be noted that some hydroquinone must be used, and the reaction time is much longer (24 h) and the total selectivity to cyclohexanol and cyclohexanone (63%) is obviously lower over the Mn/AlPO-5 catalyst than that over the Ce/AlPO-5 catalyst, in which the reaction time is 4 h and its total selectivity is 92%. Thus, compared with Mn/AlPO-5, Ce/AlPO-5 is a more environmentally friendly catalyst and more efficient catalyst for the cyclohexane oxidation.

As for bulk CeO<sub>2</sub>, although it shows activity for the cyclohexane selective oxidation (the conversion of cyclohexane

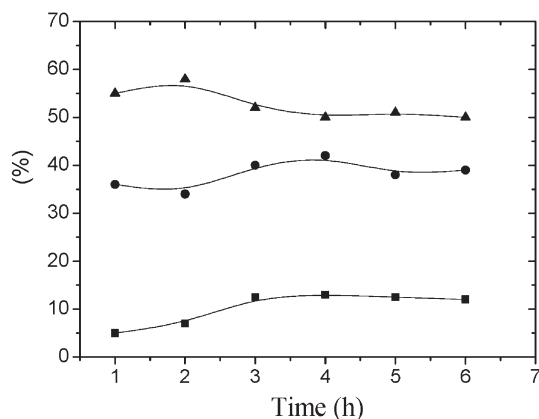


Fig. 11 Effect of reaction time on the conversion and selectivity over Ce(A)/AlPO-5. (Reaction conditions: 18 mmol cyclohexane, 12 mg catalyst, 0.5 MPa O<sub>2</sub>, at 413 K. ■: Conversion of cyclohexane; ●: selectivity to cyclohexanol; ▲: selectivity to cyclohexanone.)

is 7%), the selectivity is so low that the total selectivity to cyclohexanol and cyclohexanone is about 85%.

The effect of the reaction time on the catalytic activity of Ce/AlPO-5 was also investigated and the results are shown in Fig. 11. With increasing reaction time, the conversion of cyclohexane and the selectivity to cyclohexanone increase, but the selectivity to cyclohexanol decreases.

Fig. 12 illustrates the influence of the reaction temperature. With increasing reaction temperature, the conversion increases slightly, but the selectivity to cyclohexanol and cyclohexanone

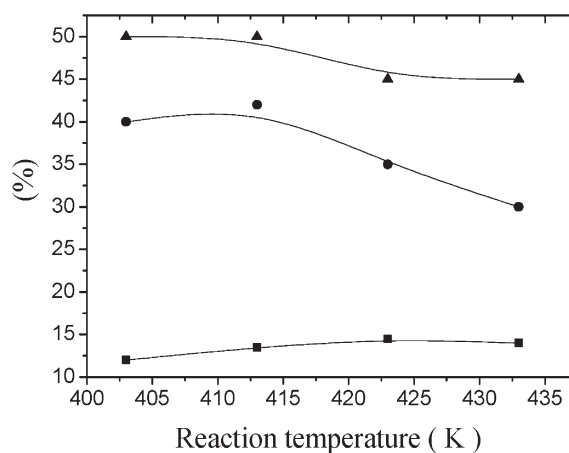


Fig. 12 Effect of reaction temperature on the conversion and selectivity over Ce(A)/AlPO-5. (Reaction conditions: 18 mmol cyclohexane, 12 mg catalyst, 0.5 MPa O<sub>2</sub>, for 4 h. ■: Conversion of cyclohexane; ●: selectivity to cyclohexanol; ▲: selectivity to cyclohexanone.)



**Table 4** Product distribution for the oxidation of cyclohexane over Ce(A)/AlPO-5<sup>a</sup>

Solvent	Products/mmol				Conversion (%)	Selectivity <sup>b</sup> (%)
	-nol	-none	n-Hexane	Adipic acid		
No solvent	0.99	1.31	—	0.20	13.5	92
Acetonitrile	0.30	0.93	—	0.34	8.7	78
Acetone	0.37	0.88	0.10	0.09	8.0	87
Acetic acid	—	—	—	1.08	6.0	—
Pyridine	0.14	0.22	—	—	2.0	100

<sup>a</sup> Reaction conditions: 18 mmol cyclohexane, 12 mg catalyst, 10 ml solvent, at 413 K for 4 h. <sup>b</sup> Selectivity =  $\sum(-\text{nol} + \text{-none})/\sum(\text{all products}) \times 100\%$ .

decreases. At higher reaction temperature, lots of n-hexane was detected.

When solvents were used in the reaction, the cyclohexane conversion decreases in the following order: no solvent > acetonitrile > acetone > acetic acid > pyridine (Table 4). Furthermore, the solvent has a considerable influence on the product distribution. In the case of the acetic acid solvent, adipic acid is the main product, only traces of cyclohexanol and cyclohexanone are detected. The formation of n-hexane and adipic acid can be strongly prevented when pyridine was used as a solvent, but only small amounts of cyclohexanol and cyclohexanone are formed with the selectivity of 100%. This indicates that the Brønsted acid sites of the AlPO-5 participate in the formation of n-hexane.

Two methods (I and II) were used in the leaching test. No cerium was detected by ICP-AES analysis in the matrix solution and no oxidative products were detected by GC analysis, after the Ce/AlPO-5 catalyst was separated from the reaction mixture under the given conditions. The results indicate that the leaching of cerium in the catalyst is very slight. This is further confirmed by analyzing the cerium contents of the fresh and recycled catalysts by ICP-AES, which shows that no obvious change in cerium content between two catalysts was observed (the sensitivity of the analysis is under 0.014  $\mu\text{g ml}^{-1}$ ).

The Ce/AlPO-5 catalyst recycling experiments have been carried out and the results are shown in Table 3. After the Ce/AlPO-5 catalyst is used repeatedly 4 times, the conversion and selectivity are hardly changed.

#### 4. Conclusion

The Ce-containing AlPO-5 catalyst was synthesized in the presence of HF. The results show that Ce(III) partially occupied the position of Al(III) and entered the framework of AlPO-5. Ce/AlPO-5 is a very efficient catalyst for the oxidation of cyclohexane with oxygen in a solvent-free system. This catalytic system is environmentally friendly. In addition, Ce/AlPO-5 catalyst in the systems is very stable, and it behaves truly as a heterogeneous catalyst.

#### Acknowledgements

This project was supported financially by the National Basic Research Program of China (No. 2004CB719500), the Commission of Science and Technology of Shanghai Municipality (No. 03DJ14006) and East China University of

Science and Technology. This project was also supported by the Postdoctoral Foundation of China (No. 2005037494).

#### References

- W. L. Faith, D. B. Keyes and R. L. Clark, *Industrial Chemicals*, Wiley, New York, 2nd edn, 1957.
- I. V. Berezin, E. T. Denisov and N. M. Emanuel, *Oxidation of Cyclohexane*, Pergamon, New York, 1968.
- S. B. Chandalia, *Oxidation of Hydrocarbons*, Sevak, Bombay, 1st edn, 1977.
- M. T. Musser, in *Encyclopedia of Industrial Chemistry*, ed. W. Gerhartz, VCH, Weinheim, 1987, p. 217.
- N. Perkas, Y. Wang, Y. Koltypin, A. Gedanken and S. Chandrasekaran, *Chem. Commun.*, 2001, 988.
- N. Sawatari, T. Yokota, S. Sakaguchi and Y. Ishii, *J. Org. Chem.*, 2001, **66**, 7889.
- A. Sakthivel and P. Selvam, *J. Catal.*, 2002, **211**, 134.
- K. Suanta and P. Selvam, *Chem. Lett.*, 2004, **33**, 198.
- C. Guo, M. Chu, Q. Liu, Y. Liu, D. Guo and X. Liu, *Appl. Catal., A*, 2003, **246**, 303.
- U. Schuchardt and V. Mano, *Stud. Surf. Sci. Catal.*, 1990, **55**, 185.
- U. Schuchardt, R. Pereira and M. Rufo, *J. Mol. Catal., A*, 1998, **135**, 25.
- R. Zhao, D. Ji, G. Lv, G. Qian, L. Yan, X. Wang and J. Suo, *Chem. Commun.*, 2004, 904–905.
- G. Lü, R. Zhao, G. Qian, Y. Qi, X. Wang and J. Suo, *Catal. Lett.*, 2004, **97**, 3–4, 115–118.
- G. Qian, G. Lv, D. Ji, R. Zhao, Y. Qi and J. Suo, *Chem. Lett.*, 2005, **34**, 2, 162.
- G. Qian, D. Ji, G. Lv, R. Zhao, Y. Qi and J. Suo, *J. Catal.*, 2005, **232**, 378–385.
- Y. Liu, T. Hayakawa, K. Suzuki, S. Hamakawa, T. Tsunoda, T. Ishii and M. Kumagai, *Appl. Catal. A*, 2002, **223**, 137.
- H. He, H. X. Dai, L. H. Ng, K. W. Wong and C. T. Au, *J. Catal.*, 2002, **206**, 1.
- L. Li, G. Li, Y. Che and W. Su, *Chem. Mater.*, 2000, **12**, 2567.
- A. Bensalem, F. Bozon Verduraz, M. Delamar and G. Bugli, *Appl. Catal.*, 1995, **121**, 81.
- B. M. Reddy, A. Khan, P. Lakshmanan, M. Aouine, S. Loridant and J. C. Volta, *J. Phys. Chem. B*, 2005, **109**, 3355.
- B. M. Reddy, A. Khan, P. Lakshmanan, M. Aouine, S. Loridant and J. C. Volta, *J. Phys. Chem. B*, 2002, **106**, 10964.
- V. R. Mastelaro, P. A. P. Nascente, A. O. Florentino and M. S. P. Francisco, *J. Phys. Chem. B*, 2001, **105**, 10515.
- F. Goubin, X. Rocquefelte, M. H. Whangbo, Y. Montardi, R. Brec and S. Jobic, *Chem. Mater.*, 2004, **16**, 662.
- M. M. Natile and A. Glisenti, *Chem. Mater.*, 2005, **17**, 3403.
- S. T. Wilson, B. M. Lok, C. A. Messian, T. R. Cannan and E. M. Flanigen, *J. Am. Chem. Soc.*, 1982, **104**, 1146.
- J. M. Thomas, R. Raja, G. Sankar and R. G. Bell, *Acc. Chem. Res.*, 2001, **34**, 191.
- R. Raja, G. Sankar and J. M. Thomas, *J. Am. Chem. Soc.*, 2001, **123**, 8153.
- J. M. Thomas, R. Raja, G. Sankar, R. G. Bell and D. W. Lewis, *Pure Appl. Chem.*, 2001, **73**, 1087.
- M. H. Zahedi-Niaki, S. M. J. Zaidi and S. Kaliaguine, *Appl. Catal., A*, 2000, **196**, 9.

- 30 M. M. J. Treacy, J. B. Higgins and R. von Ballmoos, *Collection of Simulated XRD Power Patterns for Zeolites, Zeolites* (spec. edition), Elsevier; Amsterdam, 1996.
- 31 B. M. Reddy, I. Ganesh and E. P. Reddy, *J. Phys. Chem. B.*, 1997, **101**, 1769.
- 32 C. Larese, F. C. Halisteo, M. L. Granados, R. Mariscal, J. L. G. Fierro, M. Furió and R. F. Ruiz, *Appl. Catal., B*, 2003, **40**, 305.
- 33 D. Uy, A. E. O'Neill, L. Xu, W. H. Weber and R. W. McCabe, *Appl. Catal., B*, 2003, **41**, 269.
- 34 C. Larese, F. C. Galisteo, M. L. Granados, R. M. López, J. L. G. Fierro, P. S. Lambrou and A. M. Efstathiou, *Appl. Catal. B*, 2004, **48**, 113.
- 35 J. E. Spanier, R. D. Robinson, F. Zhang, S. W. Chan and I. P. Herman, *Phys. Rev. B*, 2001, **64**, 245407.
- 36 X. M. Lin, L. P. Li, G. S. Li and W. H. Su, *Mater. Chem. Phys.*, 2001, **69**, 236.
- 37 P. Burroughs, A. Hamnett, A. F. Orchard and G. Thomson, *J. Chem. Soc., Dalton Trans.*, 1976, 1686.
- 38 C. L. F. C. Galisteo, M. L. Granados, R. Mariscal, J. L. G. Fierro, P. S. Lambrou and A. M. Efstathiou, *J. Catal.*, 2004, **226**, 443.
- 39 S. L. Suib, A. M. Winiecki and A. Kostapapas, *Langmuir*, 1987, **3**, 483.
- 40 J. M. Campelo, M. Jaraba, D. Luna, R. Luque, J. M. Marinas and A. A. Romero, *Chem. Mater.*, 2003, **15**, 3352.
- 41 T. Blasco, P. Concepción, P. Grotz, J. M. López, Nieto and A. Martínez-Arias, *J. Mol. Catal. A*, 2000, **162**, 267.
- 42 R. Raja, G. Sankar and J. M. Thomas, *J. Am. Chem. Soc.*, 1999, **121**, 11926.



90504090

**Fast  
Publishing?  
Ahead of the field**

To find out more about RSC Journals, visit

RSCPublishing

[www.rsc.org/journals](http://www.rsc.org/journals)

# Polyurethanes with pendant hydroxy groups: polycondensation of 1,6-bis-*O*-phenoxy carbonyl-2,3:4,5-di-*O*-isopropylidene galactitol and 1,6-di-*O*-phenoxy carbonyl galactitol with diamines

Günter Prömpers, Helmut Keul\* and Hartwig Höcker

Received 9th January 2006, Accepted 28th February 2006

First published as an Advance Article on the web 14th March 2006

DOI: 10.1039/b600254d

1,6-Bis-*O*-phenoxy carbonyl-2,3:4,5-di-*O*-isopropylidene galactitol (**5**) and 1,6-di-*O*-phenoxy carbonyl galactitol (**6**) were prepared from galactaric acid in four and five steps, with overall yields of 76% and 72%, respectively. These AA type monomers were reacted with  $\alpha,\omega$ -diamines ( $\text{H}_2\text{N}-(\text{CH}_2)_x-\text{NH}_2$ ;  $x = 2-10$  and 12) as BB type monomers in a polycondensation reaction to result in polyurethanes with four protected hydroxy groups **PiG2-12** or polyurethanes with four free hydroxy groups **PG2-6** per repeating unit. The polyurethanes of the **PiG**-series were transformed by hydrolysis into polyurethanes with four free hydroxy groups per repeating unit **PaG2-6**. As shown by  $^1\text{H}$  NMR spectroscopy, the polyurethanes of the **PG** series and of the **PaG** series differ in their microstructure: the polymers of the first series has urethane groups with primary and secondary carbon atoms adjacent to the urethane group, while the polymers of the second series have only primary carbon atoms adjacent to the urethane group. The molecular weights of the polyurethanes, as determined by means of gel permeation chromatography in dimethylacetamide–LiCl, are in the range of 15 000 to 63 000 for the **PiG** and the **PaG** series and 15 000 to 36 000 for the **PG**-series with polydispersity indices of about 1.6. The thermal stability of the polyurethanes was studied by means of TGA, the polyurethanes with protected hydroxyl groups being more stable than those with free hydroxy groups. The polyurethanes of the **PiG** series are semi-crystalline materials with melting points between 160 and 167 °C and glass transition temperatures between 59 and 78 °C. The polyurethanes of the **PG** and the **PaG** series show glass transition temperatures of 44 to 74 °C; no melting transition is observed before decomposition starts at about 180 °C.

## Introduction

Today new materials have to fulfil ecological requirements with respect to the raw materials used, with respect to their manufacturing technology, and with respect to waste disposal. Therefore, renewable primary materials attract a great deal of attention. Compared with the raw materials from crude oil or coal, however, raw materials from renewable resources are highly functional materials with a high content of oxygen and nitrogen, which often turns out to be impedimentary for an application.<sup>1</sup> Long-term considerations based on the availability of fossil fuels as raw materials and their influence on environmental aspects ( $\text{CO}_2$ -balance), however, make renewable raw materials attractive.<sup>2</sup> Nature produces  $170 \cdot 10^9$  t of saccharides from carbon dioxide and water; however, only 3% of this immense potential is used as a foodstuff.<sup>3,4</sup> Therefore, it is a challenge for chemists to find fields of application for renewable raw materials. Beside the polysaccharides starch and cellulose, low cost monosaccharides, such as glucose, fructose, galactose, mannose, *etc.*, are available on an industrial scale. Despite the high share of these materials on the total available biomass the amount to be used technically

is very low. A reason for this is the high functionality of these materials; a selective chemistry only is achieved by using protective groups. Mono and oligosaccharides, to a limited degree, are used already as building blocks for polymers or tenside formulations.

Polymers with monosaccharide building blocks may contain these building blocks in the main chain or in side chains. Since the fifties saccharose–phenol–formaldehyde resins<sup>4</sup> have been known and prepared by polycondensation of saccharose with phenol and formaldehyde mixtures (scheme 1).

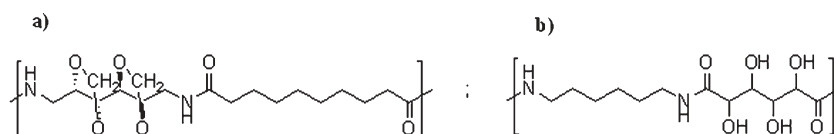
To prepare linear polymers with monosaccharide units in the main chain the saccharide building block should have only two reactive functional groups, such as amine or carboxylic acid groups, to act as suitable comonomers in polyamide synthesis (scheme 2).<sup>5-7</sup>

As is shown for the polyaddition polymerization of glucosamine and diisocyanates, in special cases, from several functional groups, two groups with higher reactivity can be used for a selective reaction. The amine group and the primary

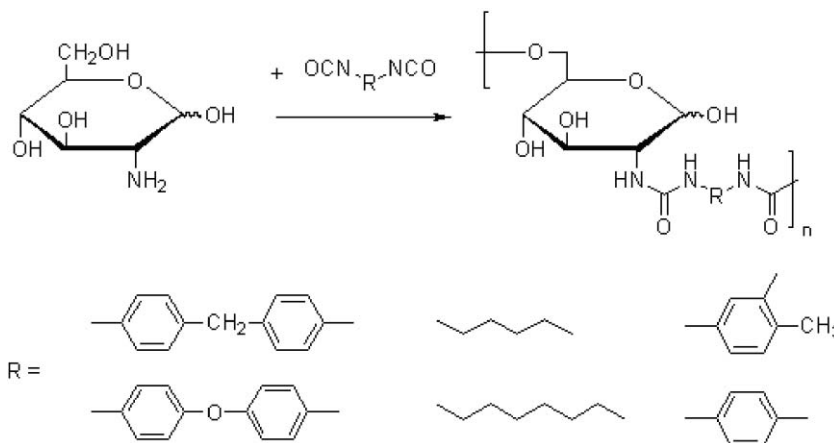


Scheme 1 Saccharose–phenol–formaldehyde resins.

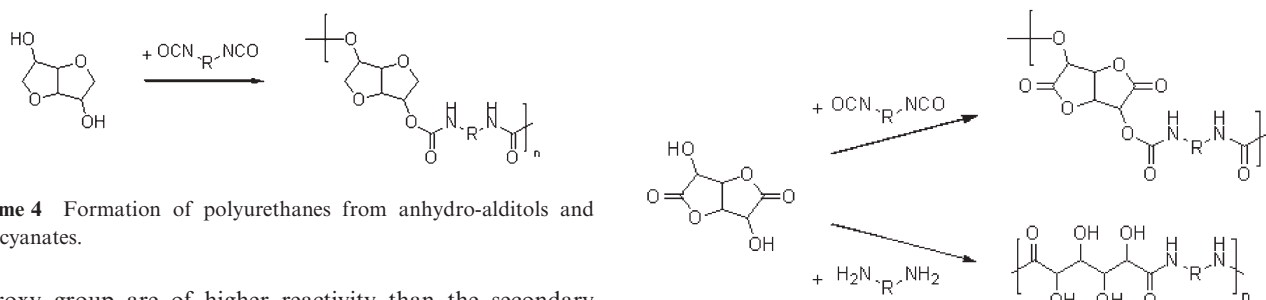
Lehrstuhl für Textilchemie und Makromolekulare Chemie der Rheinisch-Westfälischen Technischen Hochschule Aachen, Pauwelsstr. 8, 52056 Aachen, Germany. E-mail: keul@dwi.rwth-aachen.de



Scheme 2 Polyamides with monosaccharide building blocks.



Scheme 3 Formation of linear polymers from glucosamine and diisocyanates.



Scheme 4 Formation of polyurethanes from anhydro-alditols and diisocyanates.

hydroxy group are of higher reactivity than the secondary hydroxy groups (scheme 3).<sup>8</sup>

Other saccharides with only two reactive functional groups are anhydro-alditols of sorbitol or erythritol. These derivatives are suitable for production of homopolymers or copolymers with diamines, diisocyanates, phosgene or dicarboxylic acids (scheme 4).<sup>9,10</sup>

Lactones based on glucaric and galactaric acid are monosaccharide based monomers; with respect to their functional groups they are diols and/or bislactones. These monomers react with diamines by ring-opening polyaddition polymerization to result in polyamides and with diisocyanates by polyaddition polymerization to result in polyurethanes (scheme 5).<sup>11</sup>

Recently we reported on the synthesis of a new AA' monomer derived from glycerol-phenoxycarbonyloxymethyl-ethylene carbonate—which upon reaction with diamines also yields polyurethanes with one pendant primary or secondary hydroxy group per repeating unit (scheme 6).<sup>12</sup>

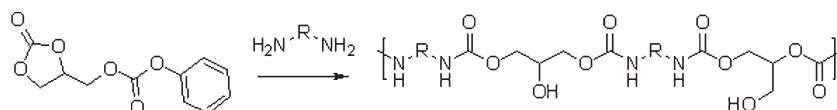
Scheme 5 Reaction of saccharic lactones with diisocyanates and with diamines.

This paper describes the synthesis of new polyurethanes with pendant hydroxy groups starting from 1,6-bis-*O*-phenoxycarbonyl-2,3,4,5-di-*O*-isopropylidene-galactitol and 1,6-di-*O*-phenoxycarbonyl-galactitol and diamines. The polyurethanes with pendant hydroxy groups obtained were characterized with respect to their microstructure and their thermal properties.

## Experimental

### Materials

Starting materials and reagents used for monomer synthesis and polymerization were of high purity and were used as received. Polymerizations were carried out in an inert



Scheme 6 Formation of polyurethanes with pendant hydroxy groups.

gas atmosphere. Nitrogen (Linde) was passed over molecular sieve (4 Å) and finely distributed potassium on aluminium oxide.

### Measurements

$^1\text{H}$  NMR and  $^{13}\text{C}$  NMR spectra were recorded on a Bruker DPX-300 FT-NMR spectrometer at 300 MHz and 75 MHz, respectively. Deuterated chloroform ( $\text{CDCl}_3$ ) and dimethylsulfoxide ( $\text{DMSO}-d_6$ ) were used as solvents, and tetramethylsilane (TMS) served as an internal standard.

Gel permeation chromatography (GPC) analyses were carried out using a high pressure liquid chromatography pump (Bischoff HPLC pump 2200) and a refractive index detector (Waters 410). The eluting solvent was dimethylacetamide with  $2.44\text{ g L}^{-1}$  of LiCl with a flow rate of  $0.8\text{ mL min}^{-1}$ . Four columns with MZ-DVB gel were applied: length of each column, 300 mm; diameter, 8 mm; diameter of gel particles, 5  $\mu\text{m}$ ; nominal pore width, 100 Å, 100 Å,  $10^3$  Å and  $10^4$  Å. Calibration was achieved using polystyrene standards of narrow molecular weight distribution from Polymer Standard Service, Mainz.

Differential scanning calorimetric analyses were performed with a Netzsch DSC 204 under nitrogen with a heating rate of  $10\text{ K min}^{-1}$ . Calibration was achieved using indium standard samples.

Thermogravimetric analyses (TGA) were performed on a TG 209 with a TA system controller TASC 414/2 from Netzsch. The measurements were performed in a nitrogen atmosphere with a heating rate of  $10\text{ K min}^{-1}$ .

### Syntheses: diethyl mucate (diethyl galactarate) (2)

Mucic acid (42.00 g, 200 mmol) (1) was suspended in ethanol (1 L), concentrated hydrochloric acid (20 mL) was added, and

the mixture was heated for 24 h to reflux. Ethanol was partly removed by distillation. After cooling, the product crystallized from the clear pale yellow solution and was separated by filtration. The product was recrystallized from ethanol. Yield: 94% (50.15 g, 188 mmol); m.p.  $153^\circ\text{--}154^\circ\text{C}$ . For the NMR assignments *cf.* scheme 7.

### $^1\text{H}$ NMR ( $\text{DMSO}-d_6$ )

$\delta_{\text{H}} = 1.21$  (tr, 6H,  $\text{CH}_3$ -1,  $^3J = 7.2$  Hz); 3.78 (d, 2H, CH-5,  $^3J = 7.5$  Hz); 4.10 (q, 4H,  $\text{CH}_2$ -2,  $^3J = 7.2$  Hz); 4.31 (d, 2H, CH-4,  $^3J = 8.2$  Hz); 4.79 (d, 2H, OH-6,  $^3J = 8.2$  Hz); 4.85 (d, 2H, OH-7,  $^3J = 8.2$  Hz) ppm.

### $^{13}\text{C}$ NMR ( $\text{DMSO}-d_6$ )

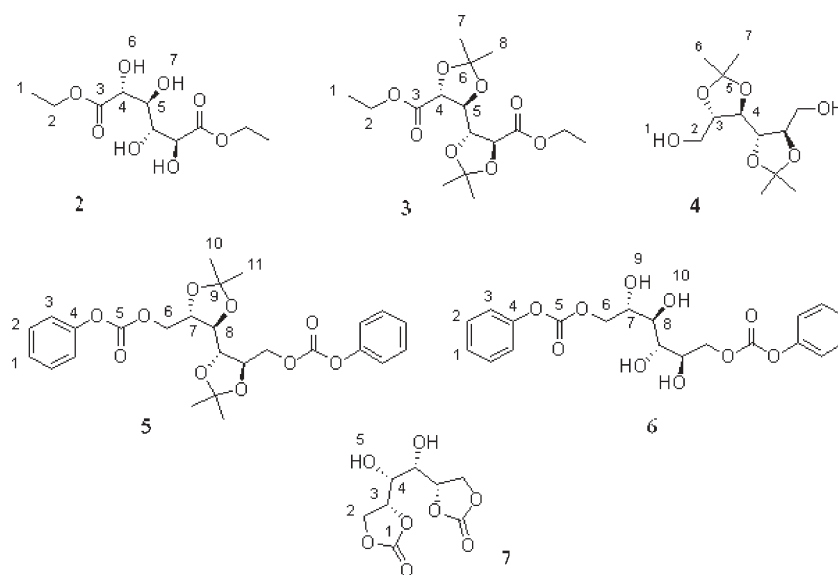
$\delta_{\text{C}} = 14.13$  (C-1, 2C); 60.08 (C-2, 2C); 70.13 (C-4, 2C); 71.19 (C-5, 2C); 73.62 (C-3, 2C) ppm.

### Galactaric acid 2,3:4,5-bis-*O*-isopropylidene diethylester (3)

Diethylgalactarate (2) (80.00 g, 300 mmol), 2,2-dimethoxypropane (65.00 g, 624 mmol), and *p*-toluenesulfonic acid (1.00 g, 6 mmol) were dissolved in acetone (1 L) and heated to reflux for 13 h in a Soxhlet apparatus containing dry molecular sieve (4 Å). The mixture was cooled and sodium carbonate was added for neutralization. After filtration of the inorganic salts the solvent was removed in vacuum. The residue was crystallized from ethanol (250 mL). Yield: 88% (91.40 g, 264 mmol); mp  $85^\circ\text{--}87^\circ\text{C}$ . For the NMR assignments, *cf.* scheme 7.

### $^1\text{H}$ NMR ( $\text{DMSO}-d_6$ )

$\delta_{\text{H}} = 1.26$  (tr, 6H,  $\text{CH}_3$ -1,  $^3J = 7.2$  Hz); 1.40 (s, 6H,  $\text{CH}_3$ -8); 1.42 (s, 6H,  $\text{CH}_3$ -7); 4.22 (q, 4H,  $\text{CH}_2$ -2,  $^3J = 7.2$  Hz); 4.41 (m, 2H, CH-5); 4.51 (m, 2H, CH-4) ppm.



**Scheme 7** Structure of diethyl mucate (diethyl galactarate) (2), galactaric acid 2,3:4,5-bis-*O*-isopropylidene diethylester (3), 2,3:4,5-di-*O*-isopropylidene galactitol (4), 1,6-bis-*O*-phenoxy carbonyl-2,3:4,5-di-*O*-isopropylidene galactitol (5), 1,6-di-*O*-phenoxy carbonyl galactitol (6), galactitol-1,2:5,6-dicarbonate (7), with numbers for NMR assignment.

**<sup>13</sup>C NMR (DMSO-*d*<sub>6</sub>)**

$\delta_{\text{C}} = 14.20$  (C-1, 2C); 26.46 (C-8, 2C); 27.32 (C-7, 2C); 61.42 (C-2, 2C); 76.50 (C-4, 2C); 79.48 (C-5, 2C); 112.20 (C-6, 2C); 173.62 (C-3, 2C) ppm.

**2,3:4,5-Di-*O*-isopropylidene-galactitol (4)**

Lithium aluminium hydride (9.00 g, 237 mmol) was suspended in dry diethyl ether (200 mL) under nitrogen and galactaric acid 2,3:4,5-bis-*O*-isopropylidene diethylester (**3**) (40.00 g, 116 mmol) in dry diethyl ether (400 mL) was added slowly at 0 °C. The solution was heated to reflux for 12 h. Workup gave a solid which was crystallized from isopropanol (30 mL). Yield: 94% (28.60 g, 109 mmol); m.p. 111°–113 °C. For the NMR assignments, *cf.* scheme 7.

**<sup>1</sup>H NMR (DMSO-*d*<sub>6</sub>)**

$\delta_{\text{H}} = 1.30$  (s, 6H, CH<sub>3</sub>-7); 1.33 (s, 6H, CH<sub>3</sub>-6); 3.46 (m, 2H, CH<sub>2</sub>-2<sup>a</sup>); 3.60 (m, 2H, CH<sub>2</sub>-2<sup>b</sup>); 3.78 (m, 2H, CH-3); 3.94 (m, 2H, CH-4); 4.82 (tr, 2H, OH-1, <sup>3</sup>*J* = 5.2 Hz) ppm.

**<sup>13</sup>C NMR (DMSO-*d*<sub>6</sub>)**

$\delta_{\text{C}} = 26.90$  (C-7, 2C); 27.10 (C-6, 2C); 61.80 (C-2, 2C); 77.52 (C-4, 2C); 80.64 (C-3, 2C); 108.71 (C-5, 2C) ppm.

**1,6-Bis-*O*-phenoxy-carbonyl-2,3:4,5-di-*O*-isopropylidene-galactitol (5)**

2,3:4,5-Di-*O*-isopropylidene-galactitol (**4**) (50.00 g, 191 mmol) in pyridine (200 mL) was treated slowly with phenyl chloroformate (60.00 g, 383 mmol) and stirred for additional 12 h at room temperature. The mixture was then cooled to –5 °C and neutralized with an aqueous solution of sulfuric acid (98% sulfuric acid (60 mL) in water (200 mL)). The product was extracted with methylene chloride and crystallized from toluene (200 mL). Yield: 98% (93.46 g, 186 mmol). For the NMR assignments, *cf.* scheme 7.

**<sup>1</sup>H NMR (DMSO-*d*<sub>6</sub>)**

$\delta_{\text{H}} = 1.37$  (s, 6H, CH<sub>3</sub>-11); 1.40 (s, 6H, CH<sub>3</sub>-10); 3.99 (m, 2H, CH-8); 4.28 (m, 2H, CH<sub>2</sub>-6<sup>a</sup>); 4.31 (m, 2H, CH-7); 4.50 (m, 2H, CH<sub>2</sub>-6<sup>b</sup>); 7.26 (m, 4H, CH-3); 7.30 (m, 2H, CH-1); 7.45 (m, 4H, CH-2) ppm.

**<sup>13</sup>C NMR (DMSO-*d*<sub>6</sub>)**

$\delta_{\text{C}} = 26.69$  (C-11, 2C); 26.78 (C-10, 2C); 67.85 (C-6, 2C); 77.06 (C-8, 2C); 77.36 (C-7, 2C); 109.92 (C-9, 2C); 121.15 (C-3, 4C); 126.18 (C-1, 2C); 129.60 (C-2, 4C); 150.69 (C-4, 2C); 152.91 (C-5, 2C) ppm.

**1,6-Di-*O*-phenoxy-carbonyl-galactitol (6)**

1,6-Bis-*O*-phenoxy-carbonyl-2,3:4,5-di-*O*-isopropylidene-galactitol (**5**) (50.00 g, 100 mmol) was treated for 20 min at room temperature with an aqueous solution of trifluoroacetic acid (trifluoroacetic acid (225 mL)–water (25 mL)). First the starting material dissolves in the mixture of solvents and later the product precipitates. For quantitative precipitation

additional water (200 mL) is added and the colourless solid is filtered off and washed with water. Yield: 95% (39.59 g, 95 mmol). For the NMR assignments, *cf.* scheme 7.

**<sup>1</sup>H NMR (DMSO-*d*<sub>6</sub>)**

$\delta_{\text{H}} = 3.55$  (s, 2H, CH-8); 4.10 (m, 2H, CH<sub>2</sub>-6<sup>a</sup>); 4.20–4.31 (m, 4H, CH<sub>2</sub>-6<sup>b</sup>, CH-7); 4.59 (br s, 4H, OH-9, OH-10); 7.27 (m, 4H, CH-3); 7.30 (m, 2H, CH-1); 7.45 (m, 4H, CH-2) ppm.

**<sup>13</sup>C NMR (DMSO-*d*<sub>6</sub>)**

$\delta_{\text{C}} = 66.74$  (C-6, 2C); 69.00 (C-8, 2C); 70.31 (C-7, 2C); 121.22 (C-3, 4C); 126.06 (C-1, 2C); 129.58 (C-2, 4C); 150.77 (C-4, 2C); 153.18 (C-5, 2C) ppm.

**Galactitol-1,2:5,6-dicarbonate (7)**

1,6-Di-*O*-phenoxy-carbonyl-galactitol (**6**) (5 g, 11.84 mmol) was suspended in toluene (100 mL) and heated for 12 h to reflux. On cooling to room temperature the product precipitates from the clear solution. Filtration yields 87% (2.42 g, 10 mmol) of colourless needles. M.p. 211°–213 °C. For the NMR assignments, *cf.* scheme 7.

**<sup>1</sup>H NMR (DMSO-*d*<sub>6</sub>)**

$\delta_{\text{H}} = 3.30$  (br s, 2H, OH-5); 4.39 (m, 2H, CH-4); 4.56 (m, 2H, CH<sub>2</sub>-2<sup>a</sup>); 5.05 (m, 4H, CH<sub>2</sub>-2<sup>b</sup>, CH-3) ppm.

**<sup>13</sup>C-NMR (DMSO-*d*<sub>6</sub>)**

$\delta_{\text{C}} = 61.44$  (C-2, 2C); 70.17 (C-3, 2C); 76.44 (C-4, 2C); 155.39 (C-1, 2C) ppm.

**Poly(2,3:4,5-di-*O*-isopropylidene-galactitol-ethylurethane) PiG2**

(a) 1,6-Bis-*O*-phenoxy-carbonyl-2,3:4,5-di-*O*-isopropylidene-galactitol (**5**) (9.13 g, 18 mmol) and 1,2-diaminoethane (1.09 g, 18 mmol) were heated in THF (180 mL) to reflux for 24 h. The solvent was removed by distillation and the product was dissolved in dimethylformamide and precipitated in ether. Yield: 59% (3.98 g, 11 mmol).  $\bar{M}_{\text{n}} = 13\,000$ ,  $\bar{M}_{\text{w}} = 20\,000$ ,  $\bar{M}_{\text{w}}/\bar{M}_{\text{n}} = 1.5$ .

(b) 1,6-Bis-*O*-phenoxy-carbonyl-2,3:4,5-di-*O*-isopropylidene-galactitol (**5**) (2.28 g, 5 mmol) and 1,2-diaminoethane (0.27 g, 5 mmol) were heated in THF (25 mL) to reflux for 24 h. The solvent was removed by distillation and the product was dissolved in dimethylformamide and precipitated in ether. Yield 67% (1.14 g, 3 mmol).  $\bar{M}_{\text{n}} = 41\,000$ ,  $\bar{M}_{\text{w}} = 63\,000$ ,  $\bar{M}_{\text{w}}/\bar{M}_{\text{n}} = 1.5$ . The <sup>1</sup>H and <sup>13</sup>C NMR spectra are shown in Fig. 3.

**Poly(galactitol-propylurethane) PG3**

1,6-Di-*O*-phenoxy-carbonyl-galactitol (**6**) (3.82 g, 9 mmol) and 1,3-diaminopropane (0.68 g, 9 mmol) in THF (90 mL) were heated under reflux for 48 h. The solvent was removed and the residue dissolved in dimethylformamide and precipitated in ether. Yield: 57% (1.60 g, 5 mmol).  $\bar{M}_{\text{n}} = 10\,000$ ,  $\bar{M}_{\text{w}} = 15\,000$ ,  $\bar{M}_{\text{w}}/\bar{M}_{\text{n}} = 1.5$ . The <sup>1</sup>H NMR spectrum is shown in Fig. 5.

### Poly(galactitol-propylurethane) PaG3

Poly(2,3:4,5-di-*O*-isopropylidene-galactitol-propylurethane) (**PiG3**) ( $\bar{M}_n = 12\,000$ ,  $\bar{M}_w = 20\,000$ ,  $\bar{M}_w/\bar{M}_n = 1.7$ ) (1.50 g) was reacted for 15 min at room temperature with 90% trifluoroacetic acid (15 mL). The solvent was partially removed in vacuum and the product was precipitated in ether. Yield: 98% (1.17 g, 4 mmol).  $\bar{M}_n = 30\,000$ ,  $\bar{M}_w = 46\,000$ ,  $\bar{M}_w/\bar{M}_n = 1.5$ . The  $^1\text{H}$  NMR spectrum is shown in Fig. 5.

### Results and discussion

Recently, it was reported that polyamides with pendant hydroxy groups prepared from aldaric acid esters (*D*-glucaric, *meso*-galactaric- and *D*-mannaric acid ester) and diamines show characteristic water solubility, depending on the conformational differences of the aldaric units and the diamine used for their preparation.<sup>13,14</sup> In this paper we report on polyurethanes with pendant hydroxy groups with galactitol and diamine segments, to study their properties and to compare their properties in a forthcoming paper with those of polyurethanes prepared from mannitol and diamines.<sup>15</sup>

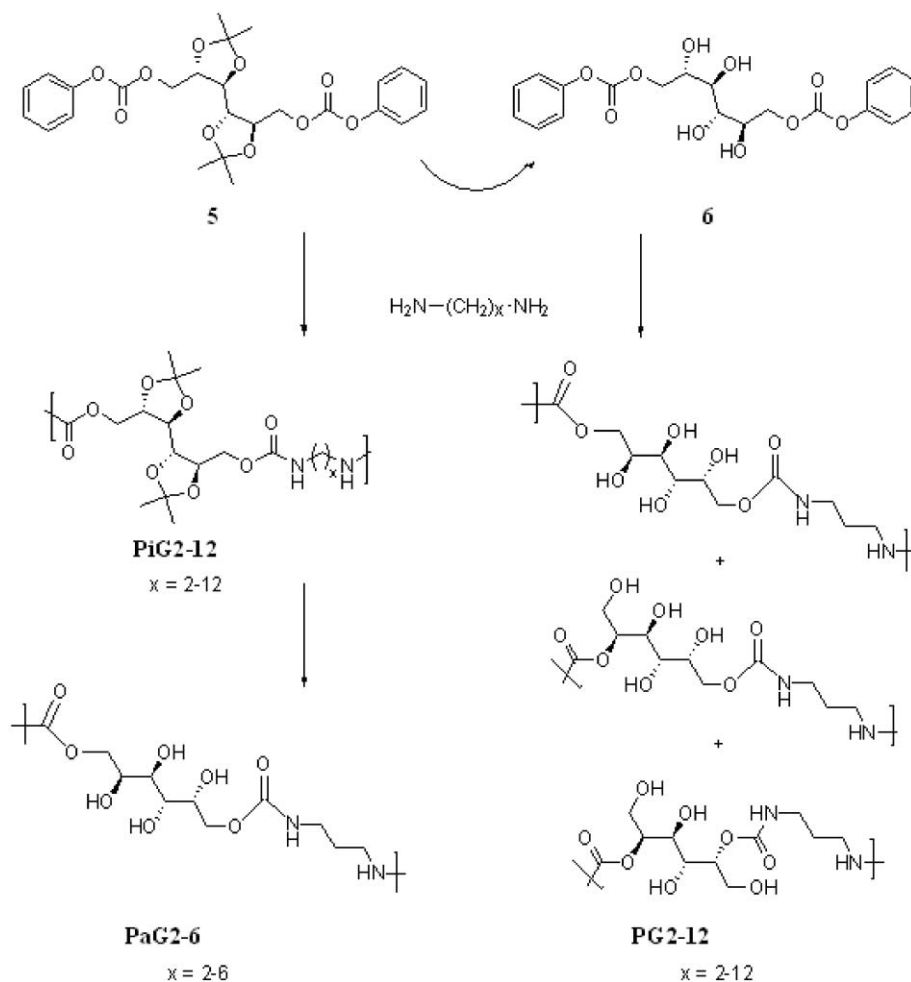
The synthetic approach to the preparation of polyurethanes with pendant hydroxy groups starts from 1,6-bis-*O*-phenoxycarbonyl-2,3:4,5-di-*O*-isopropylidene-galactitol (**5**)

and 1,6-di-*O*-phenoxycarbonylgalactitol (**6**) and diamines  $\text{H}_2\text{N}-(\text{CH}_2)_x-\text{NH}_2$  with  $x = 2-10$  and 12 as monomers. The polyurethanes starting from **5** are denoted **PiG2-12**, those starting from **6** are called **PG2-12**, where the numbers indicate the number of  $\text{CH}_2$ -groups in the diamine (scheme 8). Upon polymer analogous reaction (hydrolysis) of the **PiG**-series, polyurethanes denoted as **PaG2-6** are obtained. The reason for the difference in microstructure of polymers of the PG and PaG series will be presented later in this paper.

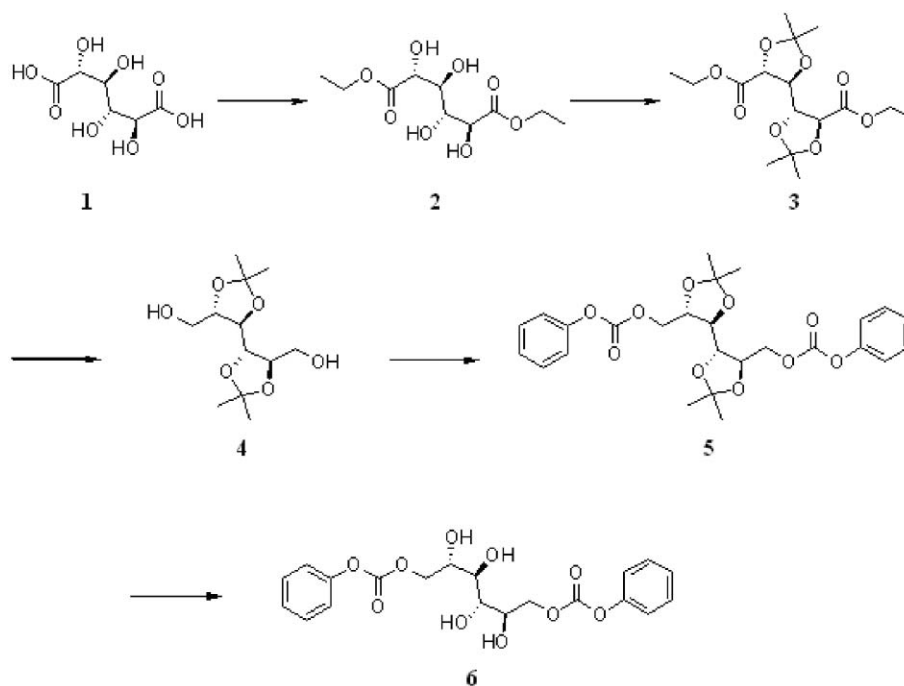
### Monomer synthesis

Phenylalkyl carbonates can be considered as activated carbonates, as phenyl esters are used as activated esters. For esters activation means acceleration of the reaction with the respective partners, for phenylalkyl carbonates in addition the direction of cleavage may be influenced, since a regio-selective cleavage determines the product yield. For phenylalkyl carbonates the direction of cleavage is determined by the thermodynamic stability of the leaving group: in the present case phenol is a better leaving group than an alcohol, and thus a regio-selective cleavage and consequently high yields are to be expected.

The starting material for the preparation of the bis(phenyl carbonate) monomers **5** and **6** is the commercially available galactaric (*mucic*) acid. The synthesis starts from the



**Scheme 8** Synthetic approach for the preparation of polyurethanes with pendant hydroxy groups.



Scheme 9 Preparation of bis(phenyl carbonate) monomers **5** and **6**.

esterification of galactaric acid with ethanol, followed by protection of the four hydroxy groups and reduction of the ester groups.<sup>16,17</sup> Finally, the phenyl carbonate group is introduced to obtain monomer **5** and, after removal of the protective groups, monomer **6** (scheme 9). The overall yield for monomer **5** is 76% and for monomer **6** is 72%.

The NMR spectra of the monomers prepared show the characteristic signals for the proposed structures, proving that during synthesis no racemization occurred. As an example, the <sup>1</sup>H NMR spectrum of 1,6-bis-*O*-phenoxycarbonyl-2,3:4,5-di-*O*-isopropylidene-galactitol (**5**) is given in Fig. 1. It shows the resonance lines of the galactitol segment at  $\delta = 4.0$ –4.5 ppm, of the protective groups at  $\delta$  ca. 4.0 ppm and of the *O*-phenyl carbonate groups at  $\delta = 7.2$ –7.5.

The <sup>13</sup>C NMR spectrum of 1,6-di-*O*-phenoxycarbonyl-galactitol (**6**) (Fig. 2) clearly reveals that the isopropylidene protective groups were effectively removed without hydrolytic cleavage of the carbonate groups. The signals of the galactitol units are around  $\delta = 70$  ppm and the phenylcarbonate groups show resonance lines between  $\delta = 120$  and 150 ppm.

### Polymer syntheses

**Polyurethanes with 2,3:4,5-di-*O*-isopropylidene-galactitol as repeating units (PiG series).** From 1,6-bis-*O*-phenoxycarbonyl-2,3:4,5-di-*O*-isopropylidene-galactitol (**5**) and diamines polyurethanes with protected hydroxy groups were obtained. Polymerizations were performed in THF solution at 80 °C for 24 h (Table 1). By increasing the monomer concentration an increase of the final molecular weight was observed. For purification the solvent was removed and the residue was dissolved in a small amount of DMF and precipitated in ether; this work-up procedure assures the removal of oligomers. In order to compare the influence of the amine on the reaction, a

homologous series of amines was subjected to polycondensation in THF solution at concentrations between 0.1 and 0.2 mol L<sup>-1</sup>. The molecular weight and the molecular weight distribution do not vary with the amine used; however, when using higher concentrations, the molecular weights obtained as well as the yields increase.

By means of <sup>1</sup>H and <sup>13</sup>C NMR analysis (Fig. 3) the structural repeating units were identified and thus the reaction course was verified. Upon nucleophilic addition of the amine to the carbonyl carbon atom phenol is selectively eliminated with formation of urethane groups; in this process the protective groups are not affected. The assignment of the signals in the <sup>1</sup>H NMR spectrum (Fig. 3(a)) is unambiguous and is shown for **PiG2** as an example. The ratio of the signals for the protective groups at  $\delta = 1.34$  and 1.37 ppm and of the protons of the galactitol moiety at  $\delta = 3.89$ , 4.05, 4.13 and 4.24 ppm of 3:3:1:1:1:1 reveals that the protective groups are not removed during polycondensation. The amide protons at  $\delta = 6.73$  and the methylene protons of the diamine unit at  $\delta = 3.12$  ppm show the expected chemical shift and integral ratio. The <sup>13</sup>C NMR spectrum confirms the proposed structure (Fig. 3(b)).

**Polyurethanes with galactitol in the repeating unit (PG and PaG series).** The polyurethanes of the **PG** and **PaG** series contain four hydroxy groups per repeating unit and were prepared either *via* direct polycondensation of 1,6-di-*O*-phenoxycarbonyl-galactitol (**6**) and diamines (**PG** series) or *via* polymer analogous reaction of the polyurethanes of the **PiG** series by removal of the protective groups (**PaG** series). Polycondensation of monomer **6** with diamines was performed under the conditions described before, *i.e.*, THF as a solvent at 80 °C for 24 h at a concentration of 0.1 mol L<sup>-1</sup>. Under these conditions, however, part of the polymer precipitates. For



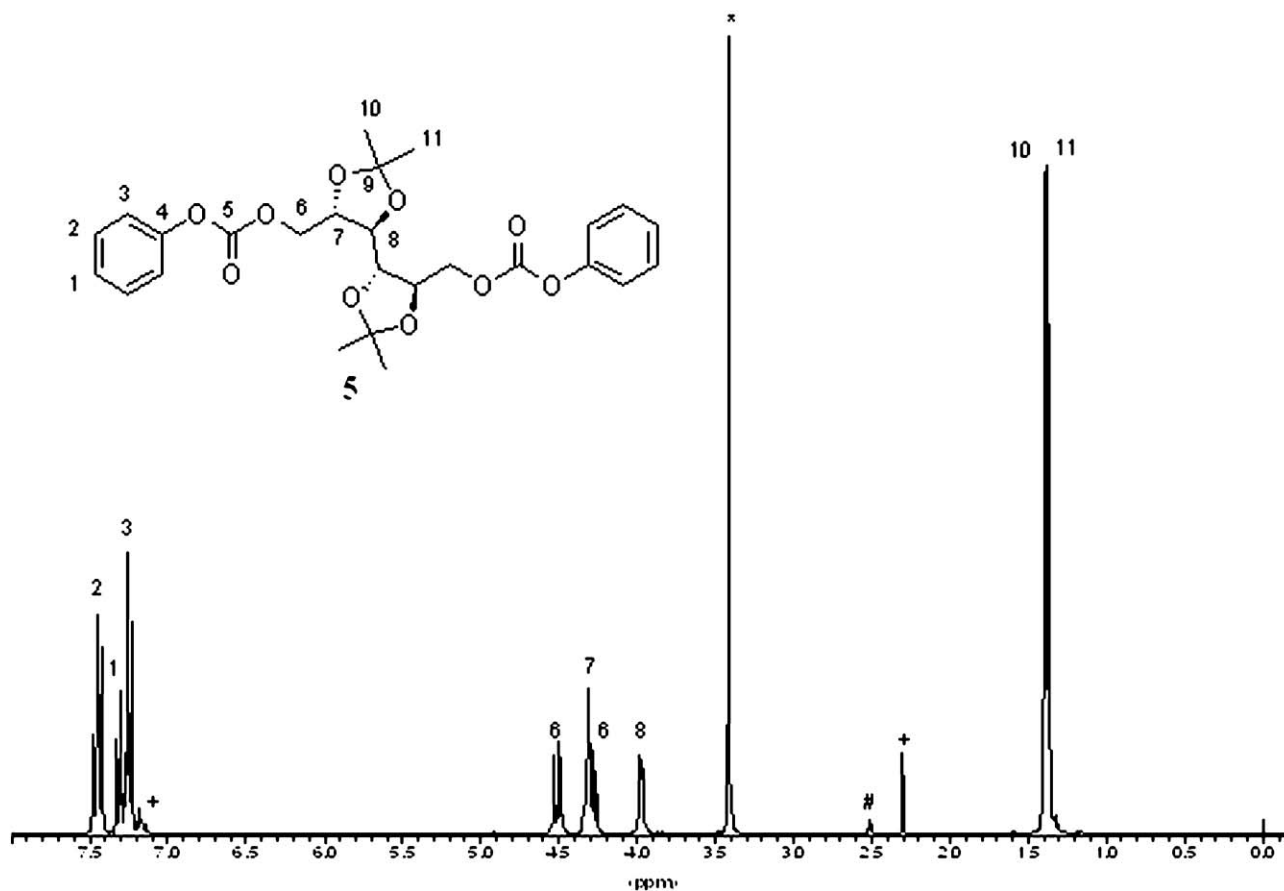


Fig. 1  $^1\text{H}$  NMR-spectrum of 1,6-bis-*O*-phenoxyacetyl-2,3,4,5-di-*O*-isopropylidene-galactitol (5) in  $\text{DMSO-}d_6$  (+ = toluene, \* =  $\text{H}_2\text{O}$ , # = DMSO).

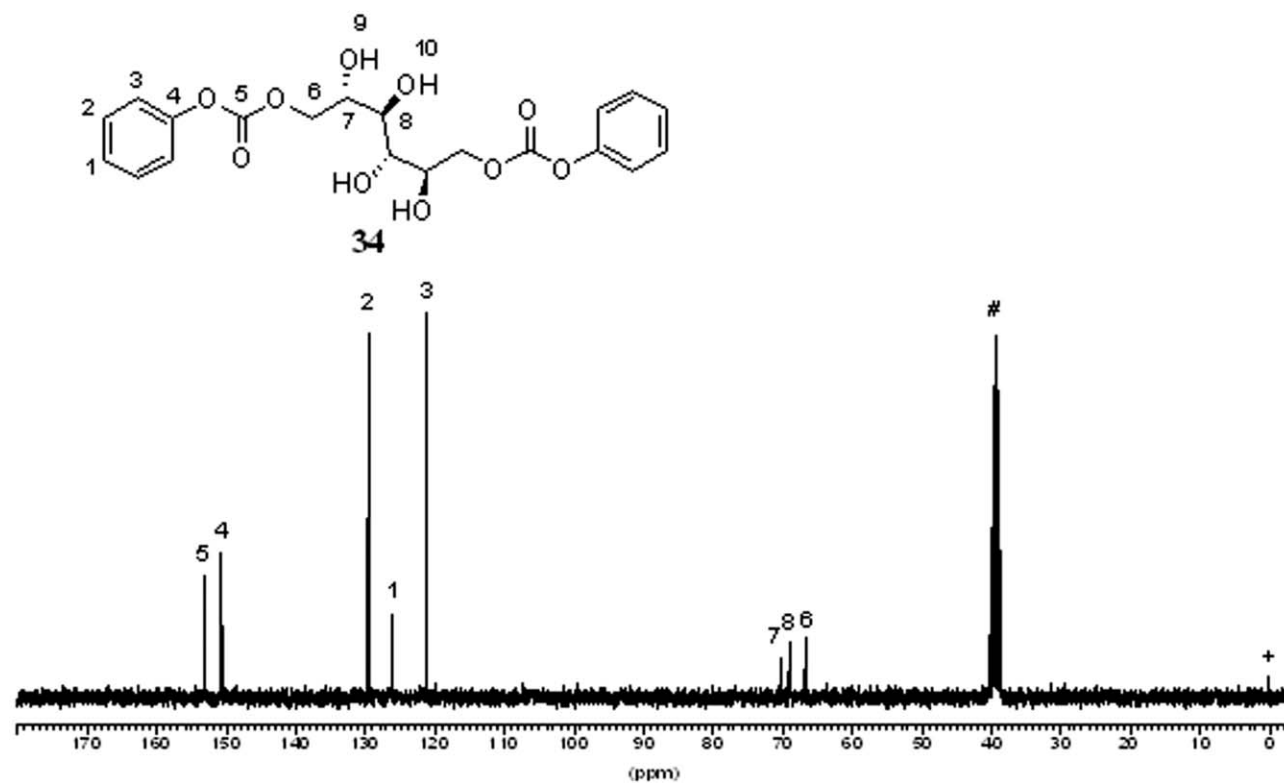
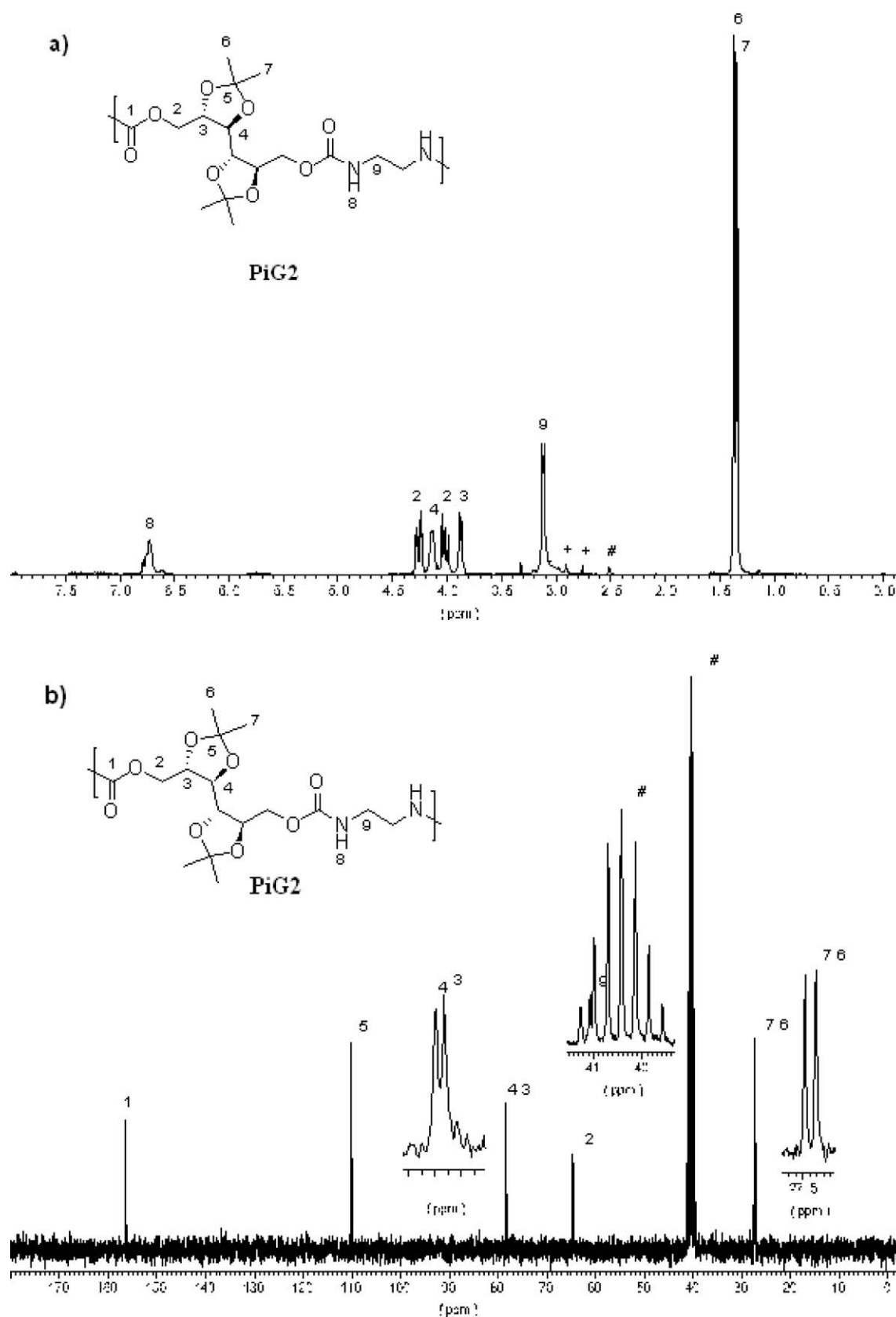


Fig. 2  $^{13}\text{C}$  NMR-spectrum of 1,6-di-*O*-phenoxyacetyl-galactitol (6) in  $\text{DMSO-}d_6$  (# = DMSO, + = TMS)



**Table 1** Polycondensation of **5** with diamines in THF ( $T = 80\text{ }^{\circ}\text{C}$ ,  $t = 24\text{ h}$ ) at two different initial concentrations: molecular weights, polydispersities and yields of the corresponding polymers **PiG2-12**

No.	Concentration <sup>a</sup> in mol L <sup>-1</sup>	Polymer	$\bar{M}_w^a$	$\bar{M}_w/\bar{M}_n^a$	Yield (%)
1	0.1	<b>PiG2</b>	20 000	1.5	59
	0.2	<b>PiG2</b>	63 000	1.5	67
2	0.1	<b>PiG3</b>	18 000	1.5	49
	0.2	<b>PiG3</b>	57 000	1.6	58
3	0.1	<b>PiG4</b>	29 000	1.5	65
	0.2	<b>PiG4</b>	42 000	1.6	54
4	0.1	<b>PiG5</b>	29 000	1.6	61
	0.2	<b>PiG5</b>	57 000	1.5	60
5	0.1	<b>PiG6</b>	41 000	1.7	62
	0.2	<b>PiG6</b>	46 000	1.5	65
6	0.1	<b>PiG7</b>	34 000	1.6	37
7	0.1	<b>PiG8</b>	34 000	1.6	57
8	0.1	<b>PiG9</b>	15 000	1.5	38
9	0.1	<b>PiG10</b>	18 000	1.5	54
10	0.1	<b>PiG12</b>	21 000	1.7	59

<sup>a</sup> These values refer to purified product.

**Table 2** Polycondensation of **6** (0.1 mol L<sup>-1</sup>) with diamines in THF ( $T = 80\text{ }^{\circ}\text{C}$ ,  $t = 24\text{ h}$ ): molecular weights, polydispersities and yields of the corresponding polymers **PG2-12**

No.	Polymer	$\bar{M}_w$	$\bar{M}_w/\bar{M}_n$	Yield (%)
1	<b>PG2</b>	18 000	1.8	82
2	<b>PG3</b>	15 000	1.5	57
3	<b>PG4</b>	16 000	1.6	63
4	<b>PG5</b>	26 000	2.0	92
5	<b>PG6</b>	29 000	1.7	67
6	<b>PG7</b>	36 000	2.6	92
7	<b>PG8</b>	33 000	2.0	86
8	<b>PG9</b>	18 000	2.0	85
9	<b>PG10</b>	28 000	1.8	85
10	<b>PG12</b>	25 000	1.9	98

**Table 3** Hydrolysis of **PiG2-6** with 90% trifluoroacetic acid: molecular weights of the starting polymer **PiG2-6** and the product polymer **PaG2-6** and yields

No.	Starting polymer	$\bar{M}_w$	Product polymer	$\bar{M}_w$	Yield (%)
1	<b>PiG2</b>	20 000	<b>PaG2</b>	50 000 <sup>a</sup>	93
				16 000 <sup>b</sup>	85
2	<b>PiG3</b>	20 000	<b>PaG3</b>	46 000 <sup>a</sup>	98
				16 000 <sup>b</sup>	84
3	<b>PiG4</b>	29 000	<b>PaG4</b>	52 000 <sup>a</sup>	99
				16 000 <sup>b</sup>	89
4	<b>PiG5</b>	29 000	<b>PaG5</b>	55 000 <sup>a</sup>	99
				16 000 <sup>b</sup>	90
5	<b>PiG6</b>	41 000	<b>PaG6</b>	62 000 <sup>a</sup>	98
				17 000 <sup>b</sup>	83

<sup>a</sup> Reaction time 15 min. <sup>b</sup> Reaction time 40 min.

purification, the solvent was removed, the residue dissolved in DMF and precipitated in ether.

The polyurethanes **PG2-12** of this series have lower molecular weights than the polymers obtained in the **PiG2-12** series at the same initial monomer concentration (*cf.* Table 2 and Table 1). All polymers of this series show poor solubility in aprotic dipolar solvents at room temperature.

An alternative route to these polymers is the hydrolytical deprotection of polyurethanes of the **PiG**-series. Samples of **PiG2-6** were hydrolyzed with 90% trifluoroacetic acid; depending on the reaction time, polymers of different molecular weight were obtained (Table 3). Obviously at short reaction times (15 min) a selective removal of the protective groups is achieved, while at longer reaction times side reactions caused by, for instance, polymer degradation occur. The polymer analogous reaction has the advantage of higher overall polymer yields and higher molecular weights as compared with the direct route.

Fig. 4 shows as an example the GPC diagrams of **PaG3** of the originating polymer **PiG3**. Even though the molecular

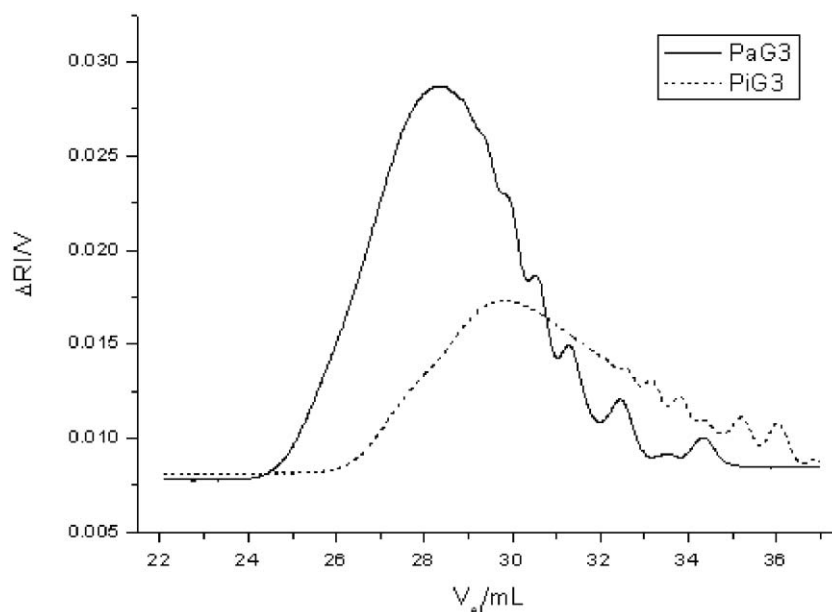


**Fig. 4** GPC-curve of **PiG3** ( $\bar{M}_w = 20\ 000$ ) and of **PaG3** ( $\bar{M}_w = 46\ 000$ ) in DMAc/2.44 g L<sup>-1</sup> LiCl (*cf.* Table 3).

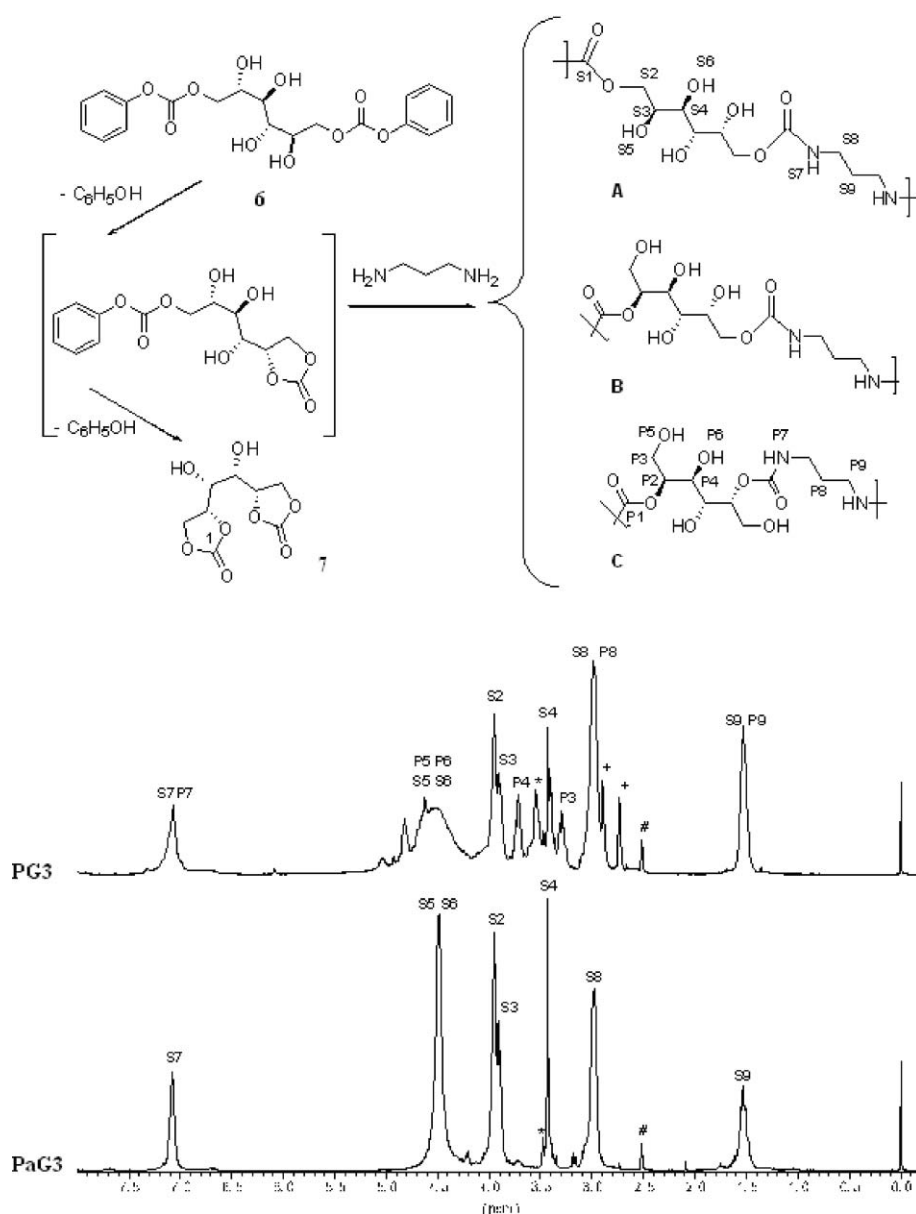


**Fig. 5**  $^1\text{H}$ -NMR-spectra of **PG3** and **PaG3** in  $\text{DMSO}-d_6$  (\* =  $\text{H}_2\text{O}$ , + = DMF, # = DMSO, TMS as internal standard, cf. Table 3) and reaction scheme for the formation of structural isomeric repeating units.

weight decreases upon deprotection an increase of the molecular weight is observed by GPC, which is caused by polymer association induced by hydrogen bonding. This explains also the low solubility of these polymers in aprotic dipolar solvents and the gelation of solutions upon cooling.

The microstructures of the polyurethanes of the **PG** series and of the **PaG** series show differences which can be explained by the different reaction course. The difference in the microstructure is exemplified in the  $^1\text{H}$  NMR spectra of **PG3** and **PaG3** (Fig. 5). The NMR spectrum of **PaG3** shows exclusively the expected signals: Due to the symmetry of the galactitol segment and the absence of structural isomers the number of signals is low. The NMR spectrum of **PG3** is more complex due to the fact that isomeric repeating units are formed during the reaction: the assignment was not possible due to strong overlapping of the signals. Obviously, under the given

conditions 1,6-di-*O*-phenoxygalactitol reacts *via* different routes: (i) reaction with the diamine leads to the microstructure **A**; (ii) intramolecular cyclization with elimination of phenol results in galactitol-1,2:5,6-dicarbonate (**7**) with 5 membered cyclic carbonate rings, since the cyclic carbonates are thermodynamically favoured. This reaction may occur only once (as shown in the scheme in Fig. 5). The substituted ethylene carbonate rings react with amines *via* ring-opening polyaddition, resulting in structurally isomeric repeating units **A**, **B**, and **C**.

#### Thermal stability

The thermal stability of the three series of polyurethanes **PiG**, **PG** and **PaG** was studied by means of thermogravimetry. For example, the mass loss as a function of temperature is shown

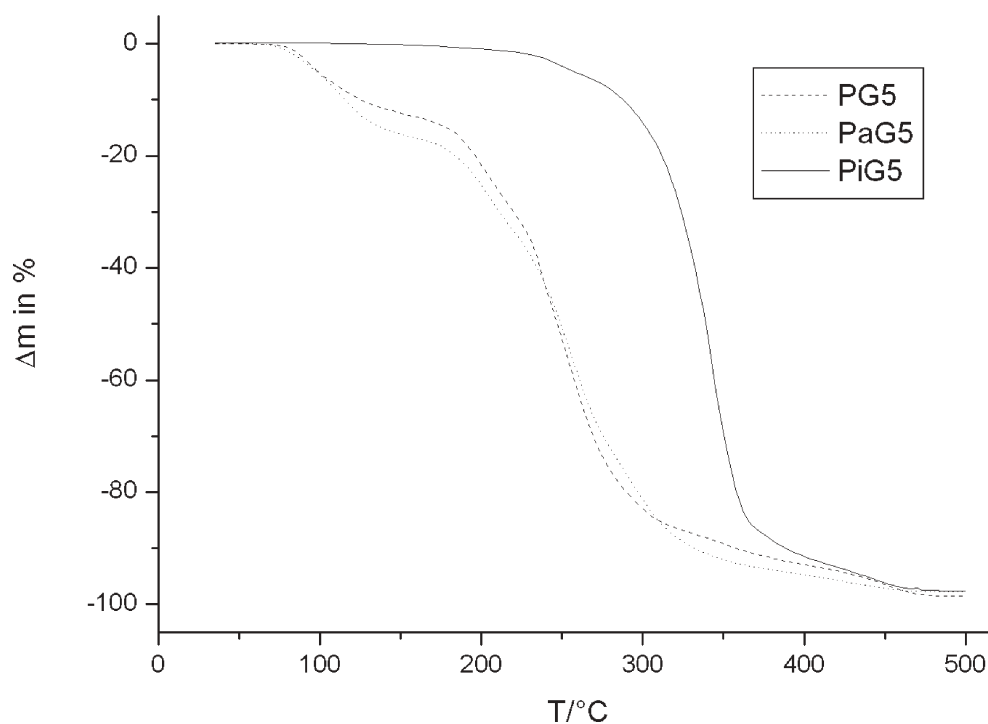


Fig. 6 TGA-curves of PaG5, PiG5 and PG5. (The measurements were performed in a nitrogen atmosphere with a heating rate of  $10 \text{ K min}^{-1}$ .)

Table 4 Thermal properties of polyurethanes PiG2-6, PG2-6 and PaG2-6 determined by means of TGA and DSC (heating rate  $10 \text{ K min}^{-1}$ )

Name	$T_{\text{dec.}}/^\circ\text{C}$	$T_{\text{m}}/^\circ\text{C}$	$T_{\text{g}}/^\circ\text{C}$	Name	$T_{\text{dec.}}/^\circ\text{C}$	$T_{\text{g}}/^\circ\text{C}$	Name	$T_{\text{dec.}}/^\circ\text{C}$	$T_{\text{g}}/^\circ\text{C}$
PiG2	270	161	78	PG2	184	59	PaG2	185	74
PiG3	282	167	74	PG3	182	54	PaG3	182	63
PiG4	293	161	72	PG4	186	52	PaG4	189	55
PiG5	298	161	69	PG5	185	45	PaG5	185	52
PiG6	303	160	59	PG6	189	44	PaG6	190	45

for PiG5, PG5 and PaG5 in Fig. 6. The polyurethane with protected hydroxy groups has a much higher stability than the polyurethanes with free hydroxy groups independent of the method of preparation of the last ones and consequently independent of their microstructure. For the polyurethanes with free hydroxy groups above  $100^\circ\text{C}$  residual water is removed before decomposition starts. The polyurethanes based on the other aliphatic diamines behave very similarly; the onset of their decomposition is summarized in Table 4.

The polyurethanes PiG2-6 are semi-crystalline materials; on first heating they show melting transitions in the range from  $160^\circ$  to  $167^\circ\text{C}$ , upon cooling no crystallization is observed and on second heating only glass transition temperatures in the range from  $59^\circ$  to  $78^\circ\text{C}$  are observed (Table 4). The polyurethanes PG2-6 and PaG2-6 show only glass transition temperatures in the range from  $44^\circ$  to  $74^\circ\text{C}$  upon first and second heating. A detailed analysis of the thermal properties will be published later.

## Conclusions

Polyurethanes with pendant hydroxy groups were prepared from 1,6-di-*O*-phenoxycarbonylgalactitol or

1,6-bis-*O*-phenoxycarbonyl-2,3:4,5-di-*O*-isopropylidene-galactitol (AA type monomers) and  $\alpha,\omega$ -diaminoalkanes (BB type monomers). The AA type monomers are derived from renewable primary materials and are highly functional monomers. These polyurethanes are not accessible *via* conventional routes starting from diisocyanates and polyols, due to the high reactivity and low selectivity of the reaction between diisocyanates and polyols which causes cross linking reactions. The polyurethanes with pendant hydroxy groups are stable up to  $180^\circ\text{C}$ , they exert hydrophilic properties and bear a high potential for adjusting the properties to the demands of a respective application by polymer analogous reactions.

## Acknowledgements

Financial support of the Fonds der Chemischen Industrie is gratefully acknowledged.

## References

- H.-J. Quadbeck-Seeger, in *Eggersdorfer/Warwell/Wulff, Nachhaltende Rohstoffe Perspektiven für die Chemie*, VCH-Verlagsgesellschaft, Weinheim, New York, Basel, Cambridge, Tokyo, 1992, XIII.
- G. A. Reinhard, in *Energie und CO<sub>2</sub>-Bilanzierung nachwachsender Rohstoffe*, F. Vieweg & Sohn Verlagsgesellschaft, Braunschweig, 1993.
- F. W. Lichtenhaler, *Zuckerindustrie*, 1991, **116**, 701–712.
- V. Prey, *Zuckerindustrie*, 1962, **87**, 548–555.
- T. B. Bird, W. A. P. Black, E. T. Dewar and D. Rutherford, *Chem. Ind.*, 1960, 1331–1332.
- O. Varela and H. A. Orgueira, *Adv. Carbohydr. Chem. Biochem.*, 2000, **55**, 137–174.
- G. A. R. Nobes, W. J. Orts and G. M. Glenn, *Ind. Crops Prod.*, 2000, **12**, 125–135.

- 8 (a) K. Kurita, N. Hirakawa and Y. Iwakura, *Makromol. Chem.*, 1977, **178**, 2939–2941; (b) K. Kurita, N. Hirakawa, Y. Iwakura and H. Morinaga, *Makromol. Chem.*, 1979, **180**, 2769–2773; (c) K. Kurita, K. Murakami, N. Masuda, S. Aibe, S. Ishii and S. I. Nishimura, *Macromolecules*, 1994, **27**, 7544–7549.
- 9 (a) J. Thiem and H. Lüders, *Starch/Stärke*, 1984, **36**, 170–176; (b) J. Thiem and H. Lüders, *Makromol. Chem.*, 1986, **187**, 2775–2785; (c) J. Thiem and F. Bachmann, *Makromol. Chem.*, 1991, **192**, 2163–2182.
- 10 (a) D. Braun and M. Bergmann, *J. Prakt. Chem.*, 1992, **334**, 298–310; (b) D. Braun and M. Bergmann, *Angew. Makromol. Chem.*, 1992, **199**, 191–205.
- 11 (a) K. Hashimoto, S. Wibullucksanakul, M. Matsuura and M. Okada, *J. Polym. Sci., Part A: Polym. Chem.*, 1993, **31**, 3141–3149; (b) K. Hashimoto, S. Wibullucksanakul and M. Okada, *J. Polym. Sci., Part A: Polym. Chem.*, 1995, **33**, 1495–1503.
- 12 L. Ubaghs, N. Fricke, H. Keul and H. Höcker, *Macromol. Rapid Commun.*, 2004, **25**, 517.
- 13 D. E. Kiely, L. Chen and T.-H. Lin, *J. Polym. Sci., Part A: Polym. Chem.*, 2000, **38**, 594.
- 14 D. W. Morton and D. E. Kiely, *J. Polym. Sci., Part A: Polym. Chem.*, 2000, **38**, 604.
- 15 G. Prömpers, H. Keul and H. Höcker, *Des. Monomers Polym.*, 2005, **8**, 547.
- 16 J. W. Cook and R. Schoental, *J. Chem. Soc.*, 1950, 47.
- 17 U. Peterson, P. Stadler, O. Lockhoff, H.-J. Zeiler and K. Metzger, *Eur. Pat. Application*, 1982, EP 56575 A1.

# Chemical Technology

A well-received news supplement showcasing the latest developments in applied and technological aspects of the chemical sciences



Free online and in print issues of selected RSC journals!\*

- **Application Highlights** – newsworthy articles and significant technological advances
- **Essential Elements** – latest developments from RSC publications
- **Free access** to the original research paper from every online article

\*A separately issued print subscription is also available

RSC Publishing

[www.rsc.org/chemicaltechnology](http://www.rsc.org/chemicaltechnology)

# Catalytic properties of several palladium complexes covalently anchored onto silica for the aerobic oxidation of alcohols

Deepak Choudhary,<sup>a</sup> Satya Paul,<sup>\*a</sup> Rajive Gupta<sup>a</sup> and James H. Clark<sup>b</sup>

Received 30th January 2006, Accepted 22nd February 2006

First published as an Advance Article on the web 10th March 2006

DOI: 10.1039/b601363e

A series of novel silica-supported palladium catalysts bearing N–N, N–S and N–O chelating ligands have been prepared and tested for the aerobic oxidation of alcohols to carbonyl compounds. The most active catalyst, **1**, was used for the oxidation of a series of primary and secondary alcohols to carbonyl compounds. The catalyst is highly selective and no over-oxidation products were detected. The catalyst **1** can also be used for the oxidation of primary benzyl alcohols to carbonyl compounds with comparable yields in the presence of atmospheric air.

## Introduction

In recent years, the search for environmentally benign chemical processes or methodologies has received much attention from chemists, because they are essential for the conservation of the global ecosystem.<sup>1</sup> The development of heterogeneous catalysts for fine chemical synthesis has become a major area of research, as the potential advantages of these materials (simplified recovery and reusability; the potential for incorporation in continuous reactors and microreactors) over homogeneous systems can lead to novel environmentally benign chemical procedures for academia and industry.<sup>2,3</sup>

The selective oxidation of alcohols to aldehydes and ketones is a highly desirable and much sought after transformation both in industrial chemistry as well as in organic synthesis, due to the wide-ranging utility of these products as important precursors and intermediates for many drugs, vitamins and fragrances.<sup>4,5</sup> In particular, the controlled oxidation of primary alcohols to aldehydes without forming over-oxidized products is a challenging task for chemists. Numerous methods are available for alcohol oxidation,<sup>6</sup> however, the development of newer methods and methodologies is currently gaining much attention due to the significance of this reaction. Traditional alcohol oxidations use toxic, corrosive and expensive oxidants such as DMSO-coupled reagents,<sup>7</sup> hypervalent iodines,<sup>8</sup> and chromium(VI) and manganese complexes, stringent conditions like high pressure or temperatures and the use of strong mineral acids.<sup>4,9</sup> Unfortunately, these oxidations result in large quantities of noxious wastes and call for the use of (at least) stoichiometric quantities of moisture-sensitive, unrecoverable and expensive reagents. Due to increasing environmental concerns, oxidations using environmentally friendly oxidants such as molecular oxygen and hydrogen peroxide are more desirable these days. Hydrogen peroxide oxidation, however, is relatively less economical due to its cost

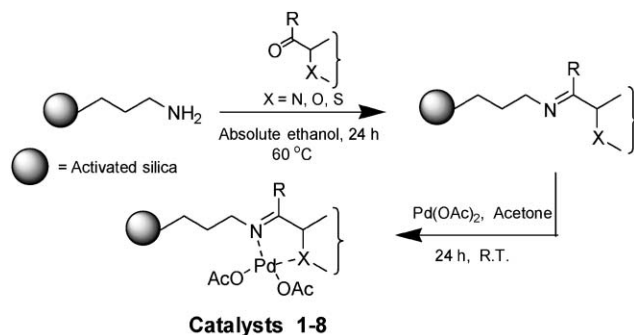
and comparatively poor efficiency and presents safety problems in transportation and storage.<sup>10</sup> Oxidations using molecular oxygen are highly attractive alternatives,<sup>6,11</sup> since they are atom efficient and produce water as the only by-product.<sup>12</sup> Recently, I<sub>2</sub>–KI–K<sub>2</sub>CO<sub>3</sub>–H<sub>2</sub>O<sup>13</sup> has been reported as a green reagent system for the selective oxidation of alcohols to carbonyl compounds.

Palladium is known to be an active catalyst for oxidations,<sup>14,15</sup> and some supported palladium catalysts have been shown to be stable in organic reaction systems. However, there are few examples of oxidations using supported palladium catalysts. Recently, it has been reported that a Pd(II) complex physisorbed onto hydrotalcite effects the aerobic oxidation of alcohols to the corresponding carbonyl compounds in the presence of pyridine as the exogenous base.<sup>16</sup> While this method is the first example of a Pd(II)-supported catalyst for application in the aerobic oxidation of alcohols, the catalyst suffers from the drawback of reduction of its activity caused by the leaching of the reactive centre (poor anchoring). Moreover, owing to the presence of a soluble ligand (pyridine) and the physisorbed nature of the Pd(II), it seems that oxidation with leached homogeneous palladium species, whereby the Pd(II) species is redeposited back on the heterogeneous surface at the end of the reaction, could be responsible.<sup>17</sup> Sahle-Demessie *et al.*<sup>18</sup> have also reported Pd/MgO as a quite efficient heterogeneous catalyst for the selective oxidation of alcohols to carbonyl compounds using molecular oxygen. However, long reaction times, low conversion and thus low turn-over frequencies (TOF) for the catalyst, make this catalytic system less practical. Palladium supported on alumina by an adsorption method has also been reported as an efficient and recyclable heterogeneous catalyst for the oxidation of alcohols using molecular oxygen.<sup>19</sup>

The problem of leaching of metals, such as palladium species, into the solution can be avoided by covalently anchoring the palladium species onto the surface of a suitable support. More recently, a palladium catalyst covalently anchored onto the surface of silica gel was reported for the selective oxidation of alcohols to carbonyl compounds.<sup>20</sup> This is a quite efficient and reusable supported palladium catalyst for the selective oxidation of alcohols to carbonyl compounds

<sup>a</sup>Department of Chemistry, University of Jammu, Jammu-180 006, India. E-mail: paul7@rediffmail.com; Fax: +91-191-2505086; Tel: +91-191-2453841

<sup>b</sup>Clean Technology Centre, Department of Chemistry, University of York, YO10 5DD, UK. E-mail: jhc1@york.ac.uk; Fax: +44 (0)1904 434550; Tel: +44 (0)1904 432559



Scheme 1

using molecular oxygen. This catalyst can be used for the oxidation of primary benzylic alcohols using atmospheric air but is less effective for aliphatic and secondary alcohols. However, with this catalyst, longer reaction times (4–14 h) are required.

In our earlier communication, we have reported<sup>21</sup> the preparation and structure–activity relationship of a series of novel, covalently anchored, silica-supported palladium catalysts bearing N–N, N–S and N–O chelating ligands for the Suzuki reaction. Keeping in view the importance of the selective oxidation of alcohols to carbonyl compounds in academia and industry, and that of heterogeneous catalysis, we report our results on the use of eight palladium catalysts covalently anchored onto the surface of silica gel (with N–N, N–S and N–O chelating ligands), for the selective oxidation of alcohols to carbonyl compounds with molecular oxygen, with a view to developing completely heterogeneous, reusable and more effective catalysts and also to further reducing the reaction time and increasing the TON. More importantly, there is interest in the development of a catalyst which could be used for the oxidation of alcohols in the presence of atmospheric air instead of molecular oxygen, which in turn could further reduce the cost and hazards of the oxidation process.

## Results and discussion

The general procedure for the synthesis of catalysts **1–8** is indicated in Scheme 1. It involves the preparation of 3-aminopropylsilica from activated silica and (3-aminopropyl)trimethoxysilane followed by the preparation of Schiff bases from 3-aminopropylsilica and *n*-butyl 2-pyridyl ketone,

**Table 1** Oxidation of benzyl alcohol to benzaldehyde using molecular O<sub>2</sub> and K<sub>2</sub>CO<sub>3</sub> in the presence of catalysts **1–8** (3 mol% of Pd) at 90 °C.<sup>a</sup>

Catalyst	Time/h	Yield <sup>b</sup> (%)
1	2.5	95
2	6	80
3	15	55
4	4.5	91
5	3.5	89
6	3.25	88
7	10	90
8	15	93

<sup>a</sup> The molar ratio of benzyl alcohol : K<sub>2</sub>CO<sub>3</sub> : catalyst is 1 : 1 : 0.03.

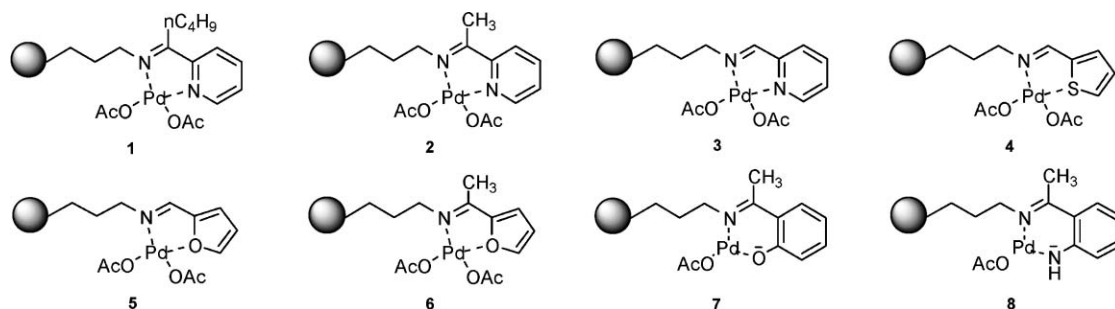
<sup>b</sup> Yield of isolated products.

2-acetylpyridine, 2-pyridinecarboxaldehyde, 2-thiophene-carboxaldehyde, 2-furancarboxaldehyde, 2-acetylfuran, 2-hydroxyacetophenone and 2-aminoacetophenone. The silica-supported palladium catalysts **1–8** were then prepared by the complexation of the Schiff base with Pd(OAc)<sub>2</sub> in acetone. For detailed procedures, and characterizations of catalysts, see refs. 21 and 22.

The probable structures of the catalysts **1–8** are given in Scheme 2.

In our earlier report, we prepared eight catalysts and among those, the most active catalyst for the Suzuki reaction was found to be **2**, which contains –CH<sub>3</sub> groups at the carbon adjacent to the imino N, with the pyridyl N as the second co-ordinating ligand. If we compare the structures of catalysts **2** and **3**, the only difference is the presence of –CH<sub>3</sub> in **2**. But the interesting thing is that there is a tremendous difference in the activity of these two catalysts for the Suzuki reaction. So keeping in view this fact, we have prepared another catalyst **1**, which contains the –(CH<sub>2</sub>)<sub>3</sub>CH<sub>3</sub> group in the place of –CH<sub>3</sub> in **2**, with a view to finding a more active catalyst.

To test the activity of these catalysts **1–8** as completely heterogeneous catalysts for the oxidation of alcohols, we selected benzyl alcohol as the test substrate. The oxidation of benzyl alcohol (1 mmol) was attempted in the presence of catalysts **1–8** (equivalent to 3 mol% of Pd) in toluene (5 mL) at 90 °C in the presence of K<sub>2</sub>CO<sub>3</sub> (1 mmol). The results are summarized in Table 1. From Table 1, it is clear that the most active catalyst is **1** (3 mol% of Pd), which oxidizes benzyl alcohol in the presence of molecular oxygen in 2.5 h at 90 °C with 100% conversion and 95% isolated yield of benzaldehyde. The high activity of catalyst **1**, compared to catalysts **2–8**, for the oxidation of alcohols to the corresponding carbonyl



Scheme 2



**Table 2** Oxidation of alcohols to the corresponding carbonyl compounds using molecular O<sub>2</sub> and K<sub>2</sub>CO<sub>3</sub> in the presence of catalyst **1** (3 mol% of Pd) at 90 °C.<sup>a</sup>

Entry	Alcohol	Time/h	Yield <sup>b</sup> (%)
1	Benzyl alcohol	2.5	95
2	4-(MeO)C <sub>6</sub> H <sub>4</sub> CH <sub>2</sub> OH	2.5	96
3	4-(Me)C <sub>6</sub> H <sub>4</sub> CH <sub>2</sub> OH	3.0	92
4	4-(Cl)C <sub>6</sub> H <sub>4</sub> CH <sub>2</sub> OH	2.5	94
5	4-(F)C <sub>6</sub> H <sub>4</sub> CH <sub>2</sub> OH	3.0	95
6	4-(NO <sub>2</sub> )C <sub>6</sub> H <sub>4</sub> CH <sub>2</sub> OH	4.5	90
7	3-(NO <sub>2</sub> )C <sub>6</sub> H <sub>4</sub> CH <sub>2</sub> OH	5	87
8	1-Pentanol	5.5	85
9	2-Butanol	5.0	82
10	Cyclohexanol	5.0	90
11	1-Phenyl ethanol	5.5	93
12	Cinnamyl alcohol	15	40

<sup>a</sup> The molar ratio of alcohol : K<sub>2</sub>CO<sub>3</sub> : **1** is 1 : 1 : 0.03. <sup>b</sup> Yield of isolated products.

compounds can be explained in a similar way to that reported in our earlier communication,<sup>21</sup> *i.e.* the presence of an alkyl group at the carbon adjacent to the imino N increases the stability of the catalyst by increasing the binding energy of Pd with the N atoms.

The oxidation of various substituted benzyl alcohols (containing both electron-withdrawing and electron-releasing groups) was attempted with catalyst **1** in toluene in the presence of K<sub>2</sub>CO<sub>3</sub> using molecular oxygen, and excellent results were found (Table 2, entries 1–7).

Once we were able to carry out the oxidation of benzyl alcohols efficiently, then attempts were made to perform the oxidation of other aliphatic alcohols. It was found that **1** is equally efficient for the oxidation of aliphatic primary and secondary alcohols as well. The results are given in Table 2 (entries 8–11). It is worth mentioning that oxidation of cinnamyl alcohol (entry 12) takes place very slowly with only 40% isolated yield of cinnamaldehyde in 15 h.

When using a supported metal catalyst, two important issues need to be addressed to qualify this as a purely heterogeneous catalyst. One is the possibility that some active metal migrates from the solid to the liquid phase, and that this leached palladium would become responsible for a significant part of the catalytic activity. To rule out the contribution of homogeneous catalysis in the results shown in Table 2, the oxidation of benzyl alcohol was carried out in the presence of **1** until the conversion was 35% and at that point, the solid was filtered off at the reaction temperature. The liquid was then transferred to another flask containing K<sub>2</sub>CO<sub>3</sub> and then again allowed to react, but no further significant conversion was observed. This indicates that no active species was present in the supernatant and that the observed catalysis is purely heterogeneous. The second important point concerning heterogeneous catalysis is the deactivation and reusability of the catalyst. To test this, a series of 7 consecutive runs of the oxidation of benzyl alcohol with catalyst **1** was carried out (1st use: 100% conversion after 2.5 h; 3rd use: 95% after 3.5 h; 5th use: 85% after 5 h; 7th use: 60% after 8 h). These results demonstrate that there is almost no change in the activity of **1** up to the 3rd use, a slight decrease in activity was observed up to the 5th use, but after the 5th use there is a tremendous

decrease in activity. This may be due to either the deactivation of active centres resulting from complexation with both starting materials and products, or microscopic changes in the structure of the catalyst.

A further improvement in the efficiency of the aerobic oxidation process can be achieved if molecular oxygen is replaced with atmospheric oxygen – then the process is more safe and economic. With catalyst **1**, we carried out the oxidation of benzyl alcohol in toluene using K<sub>2</sub>CO<sub>3</sub> (1 eq.) in the presence of atmospheric air. It was found that benzyl alcohol undergoes oxidation with 100% conversion in 7 h. However, lower yields were found in case of 1-pentanol and cyclohexanol. Thus, there is still a need to develop heterogeneous catalysts, which could be used for the oxidation of alcohols in the presence of atmospheric air. The development of new supported palladium catalysts is under active investigation in our laboratories.

## Experimental

### General

The chemicals used were either prepared in our laboratories or purchased from Aldrich Chemical Company. The products were characterized by comparison of their physical data with those of known samples or by their spectral data. The <sup>1</sup>H NMR data were recorded in CDCl<sub>3</sub> on a Bruker DPX 200 (200 MHz) spectrometer using TMS as an internal standard. The IR spectra were recorded on a Perkin–Elmer FTIR spectrophotometer using KBr windows.

**General procedure for the oxidation of alcohols to carbonyl compounds using catalyst **1**.** To a mixture of K<sub>2</sub>CO<sub>3</sub> (1 mmol) and catalyst **1** (0.260 g, 3 mol% Pd) in a three-necked round-bottomed flask, toluene (5 mL) was added. The flask was then evacuated with the help of a pump and twice refilled with oxygen (using oxygen-filled balloons). The reaction mixture was maintained at 90 °C, the alcohol (1 mmol) was injected into the flask using a syringe and the mixture was stirred under a pure oxygen atmosphere for an appropriate time (Table 2). On completion, the reaction mixture was filtered while hot and the residue was washed with hot toluene (5 mL). The product was obtained after removal of the solvent under reduced pressure. In most cases, the purity of the products was found to be greater than 98% (determined by <sup>1</sup>H NMR) without any chromatographic purification. The catalyst was recovered from the residue after washing with CH<sub>2</sub>Cl<sub>2</sub> (10 mL) followed by distilled water (200 mL) and then with CH<sub>2</sub>Cl<sub>2</sub> (15 mL). It was reused after drying at 100 °C for 5 h.

### Conclusions

In conclusion, we have reported the application of eight palladium/silica catalysts for the oxidation of benzyl alcohol using molecular oxygen and K<sub>2</sub>CO<sub>3</sub>. Out of these, the most active catalyst **1** was used for the oxidation of various types of structurally diverse alcohols to the corresponding carbonyl compounds. Catalyst **1** is completely heterogeneous, is more reusable and results in a faster reaction than the previously reported heterogeneous catalyst.<sup>20</sup> Further, it can be used for

the oxidation of primary benzylic alcohols under an air atmosphere, but is less efficient for the oxidation of other types of alcohols.

## References

- 1 *Organic Synthesis in Water*, ed. P. A. Grieco, Blackie Academic and Professional, London, 1998; C.-J. Li and T.-H. Chan, *Organic Reactions in Aqueous Media*, John Wiley and Sons, New York, 1997; U. M. Lindstorm, *Chem. Rev.*, 2002, **102**, 2751; S. Kobayashi and K. Manabe, *Acc. Chem. Res.*, 2002, **35**, 209.
- 2 *Handbook of Green Chemistry and Technology*, ed. J. H. Clark and D. J. Macquarrie, Blackwell, Oxford, 2002.
- 3 P. T. Anastas, M. M. Kirchhoff and T. C. Williamson, *Appl. Catal., A*, 2001, **221**, 3.
- 4 R. A. Sheldon and J. K. Kochi, *Metal-catalyzed Oxidation of Organic Compounds*, Academic Press, New York, 1981.
- 5 M. Hudlicky, *Oxidations in Organic Chemistry*, American Chemical Society, Washington, D.C., 1990.
- 6 R. A. Sheldon, I. W. C. E. Arends and A. Dijkman, *Catal. Today*, 2000, **57**, 157.
- 7 A. Mancuso and D. Swern, *Synthesis*, 1981, 165.
- 8 D. B. Dess and J. C. Martin, *J. Org. Chem.*, 1983, **48**, 4155; D. B. Dess and J. C. Martin, *J. Am. Chem. Soc.*, 1991, **113**, 7277.
- 9 W. P. Griffith and J. M. Joliffe, *Di-oxygen Activation and Homogeneous Catalytic Oxidation*, ed. L. L. Simandi, Elsevier, Amsterdam, 1991.
- 10 U. R. Pillai and E. Sahle-Demessie, *Appl. Catal., A*, 2003, **245**, 103.
- 11 B. Z. Zhan and A. Thompson, *Tetrahedron*, 2004, **60**, 2917.
- 12 For a general discussion of atom economy in organic synthesis see: (a) B. M. Trost, *Science*, 1991, **254**, 1471; (b) B. M. Trost, *Angew. Chem., Int. Ed. Engl.*, 1995, **34**, 259.
- 13 P. Gogoi and D. Konwar, *Org. Biomol. Chem.*, 2005, **3**, 3473.
- 14 T. Mallat and A. Baiker, *Catal. Today*, 1994, **19**, 247; G. Brink, I. W. C. E. Arends and R. A. Sheldon, *Science*, 2000, **287**, 1636; M. J. Schultz, C. C. Park and M. S. Sigman, *Chem. Commun.*, 2002, 3034; T. Nishimura, T. Onoue, K. Ohe and S. Uemura, *J. Org. Chem.*, 1999, **64**, 6750; T. Nishimura and S. Uemura, *Synlett*, 2004, 201; S. Paavola, K. Zetterberg, T. Privalov, I. Csoregh and C. Moberg, *Adv. Synth. Catal.*, 2004, **346**, 237; M. J. Schultz, S. S. Hamilton, D. R. Jensen and M. S. Sigman, *J. Org. Chem.*, 2005, **70**, 3343.
- 15 For related examples of palladium-catalyzed oxidative kinetic resolutions see: E. M. Ferriera and B. M. Stoltz, *J. Am. Chem. Soc.*, 2001, **123**, 7725; J. T. Bagdanoff, E. M. Ferriera and B. M. Stoltz, *Org. Lett.*, 2003, **5**, 835; S. K. Mandal, D. R. Jensen, J. S. Pugsley and M. S. Sigman, *J. Org. Chem.*, 2003, **68**, 4600; J. T. Bagdanoff and B. M. Stoltz, *Angew. Chem., Int. Ed.*, 2004, **43**, 353.
- 16 T. Nishimura, N. Kakiuchi, M. Inoue and S. Uemura, *Chem. Commun.*, 2000, 1245; N. Kakiuchi, Y. Maeda, T. Nishimura and S. Uemura, *J. Org. Chem.*, 2001, **66**, 6620.
- 17 For recent examples of metal colloids as reservoirs for homogeneous metal species see: S. Tasler and B. H. Lipshutz, *J. Org. Chem.*, 2002, **64**, 1190; I. W. Davis, L. Matty, D. L. Hughes and J. P. Reider, *J. Am. Chem. Soc.*, 2001, **123**, 10139.
- 18 U. R. Pillai and E. Sahle-Demessie, *Green Chem.*, 2004, **6**, 161.
- 19 H. Wu, Q. Zhang and Y. Wang, *Adv. Synth. Catal.*, 2005, **347**, 1356.
- 20 B. Karimi, A. Zamani and J. H. Clark, *Organometallics*, 2005, **24**, 4695.
- 21 S. Paul and J. H. Clark, *J. Mol. Catal. A: Chem.*, 2004, **215**, 107.
- 22 S. Paul and J. H. Clark, *Green Chem.*, 2003, **5**, 635.

# Rapid microwave-promoted synthesis of new sulfonylmethylbenzothiazoles in water

A. Gellis, N. Boufatah and P. Vanelle\*

Received 30th January 2006, Accepted 8th March 2006

First published as an Advance Article on the web 23rd March 2006

DOI: 10.1039/b601452f

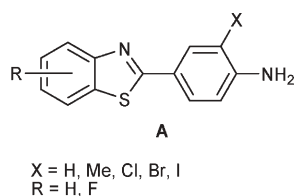
A simple, fast and inexpensive microwave-irradiated reaction permitting the synthesis of new sulfonylmethylbenzothiazoles in water by *S*-alkylation of 2-chloromethyl-6-nitrobenzothiazole **2** with different benzenesulfinic acid anions **3** is reported.

## Introduction

The development of efficient and environmentally friendly chemical processes for the preparation of new biologically active molecules constitutes a major challenge for chemists in organic synthesis. The benzothiazole nucleus is found in various synthetic drugs displaying a broad biological spectrum of activity including antiparasitic, antibacterial, antiviral and cytotoxic properties.<sup>1</sup> Novel 2-(4-aminophenyl)benzothiazoles **A** possess remarkably selective antitumour activities and represent a pharmacotherapeutic group distinct from clinically used anti-cancer agents (Scheme 1).<sup>2</sup>

The development of organic reactions in water has become an important research area, as microwave-enhanced procedures have proved highly useful in organic chemistry due to great reaction control and high reaction rates.<sup>3</sup> Among the commonly used solvents in organic synthesis, water is the cheapest, non-toxic and non-flammable. Under microwave irradiation, water is rapidly heated to high temperatures, enabling it to act as a less polar pseudo-organic solvent. Moreover, precise control of the reaction temperature is easily achieved because of the very high heat capacity of water.<sup>4</sup>

In view of the biological activity of compounds related to sulfonyl derivatives,<sup>5</sup> we became interested in devising eco-friendly synthetic methods for the preparation of new benzothiazole compounds dedicated to pharmacological evaluation. Thus we report here a practical, inexpensive, rapid and green microwave-promoted method for the preparation of sulfonylmethylbenzothiazole derivatives in water.



Scheme 1

Laboratoire de Chimie Organique Pharmaceutique, LCOP-UMR CNRS 6517, Université de la Méditerranée, Faculté de Pharmacie, 27 boulevard Jean Moulin, 13385, Marseille Cedex 5, France.  
E-mail: patrice.vanelle@pharmacie.univ-mrs.fr.; Fax: +33 04 91 79 46 77;  
Tel: +33 04 91 83 55 80

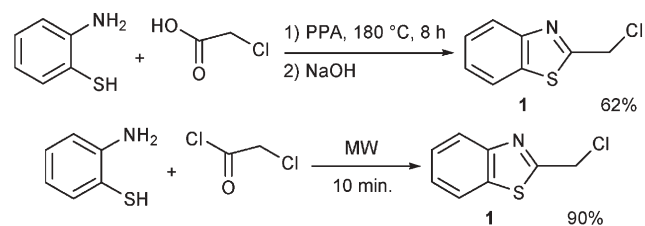
## Results and discussion

Two main synthetic routes usually allow the preparation of 2-alkylbenzothiazoles. The most commonly used method involves the condensation of *ortho*-aminothiophenols with substituted aldehydes, carboxylic acids, acyl chlorides and nitriles.<sup>6</sup> Recently, we have reported a method to prepare 2-chloromethylbenzothiazole **1**, which gives a good yield (62%) by using polyphosphoric acid (PPA) as a reactant.<sup>7</sup>

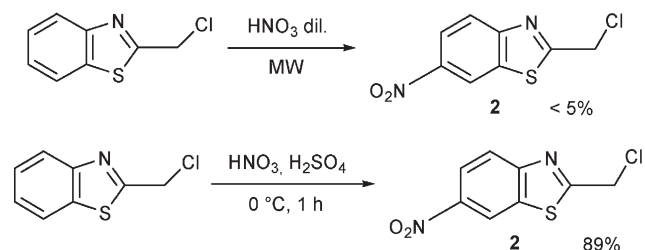
In order to improve this result, we developed a microwave-assisted procedure using less polluting reagents that are easier to use than PPA. This method uses 2-chloroacetyl chloride in acetic acid, leading to the required derivative **1**, in 90% yield in 10 minutes (Scheme 2).

With the aim of optimizing the nitration of the ring in position 6 we tried to adapt the method described by A. K. Bose on *p*-hydroxybenzaldehyde,<sup>8</sup> without much success. Indeed, the yields obtained remained very poor, and the traditional method that we described previously<sup>7</sup> was the only one that gave good results, with 89% yield for the synthesis of 2-chloromethyl-6-nitrobenzothiazole **2** (Scheme 3).

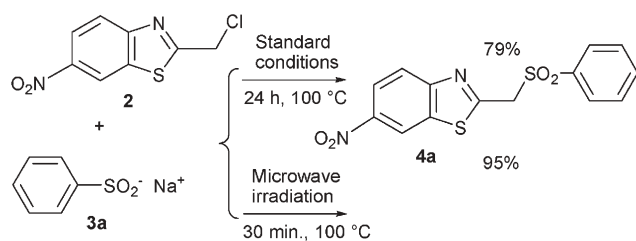
Simple addition of both 2-chloromethyl-6-nitrobenzothiazole **2** and the sodium salt of benzenesulfinic acid **3a** in an



Scheme 2



Scheme 3



Scheme 4

aqueous solution gave the corresponding *S*-alkylation product **4a** with 92% yield. Under conventional heating, a temperature of 100 °C was selected for 24 h. To evaluate the purely non-thermal microwave effects, the same temperature was applied under microwave irradiation in water for 30 min.

The use of microwave irradiation led to the same product, with higher yield (95%) in a shorter time (24 h reduced to 30 min), as shown in Scheme 4.

To generalize this procedure, we synthesized several sulfonylmethylbenzothiazole derivatives using the optimized reaction conditions: microwave irradiation, 30 min, 100 °C (Scheme 4). The use of these optimal microwave experimental conditions for the reaction of different benzenesulfinate anions **3b–j** afforded good yields of new 6-nitrobenzothiazole derivatives **4b–j**, presenting a sulfonylmethyl group in position 2 of the benzothiazole nucleus (Table 1). The obtained yields (64–95%) were similar or higher than those observed under classical conditions (45–79%).

The above results show the specific activation of the *S*-alkylation reaction by microwave heating.

The difference in yields (MW > SC) may be a consequence of both thermal effects and specific effects induced by the microwave field.<sup>9</sup>

Indeed, specific microwave effects can be observed for polar mechanisms when the polarity is increased during the reaction, from the ground state (GS) towards the transition state (TS).<sup>10</sup>

In the present case, the TS for *S*-alkylation reaction (S<sub>N</sub>2 mechanism) involves loose ion pairs as a charge-delocalised (soft) anion, whereas the GS involves a neutral electrophile and a tighter ion pair. During the course of the reaction, ionic dissociation increases, and that way polarity is enhanced from GS to TS. Thus, a favourable microwave effect can be observed.

All the sulfonylmethylbenzothiazoles obtained were to be screened for their antitumour activity. Their cytotoxicity was evaluated in triplicate on colon (HT29-D4), breast (T47D) and lung (A549) cancer cells.

The first results show that compounds **4a–j** present significant cytotoxic activity at medium concentrations, depending on the cell line. These results incite us to continue our investigations in the field of new heterocyclic sulfone synthesis according to an increasingly cleaner, more rapid and economic methodology.

## Conclusion

The present synthetic method is a simple, efficient, inexpensive and green synthesis of biologically active benzothiazole

derivatives *via* an *S*-alkylation reaction in water. As opposed to conventional heating, under controlled microwave heating the neat reaction of 2-chloromethyl-6-nitrobenzothiazole **2** with benzenesulfinate anions **3a–j** proceeds faster and in higher yields.

## Experimental

### General

Melting points were determined on a Büchi B-540 apparatus and are uncorrected. Elemental analyses were performed by the Microanalysis centers of the University of Aix-Marseille 3 and of the INP-ENSCT (Toulouse, France). Both <sup>1</sup>H and <sup>13</sup>C NMR spectra were determined on a Bruker ARX 200 spectrometer. The <sup>1</sup>H chemical shifts are reported as ppm downfield from tetramethylsilane (Me<sub>4</sub>Si), and the <sup>13</sup>C chemical shifts were referenced to the solvent peak: CDCl<sub>3</sub> (76.9 ppm) or DMSO-D<sub>6</sub> (39.5 ppm). Solvents were dried by conventional methods. The following adsorbent was used for column chromatography: silica gel 60 (Merck, particle size 0.063–0.200 mm, 70–230 mesh ASTM). TLC was performed on 5 cm × 10 cm aluminium plates coated with silica gel 60F-254 (Merck) in an appropriate solvent.

### Microwave instrumentation

The multimode reactor used was a ETHOS Synth Lab station (Ethos start, Milestone Inc.). The multimode microwave has a twin magnetron (2 × 800 W, 2.45 GHz) with a maximum delivered power of 1000 W in 10 W increments (pulsed irradiation). Built-in magnetic stirring (Teflon-coated stirring bar) was used in all operations. During the experiments, time, temperature and power were measured with the “easy WAVE” software package. The temperature was measured throughout the reaction and evaluated by an infrared detector, which indicated the surface temperature.

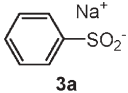
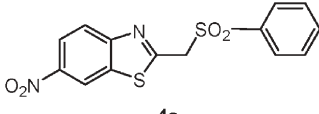
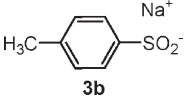
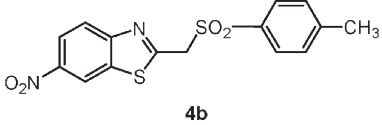
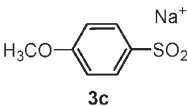
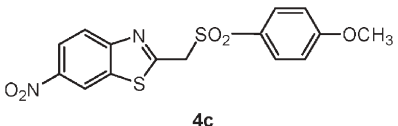
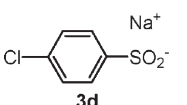
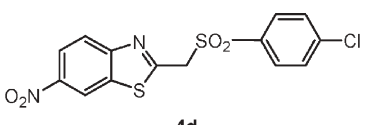
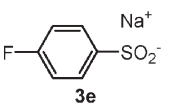
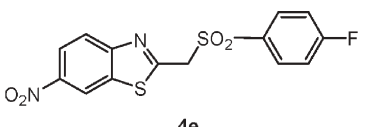
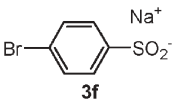
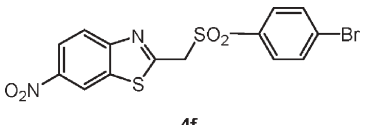
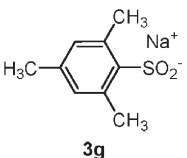
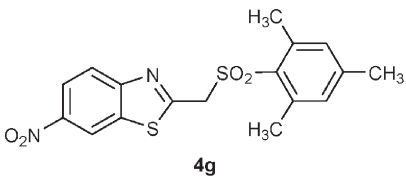
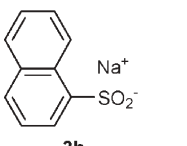
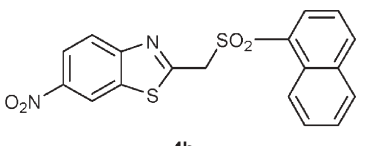
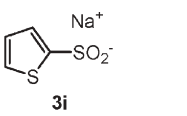
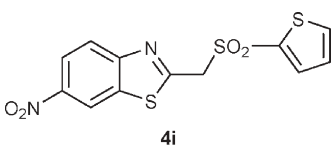
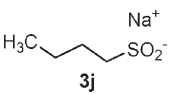
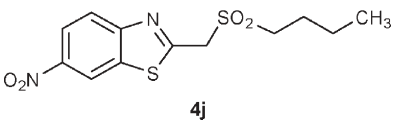
In order to compare microwave irradiation with conventional heating, the reactions were performed under similar experimental conditions (weight of reactants and temperature) using a thermostatted oil bath. The temperature was measured by the insertion of a Quick digital thermometer into the reaction mixture and the rate of the temperature rise was adjusted to be the same as measured under microwave irradiation.

### Experimental procedure

**2-Chloromethylbenzothiazole 1.** *Classical method.* A mixture of polyphosphoric acid (10 g) and chloroacetic acid (1.3 g, 13.74 × 10<sup>-3</sup> mol) was heated to 180 °C, and 2-aminobenzenethiol (1 g, 7.93 × 10<sup>-3</sup> mol) added. The mixture was stirred at reflux for 8 h. After cooling, the mixture was basified with 5 N NaOH, and the solution extracted with chloroform (3 × 20 mL). The organic layer was dried over magnesium sulfate and removed under vacuum. Purification by chromatography on silica gel, eluting with chloroform, gave 1.1 g (62%) of yellow solid **1**.

*Microwave method.* To a solution of 2-aminobenzenethiol (1 g, 7.93 × 10<sup>-3</sup> mol) in acetic acid (15 mL), 2-chloroacetyl

**Table 1** The reaction<sup>a</sup> of 2-chloromethyl-6-nitrobenzothiazole **2** with benzenesulfonic acid anions **3b–j**<sup>b</sup>

Anion	Product	Yield (%)	
		SC	MW
 <b>3a</b>	 <b>4a</b>	79	95
 <b>3b</b>	 <b>4b</b>	58	83
 <b>3c</b>	 <b>4c</b>	60	78
 <b>3d</b>	 <b>4d</b>	50	67
 <b>3e</b>	 <b>4e</b>	55	69
 <b>3f</b>	 <b>4f</b>	56	71
 <b>3g</b>	 <b>4g</b>	60	79
 <b>3h</b>	 <b>4h</b>	65	90
 <b>3i</b>	 <b>4i</b>	45	64
 <b>3j</b>	 <b>4j</b>	67	85

<sup>a</sup> The reaction time of chloride **2** with sulfone salts is 24 h under standard conditions (SC) and 30 min with the microwave methodology (MW). <sup>b</sup> All the reactions are carried out in water with 3 equivalents of sulfone salts.

chloride ( $1.35 \text{ g}, 11.89 \times 10^{-3} \text{ mol}$ ) was added dropwise. The reaction mixture was irradiated in a microwave oven (Ethos start) for 10 min at a power of 500 W. After cooling, the mixture was poured onto crushed ice (100 mL), basified with 5 N NaOH. The solution was extracted with chloroform ( $3 \times 50 \text{ mL}$ ). The organic layer was dried over magnesium sulfate and removed under vacuum. Purification by chromatography on silica gel, eluting with chloroform gave 1.97 g (90%) of yellow solid **1**.

**2-Chloromethyl-6-nitrobenzothiazole 2.** To a solution of 2-chloromethylbenzothiazole (4 g, 22 mmol) in concentrated sulfuric acid (20 mL), fuming nitric acid (5 mL) was added dropwise at  $0 \text{ }^\circ\text{C}$ . The reaction mixture was stirred at the same temperature for 1 h, poured into crushed ice (100 mL), neutralized with sodium carbonate and extracted with dichloromethane ( $3 \times 30 \text{ mL}$ ). The solvent was dried over magnesium sulfate and removed under vacuum. Purification by chromatography on silica gel, eluting with dichloromethane, and recrystallization from ethanol gave 4.5 g (89%) of yellow solid **2**, mp  $88\text{--}89 \text{ }^\circ\text{C}$  (lit.<sup>11</sup>  $87\text{--}88 \text{ }^\circ\text{C}$ ),  $^1\text{H}$  NMR ( $\text{CDCl}_3$ )  $\delta$ : 4.97 (s, 2H), 8.11 (d,  $J$  9.0 Hz, 1H), 8.33 (dd,  $J$  9.0 Hz and 2.2 Hz, 1H), 8.84 (d,  $J$  2.2 Hz, 1H).

**General procedure for the synthesis of the sulfonylmethylbenzothiazole derivatives (4a–j).** The sodium salts were commercially available or prepared as previously described.<sup>12</sup>

**Conventional conditions.** To a solution of sodium salt of substituted sulfinic acid ( $26.25 \times 10^{-3} \text{ mol}$ ) in water (30 mL) at  $100 \text{ }^\circ\text{C}$ , was added 2-chloromethyl-6-nitrobenzothiazole **2** (0.2 g,  $8.75 \times 10^{-3} \text{ mol}$ ). The reaction mixture was heated at  $100 \text{ }^\circ\text{C}$  for 24 h. After cooling, the precipitate was filtered, washed with  $3 \times 20 \text{ mL}$  of water and dried in low pressure drying oven. The product was recrystallized from ethanol.

**Microwave irradiation conditions.** To a solution of the sodium salt of the substituted sulfinic acid ( $26.25 \times 10^{-3} \text{ mol}$ ) in water (30 mL) was added 2-chloromethyl-6-nitrobenzothiazole **2** (0.2 g,  $8.75 \times 10^{-3} \text{ mol}$ ). The reaction mixture was irradiated in a microwave oven (Ethos start) for 30 min at a power of 800 W. The precipitate was filtered, washed with water ( $3 \times 20 \text{ mL}$ ) and dried in a vacuum drying oven (desiccator cabinet). The product was recrystallized from ethanol.

**2-Benzenesulfonylmethyl-6-nitrobenzothiazole 4a.** Light yellow solid, mp  $217\text{--}219 \text{ }^\circ\text{C}$ , (Found: C, 50.17; H, 2.95; N, 8.36).  $\text{C}_{14}\text{H}_{10}\text{N}_2\text{O}_4\text{S}_2$  requires C, 50.29; H, 3.01; N, 8.38%).  $\delta_{\text{H}}$  (200 MHz;  $\text{CDCl}_3$ ) 4.90 (s, 2H), 7.54 (m, 2H), 7.68–7.80 (m, 3H), 8.04 (d,  $J$  9.0 Hz, 1H), 8.33 (dd,  $J$  9.0 Hz and 2.2 Hz, 1H), 8.84 (d,  $J$  2.2 Hz, 1H).  $\delta_{\text{C}}$  (50 MHz;  $\text{CDCl}_3$ ) 57.3, 117.9, 119.2, 122.1, 126.7, 128.7, 134.4, 135.4, 138.3, 145.4, 157.3, 170.5.

**6-Nitro-2-(tosylmethyl)benzothiazole 4b.** White solid, mp  $180\text{--}182 \text{ }^\circ\text{C}$ , (Found: C, 51.69; H, 3.47; N, 8.02).  $\text{C}_{15}\text{H}_{12}\text{N}_2\text{O}_4\text{S}_2$  requires C, 51.71; H, 3.47; N, 8.04%).  $\delta_{\text{H}}$  (200 MHz;  $\text{CDCl}_3$ ) 2.44 (s, 3H,  $\text{CH}_3$ ), 4.89 (s, 2H,  $\text{CH}_2$ ), 7.30–7.69 (m, 4H, H Ar), 8.06 (d,  $J$  9.0 Hz, 1H, H Ar), 8.33 (dd,

$J$  9.0 Hz and 2.2 Hz, 1H, H Ar), 8.84 (d,  $J$  2.2 Hz, 1H, H Ar).  $\delta_{\text{C}}$  (50 MHz;  $\text{CDCl}_3$ ) 21.7, 60.9, 118.3, 121.9, 124.0, 128.6, 130.1, 134.7, 145.6, 145.9, 156.1, 159.7, 163.7.

**2-((4-Methoxyphenylsulfonyl)methyl)-6-nitrobenzothiazole 4c.** White solid, mp  $232\text{--}234 \text{ }^\circ\text{C}$ , (Found: C, 49.39; H, 3.34; N, 7.60).  $\text{C}_{15}\text{H}_{12}\text{N}_2\text{O}_5\text{S}_2$  requires C, 49.44; H, 3.32; N, 7.69%).  $\delta_{\text{H}}$  (200 MHz; DMSO) 3.90 (s, 3H,  $\text{CH}_3$ ), 5.45 (s, 2H,  $\text{CH}_2$ ), 7.10 (m, 2H, H Ar), 7.75 (m, 2H, H Ar), 8.06 (d,  $J$  9.0 Hz, 1H, H Ar), 8.33 (dd,  $J$  9.0 Hz and 2.2 Hz, 1H, H Ar), 8.84 (d,  $J$  2.2 Hz, 1H, H Ar).  $\delta_{\text{C}}$  (50 MHz; DMSO) 56.4, 59.8, 115.1, 120.1, 122.1, 123.91, 130.0, 131.1, 136.8, 145.3, 156.2, 164.2, 165.7.

**2-((4-Chlorophenylsulfonyl)methyl)-6-nitrobenzothiazole 4d.** White solid, mp  $202\text{--}204 \text{ }^\circ\text{C}$ , (Found: C, 45.54; H, 2.43; N, 7.55).  $\text{C}_{14}\text{H}_9\text{ClN}_2\text{O}_4\text{S}_2$  requires C, 45.59; H, 2.46; N, 7.60%).  $\delta_{\text{H}}$  (200 MHz; DMSO) 5.60 (s, 2H,  $\text{CH}_2$ ), 7.69–7.87 (m, 4H, H Ar), 8.12 (d,  $J$  9.0 Hz, 1H, H Ar), 8.29 (dd,  $J$  9.0 Hz and 2.2 Hz, 1H, H Ar), 9.21 (d,  $J$  2.2 Hz, 1H, H Ar).  $\delta_{\text{C}}$  (50 MHz; DMSO) 58.9, 119.8, 121.8, 123.6, 129.7, 130.4, 136.4, 137.0, 139.7, 145.0, 155.9, 164.8.

**2-((4-Bromophenylsulfonyl)methyl)-6-nitrobenzothiazole 4e.** Beige solid, mp  $228\text{--}230 \text{ }^\circ\text{C}$ , (Found: C, 40.61; H, 2.18; N, 6.70).  $\text{C}_{14}\text{H}_9\text{BrN}_2\text{O}_4\text{S}_2$  requires C, 40.69; H, 2.20; N, 6.78%).  $\delta_{\text{H}}$  (200 MHz; DMSO) 5.60 (s, 2H,  $\text{CH}_2$ ), 7.74–7.89 (m, 4H, H Ar), 8.13 (d,  $J$  9.0 Hz, 1H, H Ar), 8.30 (dd,  $J$  9.0 Hz and 2.2 Hz, 1H, H Ar), 9.21 (d,  $J$  2.2 Hz, 1H, H Ar).  $\delta_{\text{C}}$  (50 MHz; DMSO) 58.8, 119.8, 121.8, 123.6, 128.9, 130.4, 132.7, 136.4, 137.4, 145.0, 155.9, 164.8.

**2-((4-Fluorophenylsulfonyl)methyl)-6-nitrobenzothiazole 4f.** Yellow solid, mp  $158\text{--}160 \text{ }^\circ\text{C}$ , (Found: C, 47.78; H, 2.56; N, 5.41).  $\text{C}_{14}\text{H}_9\text{FN}_2\text{O}_4\text{S}_2$  requires C, 47.72; H, 2.57; N, 5.39%).  $\delta_{\text{H}}$  (200 MHz;  $\text{CDCl}_3$ ) 5.58 (s, 2H,  $\text{CH}_2$ ), 7.43–7.52 (m, 2H, H Ar), 7.87–7.94 (m, 2H, H Ar), 8.14 (d,  $J$  9.0 Hz, 1H, H Ar), 8.34 (dd,  $J$  9.0 Hz and 2.2 Hz, 1H, H Ar), 9.21 (d,  $J$  2.2 Hz, 1H, H Ar).  $\delta_{\text{C}}$  (50 MHz;  $\text{CDCl}_3$ ) 59.4, 116.6, 117.0, 119.8, 121.8, 123.6, 131.7, 131.9, 134.4, 136.4, 145.0, 155.9, 163.0, 164.9.

**2-(2,4,6-trimethylsulfonylmethyl)-6-nitrobenzothiazole 4g.** Brown solid, mp  $183\text{--}185 \text{ }^\circ\text{C}$ , (Found: C, 54.22; H, 4.25; N, 7.39).  $\text{C}_{17}\text{H}_{16}\text{N}_2\text{O}_4\text{S}_2$  requires C, 54.24; H, 4.28; N, 7.44%).  $\delta_{\text{H}}$  (200 MHz;  $\text{CDCl}_3$ ) 2.31 (s, 3H,  $\text{CH}_3$ ), 2.56 (s, 6H, 2  $\text{CH}_3$ ), 4.89 (s, 2H,  $\text{CH}_2$ ), 6.96 (s, 2H, 2 H Ar), 8.10 (d,  $J$  9.0 Hz, 1H, H Ar), 8.34 (dd,  $J$  9.0 Hz and 2.2 Hz, 1H, H Ar), 8.83 (d,  $J$  2.2 Hz, 1H, H Ar).  $\delta_{\text{C}}$  (50 MHz;  $\text{CDCl}_3$ ) 21.1, 22.9, 60.5, 118.3, 121.9, 124.0, 131.8, 132.5, 136.5, 140.6, 144.5, 144.6, 156.2, 162.9, 169.0.

**2-((Naphthalen-1-ylsulfonyl)methyl)-6-nitrobenzothiazole 4h.** Beige solid, mp  $186\text{--}188 \text{ }^\circ\text{C}$ , (Found: C, 56.20; H, 3.09; N, 7.21).  $\text{C}_{18}\text{H}_{12}\text{N}_2\text{O}_4\text{S}_2$  requires C, 56.24; H, 3.15; N, 7.29%).  $\delta_{\text{H}}$  (200 MHz;  $\text{CDCl}_3$ ) 5.08 (s, 2H,  $\text{CH}_2$ ), 7.48–7.76 (m, 4H, H Ar), 7.95–8.02 (m, 2H, H Ar), 8.15–8.20 (m, 2H, H Ar), 8.34 (dd,  $J$  9.0 Hz and 2.2 Hz, 1H, H Ar), 8.56–8.80 (d,  $J$  2.2 Hz, 1H, H Ar).  $\delta_{\text{C}}$  (50 MHz;  $\text{CDCl}_3$ ) 60.3, 118.2, 121.8, 123.6, 123.6, 124.3, 127.3, 129.3, 129.1, 129.5, 131.7, 132.6, 134.2, 135.0, 136.3, 145.5, 156.1, 162.5.

**6-Nitro-2-((thiophen-2-ylsulfonyl)methyl)benzothiazole 4i.**

Beige solid, mp 156–158 °C, (Found: C, 42.22; H, 2.30; N, 8.02. C<sub>12</sub>H<sub>8</sub>N<sub>2</sub>O<sub>4</sub>S<sub>3</sub> requires C, 42.34; H, 2.37; N, 8.23%). δ<sub>H</sub> 5.01 (s, 2H, CH<sub>2</sub>), 7.10–7.15 (m, 1H, H Ar), 7.60–7.74 (m, 2H, H Ar), 8.04–8.11 (m, 1H, H Ar), 8.33–8.40 (m, 1H, H Ar), 8.81–8.86 (m, 1H, H Ar). δ<sub>C</sub> (50 MHz; CDCl<sub>3</sub>) 60.3, 119.2, 120.5, 122.4, 128.2, 129.3, 135.7, 136.4, 144.9, 156.1, 165.6.

**2-(Butylsulfonylmethyl)-6-nitrobenzothiazole 4j.**

Beige solid, mp 119–121 °C, (Found: C, 45.82; H, 4.45; N, 8.88. C<sub>12</sub>H<sub>14</sub>N<sub>2</sub>O<sub>4</sub>S<sub>2</sub> requires C, 45.84; H, 4.49; N, 8.91%). δ<sub>H</sub> 0.87 (t, *J* 7.3 Hz, 3H, CH<sub>3</sub>), 1.36–1.48 (sextet, *J* 7.2 Hz, 2H, CH<sub>2</sub>) 1.68–1.76 (m, 2H, CH<sub>2</sub>), 3.29 (t, *J* 7.9 Hz, 2H, CH<sub>2</sub>), 4.93 (s, 2H, CH<sub>2</sub>), 8.23 (d, *J* 9.0 Hz, 1H, H Ar), 8.35 (dd, *J* 9.0 Hz and 2.2 Hz, 1H, H Ar), 9.21 (d, *J* 2.2 Hz, 1H, H Ar). δ<sub>C</sub> (50 MHz; CDCl<sub>3</sub>) 13.5, 21.0, 23.3, 52.2, 56.1, 119.7, 121.8, 123.6, 136.4, 144.9, 156.1, 165.6.

**References**

- 1 I. Hutchinson, M.-S. Chua, H. L. Browne, V. Trapani, T. D. Bradshaw, A. D. Westwell and M. F. G. Stevens, *J. Med. Chem.*, 2001, **44**, 1446; J. Koci, V. Klimesova, K. Waisser and J. Kaustova, *Bioorg. Med. Chem. Lett.*, 2002, **12**, 3275; I. Hutchinson, S. A. Jennings, B. R. Vishnuvajjala, A. D. Westwell and M. F. G. Stevens, *J. Med. Chem.*, 2002, **45**, 744; R. Paramashivappa, P. Phani Kumar and P. V. Subba Rao, *Bioorg. Med. Chem. Lett.*, 2003, **13**, 657; I. Hutchinson, T. D. Bradshaw and C. S. Matthews, *Bioorg. Med. Chem. Lett.*, 2003, **13**, 657; S. E. O'Brien, H. L. Browne, T. D. Bradshaw, A. D. Westwell, M. F. G. Stevens and C. A. Laughton, *Org. Biomol. Chem.*, 2003, **1**, 493; I. Yildiz-Oren, I. Yalcin, E. Aki-Seren and N. Ukarturk, *Eur. J. Med. Chem.*, 2004, **39**, 291.
- 2 T. D. Bradshaw, S. Wrigley, D. F. Shi, R. J. Schulz, K. D. Paull and M. F. G. Stevens, *Br. J. Cancer*, 1998, **77**, 745.
- 3 L. Bai, J. -X. Wang and Y. Zhang, *Green Chem.*, 2003, **5**, 615; N. E. Leadbeater and M. Marco, *J. Org. Chem.*, 2003, **68**, 888; V. Pironti and S. Colonna, *Green Chem.*, 2005, **7**, 43.
- 4 P. Lidström, J. Tierney, B. Wathey and J. Westman, *Tetrahedron*, 2001, **57**, 9225.
- 5 C. E. Stephens, T. M. Felder, J. W. Sowell, G. Andrei, J. Balzarini, R. Snoeck and E. De Clercq, *Bioorg. Med. Chem.*, 2001, **9**, 1123; L. Garuti, M. Roberti and E. De Clercq, *Bioorg. Med. Chem. Lett.*, 2002, **12**, 2707.
- 6 F. D. Popp and W. E. McEwen, *Chem. Rev.*, 1958, **58**, 321; Y. H. So and J. P. Heeschen, *J. Org. Chem.*, 1997, **62**, 3552.
- 7 Y. Njoya, A. Gellis, M. P. Crozet and P. Vanelle, *Sulfur Lett.*, 2003, **26**, 67.
- 8 A. K. Bose, S. N. Ganguly, M. S. Manhas, V. Srirajan, A. Bhattacharjee, S. Rumthao and A. H. Sharma, *Tetrahedron Lett.*, 2004, **45**, 1179.
- 9 C. O. Kappe, *Angew. Chem., Int. Ed.*, 2004, **43**, 6250.
- 10 L. Perreux and A. Loupy, *Tetrahedron*, 2001, **57**, 9199; A. Loupy, *C. R. Chim.*, 2004, **7**, 103.
- 11 F. M. Hamer, *J. Chem. Soc.*, 1956, 1480; H. Kristinsson, *Synthesis*, 1979, 102.
- 12 L. K. Liu, Y. Chi and K.-Y. Jen, *J. Org. Chem.*, 1980, **45**, 406.

# Vapor phase nitration of benzene using mesoporous MoO<sub>3</sub>/SiO<sub>2</sub> solid acid catalyst

S. B. Umbarkar, A. V. Biradar, S. M. Mathew, S. B. Shelke, K. M. Malshe, P. T. Patil, S. P. Dagde, S. P. Niphadkar and M. K. Dongare\*

Received 4th January 2006, Accepted 15th March 2006

First published as an Advance Article on the web 28th March 2006

DOI: 10.1039/b600094k

Nitration of benzene has been carried out in the vapor phase, using dilute nitric acid as the nitrating agent, over mesoporous MoO<sub>3</sub>/SiO<sub>2</sub> solid acid catalyst with more than 90% benzene conversion and 99.9% selectivity for mononitrobenzene. A series of MoO<sub>3</sub>/SiO<sub>2</sub> catalysts with varying MoO<sub>3</sub> loadings (1–30 mol%) were prepared using a sol–gel technique and characterized using X-ray diffraction analysis (XRD), BET specific surface area analysis, temperature-programmed desorption (TPD) of ammonia, and FTIR spectroscopic analysis of adsorbed pyridine. XRD analysis revealed the amorphous nature of the catalyst for 1 and 10 mol% MoO<sub>3</sub> loading, and the formation of a crystalline  $\alpha$ -MoO<sub>3</sub> phase on the amorphous silica support at higher MoO<sub>3</sub> loading. The BET surface area for pure silica support was 606 m<sup>2</sup> g<sup>-1</sup> and the pore size distribution in the range 40–80 Å, showing the mesoporous nature of amorphous silica. The BET surface area decreased to 583 m<sup>2</sup> g<sup>-1</sup> with incorporation of 1% MoO<sub>3</sub> and further decreased to 180 m<sup>2</sup> g<sup>-1</sup> with increasing MoO<sub>3</sub> loading up to 20%. Above 10% MoO<sub>3</sub> loading, formation of crystalline MoO<sub>3</sub> clusters on amorphous silica was observed. Ammonia-TPD showed a drastic increase in acid strength after addition of 1% MoO<sub>3</sub> compared to pure silica support and the acid strength increased with increasing MoO<sub>3</sub> content. Among the series of catalysts prepared, MoO<sub>3</sub>/SiO<sub>2</sub> containing 20 mol% MoO<sub>3</sub> was found to be the most active catalyst for benzene nitration, without showing any deactivation after more than 1000 h, showing a very high potential for commercialization.

## 1. Introduction

Nitration of aromatic substrates is a widely studied reaction because of its industrial importance. Catalytic hydrogenation of aromatic nitro-compounds is commercially practiced to produce a variety of aromatic amines that have applications as chemical intermediates and specialty chemical products. Many nitro-aromatics are extensively used as intermediates for the manufacture of dyes, pharmaceuticals, perfumeries and pesticides. Nitration of benzene, an industrially important reaction, is conventionally carried out in the liquid phase using a mixture of 56–60% (w/w) H<sub>2</sub>SO<sub>4</sub>, 27–32% (w/w) HNO<sub>3</sub>, and 8–17% (w/w) H<sub>2</sub>O as the nitrating agent at a temperature of 50–90 °C.<sup>1</sup> A large quantity of dilute sulfuric acid is generated because of water formed in the reaction. As dilute sulfuric acid cannot be used for nitration, it has to be concentrated for recycling, which is an energy intensive and costly process. The disposal of this large quantity of dilute sulfuric acid poses environmental problems, making nitration of benzene one of the most hazardous industrial processes. Nitration of benzene without use of sulfuric acid would be an attractive alternative, and various types of solid acids have been tried with limited success.

Vapor phase nitration of benzene over solid acid catalysts has been tried by Suzuki *et al.*,<sup>2</sup> however the yield of

nitrobenzene was low. Kuznetsova *et al.*<sup>3</sup> have studied vapor phase nitration of benzene using 56% nitric acid over H-ZSM-5 at 140–170 °C. However, the catalyst was found to get rapidly deactivated (<3 h) due to strong adsorption of reactants and products on the surface as well as in the pores of the zeolite, and these species were totally desorbed at only 220–250 °C, as CO, CO<sub>2</sub> and NO. Sato *et al.*<sup>4,5</sup> have studied vapor phase nitration of benzene over different solid acid catalysts, such as montmorillonite ion-exchanged with a multivalent metal ion, mixed oxides (*e.g.*, TiO<sub>2</sub>–MoO<sub>3</sub>), the same oxides treated with sulfuric acid at 500 °C and partially neutralized heteropolyacids. Although supported sulfuric acid showed good results for the vapor phase nitration of benzene, catalytic activity dropped rapidly after 144 h on-stream because of leaching of sulfuric acid.<sup>6</sup>

In continuation of our earlier efforts on the use of solid acid catalysts for nitration of aromatics,<sup>7–9</sup> we have investigated vapor phase nitration of benzene using molybdenum oxide supported on mesoporous silica as a solid acid catalyst and the results are presented in this paper.

## 2. Experimental

### 2.1. Catalyst preparation

MoO<sub>3</sub>/SiO<sub>2</sub> catalysts with varying molybdenum oxide molar concentrations (1, 10, 20 and 30 mol%) were prepared by a sol–gel technique. Ammonium heptamolybdate (AHM) and ethyl

Catalysis Division, National Chemical Laboratory, Pune 411008, India.  
E-mail: mk.dongare@ncl.res.in; Fax: +91-20-25902633;  
Tel: +91-20-25902044



silicate-40 (CAS registry no. 18945-71-7) were used as the molybdenum and silica sources, respectively.

In a typical procedure, 20 mol% MoO<sub>3</sub>/SiO<sub>2</sub> catalyst was synthesized by dissolving 14.11 g of AHM in 40 ml of water at 80 °C. This hot solution was added dropwise to a dry isopropyl alcohol solution of ethyl silicate-40 (48.0 g) with constant stirring. The resultant transparent greenish gel was air-dried and calcined at 500 °C in air in a muffle furnace for 12 h. Similarly, catalysts with 1, 10 and 30 mol% molybdenum oxide loading were prepared.

For comparison, pure, high surface area silica catalyst was prepared by adding 52 g of ethyl silicate-40 to 30 g of dry isopropyl alcohol; to this mixture 0.02 g of ammonia solution (25%) was slowly added with constant stirring. The transparent white gel thus obtained was air-dried and calcined in a muffle furnace at 500 °C for 12 h.

## 2.2. Catalyst characterization

The X-ray diffraction analysis was carried out using a Rigaku X-ray diffractometer (Model DMAX IIIVC) with Cu-K $\alpha$  (1.542 Å) radiation. Temperature programmed desorption of ammonia (NH<sub>3</sub>-TPD) was carried out using a Micromeritics Autocue 2910. BET surface area was determined using NOVA 1200 Quanta chrome instrument.

The acidity of the samples was determined by pyridine adsorption studies using a Shimadzu 8000 series FTIR spectrometer arranged for DRIFT technique.

## 2.3. Catalytic activity

Vapor phase benzene nitration was carried out using a down-flow glass reactor with a fixed catalyst bed at atmospheric pressure. In a typical nitration experiment, 10 g of granulated catalyst was loaded in a tubular glass reactor of 15 mm diameter and 25 cm length. The upper part of the reactor was packed with inert ceramic beads as a preheating zone. The glass reactor was fixed inside the heater and the reaction temperature was controlled by a thermocouple inserted in the catalyst bed.

Nitric acid (70%) and benzene were introduced into the flow reactor using peristaltic pumps with air as a carrier gas. The reaction mixture was condensed at 8 °C and collected in a receiver. The reaction mixture was extracted with diethyl ether followed by neutralization of unreacted nitric acid using sodium bicarbonate solution. After separation of the organic layer from the aqueous sodium bicarbonate layer, it was dried using Na<sub>2</sub>SO<sub>4</sub>. The organic layer was analyzed using gas chromatography (HP 6890, FID detector, column: HP-5, 60 m, 0.25 mm ID).

A few runs were also carried out using the formulated catalyst (20 mol% MoO<sub>3</sub>/SiO<sub>2</sub>) in the form of extrudates (2 mm × 5 mm) prepared using silica as binder (20 wt%) and calcined at 550 °C.

## 3. Results and discussion

The XRD patterns of 1, 10, 20 and 30 mol% MoO<sub>3</sub>/SiO<sub>2</sub> catalysts prepared by the sol-gel technique are shown in Fig. 1. For comparison, the XRD pattern of pure silica is also

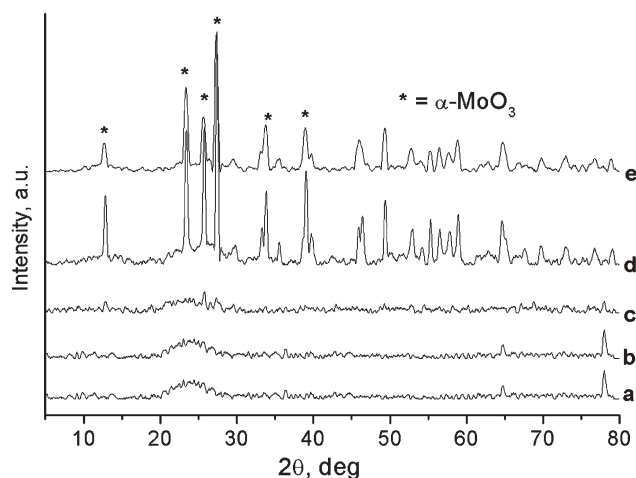


**Fig. 1** The XRD patterns of (a) silica and (b) 1, (c) 10, (d) 20 and (e) 30 mol% MoO<sub>3</sub>/SiO<sub>2</sub>.

included (Fig. 1a). The patterns show the amorphous nature of the material at lower Mo loading (Fig. 1b,c). Catalysts with 20% Mo loading (Fig. 1d) show crystalline nature with intense peaks at  $2\theta = 12.9, 23.4, 25.8$  and  $27.4^\circ$  corresponding to  $\alpha$ -MoO<sub>3</sub> in the orthorhombic phase. No  $\beta$ -MoO<sub>3</sub> phase is observed in the structure because the samples were calcined at 500 °C, a temperature at which the  $\beta$ -MoO<sub>3</sub> phase is not stable.<sup>10</sup> It is interesting to note that even though the MoO<sub>3</sub> is in the crystalline form at higher Mo loading, the silica support still retains its amorphous nature, leading to the high surface area of the catalysts.<sup>11</sup> In the case of 30 mol% MoO<sub>3</sub>/SiO<sub>2</sub>, a very clear crystalline  $\alpha$ -MoO<sub>3</sub> phase is observed (Fig. 1e). However, absence of the hump in the  $2\theta$  range of 20–30° for amorphous silica indicates the formation of bulk molybdenum oxide, as 30 mol% (~52 wt%) MoO<sub>3</sub> is quite high and forms a mixed oxide phase with amorphous silica. Up to 20 mol% MoO<sub>3</sub> loading there is uniform distribution of MoO<sub>3</sub> on the silica support, however with still higher loading MoO<sub>3</sub> becomes the bulk phase.

The surface areas of all the catalysts determined using the BET method are given in Table 1. As expected, a very high surface area of 606 m<sup>2</sup> g<sup>-1</sup> was observed in the case of pure silica because of sol-gel synthesis using ethyl silicate-40 as the silica source. Ethyl silicate-40 is a polymeric form (trimeric and tetrameric) of tetraethyl orthosilicate monomer, which on controlled hydrolysis yields silica of a very high surface area.<sup>12</sup> On controlled hydrolysis of ethyl silicate-40; the trimeric and tetrameric species form the corresponding trimeric and tetrameric silica structures, which restrict the growth of large particles. The surface area was found to decrease with

**Table 1** Surface area and acidity of the MoO<sub>3</sub>/SiO<sub>2</sub> catalysts

Catalyst	Surface area/m <sup>2</sup> g <sup>-1</sup>	Pore volume/cm <sup>3</sup> g <sup>-1</sup>	Average pore diameter/Å	NH <sub>3</sub> desorbed/mmol g <sup>-1</sup>
Silica	606	0.6132	50.49	0.0317
1% MoO <sub>3</sub> /SiO <sub>2</sub>	583	0.5934	40.69	0.1830
10% MoO <sub>3</sub> /SiO <sub>2</sub>	284	0.5656	40.56	0.7056
20% MoO <sub>3</sub> /SiO <sub>2</sub>	180	0.2327	51.64	0.9370

increasing  $\text{MoO}_3$  loading. During the sol-gel synthesis, an aqueous solution of AHM is added to ethyl silicate-40, which hydrolyzes ethyl silicate-40. However, control of the rate of hydrolysis is difficult, because of the use of excess water for dissolving AHM, which leads to a decrease in the surface area. The basic pH of the solution, due to the  $\text{NH}_3$  liberated during hydrolysis of AHM, also leads to the formation of a product with a lower surface area. It is expected that, as  $\text{MoO}_3$  loading is increased, crystalline molybdenum oxide clusters are formed that cover the amorphous silica support, reducing the total surface area of the catalyst.

The mesoporosity of the catalysts was evident from the nitrogen adsorption-desorption isotherms of all the catalysts including silica, which shows the H4 type of hysteresis. The average pore diameter for all the catalysts is given in Table 1. Since no template is used during the synthesis of pure silica or  $\text{MoO}_3/\text{SiO}_2$ , the pore size distribution does not show any specific trend. During the preparation of all the catalysts by the sol-gel method it is difficult to maintain identical process parameters. The amount of water used varies as the amount of water for dissolving AHM varies. Due to ammonia liberated during the hydrolysis of AHM, the pH of the medium is not constant. Also, due to the changes in the amount of water and the different basicities of the media, the rate of hydrolysis is not same for all the catalysts. Due to all these factors, there is no specific trend observed in average pore diameter and pore volume of the catalysts. However, pore diameters are in the range 40–80 Å, which confirms its mesoporous nature.

Ammonia-TPD experiments were carried out to determine the acid strength of the catalyst. The results are shown in Fig. 2, and the amount of  $\text{NH}_3$  desorbed is given in Table 1. The pure silica catalyst shows the lowest acidity, with  $0.0317 \text{ mmol g}^{-1}$  of ammonia desorbed at a comparatively low temperature, indicating the presence of a few weaker acid sites. Addition of 1%  $\text{MoO}_3$  to the silica support by the sol-gel method increases the acidity almost six times ( $0.183 \text{ mmol g}^{-1}$ ) with respect to the number of acid sites as well as the acid strength. The temperature for total desorption of ammonia increased (275 to  $400^\circ\text{C}$ ) with increasing  $\text{MoO}_3$  loading, up to

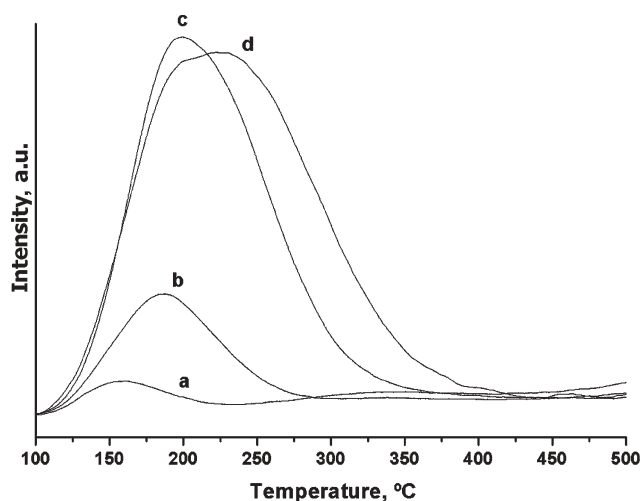


Fig. 2  $\text{NH}_3$ -TPD of (a) silica and (b) 1, (c) 10 and (d) 20%  $\text{MoO}_3/\text{SiO}_2$ .

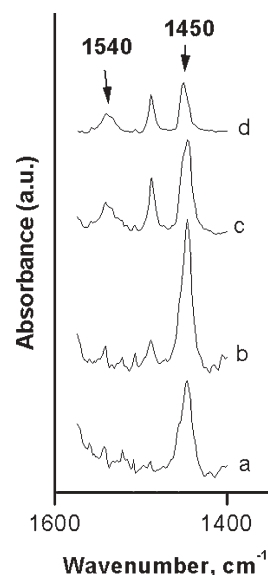


Fig. 3 FTIR spectra of pyridine adsorbed on (a) silica and (b) 1, (c) 10 and (d) 20%  $\text{MoO}_3/\text{SiO}_2$ .

20 mol%  $\text{MoO}_3/\text{SiO}_2$ , indicating corresponding increases in acid strength as well as in the number of acid sites. The catalyst with 20% Mo loading showed the maximum number of acid sites ( $\text{NH}_3$  desorbed:  $0.937 \text{ mmol g}^{-1}$ ) as well as the highest acid strength.

Pyridine adsorption studies for the determination of the nature of acidity reveal the presence of Lewis acidity in all catalysts.<sup>11</sup> Fig. 3 shows the IR spectra of pyridine adsorbed on the catalyst surface. The spectrum of pure silica (Fig. 3a) shows the presence of only Lewis acidity (peak at  $1450 \text{ cm}^{-1}$ ) with low acidity, and 1%  $\text{MoO}_3/\text{SiO}_2$  sample (Fig. 3b) shows an increase in Lewis acidity as well as acid strength. As the  $\text{MoO}_3$  loading is further increased, the samples show the presence of both Brønsted (peak at  $1540 \text{ cm}^{-1}$ ) as well as Lewis acid sites. The generation of Brønsted acidity may be correlated to the formation of polymolybdate Keggin structures.<sup>13</sup> The IR spectra of the catalyst in the framework region shows the presence of peaks at  $959$  and  $914 \text{ cm}^{-1}$ , which corresponds to polymolybdate Keggin structures, which are reported to exhibit Brønsted acidity. At temperatures of about  $500^\circ\text{C}$  transformation of the hexagonal form of molybdenum trioxide into its orthorhombic form takes place. The oxide becomes hydrated and subsequently converted into polymolybdenic trimers.<sup>14,15</sup> Such structural units are expected to show Brønsted acidity. The ratio of Brønsted to Lewis (B/L) acidity increases with increasing Mo loading. Though the Lewis acidity is found to decrease with increasing Mo loading, the Brønsted acidity observed at higher Mo loading contributes to an overall increase in the total acidity, which is seen by  $\text{NH}_3$ -TPD.  $\text{MoO}_3/\text{SiO}_2$  catalysts prepared by an impregnation technique are reported to show the presence of only Lewis acid sites without any Brønsted acidity. Ma *et al.*<sup>16</sup> have prepared a series of  $\text{MoO}_3/\text{SiO}_2$  catalysts (1–16 wt%) by an impregnation method, and the  $\text{NH}_3$ -TPD showed desorption at much lower temperature ( $<250^\circ\text{C}$ ), indicating the presence of weak acidity. The amount of ammonia desorbed for 1%  $\text{MoO}_3/\text{SiO}_2$  is reported to be only  $0.056 \text{ mmol g}^{-1}$ , which



**Scheme 1** Nitration of benzene to mononitrobenzene.

increased to 0.102 mmol g<sup>-1</sup> for 16% MoO<sub>3</sub>/SiO<sub>2</sub>. This shows that the acidity of impregnation catalysts is significantly lower compared to the catalysts prepared by sol-gel (present work).

### Catalytic activity

Nitrobenzene is the major product (99.9% selectivity for mononitrobenzene) in the nitration of benzene by nitric acid using MoO<sub>3</sub>/SiO<sub>2</sub> solid acid catalyst as in Scheme 1.

The results of the vapor phase nitration of benzene using 70% HNO<sub>3</sub> over MoO<sub>3</sub>/SiO<sub>2</sub> solid acid catalysts are shown in Fig. 4. When MoO<sub>3</sub> loading was increased from 1 to 10 mol%, only a marginal increase in benzene conversion from 70 to 74% was observed. However, a further increase in MoO<sub>3</sub> loading up to 20% led to the maximum benzene conversion of 92% without change in the nitrobenzene selectivity. Further increase in the Mo loading to 30 mol% led to a decrease in the benzene conversion to 36.6%. This shows that 20 mol% is the optimum Mo loading, which gives highest catalytic activity. Above 20% loading, MoO<sub>3</sub> forms a bulk phase on the silica surface, which does not increase the benzene conversion. Benzene conversion was calculated based on the use of 1 equivalent of nitric acid.

Considering the higher activity of 20% MoO<sub>3</sub>/SiO<sub>2</sub> catalyst, the catalyst life was tested for almost 1000 h to check the stability of the catalyst in an acid environment at higher temperature. The catalyst activity was constant, without any considerable decrease in either benzene conversion or selectivity for nitrobenzene, showing the stability of the catalyst for the nitration reaction (Table 2).

The XRD pattern of the catalyst (20% MoO<sub>3</sub>/SiO<sub>2</sub>) used for 1000 h of benzene nitration at 140 °C is shown in Fig. 5, which

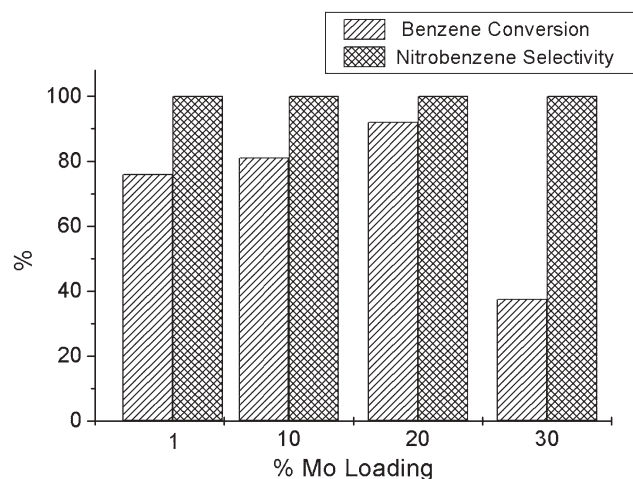
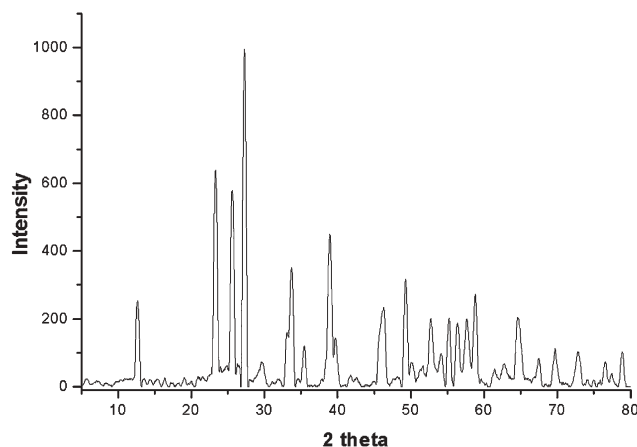


**Fig. 4** Plot of effect of different MoO<sub>3</sub> loadings on benzene conversion.

**Table 2** Vapor phase nitration of benzene over 20% MoO<sub>3</sub>/SiO<sub>2</sub> catalyst<sup>a</sup>

Time on-stream/h	Benzene conversion (%)	Nitrobenzene selectivity (%)
2	61.7	100
4	71.5	99.8 <sup>b</sup>
5	90.0	100
7	89.0	100
9	79.0	100
13	92.0	100
30	84.3	100
34	89.2	100
100	88.3	100
300	86.5	100
500	87.7	99.9 <sup>b</sup>
700	89.5	100
1000	88.4	100

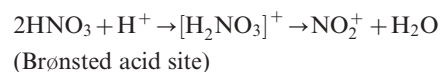
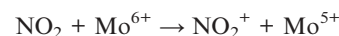
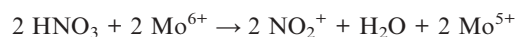
<sup>a</sup> Conditions: benzene : HNO<sub>3</sub> = 1 : 0.7; weight hourly space velocity = 0.7 h<sup>-1</sup>; 70 wt% HNO<sub>3</sub>; temp. = 140 °C. <sup>b</sup> Remaining product was dinitrobenzene.



**Fig. 5** XRD pattern of 20% MoO<sub>3</sub>/SiO<sub>2</sub> used at 140 °C for 1000 h.

showed no change in the crystalline nature of the catalyst. The chemical composition of the catalyst, verified by EDXS, also showed no change, confirming the stability of the catalyst in the nitric acid environment at 140 °C.

The maximum catalytic activity of 20% MoO<sub>3</sub>/SiO<sub>2</sub> is attributed to the higher acidity of the catalyst. The high catalytic activity of MoO<sub>3</sub>/SiO<sub>2</sub> in benzene nitration can be attributed to the redox nature of the molybdenum center. The Mo<sup>6+</sup> center acts as an electron acceptor site, which is responsible for the generation of a nitronium ion by capturing an electron occupied in the antibonding orbital of the nitrogen dioxide molecule. The nitronium ion can also be formed on the Brønsted acid sites.<sup>17</sup>



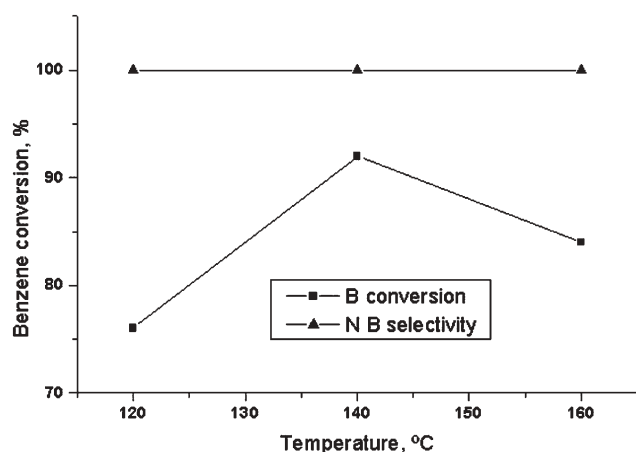


**Fig. 6** Plot for effect of temperature on benzene conversion and selectivity. Catalyst 20% MoO<sub>3</sub>/SiO<sub>2</sub> (10 g), weight hourly space velocity = 0.7 h<sup>-1</sup>, 70 wt% HNO<sub>3</sub>, benzene : HNO<sub>3</sub> = 1 : 0.7.

Nitration of benzene using dilute nitric acid can also be attributed to the polarisability of the water molecule coordinated to the cation generating the nitronium ion for the nitration reaction.<sup>5</sup>

#### Influence of temperature

The influence of reaction temperature on benzene nitration has been studied in the range 120–160 °C (Fig. 6). Initially the conversion increased from 70% to 85% with an increase in the temperature from 120 to 140 °C, and then decreased to 75% with a further increase in the temperature to 160 °C. The decrease in the conversion at high temperature is due to the thermal decomposition of nitric acid. At higher temperatures (160 °C), lots of brown fumes were observed, indicating decomposition of nitric acid, thus less nitric acid was available for the nitration of benzene leading to a decrease in the benzene conversion. The selectivity for nitrobenzene decreased marginally with increasing temperature due to the formation of dinitrobenzene.

#### Influence of weight hourly space velocity (WHSV)

The influence of WHSV on nitration of benzene was studied at 140 °C over 20% MoO<sub>3</sub>/SiO<sub>2</sub>, at nitric acid to benzene molar ratio 0.9 : 1 (Fig. 7). There was no decrease in benzene conversion when the WHSV was increased from 0.2 to 0.9 h<sup>-1</sup>, however there was slight decrease in the conversion when the WHSV was increased to 1 h<sup>-1</sup>, indicating that a WHSV of 0.9 provides optimum residence time for nitration to occur.

The high catalytic activity, selectivity and the stability of the 20% MoO<sub>3</sub>/SiO<sub>2</sub> catalyst for the nitration of benzene show its potential for commercialization. For a catalyst to be used in commercial reactors, it is essential to formulate the catalyst powder in a usable form such as pellets, extrudates *etc.* 20% MoO<sub>3</sub>/SiO<sub>2</sub> catalyst powder was formulated in the form of extrudates (2 mm × 5 mm) using silica as a binder (20 wt%). The results of the nitration of benzene using this formulated catalyst are given in Table 3. Benzene conversion using the formulated catalyst was marginally lower than the unformulated catalyst, showing high potential for commercialization of

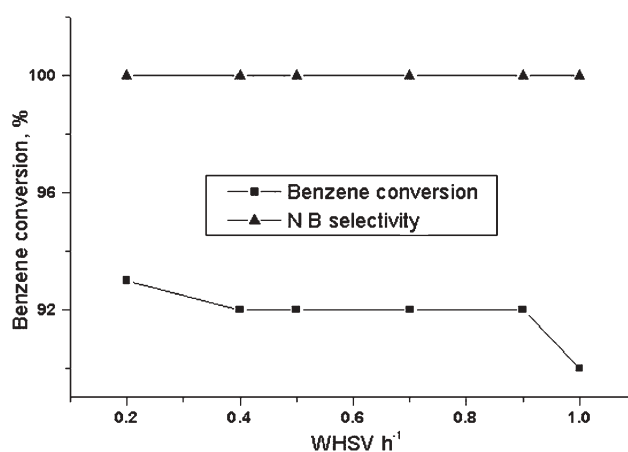


**Fig. 7** Plot of effect of weight hourly space velocity on benzene conversion and selectivity. Catalyst 20% MoO<sub>3</sub>/SiO<sub>2</sub> (10 g), 140 °C, 70 wt% HNO<sub>3</sub>, benzene : HNO<sub>3</sub> = 1 : 0.7.

**Table 3** Vapor phase nitration of benzene using formulated catalyst<sup>a</sup>

Time on-stream/h	Benzene conversion (%)	Selectivity (%)
4	71.3	100
18	72.6	100
36	70.6	99.8
50	71.8	100

<sup>a</sup> Conditions: benzene : HNO<sub>3</sub> = 1 : 0.8; weight hourly space velocity = 0.6 h<sup>-1</sup>; 70 wt% HNO<sub>3</sub>; temp. = 150 °C.

this catalyst. Use of silica as the binder led to an overall decrease in the molybdenum content of the catalyst, leading to the decrease in the benzene conversion.

## 4. Conclusion

Vapor phase nitration of benzene using dilute nitric acid over 20% MoO<sub>3</sub>/SiO<sub>2</sub> showed more than 90% benzene conversion and 99.9% selectivity for mononitrobenzene. The catalyst showed high stability for more than 1000 h on-stream. The formulated catalyst in the form of extrudates also showed similar activity, suggesting its utility on larger scale. Since sulfuric acid has been totally eliminated in this process, the process is environmentally benign and has high potential for commercialization.

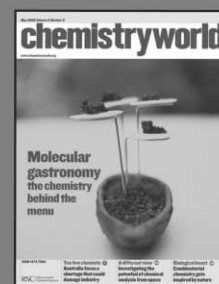
## References

- R. L. Adkins, 'Nitrobenzene and Nitrotoluenes', in: *Encyclopedia of Chemical Technology* (4th edn), Wiley-Interscience, New York, 1996, vol. 17, p. 133.
- S. Suzuki, K. Tohmori and Y. Ono, *Chem. Lett.*, 1986, 747.
- T. G. Kusnetzova, K. G. Ione and L. V. Malysheva, *React. Kinet. Catal. Lett.*, 1998, **63**, 61.
- H. Sato and K. Hirose, *Appl. Catal., A*, 1998, **174**, 77.
- H. Sato, K. Hirose, K. Nagai, H. Yoshioka and Y. Nagaoka, *Appl. Catal., A*, 1998, **175**, 201.
- H. Sato, K. Nagai and H. Yoshioka, *Appl. Catal., A*, 1999, **180**, 359.
- S. P. Dagade, S. B. Waghmode, V. S. Kadam and M. K. Dongare, *Appl. Catal., A*, 2002, **226**, 49.
- S. P. Dagade, V. S. Kadam and M. K. Dongare, *Catal. Commun.*, 2002, **3**, 67.

- 9 P. T. Patil, K. M. Malshe, S. P. Dagade and M. K. Dongare, *Catal. Commun.*, 2003, **4**, 429.
- 10 A. Kido, H. Iwamoto, N. Azuma and A. Ueno, *Catal. Surv. Jpn.*, 2002, **6**, 45.
- 11 A. V. Biradar, S. B. Umbarkar and M. K. Dongare, *Appl. Catal., A*, 2005, **285**, 190.
- 12 M. K. Dongare, P. T. Patil and K. M. Malshe, *Eur. Pat.* 1386907, 2004; M. K. Dongare, P. T. Patil and K. M. Malshe, *US Pat.* 2004024267, 2004.
- 13 W. Skupinski and M. Malesa, *Appl. Catal., A*, 2002, **236**, 223.
- 14 C. Rocchiccioli-Deltcheff, M. Amirouche, G. Herve, M. Fournier, M. Che and J. M. Tabibonet, *J. Catal.*, 1990, **126**, 591.
- 15 C. Rocchiccioli-Deltcheff, M. Amirouche, G. Herve, M. Fournier, M. Che and J. M. Tabibonet, *J. Catal.*, 1990, **125**, 292.
- 16 X. Ma, J. Gong, S. Wang, N. Gao, D. Wang, X. Yang and F. He, *Catal. Commun.*, 2004, **5**, 101.
- 17 J. S. Yoo, A. R. Sohail, S. S. Grimmer and J. Z. Shyu, *Appl. Catal., A*, 1994, **117**, 1.

# chemistryworld

A "must-read" guide to current chemical science!



**Chemistry World** provides an international perspective on the chemical and related sciences by publishing scientific articles of general interest. It keeps readers up-to-date on economic, political and social factors and their effect on the scientific community.

16050521

RSCPublishing

[www.chemistryworld.org](http://www.chemistryworld.org)

# Looking for that special research paper?

TRY one of these free news services:

## Chemical Biology

[www.rsc.org/chembiology](http://www.rsc.org/chembiology)

## Chemical Science

[www.rsc.org/chemicalscience](http://www.rsc.org/chemicalscience)

## Chemical Technology

[www.rsc.org/chemicaltechnology](http://www.rsc.org/chemicaltechnology)

- highlights of newsworthy and significant advances from across RSC journals
- free online access
- updated daily
- free access to the original research paper from every online article
- also available as free print supplements in selected RSC journals.\*

\*A separately issued print subscription is also available.

Registered Charity Number: 207890



RSC Publishing

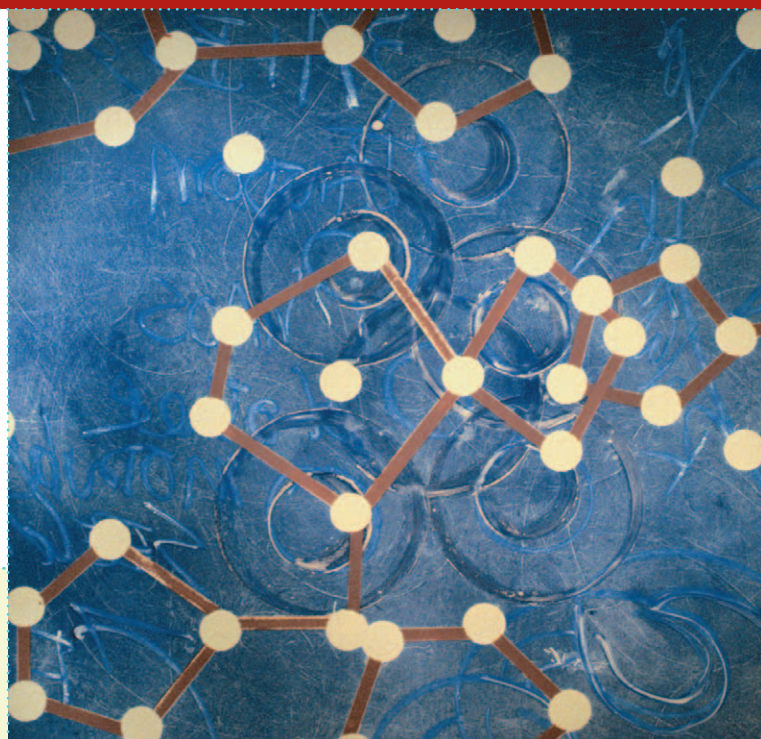
Advance Registration Deadline: June 19, 2006

# 10th Annual Green Chemistry & Engineering Conference

*Designing for a Sustainable Future*

**June 26–30, 2006**

**WASHINGTON, DC**



**The future will be  
what we design it  
to be.**

As chemists and engineers, we practice the art of design. From energy to agriculture, materials to medicine, our ability to create at

the most fundamental level gives us the power to change whole sectors of the world economy.

## Will that future be sustainable?

The simple answer is that it must be. In June 2006, designers of molecules, materials, products, processes, and systems will gather in Washington, DC to make it so.

## We need your participation.

Register now to attend this important event. This conference is centered around the theme of design, and will feature green chemistry and green engineering innovations in five core tracks:

- › *Energy*
- › *Agriculture and Foods*
- › *Resources and Renewables*
- › *Toxics and Materials*
- › *Health and Medicine*

## Register Now

Advance registration and housing are now open. To reserve a place, please visit the conference website: [www.greenchem2006.org](http://www.greenchem2006.org).

› **Deadline: June 19, 2006**

## Conference information

For additional conference information, please visit [www.greenchem2006.org](http://www.greenchem2006.org).



**GreenChem2006**

› **Advance registration closes June 19, 2006**

Visit the conference website to view the preliminary program: [www.greenchem2006.org](http://www.greenchem2006.org).

# Really readable reviews from Chem Soc Rev

**Chem Soc Rev** brings you a series of general interest reviews, carefully selected to give you an unrivalled overview of topical areas within the chemical sciences:

## Chemical forensics: every contact leaves a trace

DNA profiling methods have revolutionised crime investigation by allowing identification of the source of human tissue, and fingerprints are an invaluable aid. But when this type of evidence is not available, what other methods can be used to find the answers?



*Advances in chemistry applied to forensic science*, D. F. Rendle, *Chem. Soc. Rev.*, 2005, **34**, 1021

## Hidden Fingerprints

The continued importance of latent fingerprints as physical evidence in forensic science has created a demand for improved reagents for fingerprint development. The synthetic analogues reviewed here have shown that reagents with enhanced properties are still needed.

*The development of novel ninhydrin analogues*, D. B. Hansen and M. M. Joullié, *Chem. Soc. Rev.*, 2005, **34**, 408



## Intelligent solutions for smart packaging

Chilling and storing in modified atmosphere packaging, MAP, (a low oxygen environment) extends the shelf life of foods. Detecting oxygen levels in MAPs is therefore key to the efficacy of novel packaging. New sensor technologies, including intelligent inks, reviewed here are likely to feature strongly in future smart packaging.



*Oxygen indicators and intelligent inks for packaging food*, A. Mills, *Chem. Soc. Rev.*, 2005, **34**, 1003

For these and more great reviews,  
visit the website